

Applicability of CRISPR/Cas9-mediated
gene disruption in *Brachypodium*
distachyon (L) P. Beauv to characterise
the stress-induced 1,3- β -glucan synthase
BdGSL3 in plant defence

Dissertation

For the acquirement of the Dr. rer. nat. (*Doctor rerum naturalium*) degree at
the University of Hamburg, Faculty for Mathematics, Informatics and
Natural Sciences, Department of Biology

By

Tobias Hanak

Born 17.09.1989 in Henstedt – Ulzburg

Hamburg, September 2019

1. Reviewer: Prof. Dr. Stefan Hoth

2. Reviewer: Dr. Christian A. Voigt

Date of Disputation: 07.02.2020

Index

I. Index of abbreviations.....	VI
II. Register of illustrations.....	IX
III. Register of tables	XI
1. Introduction	1
1.1 Genome editing	1
1.1.2 Zinc-finger nucleases.....	2
1.1.3 TALEN.....	2
1.1.4 CRISPR/Cas9	3
1.1.5 Homology direct repair and non-homologous end joining.....	4
1.2 <i>Brachypodium distachyon</i> a model plant for monocotyledons	6
1.3 Plant diseases.....	8
1.3.1 The fungal leaf pathogen <i>Parastagonospora nodorum</i>	9
1.3.2 The necrotrophic fungus <i>Fusarium graminearum</i> as causal agent of Fusarium Head Blight	10
1.4 Plant Defence	12
1.5 The cell wall a first line of defence	15
1.6 Callose, a cell wall polymer and its role in plant defence	17
1.6.1 Callose and its role in plants.....	17
1.6.2 Callose synthases and callose synthesis	19
1.6.3 Regulation of callose synthases.....	21
1.7 Aim.....	23
2. Material & Methods	24
2.1 Equipment	24
2.2 Chemicals and Enzymes.....	25
2.3 Kits	25
2.4 Genetical resources and oligonucleotides	26
2.4.1. Oligonucleotides.....	26
2.4.2. DNA-Plasmids.....	28
2.5 Cultivation media and broths.....	28
2.6 Biological resources and cultivation	30
2.6.1 Plant material.....	30
2.6.2 Microorganisms	30
2.6.2.1 <i>Agrobacterium tumefaciens</i>	30
2.6.2.2 <i>Fusarium graminearum</i>	31

2.6.2.3 <i>Stagonospora nodorum</i> SN15	31
2.7 Methods	31
2.7.1 Generating of transgenic <i>B. distachyon</i> plants	31
2.7.2 Isolation of DNA	32
2.7.3 Isolation of RNA and qPCR analysis	33
2.7.3.1 Isolation of plant RNA from <i>Brachypodium distachyon</i>	33
2.7.3.2 cDNA synthesis	33
2.7.3.3 Gene expression analysis via qPCR	33
2.7.4 Genotyping of transformed plants	35
2.7.4.1 PCR based screening for <i>BdGSL3</i> mutations.....	35
2.7.4.2 Screening for the <i>hpt</i> gene in transformed plants	36
2.7.4.3 PCR based off-site target screening.....	36
2.7.4.4 Agarose gel electrophoresis of screening PCR products.....	37
2.7.5 Infection and wounding experiments	37
2.7.5.1 Wounding of <i>B. distachyon</i> leaves.....	38
2.7.5.2 Inoculation of <i>B. distachyon</i> leaves with the necrotrophic leaf pathogen <i>S. nodorum</i> .	38
2.7.5.3 Inoculation of <i>B. distachyon</i> spikelets with <i>F. graminearum</i> 8/1	38
2.7.5.4 Evaluation of the Disease Score after 7- and 14-days post inoculation	39
2.7.5.5 Measuring the relative area covered with callose depositions in inoculated <i>B. distachyon</i> florets	40
2.8 Microscopy and visualization.....	41
2.8.1 Macroscopic pictures.....	41
2.8.2 Stereo microscopy	41
2.8.3 Confocal laser scanning microscopy	41
2.9 <i>In silico</i> methods	42
3. Results	44
3.1 Overview of <i>BdGSL3</i> and its homology to <i>PMR4</i>	44
3.2 Generating and identifying genome edited plants	46
3.3 Phenotyping of four genome edited <i>B. distachyon</i> lines	54
3.4 Infection analysis of genome edited plants.....	58
3.5 Wounding and pathogen induced callose response in leaves of <i>B. distachyon</i>	68
3.6 qPCR analysis of the <i>Brachypodium distachyon</i> GSL Gene family	73
3.7 Analysis of pathogen responsive genes of <i>B. distachyon</i> and virulence genes of <i>F. graminearum</i> after inoculation.....	80
4. Discussion	83
4.1 Genome editing as new breeding technology for crops	83
4.1.1 CRISPR/Cas9 in <i>Brachypodium distachyon</i> and prospects for plant breeding.....	83

4.1.2 CRISPR/Cas9 in <i>Brachypodium distachyon</i> a look into the major concern of unspecific off-site mutations.....	84
4.2 The loss of function of BdGSL3 and the possible role in <i>Brachypodium distachyon</i>	86
4.2.1 CRISPR/Cas9 mediated loss of function mutants of BdGSL3.....	86
4.2.2 Vegetative phenotype of genome edited <i>Brachypodium distachyon</i> plants	88
4.2.3 Is BdGSL3 responsible for the formation of callose depositions after infection of <i>Fusarium graminearum</i> in spikelets?	89
4.2.4 BdGSL3 as a universal answer to stress in <i>Brachypodium distachyon</i> ?	91
4.2.5 The genome editing and loss of function of BdGSL3 and its impact on transcriptional level to the callose synthase gene family in <i>Brachypodium distachyon</i>	94
4.2.6 How does the plant respond to the absence of callose after inoculation with <i>Fusarium graminearum</i> on transcriptional level?.....	96
4.2.7 A prospect on BdGSL2 and BdGSL3 and their role in <i>B. distachyon</i>	101
4.3 The role of callose during <i>F. graminearum</i> infection	103
4.4 Conclusion.....	104
5. Abstract	107
6. Zusammenfassung	109
7. References	111
8. Supplement.....	143
Acknowledgments	XII
Declaration of authorship	XIII
Confirmation of Linguistic Correctness	XIV

I. Index of abbreviations

AA	Amino acid/ Amino acids
Act	<i>ACTIN</i>
ANOVA	Analysis of Variance
Appx.	Approximately
ASL39	<i>ASYMMETRIC LEAVES2-LIKE</i> 39
ASN	Asparagine
At	<i>Arabidopsis thaliana</i>
Avr	Avirulence
BAK1	<i>BRASSINOSTEROID INSENSITIVE</i> 1
BBCH	B iologische B undesanstalt, B undessortenamt und C hemische Industrie
Bd21	<i>Brachypodium distachyon</i> inbred line 21
Bp	basepair
CalS	Callose Synthase
Cas	CRISPR associated gene
CC	Coiled-Coiled domain
cDNA	Complementary DNA
CDS	Coding Sequence
CEBiP	CHITIN ELICITOR-BINDING PROTEIN
CERK1	CHITIN ELICITOR RECEPTOR KINASE
CesA	Cellulose synthase
Chit8	<i>CHITINASE</i> 8
CIM	Callus induction medium
CLSM	Confocal laser scanning microscopy
CMPG1	RING-type E3 ubiquitin transferase
CRISPR	Clustered Regularly Interspaced Short Palindromic Repeats
crRNA	CRISPR RNA
CSC	Cellulose synthase complex
CSN2	<i>COP9 SIGNALOSOME COMPLEX SUBUNIT</i> 2
D	Aspartic acid / aspartate
DNA	Desoxyribonucleic acid
Dnase	Desoxyribonuclease
DON	Deoxynivalenol
Dpi	Days post inoculation
DSB	Double strand break
ETI	Effector triggered immunity
Exo70	<i>EXOCYST COMPLEX COMPONENT</i> 70
fgl1	<i>FUSARIUM GRAMINEARUM LIPASE</i> 1
FHB	Fusarium head blight
FKS1	Catalytic subunit of 1,3- β -glucan synthase
flg22	Flagellin Fragment 22
FLS2	LRR receptor-like serine/threonine-protein kinase FLS2
<i>FokI</i>	Restriction endonuclease from <i>Flavobacterium okeanoikoites</i>
G	Glycine
GAsP	Gallium arsenide phosphide
gDNA	Genomic DNA
GM	Germination medium
GSL	GLUCAN SYNTHASE LIKE

H	Histidine
HDR	Homology directed repair
HNH	Active nuclease domain of cas9
Hpi	Hours post inoculation
Hpt	Hypoxanthine phosphoribosyltransferase
Hrp	Hypersensitive response and pathogenicity
Hv	<i>Hordeum vulgare</i>
I	Isoleucine
Indel	Insertion-Deletion
K	Lysine
Kbp	Kilo basepair
KD	Kilo dalton
LBD37	LOB DOMAIN-CONTAINING PROTEIN 37
LKH	LEUKOTRIENE A-4 HYDROLASE HOMOLOG
LRR	Leucin Rich Repeat
LysM	Lysin Motif Domain
MALDI	Matrix-assisted laser desorption/ionization
MAPK	Mitogen-activated protein kinase
MAPKK	Mitogen-activated protein kinase kinase
MAPKKK	Mitogen-activated protein kinase kinase kinase
Mbp	Mega basepairs
MLO	MILDEW RESISTANCE LOCUS
MQTL	Meta Quantitative trait locus
MSB	Murashige-Skoog Broth
MS-Salt	Murashige-Skoog Salt
N	Asparagine
NADPH	Nicotinamide adenine dinucleotide phosphate
NBT	New breeding technology
NHEJ	Non-homologous end joining
ORF	Open reading frame
Os	<i>Oryza sativa</i>
p. a.	postero-anterior
PAM	Protospacer adjacent Motif
PAMP	Pathogen associated molecular pattern
PCR	Polymerase chain reaction
PMR4	POWDERY MILDEW RESISTANT 4
PR Gene	Pathogenesis-related gene
PRR	Pattern recognition receptor
PTI	Pattern triggered immunity
qPCR	Quantitative PCR
QTL	Quantitative trait locus
R Gene	Resistance gene
RBOHD	RESPIRATORY BURST OXIDASE HOMOLOG PROTEIN D
RIN4	RPM1-INTERACTING PROTEIN 4
RLK	Receptor like kinase
RM	Regeneration medium
RNA	Ribonucleic acid
RNase	Ribonuclease
RNS	Reactive nitrogen species
ROS	Reactive oxygen species
RPM	Revolutions per minute

RPM1	DISEASE RESISTANCE PROTEIN RPM1
RPS2	RESISTANCE TO P. SYRINGAE 2
RuvC	Active nuclease domain of cas9
RVD	Repeat variable diresidues
sgRNA	single-guide RNA
SNB	Septoria nodorum blotch
SSB	Single strand break
SUSY	Sucrose synthase
TALLEN	Transcription activator-like effector nucleases
T-DNA	Transfer-DNA
TIR	TOLL/INTERLEUKIN-1 RECEPTOR
tracrRNA	Trans-activating crRNA
Tri5	TRICHODIENE SYNTHASE 5
Tyr	Tyrosine
UBC18	UBIQUITIN 18
Ubi	UBIQUITIN
UGT74f2	UDP-GLYCOSYLTRANSFERASE 74F2
upH ₂ O	Ultrapure H ₂ O
UV	Ultraviolet
v/v	volume percent
w/v	Mass concentration
WGA	Wheat germ agglutinin
WGLUC5	WHEAT GLUCANASE5
WRKY	WRKY transcription factors
WT	Wild-type
ZFN	Zinc-finger nuclease

II. Register of illustrations

Figure 1: Overview of the active form of cas9 endonuclease and the repair mechanisms for DNA in cells.....	5
Figure 2: The grass model plant <i>Brachypodium distachyon</i>	7
Figure 3: Disease Score ranking system for evaluation of the infection of the FHB disease causing pathogen <i>F. graminearum</i> in <i>B. distachyon</i>	39
Figure 4: <i>B. distachyon</i> floret with the marked area used to measure the relative area occupied by callose depositions.....	40
Figure 5: Overview of the CDS of the 1,3- β -glucan synthase <i>BdGSL3</i> from <i>Brachypodium distachyon</i>	44
Figure 6: Comparison of the characterised stress induced 1,3- β -glucan synthase AtGSL5 (PMR4) and the 1,3- β -glucan synthase <i>BdGSL3</i> from <i>Brachypodium distachyon</i> with unknown function.....	45
Figure 7: PCR based screening of the T ₀ -Generation for differences in the genome editing target region.....	46
Figure 8: PCR based screening from the T ₁ -Generation to further describe the genome editing process	47
Figure 9: Final PCR based screening for the T ₆ -Generation to identify the <i>BdGSL3</i> genotype and the presence of T-DNA.....	48
Figure 10: Sequence alignment of sequenced PCR products compared to the <i>BdGSL3</i> gDNA reference	50
Figure 11: Sequence alignment of the expected protein sequences of <i>BdGSL3</i> with the wild-type protein as reference	50
Figure 12: Off-Site target screening for the identified mismatching regions in the genome of Bd21	52
Figure 13: Growth of <i>B. distachyon</i> wild-type and the four genome edited lines for an eight weeks life cycle	54
Figure 14: Overview of different growth stages for <i>B. distachyon</i> wild-type Bd21 and the four genome edited lines	56
Figure 15: Disease Score mediated evaluation of <i>F. graminearum</i> 8/1 infection in <i>B. distachyon</i> at 14 dpi.....	58
Figure 16: Evaluation of FHB Disease Score of <i>B. distachyon</i> spikelets at 7 dpi with <i>F. graminearum</i> 8/1	60

Figure 17: Overview of the <i>F. graminearum</i> mediated FHB disease at 7 dpi on the <i>B. distachyon</i> wild-type Bd21 and the four genome edited lines.....	62
Figure 18: Confocal Laser Scanning Microscopy of inoculated <i>B. distachyon</i> florets at 7 dpi with <i>F. graminearum</i> strain 8/1.....	63
Figure 19: Callose depositions in spikelets of <i>B. distachyon</i> 3 dpi with <i>F. graminearum</i> 8/1	65
Figure 20: Mean relative area of callose depositions in 3 dpi spikelets of <i>Brachypodium distachyon</i>	66
Figure 21: Wounding induced callose depositions in <i>B. distachyon</i> leaves six hours after wounding	68
Figure 22: Wounding induced stress response and callose forming of <i>B. distachyon</i> leaves 16 hours after wounding.....	69
Figure 23: Mean relative area of callose depositions at wounded tissue 16 hours after wounding	70
Figure 24: Confocal Laser Scanning Microscopy of <i>P. nodorum</i> strain SN15 infection on <i>B. distachyon</i> leaves 7 days post inoculation.....	72
Figure 25: Relative gene expression of <i>BdGSL</i> gene family in leaves of three weeks old <i>B. distachyon</i> plants	74
Figure 26: Gene expression of <i>BdGSL</i> gene family in stem tissue of five weeks old <i>B. distachyon</i> plants	76
Figure 27: <i>BdGSL</i> gene family expression in spikelets of <i>B. distachyon</i> during anthesis	78
Figure 28: Relative gene expression of the pathogen responsive gene <i>PR2</i> at 0 dpi and 2 dpi in spikelets of <i>B. distachyon</i>	81
Figure 29: Relative gene expression for the two fungal virulence genes <i>fgl1</i> and <i>tri5</i> in 2 dpi spikelets	82

III. Register of tables

Table 1: Equipment list used during this work	24
Table 2: Overview of the uncommon chemicals used during this work	25
Table 3: Overview of important kits for the declared applications during this work	25
Table 4: Overview of the used primer in this work.....	26
Table 5: Description of the used binary vector for plant transformation and CRISPR/Cas9 mediated genome editing	28
Table 6: Overview of the used media and broths and their compositions	28
Table 7: Brief overview of the used microorganisms and their background	30
Table 8: Used buffers for the gDNA isolation from <i>B. distachyon</i>	32
Table 9: Amplification protocol for the RealTime ready Custom Panel qPCR.....	34
Table 10: Overview of the analysed <i>B. distachyon</i> genes and the associated loci.....	34
Table 11: Overview of the analysed PR and virulence genes of <i>B. distachyon</i> and <i>F. graminearum</i>	35
Table 12: Amplification protocol for the expression analysis of <i>B. distachyon</i> PR genes and <i>F. graminearum</i> virulence genes	35
Table 13: PCR program used for the screening for mutations in <i>BdGSL3</i>	36
Table 14: PCR program for amplification of an <i>bar</i> gene fragment from the T-DNA.....	36
Table 15: PCR amplification program for off-site target screening in <i>B. distachyon</i>	36
Table 16: Buffers used for the agarose gel electrophoresis of the PCR products	37
Table 17: Overview of the used fluorescence dyes and composition for the fluorescence microscopy	41
Table 18: Overview of the excitation and detection of the used fluorescence dyes	42
Table 19: Predicted Motifs for BdGSL3 at the genome edited region of the protein	51

1. Introduction

One of the major global challenges is the production of food with its aims to achieve food security and food safety. Even though yields substantially increased over the last century for major crops, research indicates that the climate change might affect those yields negatively (Erda et al. 2005; Lobell and Field 2007; Schmidhuber and Tubiello 2007). The abiotic stresses for crops like drought, floods, natural disasters or extreme temperatures are currently rising in its frequencies (Brito et al. 2018; Han et al. 2016; Khan et al. 2015). In addition, biotic stresses are a rising factor in agriculture for food production and food safety (CARVER and GRIFFITHS 1981; Conner et al. 2003; GOSWAMI and KISTLER 2004; Madgwick et al. 2011; Matny 2015; West et al. 2012). Therefore, the combination of new breeding technologies and new breeding targets for plant protection might be a key to cope with the new emerging challenges (Fears et al. 2014; Lusser et al. 2012; Schaart et al. 2016; Tester and Langridge 2010).

1.1 Genome editing

Plant breeding is an old technique used by humans to influence agronomical traits of crops used in agriculture (Berry 2019; Bradshaw 2016; Mudge et al.). Gregor Mendel who conducted crossing experiments is often credited as the father of genetics and laid the foundation for the green revolution and modern breeding. The last major change in breeding was during the 80's of the last century introducing genomics assisted breeding (Collard Bertrand and Mackill David 2008; Desta and Ortiz 2014; Varshney et al. 2005). This nowadays often referred to as classical breeding got in recent years a lot additional tools helping to identify new traits via transcriptomics (Jiao et al. 2009; Lu et al. 2010; Zhao et al. 2012). New sequencing methods and genome assembly (Edwards et al. 2013; Jorin-Novo et al. 2009; Morrell et al. 2012), metabolomics and proteomics (Chawade et al. 2016; Fernie and Schauer 2009; Kushalappa and Gunnaiah 2013) assist breeders nowadays. However, the classical breeding approach comes with several drawbacks regarding the effort, the efficiency and the time needed compared to new breeding technologies (NBT) (Lusser et al. 2012; Schaart et al. 2016; Tester and Langridge 2010). A novel approach for changes in the genome of an organism is genome editing. It enables specific desired changes in the DNA of the target organism. The top three techniques used for genome editing are Zinc-finger nucleases (ZFN), the transcription activator-like nucleases (TALENs) and maybe the most recent technique CRISPR/Cas nucleases (Seyran and Craig 2018).

1.1.2 Zinc-finger nucleases

Zinc-finger nucleases are artificial protein complexes resulting from the idea to generate new endonucleases with the ability to choose the target sequence. The first generated ZFN used the non-sequence-specific cleavage domain of the *FokI* type II endonuclease fused to a homeobox domain from *Drosophila melanogaster* (Kim and Chandrasegaran 1994). Later it was possible to use instead of the homeobox domain zinc-finger sequences or the yeast Gal4 DNA-binding domain (Kim et al. 1996; Kim et al. 1998). The identification of the crystal structure of zinc-fingers enabled the modular assembly to identify and generate specific zinc-fingers for a given sequence (Pavletich and Pabo 1991; Segal et al. 2003). This led to the generation of specific zinc-fingers for most triplets occurring in the DNA (Bae et al. 2003; Choo and Klug 1994; Dreier et al. 2001; Dreier et al. 2005; Jamieson et al. 1994; Rebar and Pabo 1994; Segal et al. 1999). Research on ZFNs discovered favourable designs which lead to the conclusion that a construct with dimers inversely oriented and separated by six nucleotides is the most efficient way (Bibikova et al. 2001; Pabo et al. 2001). ZFNs have been widely used to induce DSBs to alter the DNA sequence of different model organisms like the common fruit fly, rats, plants and humans (Lloyd et al. 2005; Mashimo et al. 2010; Porteus and Baltimore 2003; Zhang et al. 2010a).

1.1.3 TALEN

A similar approach to genome editing with Zinc-finger nucleases are transcription activator-like nucleases. TALEN originated from effectors of phytopathogenic bacteria of the *Xanthomonas* genus (Kay et al. 2009; Römer et al. 2010). The discovered transcription activator-like effectors were found to bind to host DNA sequences (Boch et al. 2009; Moscou and Bogdanove 2009). TAL effectors tend to contain 5 to 30 tandem monomer repeats each consisting of 33 to 35 residues with each tandem repeat determines the specificity of the target sequence binding (Boch and Bonas 2010; Deng et al. 2012; Mak et al. 2012). A pair of these residues, often referred to repeat variable diresidues (RVD), is responsible for binding to the target sequence, whereas NI (Asn Ile) binds to adenine, HD (His Asp) to cysteine, NN (Asn Asn), NH (Asn His) and NK (Asn Lys) to guanine and NG (Asn Gly) to thymine (Boch et al. 2009; Moscou and Bogdanove 2009). From the three candidates binding to guanine, the highest affinity was shown for NH (Cong et al. 2012; Streubel et al. 2012). Due to the pioneer work with ZFNs, TALEN can be used with numerous proteins for targeted genetic modifications. Some possibilities are site-directed modifications with nucleases like *FokI* (Christian et al. 2010; Li et al. 2012; Miller et al. 2010) or transcriptional activators (Zhang et al. 2011).

There are several benefits of TALENs compared to ZFNs, which led to the creation of a TALEN library for humans with over 18000 targets (Gaj et al. 2013; Kim et al. 2013; Wei et al. 2013).

1.1.4 CRISPR/Cas9

TALEN and ZFN both rely heavily on large protein structures needed for specific binding to the target DNA. This requires large constructs with limitations for cloning and target design (Gaj et al. 2013; Urnov et al. 2010; Wei et al. 2013). However, a new method for genome editing might solve these complications and challenges if the binding to target regions is impossible with large protein structures used by TALEN or ZFN.

First hints for this new method were discovered in the gram-negative bacteria *Escherichia coli*, where clustered regularly interspaced palindromic sequences (CRISPR) were found (Ishino et al. 1987). These sequences were later discovered in numerous other organisms from the two kingdoms of archaea and bacteria (Mojica et al. 2000). Research on these CRISPR sequenced revealed their origin in acquired DNA or plasmid DNA and further research revealed that CRISPR sequences heavily undergo horizontal gene transfer and even closely related species can differ in their CRISPR sequences (Bolotin et al. 2005; Garneau et al. 2010; Godde and Bickerton 2006; Makarova et al. 2006; Mojica et al. 2005; Pourcel et al. 2005). First ideas came up, that CRISPR sequences might be involved in an acquired prokaryotic immune system due to the association with different DNA modifying enzymes (CRISPR-associated genes; cas) (Bondy-Denomy et al. 2013; Garneau et al. 2010; Haft et al. 2005; Horvath and Barrangou 2010; Jansen et al. 2002; Makarova et al. 2006; Terns and Terns 2011). Evidence for CRISPR-Cas mediated immunity was provided by experiments in *Streptococcus thermophilus* (Makarova et al. 2006). The combination of CRISPR sequences with cas enzymes were quickly propagated for biotechnology purposes like phage resistance or eliminating of unwanted traits of bacteria (Barrangou and Horvath 2012).

Cas9 was identified as a large multifunctional protein, consisting two nuclease subunit domains (Makarova et al. 2002; Makarova et al. 2006). In its native form, this enzyme would lead to double-stranded DNA cleavage, but deleting either the HNH or the RuvC domain single-stranded DNA cleavage occurs (nickases) (Gasiunas et al. 2012; Jinek et al. 2012). In the c-terminal domain of the cas9 protein, a short protospacer adjacent motif (PAM) is identified which is needed for interrogation of the DNA to the matching PAM sequence (Jiang and Doudna 2017; Jinek et al. 2014a). In its inactive state this region is largely disordered to prevent cleavage at the PAM site (Barrangou and Doudna 2016; Sternberg et al. 2014). Cas9 needs a combination of transactivating RNA (tracrRNA) for the activation of the protein complex and

a crispr RNA (crRNA) for the binding to the complementary DNA sequence (Deltcheva et al. 2011; Jinek et al. 2012). Only the combination of tracrRNA and crRNA (Fig. 1 A) leads to the activation of cas9 (Brouns et al. 2008; Jinek et al. 2012; Perez-Rodriguez et al. 2011). Modifications of this tracrRNA:crRNA duplex led to the construction of single-guide RNA (sgRNA) (Fig. 1 B) which fused the crRNA directly to the tracrRNA with a linker loop resulting in a working CRISPR/Cas9 construct and enabling the design for genome editing constructs (Anders et al. 2014; Jinek et al. 2012; Jinek et al. 2014b). Currently, a lot of effort is invested in engineering better cas enzymes to increase specificity or modifying the enzyme to unlock new targeting sites with changes to the PAM sequence (Fu et al. 2014; Slaymaker et al. 2016; Tsai and Joung 2016).

CRISPR/Cas9 is used in many different ways of understanding diseases in humans, functions of proteins, or as a new therapy (Ghorbal et al. 2014; Hwang et al. 2013; Matano et al. 2015; Paquet et al. 2016). The possibilities with CRISPR/Cas9 are enormous and are highly discussed in science (Doudna and Charpentier 2014; Xue et al. 2016; Zhang et al. 2014). CRISPR/Cas9 was already used to identify new interesting traits for plants. Multiplex mutations in three different rice genes resulted in a rapid increase in grain weight (Xu et al. 2016). In tomato the fruit ripening, shelf life and γ -aminobutyric acid levels could be modified (Ito et al. 2015; Li et al. 2018; Yu et al. 2017). In wheat, the resistance to powdery mildew could be increased and a low-gluten wheat was engineered (Sánchez-León et al. 2018; Wang et al. 2014; Zhang et al. 2017).

1.1.5 Homology direct repair and non-homologous end joining

The modification of the genome via genome editing with all three methods results in double- or single-strand breaks (DSB, SSB) of the targeted DNA. Damage to the DNA is quite common and two different repair mechanisms have been evolved as a solution (Weterings and Chen 2008). Non-homologous end joining (NHEJ) is the most common repair mechanism in eukaryotes used to repair DSBs and in the most cases is sufficient to repair the damaged DNA (Budman and Chu 2005; Lieber et al. 2003; Moore and Haber 1996; Weterings and Chen 2008; Wilson and Lieber 1999).

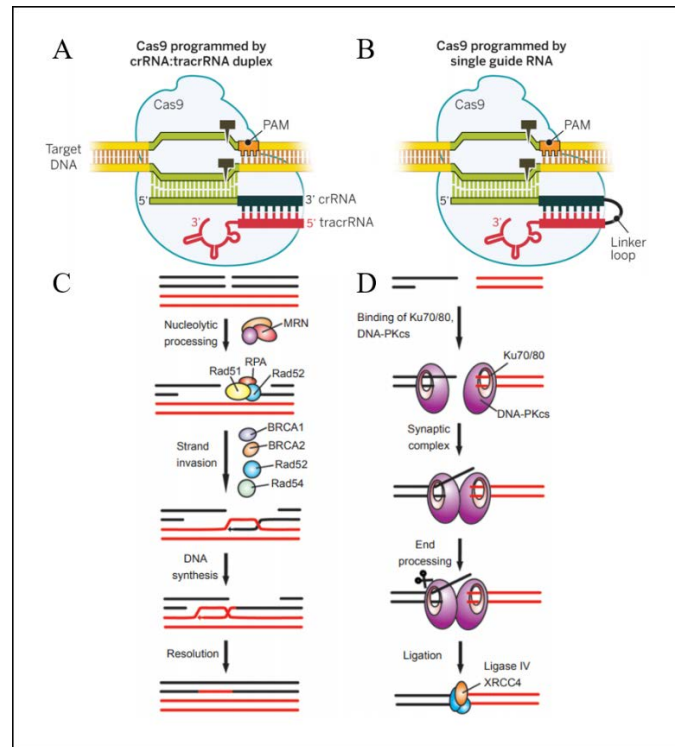


Figure 1: Overview of the active form of cas9 endonuclease and the repair mechanisms for DNA in cells

A) The active form of cas9 with the in bacteria found duplex of crRNA:tracrRNA. The crRNA binds homologous to the specific sequence on the genome. The tracrRNA activates the cas9 complex and enables the PAM interrogation. The DSB is induced at the PAM site (Doudna and Charpentier 2014). **B)** The active form of cas9 with sgRNA. The introduction of a linker loop enabled the use of an artificial designed crRNA without the maturation step in bacteria (Doudna and Charpentier 2014). **C)** HDR of a DSB damaged DNA sequence. HDR utilizes ectopic or adjacent homologous sequences to repair the DSB. The DNA ends are processed by a protein complex. After the preparations a joint molecule is formed by a damaged and an undamaged strand. Template guided DNA synthesis repairs the stands (Weterings and Chen 2008). **D)** NHEJ of a DSB begins with the binding and formation of a synaptic complex which brings both ends together. Non compatible DNA ends are processed to form ligatable ends, which are then ligated to repair the DSB (Weterings and Chen 2008).

When a DSB is repaired via NHEJ, the loose ends of the DNA are ligated (Puchta 2004; Wilson and Lieber 1999). In the majority of cases, homologous ends of up to five bp are religated to successfully repair the damaged DNA strand (Fig. 1 D). However, sometimes this can result in major changes in the sequence resulting in insertions, deletions, duplications or translocations (Britt 1999; Gorbunova and Levy 1999; Vonnarx et al. 1998).

Homology direct repair (HDR) was first described in yeasts (Petes et al. 1991). Research in other organisms also identified the HDR repair mechanism, however the frequency is rather low compared to yeasts (Britt 1999; Liang et al. 1998). Research in *Arabidopsis thaliana* has indicated that HDR frequencies were higher during meiosis than in somatic cells (Caryl et al. 2003; Jones et al. 2003; Keeney 2001). HDR functions different to NHEJ (Fig. 1 C).

During HDR the DSB is repaired with the help of homologous regions of the damaged DNA sequence either ectopic from other regions of the genome or with homologous regions in the close proximity of the damaged sequence (Britt 1999; Puchta 2004; Vonarx et al. 1998). This mechanism is highly interesting for researchers because it enables the possibility to introduce specific changes in the sequence of the genome (Chu et al. 2015; Cong et al. 2012; Lee et al. 2015; Lin et al. 2014; Ran et al. 2013; Wu et al. 2013).

1.2 *Brachypodium distachyon* a model plant for monocotyledons

The annual grass *Brachypodium distachyon* (L) P. Beauv was for a long time thought to be the only annual member of the genus *Brachypodium* with three different cytotypes (Robertson 1981; Schippmann 1991; Scholthof et al. 2018). Newer research identified that these three different cytotypes are independent species and a group of three annual member of the *Brachypodium* genus, *Brachypodium distachyon*, *B. hybridum* and *B. stacei* were defined (Catalan et al. 2012). Evolutionary the oldest member of the species is *B. stacei* splitting from the most common ancestor around 10 million years, followed by the divergence of *B. distachyon* 7 million years later and the most recent divergence of *B. hybridum* around 3 million years ago (Catalan et al. 2012; Sancho et al. 2018). *B. distachyon* prefers colder temperatures between sea level and 2000 m altitude and grows on xeric to mesic pastures or open woodlands in central Europe, North and South America, South Africa or Australia (Garvin 2007; Mur et al. 2011; Schippmann 1991; Vogel and Bragg 2009). In controlled environments, *B. distachyon* reaches heights between 15 and 30 cm. It has a high germination rate, a short life-cycle of approximately 8 weeks (Fig. 2 B) from seeds to seeds and its self-fertility enables the generation of pure inbred lines (Garvin 2007; Mur et al. 2011; Vogel and Bragg 2009; Vogel et al. 2009).

On a genetic level *B. distachyon* has additional features facilitating its role as a model plant for important crops. The genome of the *B. distachyon* inbred line Bd21 is completely sequenced and one of the smallest genomes for monocots and grasses with only 272 Mbp on 5 chromosomes (Initiative 2010; Ozdemir et al. 2008; Wolny and Hasterok 2009). Analyses of the DNA sequence of the *B. distachyon* genome furthermore indicates only few repetitive or methylated sequences (Draper et al. 2001). Phylogenetically, *B. distachyon* is closely related to wheat and barley, two of the most important crops of the *Triticeae* tribe (Brkljacic et al. 2011; Catalan et al. 1997; Catalan et al. 2016; Group et al. 2001; Vogel et al. 2006b). This makes *B. distachyon* a perfect candidate for a monocot model plant. However, an efficient transformation of *B. distachyon* is required to utilise all its features for research.

Two different transformation methods have been established for *B. distachyon*. The biolistic transformation with particle bombardment was established and yielded relative high transformation rates of roughly 5 % (Christiansen et al. 2005; Draper et al. 2001). Additionally, the transformation with *Agrobacterium tumefaciens* was also established in *B. distachyon* for callus tissue isolated from mature or immature embryos resulting in transformation efficiencies of 40 % to 80 % (Alves et al. 2009; Bablak et al. 1995; Bragg et al. 2015; Păcurar et al. 2008; Sogutmaz Ozdemir and Budak 2018; Vain et al. 2008; Vogel and Hill 2008; Vogel et al. 2006a; Vunsh 2018). With the aid of these transformation protocols, a large T-DNA insertion library was established containing more than 20.000 different lines (Bragg et al. 2012; Hsia et al. 2017; Thole et al. 2010). In addition to the T-DNA mutant library, a collection of different retrotransposon lines and chemical mutagenesis lines is accessible (Dalmais et al. 2013; Gill et al. 2018).

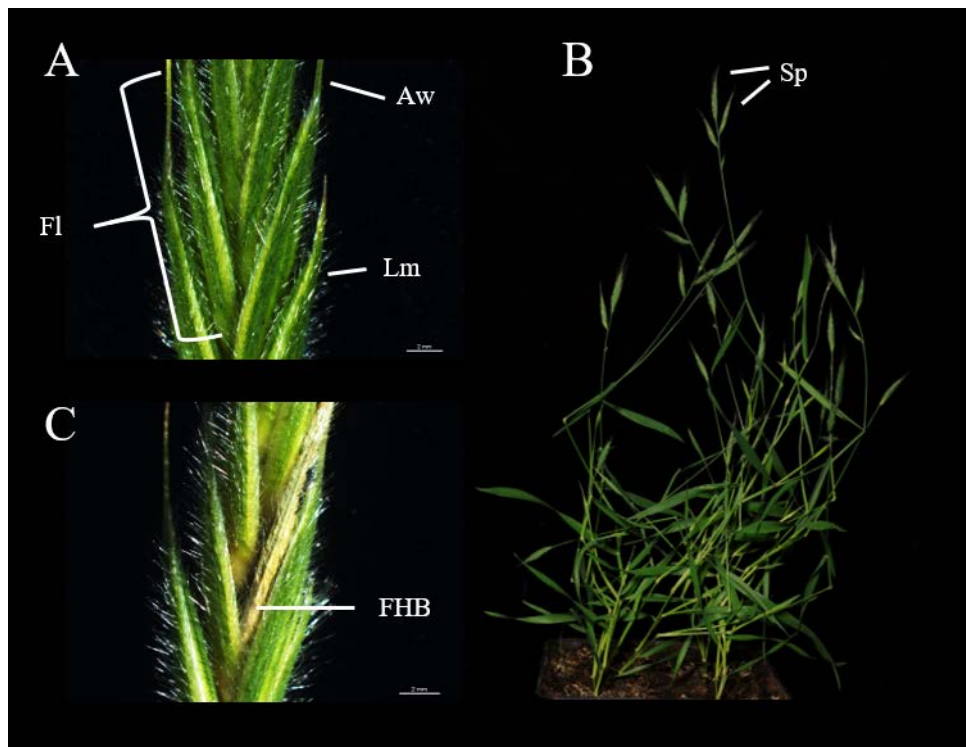


Figure 2: The grass model plant *Brachypodium distachyon*

A) Mature spikelet of *B. distachyon*. It contains several individual florets for reproduction. One *B. distachyon* plant can produce several independent spikelets. Fl = one independent floret in a spikelet. Aw = awns at the top of the lemma. Lm = Lemma of a *B. distachyon* spikelet. The palea on the internal site is not visible. **B)** Overview of the growth phenotype of the *B. distachyon* inbred line Bd21. At this 8-week-old stage, several spikelets for reproductions are formed (Sp). Typical for *B. distachyon* is a terminal spikelet followed by two lateral spikelets. **C)** Infected spikelet of *B. distachyon* inoculated with *F. graminearum*. The necroses typical for the Fusarium Head Blight (FHB) disease are present (FHB).

B. distachyon has been established as a suitable model organism to study different pathogen-host interactions (Fitzgerald et al. 2015). Research with the rice blast causing pathogen *Magnaporthe grisea* revealed that *B. distachyon* evolved resistant and susceptible ecotypes (Parker et al. 2008; ROUTLEDGE et al. 2004; William Allwood et al. 2006). Other host-pathogen interactions between *B. distachyon* and *Puccinia garminis*, *Mycosphaerella graminicola* or *Parastagonospora nodorum* were studied (Ayliffe et al. 2013; Falter and Voigt 2014; Figueroa et al. 2013; Gill et al. 2015; O'Driscoll et al. 2015; Sandoya and Buanafina 2014). The natural resistance to powdery mildews of *B. distachyon* was linked to several new *MILDEW RESISTANCE LOCUS (MLO)* genes (Ablazov and Tombuloglu 2016; Fitzgerald et al. 2015). *B. distachyon* was also found to be a suitable tool to study the host-pathogen interactions to the Fusarium Head Blight causing pathogen *Fusarium graminearum* (Peraldi et al. 2011). Several important interactions between *F. graminearum* and *B. distachyon* were revealed in different studies, and transgenic experiments were able to translated resistances into wheat (Blümke et al. 2015; Gatti 2017; Gatti et al. 2019; Schmeitzl et al. 2015).

1.3 Plant diseases

The impact of pests and diseases on plants is a severe challenge for agriculture. Yield losses due to pests are an important factor in agriculture ranging from 4 % to 40 % depending on several variables (Fried et al. 2017; Oerke 2006; Savary et al. 2019). Several different kinds of pests can affect the plants, ranging from herbivore insects, oomycetes, bacteria to fungi (Bebber and Gurr 2015; Fillinger and Elad 2016; Martins et al. 2018; Myers and Sarfraz 2017; Savary et al. 2019). The oomycete *Phytophthora infestans* for example was responsible for the potato blight in the 19th century causing a severe food shortage in Europe (Goss et al. 2014; Haas et al. 2009; Raffaele et al. 2010). Powdery mildews, a group of biotrophic fungi, are causing a strong reduction in photosynthesis in wheat and barley leading to a significant yield and quality loss (CARVER and GRIFFITHS 1981; Conner et al. 2003; Griffey et al. 1993; Johnson et al. 1979; Rabbinge et al. 1985). Major problems not only on a global scale but dominantly in Europe is caused by the four wheat pathogens *Zymoseptoria tritici*, *Puccinia graminis* f. sp. *tritici*, *Phaeosphaeria nodorum* and *Fusarium graminearum* (Figueroa et al. 2018; Fones and Gurr 2015; Singh et al. 2008; Singh et al. 2016; Torriani et al. 2015).

1.3.1 The fungal leaf pathogen *Parastagonospora nodorum*

The causing pathogen of the Stagonospora nodorum blotch or Septoria nodorum blotch (SNB) is the ascomycete *Parastagonospora nodorum* (Berk.) Quaedvlieg, Verkley & Crous (Teleomorph: *Phaeosphaeria nodorum* [Müll.] Hedjar) (Quaedvlieg et al. 2013; Solomon et al. 2006). *Parastagonospora nodorum* is mostly associated as a wheat or barley pathogen, but wild grasses like *B. distachyon* can also be infected (Cunfer and Ueng 1999; Falter and Voigt 2014; Krupinsky 1989; Osbourn et al. 1986; Williams and Jones 1973). *P. nodorum* is capable of destroying up to 31% of the yield resulting in potential losses of up to \$230 million per year in Australia (Bhathal et al. 2003; Murray and Brennan 2009). The life cycle of *P. nodorum* involves an asexual and a sexual phase. During non-growing season, pycnidia survive on residual biomass forming pseudothecia and undergo a sexual reproduction (Arseniuk et al. 1998; Bathgate and Loughman 2001; Shah et al. 1995; Shah et al. 2001). Ascospores formed during this stage are then transferred through wind or other vectors onto leaf surfaces (Bathgate and Loughman 2001; Shah et al. 2001). The transferred conidia germinate and infect the leaf tissue of host plants. After an intracellular growth phase, pycnidia are produced which then dispose pycnidiospores to adjacent tissue resulting in a polycyclic infection cycle (Arseniuk et al. 1998; Oliver et al. 2011; Shah et al. 2001). The infection cycle of *P. nodorum* starts with the direct penetration of the cuticula with an penetration peg or in rare occasions via growth through stomata (Bird and Ride 1981; Karjalainen and Lounatmaa 1986). To penetrate the cuticula *P. nodorum* releases a wide range arsenal of different cell wall degrading enzymes, proteases and metabolites (Carlile et al. 2000; Chooi et al. 2014; Lehtinen 1993; Solomon et al. 2004). In response to this attack, the plant forms a papilla to prevent the intruder in entering the cell. This response is often coupled with a lignification of these papillae and in most cases sufficient to prevent *P. nodorum* infection (Bird and Ride 1981; Ride and Pearce 1979; Zinkernagel et al. 1988). However, *P. nodorum* developed a wide arsenal of effectors and toxins to overcome the plant defence due to suppression of host defence responses (Figueroa et al. 2018; Oliver et al. 2011). *SnTox1* was identified as a gene with a function to protect *P. nodorum* from host chitinases and interaction to *Snn1* results in the formation of necrosis (Liu et al. 2016). The two effectors *SnToxA* and *SnTox3* both target genes of the *PR1* class in wheat (Breen et al. 2016; Lu et al. 2014). Recently new effector candidates were discovered in a screening of Australian wheat cultivars (Tan et al. 2014). One new effector described in *P. nodorum* is *SnTox6*. *SnTox6* interacts with a wheat gene described as *Snn6* (Gao et al. 2015). It was revealed that *SnTox6* activity is dependent on light and the presence of *Snn6* resulting in the formation of necrosis (Gao et al. 2015).

1.3.2 The necrotrophic fungus *Fusarium graminearum* as causal agent of Fusarium Head Blight

Fusarium graminearum Schwabe (Teleomorph: *Gibberella zeae* [Schweinitz] Petch) is a filamentous ascomycete and the main cause of the Fusarium Head Blight disease (FHB), a disease described since the early 20th century (MacInnes and Fogelman 1923; Stack 2000). FHB is still a severe disease in North and South America, China, Australia and Europe (GOSWAMI and KISTLER 2004; Madgwick et al. 2011; McMullen and Stack 2008; Palazzini et al. 2015) resulting in high economical costs of up to \$1.47 billion for wheat and barley in the USA (Matny 2015; Wilson et al. 2018; Windels 2000). The main hosts of *F. graminearum* are small grains grasses like wheat, barley and oats but maize and *Brachypodium distachyon* can also be infected (Fig. 2 C) (McMullen and Stack 2008; Peraldi et al. 2011). The life cycle of *F. graminearum* is separated into a sexual and asexual phase depending on the environment (Markell and Franc 2003; Parry et al. 1995; Sutton 1982; Trail et al. 2002). During winter *F. graminearum* survives as spores or saprophytic mycelia on crop residues (Parry et al. 1995). During spring, when warmer temperatures are present, and the moisture is favourable for *F. graminearum* the spores are transported by wind, insects or rain to host plants (Parry et al. 1995; Sutton 1982). On the infected host plants, *F. graminearum* is then producing either asexual conidiospores or perithecia producing sexual ascospores which get forcibly discharged (Markell and Franc 2003; Trail et al. 2002).

The infection cycle of *F. graminearum* begins with the germination of the conidia roughly 6 to 12 hours after attaching to the host (Brown et al. 2010; Xu and Nicholson 2009). During anthesis and the exposed anthers the spores are able to get directly into the florets (Parry et al. 1995). There, *F. graminearum* begins to colonise the palea and lemma with runner hyphae (Boenisch and Schäfer 2011). Infection of the host cells is performed with three different infection structures. From the runner hyphae, small infection hyphae called foot structures are formed for direct infection of the adjacent host cell (Boenisch and Schäfer 2011). These infection structures are considered in the primary infection stage. In the secondary infection stage, the two other infection structures are formed (Boenisch and Schäfer 2011; Bormann et al. 2014). The more complex structure of lobate appressoria are formed by aggregation of several hyphae at the infection site. If several lobate appressoria aggregate at one site infection cushions are formed (Boenisch and Schäfer 2011). The secondary infection stage is also referred to as the main infection stage (Bormann et al. 2014).

The colonisation of the host tissue begins after primary infection of the host cells and results in the invasion of the caryopsis and the rachis node (Brown et al. 2010; Jansen et al. 2005). At 5 days post inoculation in wheat, *F. graminearum* penetrates the rachis node reaching the rachis and continues to colonise the host and apically florets (Brown et al. 2010; Jansen et al. 2005). This leads to the typical FHB symptom and the bleaching of the spike upwards of the primary infected floret (Miller et al. 2004).

For colonisation of the host, *F. graminearum* is producing a group of toxins known as trichothecenes (Döll and Dänicke 2011). The most prominent member of the trichothecenes is deoxynivalenol (DON), which is produced by *F. graminearum* during colonisation but is not required for the primary infection (Jansen et al. 2005). The current opinion is that DON is needed to suppress plant defence and prepares the plant tissue for the colonisation of the pathogen (Jansen et al. 2005; Proctor et al. 1995; Proctor et al. 1997). Research with a DON deficient *F. graminearum* strain showed an impaired ability to colonise the host and the pathogen is contained in the inoculated spikelet not able to penetrate the rachis node (Hohn et al. 1998; Jansen et al. 2005; Proctor et al. 1995; Proctor et al. 1997). DON is considered as a major virulence factor for *F. graminearum*. Following research identified the secreted lipase FGL1 (FUSARIUM GRAMINEARUM LIPASE 1) as second, major virulence factor (Bai et al. 2002; Voigt et al. 2005). The lipase-deficient strain $\Delta fgl1$ was only able to infect the inoculated spikelet but not able to further colonise the host wheat spike (Voigt et al. 2005). It was shown in wheat, that *F. graminearum* uses FGL1 to release free fatty acids which suppresses plants-defence-related callose deposition (Blümke et al. 2014). To compensate for the loss of the lipase activity, *F. graminearum* increases the mycotoxin production, which is not sufficient for compensation, supporting the importance of the lipase FGL1 as a virulence factor (Blümke et al. 2014; Voigt et al. 2007).

1.4 Plant Defence

Plants are frequently exposed to pathogens trying to infect them, to sustain the constant pressure plants developed an immune system (Jones and Dangl 2006). The current model for the plant immune system consists of two interconnected receptor pathways, one pathway responsible for the intracellular response and a second pathway for the extracellular space (Dangl et al. 2013; Jones and Dangl 2006). The extracellular pathway is activated with receptors on the extracellular side of the membrane and cell wall known as pattern-recognition receptors (PRR) (Dangl et al. 2013; Jones and Dangl 2006). PRRs are receptor-like kinases (RLK) or receptor-like proteins (RLP) interacting with specific conserved pathogen-associated molecular patterns (PAMPs) like flagellin or chitin (Felix et al. 1999; Gómez-Gómez et al. 2001; Gómez-Gómez and Boller 2000; Gómez-Gómez et al. 1999; Monaghan and Zipfel 2012). The PRR FLS2 recognizes the flagellin peptide flg22 (Gómez-Gómez et al. 2001; Gómez-Gómez and Boller 2000; Gómez-Gómez et al. 1999). After binding to the FLS2 receptor, FLS2 forms a complex with BAK1 a receptor-like kinase (Chinchilla et al. 2007; Heese et al. 2007; Sun et al. 2013). The current model for this interaction is described by Boller and Felix (2009), after the binding of FLS2 and BAK1 both intracellular kinase domains are in close proximity of each other which could lead to transphosphorylation and the activation of a defence pathway.

Another already discovered PAMP and PRR interaction is the chitin receptor CERK1 (*CHITIN ELICITOR RECEPTOR KINASE 1*) from *Arabidopsis thaliana* or the rice equivalent CEBiP (*CHITIN ELICITOR BINDING PROTEIN*) which both present a lysine motif (LysM) for chitin binding (Kaku et al. 2006; Kouzai et al. 2014; Miya et al. 2007). In rice CEBiP forms a complex with the LysM-RLK OsCERK1 resulting in the phosphorylation of OsRLCK185 and activation of a MAPK pathway (Hayafune et al. 2014; Shimizu et al. 2010; Yamaguchi et al. 2013). A similar pathway is observed in *Arabidopsis thaliana*, where CERK1 forms a complex with the LysM-containing receptor kinases LYK4 and LYK5, resulting in the phosphorylation of a OsRLCK185 orthologue and the activation of a MAPK defence pathway (Cao et al. 2014; Erwig et al. 2017; Liu et al. 2012; Shinya et al. 2014; Wan et al. 2012). This first line of defence reactions is described as pattern-triggered immunity (PTI), and takes place minutes to hours after first recognition of the PAMP (Boller and Felix 2009; Jones and Dangl 2006). To overcome this PTI, adapted pathogens evolved the ability to use countermeasures, so called effectors, to disrupt the plant defence (Jones and Dangl 2006). Effectors are used from bacteria, fungi, oomycetes and other pathogens (Baltrus et al. 2011; Koeck et al. 2011; Raffaele et al. 2010).

They can have different activities ranging from molecular to enzymatic abilities (Grant et al. 2006). One well-studied interaction is *Pseudomonas syringae* and *Arabidopsis thaliana*. The AvrPto and AvrPtoB effectors of *P. syringae* were shown to suppress the FLS2-BAK1 complex. AvrPto is shown to be a kinase inhibitor, inhibiting the FLS2:BAK1 activity (Shan et al. 2008; Xing et al. 2007). AvrPtoB serves two functions, the n-terminal domain was shown to be sufficient for flg22 response suppression, while the c-terminal domain has an E3 ligase domain for ubiquitination of kinases (Göhre et al. 2008; Xiang et al. 2008; Zhang et al. 2010b). Additionally, the interference between the FLS2:BAK1 complex and AvrPtoB was shown to interact also with other PRR like CERK1 and LysM-RLK in tomato (Gimenez-Ibanez et al. 2009; Zeng et al. 2012). However, effectors can work not only in suppression of the PRR-PTI pathway but also in other pathways. The *Xanthomonas spp.* effector transcription-activator like (TAL) for example induces expression of specific host genes (Kay and Bonas 2009) and the *Phytophthora infestans* effector Avr3a is suppressing immunity due to an interaction with the E3 ligase CMPG1 (Bos et al. 2010; Bos et al. 2006).

As mentioned in the beginning of this chapter, plants have developed mechanisms to sense and interact with secreted effectors (Jones and Dangl 2006). Intracellular receptors have been identified which are specialized on sensing pathogen effectors (Chisholm et al. 2006; Jones and Dangl 2006). These receptors consist of a nucleotide-binding domain (NB) and a leucine rich repeat domain (LRR) and are divided into two classes, a Toll/interleukin 1-like receptor (TIR) class and a coiled-coiled domain (CC) class (Bernoux et al. 2011; Dodds and Rathjen 2010; Lukasik and Takken 2009; Maekawa et al. 2011; Takken and Govers 2012). How these NB-LRR or R genes function in the effector-triggered immunity (ETI) is still under investigation, but the current data proposed a model with three possible functions. R genes could function either in a direct interaction with the effector, they could act as a guard or decoy or as a third function as a possible bait (Collier and Moffett 2009; Dangl and Jones 2001; Dodds and Rathjen 2010; Jones and Dangl 2006; van der Hoorn and Kamoun 2008). Two examples for a direct interaction between an effector and a plant R gene are found in the rice – *M. oryza* interaction. The rice CC-NB-LRR Pi-ta is directly interacting with the fungal effector AvrPita and Exo70 is directly interacting with the *M. oryza* effector AvrPii (Fujisaki et al. 2015; Jia et al. 2000). For the guard/decoy model, the most famous interaction is described in *Arabidopsis thaliana*. In *A. thaliana* the RIN4 protein forms complexes with the R genes RPM1 and RPS2 (Axtell and Staskawicz 2003; Mackey et al. 2003).

Phosphorylation of RIN4 by AvrB or AvrRPM1 from *P. syringae* leads to the activation of RPM1 while the degradation of RIN4 through the AvrRpt2-effector causes the activation of RPS2 (Axtell and Staskawicz 2003; Mackey et al. 2003). A decoy R-gene was identified in tomato, where the R gene Prf, which contains a kinase relative to FLS2 or CERK1 which both are targets of AvrPto or AvrPtoB effectors, forms a complex with Pto (Gimenez-Ibanez et al. 2009; Mucyn et al. 2006; Zipfel and Rathjen 2008). Recently it was identified, that NB-LRR R genes can work in pairs, which lead to the idea of the bait or bait and switch model (Collier and Moffett 2009; Eitas and Dangl 2010; Saucet et al. 2015). Evidence for the existence of this model was found with the identification of a NB-LRR pair, where one partner exposes a WRKY DNA binding domain and the other partner promotes the defence response, leading to the bait of pathogen effectors that broadly target the WRKY domain and switching a defence pathway on (Sarris et al. 2015). A recent review of the last 25 years of R gene research came to the conclusion that we might have to change our current model into a more sophisticated one (Kourelis and van der Hoorn 2018).

A recognized pathogen can get repelled on different ways and plants developed a wide arsenal of defence reactions (Chisholm et al. 2006; Dangl et al. 2013; Jones and Dangl 2006). One of the earliest responses is an ion influx of Ca^{2+} in the first 5 minutes (Blume et al. 2000; Boller 1995; Jeworutzki et al. 2010; Lecourieux et al. 2006; Ranf et al. 2011). Research showed that BAK1 is a positive regulator of this defence response after forming a complex with FLS2 (Li et al. 2014). This Ca^{2+} ion influx opens the door for other membrane transporters resulting in a depolarization of the membrane and an alkalisation of the extracellular space (Blume et al. 2000; Boller 1995; Jeworutzki et al. 2010; Li et al. 2014). This leads to a signal transduction regulating sodium dependent proteins, secretion of reactive oxygen species (ROS) and regulation of transcription factors (Blume et al. 2000; Moore et al. 2011; Ogasawara et al. 2008; Sierla et al. 2013). A direct interaction between Ca^{2+} and ROS production was identified for the regulation of the NADPH oxidase RBOHD (Ogasawara et al. 2008). Recently, a new reactive compound group was connected to plant defence based on reactive nitrogen species (RNS) (Groß et al. 2013). Another early response connected to the Ca^{2+} burst is the forming of cell wall thickenings at the penetration site, referred to as papilla, a viscoelastic barrier that contain several cell wall polymers like callose, cellulose, lignin but also ROS (Aist 1976; Israel et al. 1980; Thordal-Christensen et al. 1997; Zeyen et al. 2002).

Plant hormones play also a crucial role in pathogen defence and can regulate different responses (Alazem and Lin 2015; Bari and Jones 2009; Kammerhofer et al. 2015; Verhage et al. 2010). Salicylic acid for example is associated with the regulation of the pathogenesis related (PR) genes of the classes 1, 2 and 5 (Malamy et al. 1990; Stintzi et al. 1993; Zhang et al. 1999). Two other plant hormones, jasmonic acid and ethylene, were shown to be synergistic in the regulation of PR genes from the classes 3 and 12 (Pieterse and van Loon 1999; Samac et al. 1990; Xu et al. 1994).

PR genes are defined as genes induced in presence of a pathogen but are not necessarily anti-pathogenic (Gianinazzi 1970; Hammond-Kosack and Jones 1996; Van Loon and Van Kammen 1970). The classification of PR genes is based on their properties and until now, 17 classes are described, whereas PR1 genes have antifungal activities, PR2 genes are 1,3- β glucanases and the two classes PR3 and PR4 contain different chitinases (Jain and Khurana 2018; Van Loon and Van Strien 1999). Contradictory to what is known from other plants regarding the regulation of PR1 genes, in monocots a member of the PR1 class was shown to be suppressed after treatment with all three phytohormones (Kouzai et al. 2016). In addition, a member of the PR2 class was shown to be induced by jasmonic acid (Agrawal et al. 2000; Desmond et al. 2005; Mei et al. 2006). Even though, PR genes are not necessarily anti-pathogenic, overexpression studies with glucanases and chitinases revealed an increased protection against fungal attacks (Jach et al. 1995; Jongedijk et al. 1995; Zhu et al. 1994).

1.5 The cell wall a first line of defence

The first line of defence for plant cells are their characteristic cell walls. Cell walls are barriers in plants consisting of a mixture of different glucose polymers that form a tough network (Keegstra 2010; McCann et al. 2001; O'Neill and York 2003; Somerville et al. 2004; Vorwerk et al. 2004). Plants form two different kinds of cell walls, a primary cell wall and a secondary cell wall. The primary cell wall is the most common cell wall and found in almost all growing and dividing plant cells. The secondary cell wall is formed in plant cells that have reached a steady state and contributes to cell wall thickening (Keegstra 2010; McCann et al. 2001; O'Neill and York 2003; Somerville et al. 2004). Secondary cell walls differ from primary cell walls. An increased incorporation of cellulose fibrils and hemicelluloses result in a stiffened and more compact cell wall (Keegstra 2010; McCann et al. 2001; Ochoa-Villarreal et al. 2012). Since the primary cell wall is more abundant in plants, the following description refers to the composition and synthesis of this cell wall type.

The major three components of the primary cell wall are cellulose, hemicelluloses and pectin (Keegstra 2010; McCann et al. 2001; O'Neill and York 2003; Ochoa-Villarreal et al. 2012). Cellulose is a polysaccharide formed by several microfibrils each consisting of 1,4- β -linked glucan molecules synthesized by cellulose synthases (CesA) (Diotallevi and Mulder 2007; Keegstra 2010; McFarlane et al. 2014; Schneider et al. 2016). To synthesise these cellulose microfibrils, a cellulose synthase complex (CSC) is formed consisting of three different CesAs in an equimolar ratio (Gonneau et al. 2014; Hill et al. 2014). The structure of these microfibrils is still debated. Until recently, it was proposed that a hexagonal arrangement of 36 chains is present (Ding et al. 2014; McFarlane et al. 2014). However, later research found evidence for a model favouring 18 – 24 chains (Cosgrove 2014; Ding et al. 2014; Fernandes et al. 2011; Newman et al. 2013; Schneider et al. 2016). The cellulose microfibrils have distinct regions of hydrophobic and hydrophilic surfaces, which are important for the binding of hemicelluloses like xylan or xyloglucan (Busse-Wicher et al. 2014; Zhao et al. 2014).

Hemicelluloses are polysaccharides which are not only composed of glucose molecules but also incorporate mannose and xylose, and therefore differ from cellulose and pectin (Scheller and Ulvskov 2010). Hemicelluloses are part of the plant cell wall and can differ in plants leading to the classification of two types of hemicellulose compositions in plant cell walls (Carpita and Gibeaut 1993). The first type of hemicelluloses are the most abundant form found in the majority of plants and to a large extent in monocotyledons (Carpita and Gibeaut 1993). The major compound responsible for the connection of cellulose fibrils in this type are xyloglucans (Carpita and Gibeaut 1993; Vogel 2008). The second type is present dominantly in grasses. Type II hemicellulose fractions incorporate glucuronoarabinoxylan with unregularly branches of different sugars. Mixed linkage glucans are also incorporated in this kind of hemicelluloses (Carpita and Gibeaut 1993; Scheller and Ulvskov 2010; Vogel 2008).

The last major compound of plant cell walls is pectin. Pectin is a 1,4- α -linked galacturonic acid molecules forming a gel like matrix around celluloses and hemicelluloses in plant cell walls (Carpita and Gibeaut 1993; McCann et al. 2001; O'Neill et al. 1990; Ridley et al. 2001). Interestingly, pectin plays a crucial role in plant–pathogen interaction. Fungal pathogens are secreting pectinases, enzymes degrading the pectin of plant cell walls, to increase the accessibility of the cell wall to other cell wall degrading enzymes (D'Ovidio et al. 2004; Have et al. 1998; Lionetti 2015; Riou et al. 1991; Salmond 1994).

1.6 Callose, a cell wall polymer and its role in plant defence

Callose is a 1,3- β -glucan consisting of 1,3- β -linked glucose molecules with 1,6- β -branches and was identified in plants in the late 19th century but is also common in cell walls of yeasts, filamentous fungi and bacteria (Aist 1976; Aspinall 1957 ; Currier 1957; Kauss 1996; Stone 1992). Callose is produced as helical chains resulting in a gel like structure used to plug and seal damaged cell walls (Verma and Hong 2001). It is produced by a class of enzymes localized in the plasma membrane and is incorporated into the cell wall (Aist 1976; Verma and Hong 2001). New visualisation techniques hint to a direct interaction of callose and cellulose microfibrils suggesting a permeability of callose (Anderson et al. 2010; Eggert et al. 2014). However, in contrast to the other cell wall polymers already introduced, callose is found only in relative low amounts in the cell wall of land plants (Falter et al. 2015).

1.6.1 Callose and its role in plants

Callose is involved in many important plant developmental pathways or in stress responses. In *A. thaliana* it was shown that AtGSL1 and AtGSL5 are partially redundant for pollen development and fertility (Dong et al. 2005; Enns et al. 2005; Østergaard et al. 2002). In deficient mutants the pollen grains were inviable and collapsed or abnormally large with unusual structures because of a missing callose wall for tetrad separation (Enns et al. 2005). The role of AtGSL5 in particular was found to be in the meiocytes, tetrads, microspores and mature pollen indicating its role in these tissues (Dong et al. 2005; Shi et al. 2016; Shi et al. 2014). Callose is also found in pollen tubes, but not at the pollen tube tip, and important for formation of the second cell wall in pollen tubes (Kroh and Knuiman 1982; Lennon and Lord 2000; Steer and Steer 1989). Another role of callose in plant development is the formation of a callose wall around fertilized zygotes shown in *Rhododendron spp.* (Williams et al. 1984). But also in the development of somatic tissue, callose is involved in crucial steps of phloem transport, phloem development, inflorescence growth, root hair development, cytokinesis and cell patterning (Barratt et al. 2011; Chen et al. 2009; Somssich et al. 2016; Xie et al. 2011). One interesting role of callose is the regulation of plasmodesmata. The synthesis of callose at the plasmodesmata stops cell-to-cell transfer, while the degradation of callose enables cell-to-cell transfer (Botha et al. 2000; Radford et al. 1998; Vatén et al. 2011). Callose mediated plasmodesmata regulation is important for several developmental steps such as transport of transcription factors, establishing the auxin gradient and signalling or regulation of cotton fibre elongation (Han et al. 2014; Ruan et al. 2004; Vatén et al. 2011).

It plays also a crucial role in the containment of plant viruses to prevent spreading in adjacent cells (Fridborg et al. 2003; Iglesias and Meins Jr 2000; Zavaliev et al. 2011). This callose reaction can also be considered as a stress induced reaction, which indicates the second important role of callose in plants, the response to biotic and abiotic stress. A connection between abiotic stress and callose response was described in mechanically stressed plants (Jaffe and Telewski 1984). In *A. thaliana*, connections between the callose response to abiotic stresses and the *calmodulin* expression after rain, wind and mechanical stress were found leading to the identification of a CalS responsible for callose formation after wounding (Braam and Davis 1990; Jacobs et al. 2003). Callose formation was also observed in *Gossypium hirsutum* after heat stress, in *Prunus cerasus* after bruising and after wounding experiments in *Allium cepa* and stems of *Loquidambar styraciflua* (Currier and Strugger 1956; Dekazos and Worley 1967; McNairn 1972; Moore 1978). This wound-sealing callose formation is also described in *A. thaliana* and *B. distachyon* (Blümke 2013; Jacobs et al. 2003). The formation of callose to aluminium exposure in soil was described for different plant species like *Glycine max*, *Picea abies*, *Zea mays*, *Phaseolus vulgaris* and wheat (Horst et al. 1997; Jorns et al. 1991; Rincón and Gonzales 1992; Wissemeier et al. 1987; Yang et al. 2012). Callose formation prevents the transport of aluminium through the roots but results in a trade off and the formation of the typical aluminium toxicity phenotype (Sivaguru et al. 2000). It is proposed that callose formation could be used as a breeding marker for aluminium tolerance (Eticha et al. 2005; Wissemeier et al. 1992). Exposure to other abiotic stressor metals like Cu, Zn or Ni results in a comparable callose formation response (Kartusch 2003; Peterson and Rauser 1979; Qin et al. 2007).

Not only abiotic stress is an inducer of callose formation, different biotic stresses can induce callose synthesis and formation. The herbivore pathogen *Nilaparvata lugens* for example is feeding from rice phloem sap which results in a callose response to stop phloem transport (Hao et al. 2008). Newer research revealed a possible mechanism by the pathogen which is secreting 1,3- β -glucanases to prevent the formation of callose in the phloem (Liu et al. 2017). A similar response is also found after infections with aphids in wheat and *A. thaliana* (Botha et al. 2004; Kempema et al. 2007; KUŚNIERCZYK et al. 2008; Will and van Bel 2006). Callose response is also detected after nematode infection in plants (Ali et al. 2013; Hofmann et al. 2010; Hussey et al. 1992; Williamson and Hussey 1996). Bacterial infections from *Pseudomonas syringae* or *Xanthomonas spp.* can cause callose formation as a plant defence reaction; however, both bacterial pathogens evolved efficient ways to suppress plant defence and the formation of callose depositions (Hauck et al. 2003; Li et al. 2005; Yun et al. 2006; Zhang et al. 2010b).

Fungal pathogen infections are also a major stress causing formation of callose depositions and papillae (Aist 1976; Israel et al. 1980; Voigt 2014). A common plant response to powdery mildews is the response with callose depositions (Frye and Innes 1998; Jørgensen 1992; Nishimura et al. 2003; Skou et al. 1984). In *A. thaliana* and barley the importance for callose depositions as plant defence could be shown (Blümke et al. 2013; Chowdhury et al. 2016; Ellinger et al. 2013). A knockout of the stress induced callose synthase *PMR4* from *A. thaliana* resulted in a resistance to powdery mildew caused by an elevated salicylic acid-dependent defence mechanism (Nishimura et al. 2003). However, in barley a knock-down of a *PMR4* orthologue, *HvGSL6*, resulted in increased penetration success and a more severe disease (Chowdhury et al. 2016). Interestingly, in both plants an overexpression of *PMR4* lead to an increased penetration resistance indicating the importance of callose depositions against biotrophic fungi and a possible approach for plant breeding (Blümke et al. 2013; Eggert et al. 2014; Ellinger et al. 2013).

Callose deposition is also a known defence mechanism against necrotrophic fungi. For the two necrotrophic fungi *Alternaria brassicicola* and *Plectosphaerella cucumerina* research revealed that callose depositions are a successful defence when induced by β -amino-butyric acid (Flors et al. 2008; Ton and Mauch-Mani 2004). Also against the necrotrophic fungus *Botrytis cinera* callose plays a major role in plant defence reaction (Garcia-Arenal and Sagasta 1977). However, it seems that successful pathogens somehow suppress the plant defence response and the formation of callose. This has also been discovered for *Fusarium graminearum*. The importance for callose as a repellent could be shown with the lipase deficient $\Delta fgl1$ *F. graminearum* strain which is unable to suppress the callose response of wheat (Voigt et al. 2005). As a response to this successful defence *F. graminearum* is trying to compensate with an increased toxin production (Voigt et al. 2007). Since callose is involved in several abiotic and biotic stress responses for a successful defence or repair it is apparent how important a functional callose reaction is for plants.

1.6.2 Callose synthases and callose synthesis

Callose is produced by enzyme complexes at the membrane of cells (Brownfield et al. 2009; Verma and Hong 2001). In Arabidopsis 12 members of the *GLUCAN SYNTHASE LIKE* (GSL) family were identified and phylogenetic analyses revealed homologues in sorghum, rice and barley (Chowdhury et al. 2016; Verma and Hong 2001; Yamaguchi et al. 2006). Blümke (2013) identified 11 *GSL* genes in the genome of *B. distachyon* based on the sequence of *AtGSL5*.

A phylogenetic analysis with the *A. thaliana* GSL genes, the identified rice *GSLs* and the *B. distachyon* *GSLs* revealed a ancestry between *AtGSL5* and two *B. distachyon* *GSLs* *BdGSL2* and *BdGSL3* (Blümke 2013). The Arabidopsis gene family is separated into two major groups (Verma and Hong 2001). Group I is responsible for plant cell pathways, fertility and cell division consisting of *GSL1*, *GSL2*, *GSL6*, *GSL8*, *GSL10* and Group II provides cell wall reinforcements consisting of *GSL5*, *GSL7* and *GSL12* (Schneider et al. 2016; Verma and Hong 2001). The remaining *GSLs* have not been conclusively studied to provide clear evidence regarding their function. Structural predictions revealed that *GSLs* contain 12-16 transmembrane helices and the *GSL* complexes are around 200 kD large protein complexes (Li et al. 2003; Østergaard et al. 2002). The n-terminal part of *GSL* proteins revealed a high diversity in its aa sequence throughout the whole gene family, indicating a regulatory function (Cui et al. 2001; Verma and Hong 2001). However, the intracellular loop between the transmembrane helices showed a high sequence homology between several *GSL* proteins and FKS1 from *Saccharomyces cerevisiae* (Inoue et al. 1995; Østergaard et al. 2002; Verma and Hong 2001). Later research with PMR4 confirmed the proposed function of the IL revealing a callose synthase activity (Sode 2015). The complete callose synthase (CalS) complex is not yet identified, but several studies indicate some associated proteins essential for a functional CalS complex (Verma and Hong 2001). It was possible to identify annexins in cotton fibre, which are proteins associated with Ca^{2+} binding and callose synthases (Andrawis et al. 1993; Delmer and Potikha 1997; Laohavisit and Davies 2011). Another protein complex associated to CalS and CesA complexes are sucrose synthases (SUSY) (Amor et al. 1995). In vitro assays with this enzyme revealed that sucrose could be used for callose and cellulose synthesis (Amor et al. 1995). In *A. thaliana* it was possible to partially purify *AtGSL6*, which led to the identification of two associated proteins; a UDP-Glycosyltransferase (UGT1) and a Rho-like GTPase (ROP1) (Hong et al. 2001b). The regulatory pathway of ROP1 is connected with Ca^{2+} regulation, as shown for annexins from cotton fibre and the regulation of pollen tube tip growth (Li et al. 1999; Shin and Brown 1999). The binding of UGT1 to ROP1 occurs only in ROP1 GTP-bound state suggesting its functional significance for callose synthesis based on the conserved mechanism already described for FKS1 in *S. cerevisiae* (Hong et al. 2001b; Li et al. 1999; Qadota et al. 1996; Zheng and Yang 2000). Research on *AtGSL5* identified an interaction with the GTPase RabA4c (Ellinger et al. 2014a). After biotic stress, RabA4c is enhancing the early CalS activity and helps in formation of early callose depositions indicating that GTPases are an early activator for CalS in plants (Ellinger et al. 2014a).

However, for the basic synthesis of callose in vitro, no additional proteins are needed as shown for AtGSL5 and its intracellular loop (Sode 2015). A sequence analysis of the exon and intron structure of all *B. distachyon* *GSLs* revealed that *BdGSL2* and *BdGSL3* have no introns, a typical structure found in the stress induced CalS *AtGSL5* (Blümke 2013). Additionally, Blümke (2013) could show that both *BdGSLs* are upregulated after wounding stress. The overexpression of *AtGSL5* in *B. distachyon* resulted in an increased resistance to *F. graminearum* (Blümke 2013). And experiments in wheat and barley lines overexpressing *AtGSL5* showed a similar resistance to *F. graminearum* (unpublished data). Based on these results, *BdGSL2* and *BdGSL3* are two candidates for stress induced CalS in *B. distachyon*. An overexpression of *BdGSL3* in *B. distachyon* further backs the idea of *BdGSL3* as a stress induced CalS since it showed a similar phenotype like the *AtGSL5* overexpression as described by Blümke et al. (2013) (unpublished data).

1.6.3 Regulation of callose synthases

The regulation and activation of callose synthases is linked to different pathways. Research with plant extracts from different plants revealed the important role of Ca^{2+} for the activity of wounding activated callose synthesis (Hayashi et al. 1987; Kauss 1996; Kauss and Jeblick 1986b; Kauss et al. 1983; Kauss et al. 1990; Morrow and Lucas 1986). It was shown that calmodulin, a protein already associated with callose synthesis, plays a crucial role in the activity of CalS complexes (Braam and Davis 1990; Koo et al. 2009; Leba et al. 2012; Tirlapur and Willemse 1992; Xu et al. 2017). Additionally, in *G. hirsutum* it was possible to identify a calmodulin binding site (Cui et al. 2001). The actual pathway of calmodulins for the CalS activity is not yet identified, however the data suggests that calmodulins play an important role for several stress responses (Bender and Snedden 2013; McCormack et al. 2005). One hypothesis is, that calmodulin changes its secondary and tertiary structure after Ca^{2+} binding resulting in the exposure of a protein binding domain (Bender and Snedden 2013). This enables binding to other proteins and changes in their structure resulting in the moderation of protein activity for proteins not directly interacting with Ca^{2+} (Bender and Snedden 2013; Zielinski 1998). However, not all callose synthases are associated to calmodulin and Ca^{2+} mediated activity since the discovery of a Ca^{2+} independent callose synthase in tabaco (Schlupmann et al. 1993). It is highly possible, that the membrane environment plays a crucial role in callose synthesis (Bessueille et al. 2009; Iswanto and Kim 2017; Škalamera and Heath 1995; Srivastava et al. 2013). It was observed, that in detergent-resistant plasma membrane microdomains more than 70 % of the membrane associated callose synthesis is present (Bessueille et al. 2009).

Furthermore, it was possible to show the influence of lipid rafts on the plasmodesmata callose homeostasis (Iswanto and Kim 2017). Earlier research on the activity of callose synthases and the influence of unsaturated fatty acids revealed a strong suppression of CalS activity when exposed to unsaturated fatty acids (Kauss and Jeblick 1986a). A major defence suppression pathway of *F. graminearum* in wheat infection is the secretion of a lipase to increase the concentration of unsaturated free fatty acids which suppresses the formation of callos for plant defence (Blümke et al. 2014; Voigt et al. 2005).

One important regulatory mechanism is the post-translational phosphorylation or de-phosphorylation of callose synthases. Phosphorylation in general is a highly important mechanism in animals, plants and bacteria (Cohen 1988; Huber 2007; Hunter 1995; Iakoucheva et al. 2004; Jers et al. 2008; Nardozzi et al. 2010). Phosphorylation as a regulatory mechanism for callose synthases was first described in yeasts, where the GTPase Rho1 induces changes in the phosphorylation pattern (Huang et al. 2005; Qadota et al. 1996). A similar mechanism is assumed for AtGSL6 based on the identification of UGT1 and the GTPase Rop1 (Hong et al. 2001a). Additionally, topological analysis of AtGSL6 identified several possible phosphorylation sites (Hong et al. 2001a). For AtGSL5 two possible phosphorylation sites were identified in the context of stress responses (Benschop et al. 2007; Nühse et al. 2007). Phosphomimic experiments with these two serine at position 1041 and 1053 of AtGSL5 revealed key regulatory function (Sode 2015). The phosphorylation of the serine at 1053 is essential for the activity of the callose synthase whereas the phosphorylation state of the serine 1041 is regulating the transport of the CalS complex (Sode 2015). A further hint on the importance of post-translational regulation for stress induced callose synthases was provided by studies in *PMR4* overexpression lines (Ellinger et al. 2013). After infection with powdery mildew no significant changes in *PMR4* expression was observed, however it was possible to detect the PMR4:GFP signal in the plasma membrane before infection and at the infection site after infection (Ellinger et al. 2013). This backs up the idea that post-translational phosphorylation or de-phosphorylation is an important regulatory pathway for callose synthesis and transport of stress induced callose synthases.

1.7 Aim

The current challenges for humanity in providing food security and safety for a growing global population is linked to the adaptation of new breeding technologies. The most recent representative of these technologies is CRISPR/Cas9 mediated genome editing. In the first part of this work, the aim was to study the applicability of CRISPR/Cas9 mediated genome editing in *B. distachyon* as a new technology to study host-pathogen interaction and generation of mutants with possible new targets for plant breeding. One possible target for new breeding approaches are stress induced callose synthases. Studies in *A. thaliana* revealed the importance of callose in host-pathogen interactions; therefore, it is highly interesting to identify stress induced callose synthases in *B. distachyon* a model plant for crops like wheat or barley. Previous work in *B. distachyon* identified BdGSL3 as a possible stress- and pathogen-induced callose synthase. Therefore, it was an interesting target to study a loss-of function mutant in *B. distachyon* to give insights into the role of BdGSL3 in plant defence to fungal infections. In this work, a CRISPR/Cas9 mediated disruption in *BdGSL3* was generated to study the applicability of CRISPR/Cas9 in *Brachypodium distachyon*. After the identification of successful manifested mutants, a characterization of these mutants was performed. An overall acquisition of the general phenotype of the generated mutants was done to find possible impacts of the absence of BdGSL3. To study different stress responses of the generated mutants, abiotic wounding was inflicted and analysed. Additionally, biotic stress as the key interest was examined with two important necrotrophic pathogens. The role of BdGSL3 in response to the necrotrophic leaf pathogen *Parastagonospora nodorum* was analysed with microscopy. To study the effect of BdGSL3 on FHB disease, infections with *Fusarium graminearum* were in-depth examined to reveal the role of BdGSL3 in this host-pathogen interaction. Furthermore, a transcriptional analysis of different organs was performed to examine changes in the transcription of other members of the *BdGSL* gene family. With the aid of these experiments, the role of BdGSL3 should be uncovered and described.

2. Material & Methods

2.1 Equipment

The technical equipment needed for the tasks are listed in the following table (Tab. 1).

Table 1: Equipment list used during this work

No.	Name	Specification	Manufacturer
1	Camera	D300s	Nikon Corp. (Shinagawa, Tokyo, Japan)
2	Centrifuge	Refrigerated Centrifuge 5403	Eppendorf AG (Hamburg, Germany)
3	Centrifuge	Labnet MiniCentrifuge	neoLab Migge Laborbedarf-Vertriebs-GmbH (Heidelberg, Germany)
4	Centrifuge	MiniSpin®	Eppendorf AG (Hamburg, Germany)
5	Centrifuge	Zentrifuge 5430	Eppendorf AG (Hamburg, Germany)
6	Centrifuge	Zentrifuge 5810R	Eppendorf AG (Hamburg, Germany)
7	CLSM	Zeiss Axio Imager Z2 coupled to the Zeiss LSM780	Carl Zeiss Microscopy GmbH (Jena, Germany)
8	Electroporator	Electroporator 2510	Eppendorf AG (Hamburg, Germany)
9	Gel documentation	GENE Genius	Synoptics Ltd (Cambridge, UK)
10	Gelelectrophoresis chamber	Mupid-One System	Biozym Scientific GmbH (Hessisch Oldenburg, Germany)
11	Light microscope	Leitz Laborlux 11	Leica Microsystems GmbH (Wetzlar, Germany)
12	Magnetic stirrer	Kamag® RH	IKA® - Werke GmbH & CO. KG (Staufen, Germany)
13	Magnetic stirrer	MSH basic	IMLAB sarl (Lille, France)
14	Micro scale	AW - 224	Sartorius AG (Göttingen, Germany)
15	Mixing block	Mixing Block MB-102	Bioer Technology Cor. Ltd (Cheshire, UK)
16	NanoVue	GE NanoVue Plus	GE Healthcare (Chicago, IL, USA)
17	Orbital shaker	GFL 3015	GFL Gesellschaft für Laborgeräte mbH (Burgwedel, Germany)
18	PCR - Cyclor	TProfessional Thermocycler	Biometra GmbH (Göttingen, Germany)
19	PCR - Cyclor	TGradient96 – Gradient Thermocycler	Biometra GmbH (Göttingen, Germany)
20	pH - Meter	FiveEasy	Mettler-Toledo Inc. (Columbus, USA)
21	Real-Time PCR Cyclor	LightCycler® 480	Roche Diagnostics GmbH (Mannheim, Germany)
22	Scale	KERN 572	Kern & SOHN GmbH (Balingen, Germany)
23	Scale	KB 2400-2N	Kern & SOHN GmbH (Balingen, Germany)
24	Stereo microscope	Leica MZFL III	Leica Microsystems GmbH (Wetzlar, Germany)
25	UV/VIS Spectrometer	Ultrospec 2000	Pharmacia AG (Uppsala, Sweden)
26	Vibratory mill	MM200	RETSCH GmbH (Haan, Deutschland)
27	Vortex mixer	Vortex-Genie® 2	Scientific Industries, Inc. (Bohemia, NY, USA)

2.2 Chemicals and Enzymes

The chemicals and reagents during this work, if not extra listed, were purchased from the following suppliers: Biozym Scientific GmbH (Hessisch Oldendorf, Germany), Carl Roth GmbH&Co.KG (Karlsruhe, Germany), Merck KGaA (Darmstadt, Germany), New England Biolabs GmbH (Ipswich, MA, USA), Sigma-Aldrich Co. LLC (St. Louis, MO, USA) and Thermo Fisher Scientific Inc. (Waltham, MA, USA). Uncommon chemicals used during this work are listed below (Table 2).

Table 2: Overview of the uncommon chemicals used during this work

Chemical/Enzyme	Supplier
Aniline blue	02570-25, Polysciences, Inc., Warrington, PA, USA
DNase I, RNase-free	Thermo Fisher Scientific Inc. Waltham, MA, USA
Orange G	0138.2, Sigma-Aldrich Co. LLC St. Louis, MO, USA
OneTaq 2x MasterMix	New England Biolabs Inc. Ipswich, MA, USA
Q5 High-Fidelity DNA Polymerase	New England Biolabs Inc. Ipswich, MA, USA
RNase A, DNase and Protease free	Thermo Fisher Scientific Inc. Waltham, MA, USA
WGA-CF TM -488A (Wheat Germ Agglutinin)	Biotium, CA, USA

2.3 Kits

During this work, the following Kits were used for tasks as indicated in table 3.

Table 3: Overview of important kits for the declared applications during this work

Kit	Application	Supplier
GenepHlow TM Gel/PCR Kit	Gel/PCR product DNA clean up	Geneaid Biotech Ltd. (New Taipei City, Taiwan)
innuPep Plant RNA Kit	Isolation of RNA	Analytik Jena AG (Jena, Germany)
LightCycler® 480 SYBR Green I	Quantitative Real-Time PCR	F. Hoffmann-La Roche Ltd (Basel, Swiss)
LightCycler® 480 Probes Master	Quantitative Real-Time PCR	F. Hoffmann-La Roche Ltd (Basel, Swiss)
RevertAid First Strand cDNA Synthesis Kit	cDNA synthesis	Thermo Fisher Scientific Inc. (Waltham, MA, USA)

2.4 Genetical resources and oligonucleotides

2.4.1. Oligonucleotides

The oligonucleotides and primer for this work were synthesised by Eurofins MWG Operon (Ebersberg, Germany). Sequencing of DNA fragments required for this work was performed by Genewiz UK (Takeley, United Kingdom).

Table 4: Overview of the used primer in this work

Name	Target	Sequence	T _m °C
TH23	bradi2g50140	TGTATGCACTTCCTCCTCTC	56
TH30	bradi2g50140	CCTGGTGGCACAAGAAG	55
TH56	bradi2g50140	GGCACAAGAAGCCCCTTGAA	61
TH57	bradi2g50140	GATCCAGAACGTGCTGATGC	59
TH81	<i>bar</i>	TTCAGCAGGTGGGTGTAGAG	59
TH82	<i>bar</i>	GACAAGCACGGTCAACTTCC	59
TH89	XM_003567251	GGAGCAGCTCTTGGTGTCAT	60
TH90	XM_003567251	GGCGACTCAGTTCAGGACAA	59
TH91	No gene	AGCGTGATACGTTCCCATCC	59
TH92	No gene	CGACCGAGGACAACACTACC	60
TH93	XM_003563657	CTACTCGCTCCTCCTCAACG	59
TH94	XM_003563657	CTTTGATCACGGTTGGCGTG	60
TH95	XM_003557154	GCCACACTTCACTACAAGCG	59
TH96	XM_003557154	GAGGTGTCTTGAGGTGCTC	60
TH97	XM_024461141	CGTGTAATCAGCCGCCAATG	59
TH98	XM_024461141	TATTAGTGGGGCAAAGCGCA	60
TH99	XM_003561622	CACGTTTGATCCTTCCCCGA	60
TH100	XM_003561622	GGACCTGCATGTAGGAGTCG	59
TH101	XM_014897740	CCCACGAGAATTGCTGGAGA	59
TH102	XM_014897740	AATCGGAATGAGTGGTGCGT	60
TH103	No gene	ACTGTTTGAAAACGAAGTGCTTG	58
TH104	No gene	CATGCATGTGCAGTTCGGAG	59
TH105	XR_002963839	GCCGATTGATTCATCTTGGCA	59
TH106	XR_002963839	TGTGGACACATCCTTCATCCG	60
TH107	XM_003569230	CGGAAGCCCCAAGTCTGAAA	60
TH108	XM_003569230	TGATGTGTCAGCTGCCTTGT	59
TH109	XM_003562738	GTTGGTATGGTACCAGGGCG	60
TH110	XM_003562738	GGTCCAATCCCCGATCCAAC	60
TH111	No gene	TTGTGGATCGTACACACGGG	60
TH112	No gene	CGGGCAACACAATCATGCAA	60
TH113	NC_016132	GATGTGCGTCTTTTGCTCCC	59

Table 4 continued: Overview of the used primer in this work

TH114	NC_016132	TGCATTTGGGTTTGCACACTACG	60
TH115	XM_003564549	TAATCTCAGAGGCGGACGGA	60
TH116	XM_003564549	CGATCATCGGCACGATCAGG	61
TH117	XM_003566025	GGAGGTCTTTCCGTTCCCTG	60
TH118	XM_003566025	CAGAAGATCGAGAGCGTCGT	59
TH119	No gene	CCCGACTGCCTTGATGTCTT	60
TH120	No gene	GAGTAGTCGACGCCGGAAT	59
TH121	No gene	GGCCAGCCGGTTTAGTAGTT	60
TH122	No gene	GCCTTGCAATAGCCAGCAAG	60
TH123	No gene	CAGAAAAGGCAGCAGAGGGA	59
TH124	No gene	AATCGCAACGAAAACCACCG	60
BdUBC18-exp2-fw	Bradi4g00660	GTCACCCGCAATGACTGTAAGTTC	61
BdUBC18-exp2-rev	Bradi4g00660	TTGTCTTGCGGACGTTGCTTTG	62
BdPR1-exp-fw	Bradi1g57540	AAGAACGCCGTGGACATGTG	61
BdPR1-exp-rev	Bradi1g57540	ACCCGGAGGATCATAACTAC	56
BdPR2-exp-fw	Bradi2g60490	AGCCATCCAGCTCAACTAC	57
BdPR2-exp-rev	Bradi2g60490	CCTTGCCAACATGGTCAATC	57
BdXET-exp-fw	Bradi1g33827	AGCACAGGAACAGGGAGAC	60
BdXET-exp-rev	Bradi1g33827	GTCCAGCTCCTGGTACATC	58
BdMAPKK-exp-fw	Bradi2g17840	CCATGCCGACCTTGATAGAG	58
BdMAPKK-exp-rev	Bradi2g17840	CCTGAAACTTTGGGCGAGAG	59
BdChit8-exp-fw	Bradi3g32340	CTGCTTCAAGGAGGAGATAAAC	55
BdChit8-exp-rev	Bradi3g32340	TCATCCAGAACCACATGGC	58
BdUDP74f2-exp-fw	Bradi5g03300	GAATTCCACATTGGGCAGAC	57
BdUDP74f2-exp-rev	Bradi5g03300	CCTTCCTCTCACTATCCATCAC	57
BdAct-exp-fw	Bradi4g41850	GCTGGGCGTGACCTAACTGAC	64
BdAct-exp-rev	Bradi4g41850	ATGAAAGATGGCTGGAAAAGGACT	59
FgTub-expr-fw	FGSG_06611	TCAACATGGTGCCCTTCC	58
FgTub-expr-rev	FGSG_06611	TTGGGGTCGAACATCTGC	58
FgAct-expr-fw	FGSG_07335	ATGGTGTCACTCACGTTGTCC	60
FgAct-expr-rev	FGSG_07335	CAGTGGTGGAGAAGGTGTAACC	60
FgTRI5-expr-fw	FGSG_03537	GATGAGCGGAAGCATTTC	57
FgTRI5-expr-rev	FGSG_03537	CGCTCATCGTCGAATTC	53
FgFGL1-expr-fw	FGSG_05906	CGCCGCAGCATACT	55
FgFGL1-expr-rev	FGSG_05906	GGGTCCTTGGCGTTCGT	62

2.4.2. DNA-Plasmids

Dr. Johannes Stuttmann from the Martin – Luther University in Halle – Wittenberg, Germany provided the CRISPR/Cas9 containing binary DNA plasmid used in this work. An overview of this vector is presented below (Table 5 + Figure Supplement 1). To increase the chance of indels in the 5' region of *BdGSL3* a construct with four independent targets were used with the following sequences: Target 1: 5' CTACTCCGTTCCCCGGGCCA 3'; Target 2: 5' GGTGCGCGTACCTCGGCCAG 3'; Target 3: 5' CTGACATCCGCAGGGACCTCA 3'; Target 4: 5' TTTGTACCTGCTAATCTGGGG 3'.

Table 5: Description of the used binary vector for plant transformation and CRISPR/Cas9 mediated genome editing

Name	Description	Features
pMGE546	Size: 14355 bp. Binary vector for agrobacteria-mediated transformation of <i>B. distachyon</i> .	pVS1 backbone, <i>nptII</i> , LB, 35S ter, <i>bar</i> , TMV omega, OcsT, hCas9, Zm_Ubi1, 4 x (pOsU6, TATA, crRNA), RB

2.5 Cultivation media and broths

The media and broths used during this work were prepared as stated. Every broth and media were autoclaved after preparation if not other stated. The solvent used for the media and broths was ultrapure Water (upH₂O) (ELGA PURELAB® flex, Veolia).

Table 6: Overview of the used media and broths and their compositions

Media	Composition
LB-Agar	40 g/L LB-Agar (Luria/Miller) in upH ₂ O
LB-Broth	25 g/L LB-Broth (Luria/Miller) in upH ₂ O
SOC (Super Optimal Broth with Catabolite Repression)-Medium	2 % (w/v) Bacto-Trypton 0.5 % (w/v) Yeast extract 10 mM NaCl In upH ₂ O; After autoclaving add 10 mM MgCl ₂ 10 mM MgSO ₄ 0.4 % (v/v) Glucosesolution
Wheat-Broth	15 g/L fresh Wheat leaves
Callus-Induction-Agar (CIM)	4.3 g/L MS-Salt 30 g/L Saccharose 1 mL/L Fe-EDTA (40 mg/mL) 1 mL/L CuSO ₄ (0,6 mg/mL) 2 g/L Phytagel 250 µL/L 2,4-Dichlorophenoxyacetic acid 500 µL/L MS-Vitamins (103 mg/mL) pH 5.8 with 1 M KOH

Table 6 continued: Overview of the used media and broths and their compositions

Murashige – Skoog-Broth (MSB)	4.3 g/L MS-Salt 10 g/L Saccharose 10 g/L Mannitol 1 mL/L Fe-EDTA (40 mg/mL) 1 mL/L CuSO ₄ (0,6 mg/mL) pH 5.5 with 1 M KOH
Selection medium (SM)	4.3 g/L MS-Salt 30 g/L Saccharose 1 mL/L Fe-EDTA (40 mg/mL) 1 mL/L CuSO ₄ (0,6 mg/mL) 2 g/L Phytigel 500 µL/L 2,4-Dichlorophenoxyacetic acid 1 mL/L MS-Vitamins (103 mg/mL) 700 µL/L Timentin (320 mg/mL) 300 µL/L Basta (10 mg/mL) pH 5.8 with 1 M KOH
Regeneration medium (RM)	4.3 g/L MS-Salt 30 g/L Saccharose 1 mL/L Fe-EDTA (40 mg/mL) 1 mL/L CuSO ₄ (0,6 mg/mL) 2 g/L Phytigel 500 µL/L 2,4-Dichlorophenoxyacetic acid 1 mL/L MS-Vitamins (103 mg/mL) 700 µL/L Timentin (320 mg/mL) 300 µL/L Basta (10 mg/mL) 1 mL/L Kinetin (0.2 mg/mL) pH 5.8 with 1 M KOH
Germination medium (GM)	4.3 g/L MS-Salt 30 g/L Saccharose 1 mL/L Fe-EDTA (40 mg/mL) 2 g/L Phytigel 500 µL/L 2,4-Dichlorophenoxyacetic acid 1 mL/L MS-Vitamins (103 mg/mL) 700 µL/L Timentin (320 mg/mL) 300 µL/L Basta (10 mg/mL) 1 mL/L Kinetin (0.2 mg/mL) pH 5.8 with 1 M KOH
Completemedia (CM) (Leach et al. (1982))	2 g/L Yeast extract 10 g/L Glucose 1 g/L Ca(NO ₃) ₂ • 4 H ₂ O 0.2 g/L KH ₂ PO ₄ 0.25 g/L MgSO ₄ • 7 H ₂ O 0.15 g/L NaCl 1 mL/L MNS (Micronutrient solution)
V8-media mod.	500 mL albi Vegetable juice 0,15 % CaCO ₃ 1.5 % Agar pH 6.8 with NaOH

2.6 Biological resources and cultivation

The used biological resources are described in this chapter with the used cultivation environment.

2.6.1 Plant material

Brachypodium distachyon inbreed line Bd21 (Garvin 2007) and the transformed mutants were cultivated in climate chambers with 16 h / 8 h day-night cycle at 22 °C and 50 % humidity. The seeds were sowed into a Soil-Sand Mix (3:1, Werner Tantau GmbH & Co KG, Uetersen, Germany), and vernalized for 8 days at 8 °C in a dark place. After vernalisation, the trays were moved into the climate chamber and the pots were kept under a transparent hood for one week.

2.6.2 Microorganisms

An overview of the microorganisms is presented in this chapter. For a brief overview a table with the used microorganisms is presented here. A detailed description of the cultivation conditions follows.

Table 7: Brief overview of the used microorganisms and their background

Name	Description	Reference
<i>Agrobacterium tumefaciens</i> GV3101	Virulent strain used for transformation containing the virulence vector pMP90RK	Koncz and Schell (1986)
<i>Fusarium graminearum</i>	Strain 8/1	Miedaner et al. (2000)
<i>Parastagonospora nodorum</i>	Strain SN15	FGSC #10173

Legend: For the used *Parastagonospora nodorum* strain SN15 the catalogue number for the Fungal Genetics Stock Center is given.

2.6.2.1 *Agrobacterium tumefaciens*

For the transformation of *Brachypodium distachyon* Bd21 the *Agrobacterium tumefaciens* strain GV3101 was used (Koncz und Schell, 1986). Competent Agrobacteria were transformed with the desired plasmid via electroporation (Nagel et al. 1990) and plated on LB-agar containing the antibiotics Rifampicin (100 µg/mL), Spectinomycin (50 µg/mL) and Gentamycin (50 µg/mL). Modifications to the electroporation protocol by Nagel et al. (1990) were the use of LB-broth.

2.6.2.2 *Fusarium graminearum*

The *Fusarium graminearum* wild-type strain 8/1 was used for the spikelet inoculation experiments. For conidiation conidia were plated on CM agar plates and cultivated at 28°C in the absence of light for 3-4 days. To induce conidiation, small agar blocks with young mycelia were transferred into sterile wheat broth for 7-10 days, shaking at 144 rpm at 28°C.

2.6.2.3 *Stagonospora nodorum* SN15

The used *Stagonospora nodorum* strain SN15 was provided by the Fungal Genetics Stock Center (FGSC #10173). For conidiation SN12 was cultivated on V8-media mod. and kept in the lab under room temperature conditions on the windowsill exposed to sunlight. After two weeks, conidia could be harvested for infection studies.

2.7 Methods

2.7.1 Generating of transgenic *B. distachyon* plants

The generation of transgenic *B. distachyon* plants was done in cooperation with the technical assistance Petra von Wiegen (AG Molecular Phytopathology, Institute for Plant Science and Microbiology). The protocol is adapted from Alves et al. (2009) and will be described briefly. The used media and broths are stated in table 6. For the agrobacterium-mediated transformation of *B. distachyon* premature embryos were isolated from caryopses of seven weeks old plants (BBCH 73-75, Hong et al. (2011)). The isolated embryos were then placed on Callus-Induction-Agar (CIM) to facilitate the forming of callus tissue. The generated calluses were divided after three weeks and transferred on fresh CIM. This procedure was repeated after additional two weeks, and again after one additional week to facilitate proper callus formation. At the end of this callus generating step, positive transformed *A. tumefaciens* clones containing the desired plasmid pMGE546 were transferred to a 5 mL LB-Broth preculture containing the antibiotics Rifampicin (100 µg/mL), Kanamycin (50 µg/mL) and Gentamycin (50 µg/mL) for selection. After two days of incubation at 28°C, 144 RPM in the absence of light on an orbital shaker (Tab. 1, No. 17), 1 mL of preculture was used to inoculate the 400 mL main culture. The main culture consists of LB-Broth containing the already noted antibiotic concentrations for selection purpose. After another two days under identical growth conditions, the bacteria were harvested at 3000 x g (Tab. 1, No. 6) and suspended in 10 mL of MSB supplemented with 45 mg/mL Acetosyringone. After an incubation of one hour, the isolated calluses were soaked in the *A. tumefaciens* MSB suspension for five minutes. After the incubation, the calluses were transferred onto sterile dry filter paper and quickly dried before placed onto sterile petri dishes.

The sterile petri dishes contained filter paper soaked with Acetosyringone supplemented MSB. Co-cultivation was performed at RT in the dark for two days before the calluses were placed on SM. Positive transformed calluses were transferred onto RM to facilitate the formation of roots and hypocotyls before a last transfer on GM was done. The surviving small plantlets were transferred into soil and kept under the stated controlled environment until further tests or seeds were formed. All plants transformed with the described construct pMGE546 were labelled with the transformation label Agro250.

2.7.2 Isolation of DNA

Table 8: Used buffers for the gDNA isolation from *B. distachyon*

Buffer	Composition
TE-Buffer	0.01 M Tris-HCl pH 8 1 mM Na ₂ EDTA pH 8 in upH ₂ O
Waite DNA-Extraction buffer Pallotta et al. (2000)	1 % (v/v) N-lauryl-sarcosin 100 mM Tris-HCl, pH 8 10 mM Na ₂ EDTA, pH 8 100 mM NaCl in upH ₂ O

For the isolation of genomic DNA from *Brachypodium distachyon* the protocol from Pallotta et al. (2000) was used. Appx. 100 mg of plant material was taken into prepared screwcap tubes with two steel beads. The material was frozen in liquid nitrogen and milled for 90 s in a vibratory mill (Tab. 1, No. 26) at 30 hz. Afterwards the milled material was resolved in 800 µL Waite DNA-Extraction buffer and thoroughly mixed. After mixing 800 µL of Phenol:Chloroform:Isoamyl Alcohol (25:24:1) were added and mixed again for two minutes. Centrifugation at 4°C, 5000 x g (Tab. 1, No. 2) for 3 minutes was performed to separate nucleic acids from cell debris and proteins. The upper hydrous phase was carefully transferred into a new 2 mL tube. 800 µL ice-cold propan-2-ol and 80 µL pH 5.2 3 M Sodium acetate were added and mixed via inverting of the tubes. A centrifugation at 4°C, 12500 x g (Tab. 1, No. 2) for 10 minutes was performed to precipitate nucleic acids. The supernatant was removed, and the pellet was washed with ice-cold 70% Ethanol (p.a.). After washing a second centrifugation, same conditions as before, was performed and the supernatant removed. The pellets were air dried and resolved in 100 µL TE-Buffer. An RNAase (40µg/mL) treatment was performed for 30 min at 37°C (Tab. 1, No. 15) and the DNA was kept at 4°C overnight.

2.7.3 Isolation of RNA and qPCR analysis

2.7.3.1 Isolation of plant RNA from *Brachypodium distachyon*

The isolation of RNA from *Brachypodium distachyon* was performed with three different tissues, and therefore different preparations were performed. For the leaf RNA three weeks old leaves were harvested and in screw cap tubes with two steel beads frozen in liquid nitrogen. The leaves were homogenized in a vibratory mill (Tab. 1, No. 26) at 30 hz for 90s. The stem RNA was isolated from five weeks old plants, the stems were cut into small pieces and frozen in screw cap tubes with two steel beads in liquid nitrogen. The plant material was homogenized in a vibratory mill (Tab. 1, No. 26) at 30 hz for 90s, then frozen again in liquid nitrogen. This procedure was repeated two to three times until the stem material was completely milled into fine powder. This procedure was also done for the spikelets from *Brachypodium distachyon*, which were either taken 2 dpi or at anthesis. After material preparation the total RNA was isolated following the instructions of the innuPREP Plant RNA Kit. RNA quality control was performed on agarose gel electrophoresis and concentration was measured via photometric absorption.

2.7.3.2 cDNA synthesis

Before cDNA synthesis, the RNA had to undergo a DNase I treatment to remove possible gDNA impurities. This was performed as described by the supplier (Tab. 2). After DNase I treatment and inactivation, the cDNA was synthesized with the RevertAid First Strand cDNA Synthesis Kit. The synthesis was done as described in the protocol from the supplier (Tab. 3). For every cDNA synthesis reaction, a total of 500 ng isolated RNA was used.

2.7.3.3 Gene expression analysis via qPCR

To analyse the gene expression in different tissue two different methods for qPCR were used. The first method is a probe-based method provided by Roche for the LightCycler® 480, called the RealTime ready Custom Panel system. In this system, a 96 Well plate gets prepared with custom chosen probes, with a guaranteed 100% \pm 10% efficiency (Mauritz et al. 2005) for targets and reference genes. The reaction set up for one well consists of 5 μ L of cDNA (1:20), 5 μ L of nucleic-acid free water and 10 μ L of the LightCycler® 480 Probes Master. Therefore, for each line a master-mix was prepared. The following amplification protocol was used (Tab. 9).

Table 9: Amplification protocol for the RealTime ready Custom Panel qPCR

Step	Temperature °C	Time s	Cycles
Pre-Incubation	95	600	1
Denaturation	95	10	
Annealing	60	30	45
Elongation	72	1	
Fluorescence measurment	After every cycle		

Table 10: Overview of the analysed *B. distachyon* genes and the associated loci

Gene	Locus
<i>BdGSL1</i>	bradi1g51757.1
<i>BdGSL2</i>	bradi2g46250.1
<i>BdGSL3</i>	bradi2g50140.1
<i>BdGSL4</i>	bradi2g40460.1
<i>BdGSL5</i>	bradi1g47427.1
<i>BdGSL6</i>	bradi3g60790.1
<i>BdGSL7</i>	bradi1g29622.1
<i>BdGSL8</i>	bradi1g77247.1
<i>BdGSL9</i>	bradi3g09317.1
<i>BdGSL10</i>	bradi1g76617.1
<i>BdGSL11</i>	bradi2g40430.1
<i>BdUbi</i>	bradi4g00660.1

For the PR and virulence gene expression analysis, a dye-based qPCR analysis was performed. The LightCycler® 480 SYBR Green I was used as described by the manufacturer (Tab. 3). This qPCR analysis was done in cooperation with Dr. Christian Voigt from the Voigt Lab in Sheffield, UK due to the movement of the LightCycler 480 system. The Samples were prepared and send to the Voigt lab, the qPCR was performed on the following genes (Tab. 11). The results were then sent to me. The primers used for the qPCR analysis are listed in the corresponding table (Tab. 4).

Table 11: Overview of the analysed PR and virulence genes of *B. distachyon* and *F. graminearum*

Gene	Locus
<i>PR1.3</i>	Bradi1g57540
<i>PR2</i>	Bradi2g60490
<i>BdMAPKKK</i>	Bradi2g17840
<i>BdChit8</i>	Bradi3g32340
<i>BdUGT74f2</i>	Bradi5g03300
<i>BdAct</i>	Bradi4g41850
<i>BdUBC18</i>	Bradi4g00660
<i>Fgl1</i>	FGSG_05906
<i>Tri5</i>	FGSG_03537
<i>Actin</i>	FGSG_07335
<i>Tubulin</i>	FGSG_06611

Table 12: Amplification protocol for the expression analysis of *B. distachyon* PR genes and *F. graminearum* virulence genes

Step	Temperature °C	Time s	Cycles
Pre-Incubation	95	600	1
Denaturation	95	10	
Annealing	60	10	45
Elongation	72	10	
Fluorescence measurement	After every cycle		
Melting curve	58 - 95	5 / °C	1

The analysis of acquired data of both qPCRs was done using Microsoft Excel, IBM SPSS Statistics 24 and according to the published method (Pfaffl 2001).

2.7.4 Genotyping of transformed plants

2.7.4.1 PCR based screening for *BdGSL3* mutations

To identify possible genome edited plants, a screening for the genotype of the targeted area was performed. Therefore, a PCR based screening system was established. The isolated gDNA was used in a PCR with specific designed Primers flanking the interesting region. Two primer sets were used during this work (Tab. 4).

Table 13: PCR program used for the screening for mutations in *BdGSL3*

Step	Temperature °C	Time s	Cycles
Initial Denaturation	95	180	
Denaturation	95	30	
Annealing	62.3	30	35
Elongation	69	70	
Final Elongation	69	180	
Pause	13	∞	

2.7.4.2 Screening for the *bar* gene in transformed plants

To screen for the T-DNA integration into the genome, a PCR for the *bar* gene, which causes to the BASTA® resistance, was performed. A specific primer set was designed which only binds in the specific gene (Tab. 3). The screening PCR was performed with the following conditions (Tab. 14).

Table 14: PCR program for amplification of an *bar* gene fragment from the T-DNA

Step	Temperature °C	Time s	Cycles
Initial	95	180	
Denaturation			
Denaturation	95	30	
Annealing	56	30	35
Elongation	69	25	
Final Elongation	69	90	
Pause	13	∞	

2.7.4.3 PCR based off-site target screening

To screen for possible indels in the off-site targets found by *in silico* analysis, a PCR screening was used. The results of the *in silico* analysis are provided in the supplement (Fig. S. 2) The primer pairs designed for each off-site target are presented in the primer table (Tab. 3).

Table 15: PCR amplification program for off-site target screening in *B. distachyon*

Step	Temperature °C	Time s	Cycles
Initial	95	180	
Denaturation			
Denaturation	95	30	
Annealing	55	30	35
Elongation	69	25	
Final Elongation	69	90	
Pause	13	∞	

2.7.4.4 Agarose gel electrophoresis of screening PCR products

Table 16: Buffers used for the agarose gel electrophoresis of the PCR products

Buffer	Composition
TBE 10x	890 mM Tris Base 890 mM Boric acid 20 mM Na ₂ EDTA pH 8.0 in upH ₂ O
6x Loading Dye	30 % (w/v) Glycerol Add. Small amounts of Orange G
TBE 1x	100 mL TBE 10x in 1 L upH ₂ O

The PCR products amplified in screening PCRs were separated in agarose gel electrophoresis. The concentration for the agarose gels were determined on the expected size of the amplified product. For PCR products around 1 kb a concentration of 1.5 % agarose in 1 x TBE was used. For PCR products around 500 bp 2 % agarose were used. The gel was loaded with 3 µL of PCR product, 1 µL of 6x Loading Dye and 2 µL of upH₂O. The Marker used for the gel electrophoresis was the GeneRuler 1kb+ (ThermoFisher Scientific, USA). Gels were run on 100 v until the loading dye was at the lower end of the gel (Tab. 1, No. 6). Gels were then stained for 15 min in a 0.5 µg/ml EtBr solution. Stained gels were documented in a gel documentation (Tab. 1, No. 5).

2.7.5 Infection and wounding experiments

Conidia of *F. graminearum* and *S. nodorum* were harvested under sterile conditions in a laminar flow cabinet. The liquid wheat broth containing *F. graminearum* was directly filtered through a 50 µm sieve. The conidia of *S. nodorum* were washed and gently scraped from the agar plates and filtered through a 50 µm sieve. The filtered conidia were pelleted at 4 °C and 3000 x g (Table 1 No. 6). The supernatant was removed, and the pellet washed with sterile water before pelleted again. The pellet was then resuspended in 10 mL sterile water and conidia concentration was counted under a microscope with a Fuchs–Rosenthal counting chamber. The desired conidia concentration was set by adding water or pelleting and removing supernatant. Harvested conidia were stored at -70°C for up to six months in aliquots.

2.7.5.1 Wounding of *B. distachyon* leaves

To study the stress response of *B. distachyon* in leaves to wounding, a wounding assay was performed. Leaves of 5 weeks old plants were wounded with the aid of a needle array. With this needle array several wounds were inflicted in the leaves of *Brachypodium distachyon* wild-type and the four genome edited lines. After wounding the plants were kept under controlled growing environment until samples were taken. After 6 hours and after 16 hours samples were taken for each time point. The harvested leaves were transferred into 2 mL reaction tubes and fixed in 70 % ethanol. For three successive days, the ethanol was changed. The samples were stored for Confocal Laser Scanning Microscopy. To quantify the mean relative area of callose at 16 hours after wounding, the callose formation area was measured and set in relation to the wounded tissue area.

2.7.5.2 Inoculation of *B. distachyon* leaves with the necrotrophic leaf pathogen *S. nodorum*

To evaluate the infection of *S. nodorum* on *B. distachyon* leaves, detached leaf assays were performed. The droplet inoculation on detached leaves was performed as described by Falter and Voigt (2014) with some minor modifications. Leaves from 5 weeks old plants were placed in sterile petri dishes and fixed between sterile filter paper. The leaves were inoculated with 10 μ L of conidia suspension with a concentration of 100 conidia/ μ L. The filter paper was wetted to keep the leaves hydrated and the petri dishes were sealed with Parafilm® during the 7 days incubation. The inoculated leaves were kept in the growing chambers at the controlled growing environment. After incubation the leaves were transferred into reaction tubes and fixed in 70 % Ethanol.

2.7.5.3 Inoculation of *B. distachyon* spikelets with *F. graminearum* 8/1

To study the FHB disease in *B. distachyon* and the four genome edited lines point inoculations of spikelets were performed. Flowering spikelets of around 6 weeks old *B. distachyon* (BBCH: 61 – 65; Hong et al. (2011)) were used and inoculated with *F. graminearum* conidia or water. The determining factor for the point inoculation of florets were the visibility of anthers. If the anthers are visible in the floret, a 1 μ L droplet of the conidia suspension or water was injected into the floret. The inoculation procedure is based on previous work (Blümke 2013; Blümke et al. 2015; Pritsch et al. 2001). The droplet was injected between the lemma and palea of the identified floret in the spikelet. Opposed to wheat inoculations, in *B. distachyon* only a single floret per spikelet was inoculated. Inoculations were done at the early evening and the inoculated spikelets were wrapped in plastic bags sprayed with water. This procedure should ensure a high humidity to support the primary infection of *F. graminearum*.

The plants were transferred into infection chambers with adapted environmental settings. The day and night cycle were kept at 16 h daylight and 8 h night and temperature stayed at 22 °C. The humidity was increased to 65 % to facilitate the infection with *F. graminearum*. The plants were kept until the desired time point at 2 dpi, 3 dpi, 7 dpi or 14 dpi were reached, and the experiments could be carried out. Spikelets used for microscopy were directly fixed in 70 % ethanol. Spikelets used for RNA isolation were shock frozen in liquid nitrogen and if not directly used stored at -70 °C until used.

2.7.5.4 Evaluation of the Disease Score after 7- and 14-days post inoculation

The evaluation of the FHB disease in *Brachypodium distachyon* was done according to the established Disease Score by Blümke (2013); Blümke et al. (2015). At the specific time points 7 days and 14 days after inoculation, the inoculated spikelets were visually evaluated and scored appropriate to the Disease Score (Fig. 3).



Figure 3: Disease Score ranking system for evaluation of the infection of the FHB disease causing pathogen *F. graminearum* in *B. distachyon*

The figure is from Blümke et al. (2015) showing an overview of different infection scores. The scale bar equals 2 mm and the L indicates the lemma. **A)** Uninfected floret without any necrosis or other disease symptoms, Disease Score 0.0. **B)** Weak infection with restricted necrosis (N) at the rachis node of the floret, Disease Score 0.1. **C)** Moderate infection covering up to 50 % of the floret with necrotic lesions, Disease Score 0.5. **D)** Fully necrotic floret or more than 50 % of the floret is covered in necrotic lesions, Disease Score 1.0. The florets of each inoculated spikelet were rated at either 7 dpi or 14 dpi based on this scoring system.

The evaluation of the FHB disease in *B. distachyon* was based on the Disease Score system (Fig. 1). The florets of inoculated spikelets were individually scored. Florets with no visual necrotic tissue or lesions were ranked with 0.0 (Fig. 3, A). Florets with weak infections having necrotic lesions at the basal tissue, rachis node or caryopsis received a score of 0.1 (Fig. 3, B). While florets showing more lesions or are up to 50 % necrotic were rated at 0.5 (Fig. 3, C). Florets having a stronger infection than 50 % and up to fully necrotic or showing several lesions were rated with 1.0 (Fig. 3, D). The score of all florets of an inoculated spikelet were added and the final Disease Score was calculated.

2.7.5.5 Measuring the relative area covered with callose depositions in inoculated *B. distachyon* florets

To measure and calculate the relative area covered with callose depositions in the rachis of inoculated florets confocal scanning microscopy pictures of the 3 dpi stage were taken. These pictures were used to measure the whole rachis area of the inoculated floret and the area of the callose depositions in this area (Fig. 4).

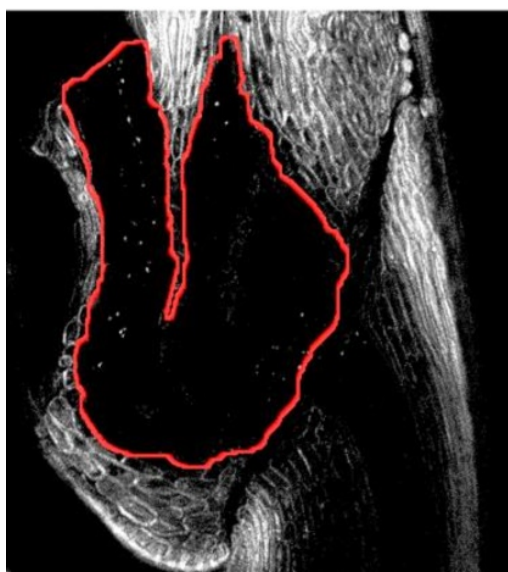


Figure 4: *B. distachyon* floret with the marked area used to measure the relative area occupied by callose depositions

The figure is taken from Blümke (2013) who established this method. In an inoculated floret 3 days post inoculation the amount of callose depositions was measured. The area in red was used for the measuring and the callose depositions inside this area were manually marked and measured with the Fiji distribution of ImageJ2 (Rueden et al. 2017; Schindelin et al. 2012).

To calculate the relative area covered with callose depositions in the rachis area of *B. distachyon* spikelets 3 days post inoculation microscopy pictures were used (Fig. 4). The area marked in red (Fig. 4) was measured in ImageJ2, Fiji (Rueden et al. 2017; Schindelin et al. 2012). Additionally, the area of each callose deposition inside the marked area was measured by hand

with the free hand marking tool of ImageJ and both measurements were transferred into Excel for further calculations. With the acquired data, the calculation of the relative area covered could be performed. The formula used for the calculation is:

$$relative\ area = \left(\frac{100}{rachis\ area} \right) \times area\ of\ callose\ depositions$$

With the calculated relative area covered by callose depositions, comparisons between the wild-type Bd21 and the four genome edited lines were done.

2.8 Microscopy and visualization

The visualization of plants and the different tissues used for experiments during this work was done with three different methods. Macroscopic pictures were taken by camera; the spikelets at 7 dpi pictures were taken with a stereo microscope and a coupled camera. The microscopy pictures were taken with a confocal laser-scanning microscope (CSLM).

2.8.1 Macroscopic pictures

Macroscopic pictures during this work were taken with the single-lens reflex camera Nikon D300s coupled with a macro objective (Nikon, Japan). The pictures were taken with the camera mounted on a tripod and connected to a PC. The software used for the pictures was the Camera Control Pro 2 software by Nikon.

2.8.2 Stereo microscopy

To take pictures of inoculated spikelets with either *F. graminearum* or H₂O as a negative control, the inoculated spikelets were cut into longitudinal cross sections. The prepared spikelets were then placed on black velvet under the stereo microscope Leica MZ FL III that is coupled with the Leica DFC500 camera and connected to a PC. Pictures were taken with the Leica Application Suite V. 3.8 software.

2.8.3 Confocal laser scanning microscopy

Table 17: Overview of the used fluorescence dyes and composition for the fluorescence microscopy

Stain	Composition
Aniline blue 10x	0.01 % (w/v) Aniline blue in upH ₂ O
Aniline blue working solution	0.001 % (v/v) in 150 mM K ₂ HPO ₄
WGA-CF TM - Alexa 488 Stock	2 mg/mL
WGA-CF TM - Alexa 488 working solution	0.08 mg/mL in upH ₂ O

The microscopy in this work was done with the Zeiss LSM780 coupled to the Zeiss Axio Imager Z2. Pictures were taken and analysed with the Zeiss Zen 2010 software. The pictures were taken either with a 10x objective (EC Plan-Neofluar 10x/0.30 M27) or a 20x objective (LD LC1 Plan-Apochromat 25x/0.8 O/W/G M27). The in ethanol fixed samples were prior staining washed with upH₂O to remove the ethanol. After washing the samples were stained for 16 to 24 hours with aniline blue (Tab. 17). Aniline blue staining was used to stain the cell wall polymer 1,3- β -glucan, which is also present in papillae (Kauss 1989; Stone et al. 1984). To visualise the pathogen after destaining with ethanol, the Alexa 488 fluorescence dye conjugated to the chitin targeting wheat germ agglutinin was used (Monsigny et al. 1980; Panchuk-Voloshina et al. 1999).

Table 18: Overview of the excitation and detection of the used fluorescence dyes

Stain	Excitation	Emission
Aniline blue	405 nm with UV-Diode	427-490 nm with GAsP
WGA-CF TM - Alexa 488	488 nm with Argon Laser	499-551 nm with GAsP

Legend: The hybrid photo detector used consists of gallium arsenide phosphide (GAsP)

2.9 *In silico* methods

During this work, several different software and online tools were used for different methods. An overview of the used software and tools is given here. For the work with nucleic acid sequences, the client-based software Clone Manager 9 from Sci Ed Software and the online cloud-based software Benchling (www.benchling.com) were used. The primer were designed using the Benchling primer wizard based on the Primer3 algorithm (Kõressaar et al. 2018; Koressaar and Remm 2007; Untergasser et al. 2012). The sequence alignments were done with the Clustal Omega or MAFFT algorithm (Sievers et al. 2011; Standley and Katoh 2013).

Analysis of the protein sequence for possible predicted protein domains were done with online tools. The transmembrane helices prediction was performed with the TMHMM prediction method (Krogh et al. 2001). The cross-species search for homologue proteins was performed with PLAZA 4.0 (Van Bel et al. 2017; Vandepoele et al. 2013). For the MOTIF prediction, the database query search MyHits was used (Hau et al. 2007; Junier and Pagni 2000; Junier et al. 2001; Pagni et al. 2004; Pagni et al. 2007; Pagni et al. 2001; Sigrist et al. 2010; Sperisen et al. 2004; Sperisen and Pagni 2005). Off-site target search in the Bd21 genome for the four targets was done with the web based tool Cas-OFFinder (Bae et al. 2014).

For the measurement of callose depositions in this work, the Fiji distribution of ImageJ2 was used (Rueden et al. 2017; Schindelin et al. 2012). Further software used during this work was the spreadsheet Excel and the word processor Word from Microsoft. The statistical analysis of the data acquired during this work was done with the help of IBM SPSS Statistics 24. IBM SPSS Statistics 24 was also used for the charts presented in this work.

3. Results

To identify the function of BdGSL3 in *Brachypodium distachyon* defence response to fungal infections, the CRISPR/Cas9-mediated genome editing approach was chosen to disrupt the target gene. The acquired mutant lines were analysed and the results are presented in this chapter.

3.1 Overview of *BdGSL3* and its homology to *PMR4*

BdGSL3 is a 5379 bp large gene, located on the second chromosome. *In silico* analysis predicted a 1,3-beta-D-glucan-UDP glucosyltransferase (FKS1) subdomain followed by five transmembrane helices, an intracellular region and another six transmembrane helices (Fig. 5). The four targets chosen for genome editing are in the 5'-end of the coding sequence (CDS) of *BdGSL3* (Fig. 5).

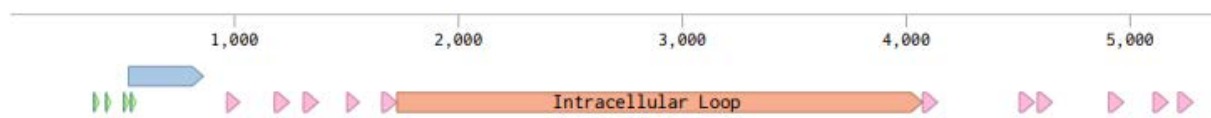


Figure 5: Overview of the CDS of the 1,3- β -glucan synthase *BdGSL3* from *Brachypodium distachyon*

The 1,3- β -glucan synthase BdGSL CDS consists of 5379 bp. Based on data available in the uniprot database (<https://www.uniprot.org/>) and the transmembrane helices prediction software TMHMM V2.0 the predicted domains were annotated. The sgRNA targets for the endonuclease Cas9 are located at the 5'-end upstream of the FKS1 subunit domain. The sgRNA targets are indicated in green, the FKS1 subunit domain in blue. The two groups of transmembrane helices are indicated in pink, in between is the intracellular loop located, represented in orange.

When compared with PMR4, a described stress induced callose synthase, similarities in protein structure and subunit domains are found (Fig. 6). Both enzymes have a similar size of 1780 AA for PMR4 and 1792 AA for BdGSL3, both contain a predicted FKS1 subunit domain in the n-terminal region of the protein followed by several *in silico* predicted transmembrane helices (Fig. 6). Between the two groups of transmembrane helices lies an intracellular loop (Fig. 6).

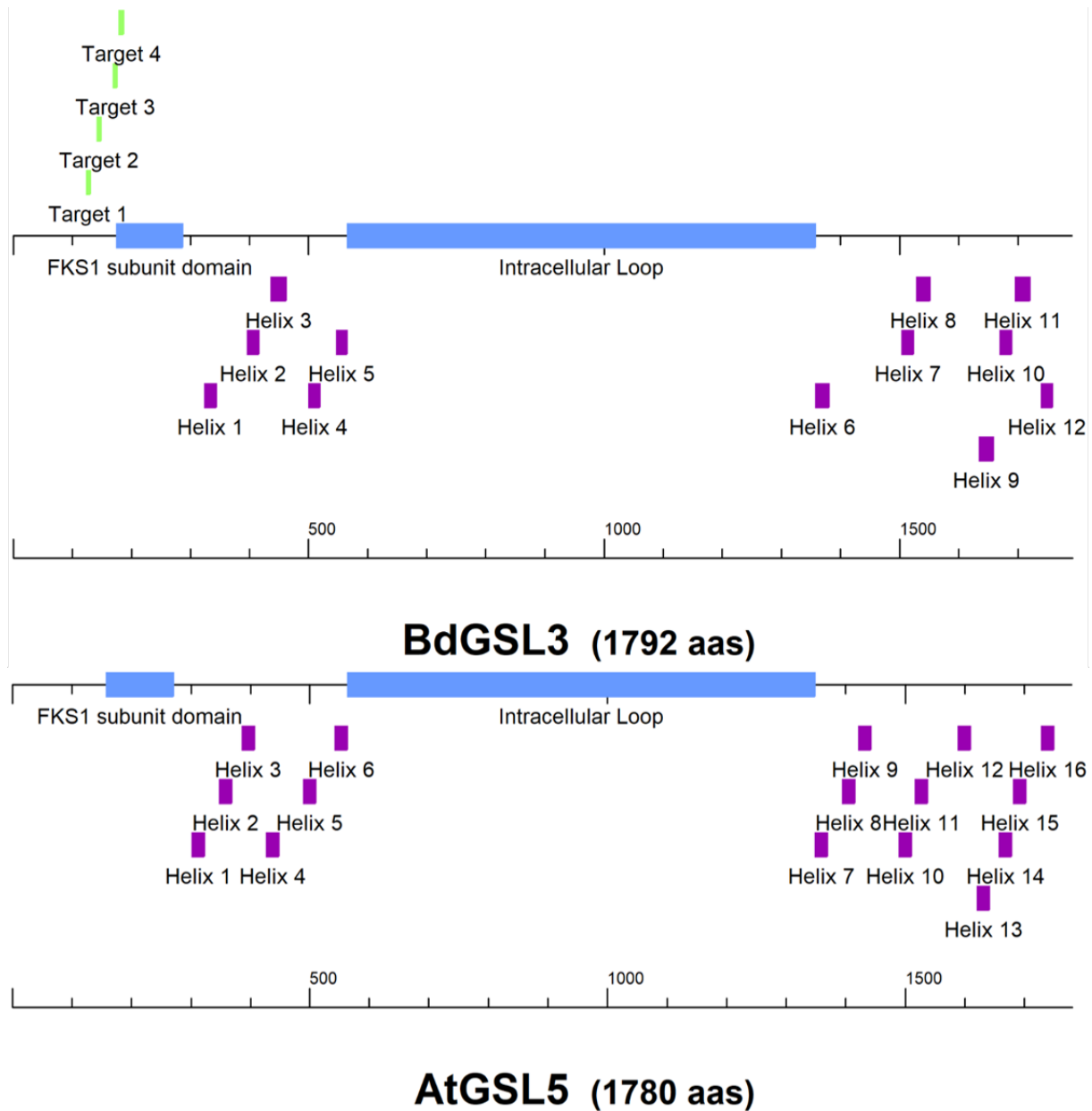


Figure 6: Comparison of the characterised stress induced 1,3-β-glucan synthase AtGSL5 (PMR4) and the 1,3-β-glucan synthase BdGSL3 from *Brachypodium distachyon* with unknown function

The alignment was performed with CloneManager V.9 and the ClustalW algorithm. The annotations were added manually with the aid of the uniprot database (<https://www.uniprot.org/>) for each protein. The prediction for the transmembrane helices were predicted with the TMHMM V.2.0 software. Both proteins share a similar structure. They are similar in size and contain a FKS1 subunit at the n-terminal region of the protein. Both proteins have an intracellular loop flanked by a set of n-terminal and c-terminal transmembrane helices. The homologue region for the sgRNA were transferred into the amino acid sequence for BdGSL3 as a visual aid.

The major differences on structural level is the reduction of transmembrane helices for BdGSL3 (Fig. 6). PMR4 includes 16 transmembrane helices, whereas in BdGSL3 only 12 are predicted (Fig. 6). Otherwise, both proteins share several similarities in the overall annotated features and structure.

3.2 Generating and identifying genome edited plants

The T₀-Generation was screened to investigate the function of the used genome editing construct and to determine whether the endonuclease is active during the haploid callose phase, or during plant regeneration. DNA was extracted from leaves of five weeks old plants. In T₀-Generation four out of 18 independent transformants (Fig. 7) showed possible genome editing events. PCR screening revealed two lines with a double band, the lines #2 and #11, and twice an unclear PCR product with 3 possible bands, for the lines #1 and #16, at the expected size (Fig 7).

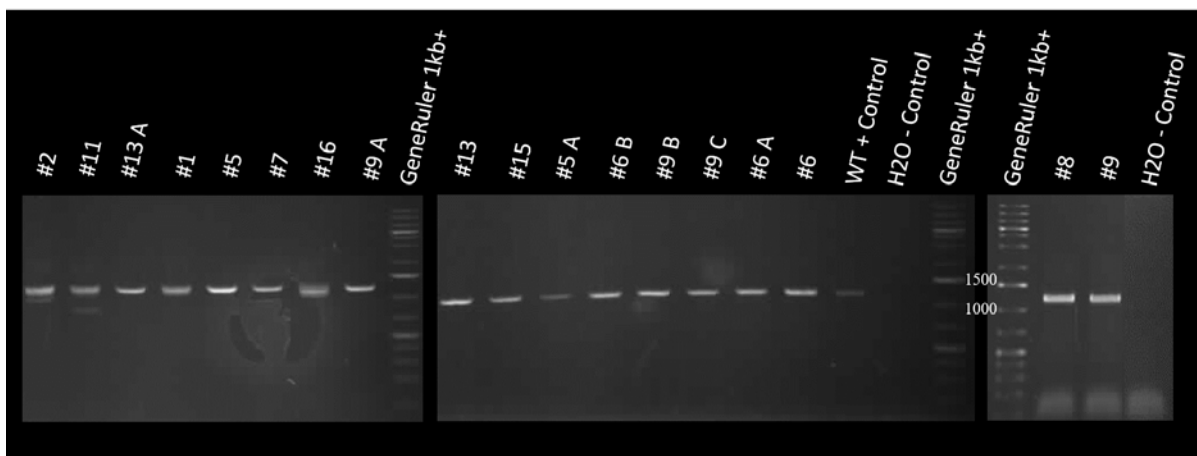


Figure 7: PCR based screening of the T₀-Generation for differences in the genome editing target region

The Marker GeneRuler 1kb+ supplied by ThermoFisher Scientific was used to determine the size; numbers are indicating size in bp. The wild-type (WT) gDNA was used as a positive control and was expected to be 1.1 kbp large. For the Lines #1, #2, #11 and #16 differences in product size could be detected. The lines #2 and #11 showed a distinct second lower band, indicating a deletion in the amplified region. The Lines #1 and #16 showed an indistinct PCR product. This indicates some form of mosaicism with different genotypes in different cells. Negative control (H₂O – Control) showed no amplification. Primers used for this PCR are TH23 and TH30 (Tab. 4).

To study the activity of the transformed endonuclease construct during several plant generations, 20 seeds from each of the four already identified lines plus the line #1 were sowed and the PCR based screening was repeated.

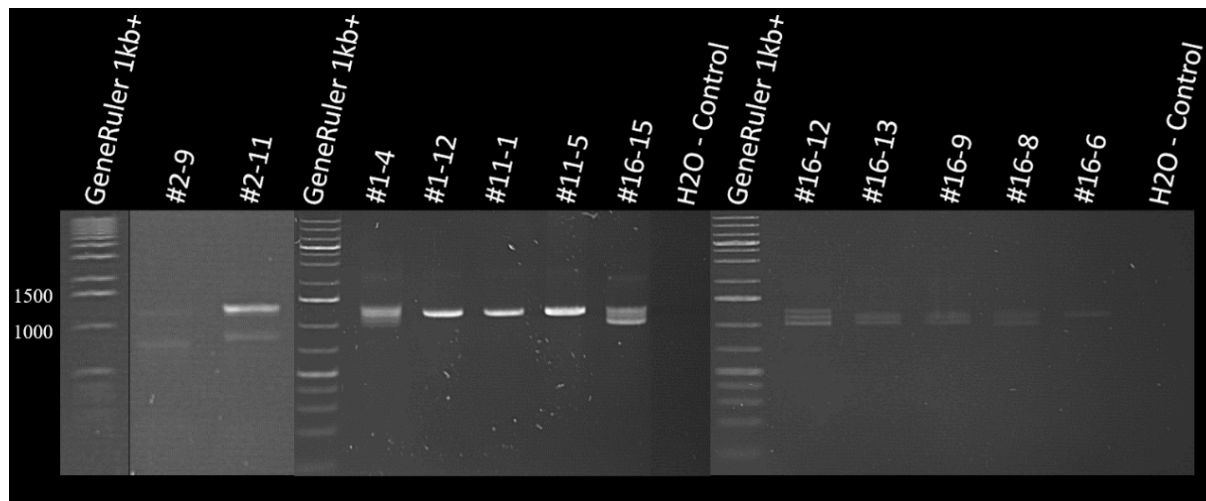


Figure 8: PCR based screening from the T₁-Generation to further describe the genome editing process

The Marker used was the GeneRuler 1kb+ from ThermoFisher Scientific, numbers are indicating size in bp. A PCR product at 1.1 kbp was expected for the wild-type undisrupted locus. For the Line #2-9 and #2-11 a heterozygotic genotype with a deletion was detected. The Line #1-4 showed an indistinct PCR product as previously found in the T₀-Generation, indicating an active construct. The Lines #16-15 and #16-12 showed mosaicism with three distinct bands. The Lines #16-13, #16-9 and #16-8 were also heterozygotic. Primers used for this PCR are TH23 and TH30 (Tab. 4).

The screening of the T₁-Generation revealed eight interesting lines with changes in the genetic background of the *BdGSL3* gene (Fig. 8). Two lines showed the previously identified mosaicism on gDNA level, indicating an active endonuclease during the generation cycle of the T₁-Plants (Fig. 4, #16-12 and #16-15). Both lines had three distinct bands on the agarose gel compared to the other lines which contained the wild-type allele and a modified allele. Since the construct used has four different targets (Fig. 5), different intermediate conditions could be expected. This explains the found mosaicism for #16-12 and #16-15. The lines #2-9, #2-11, #16-13, #16-9 and #16-8 had two distinct PCR products on the agarose gel (Fig. 8). The deletions for the lines #2-9 and #2-11 are larger compared to the deletions of the lines #16-13, #16-9 and #16-8 (Fig. 8). This indicates two different kind of deletions, which is caused by endonuclease activity on different targets. Because of this possible endonuclease activity, the observed PCR product for line #1-4, which contained a wild-type sized fragment and smaller fragments were possible (Fig. 8).

From the T₁-Generation the following five lines were chosen: #1-12, #2-9, #2-11, #16-8 and #16-12 and further PCR based screenings with the offspring from each line were performed to monitor the development of the genotypes until the T₆-Generation. For the final screening in the T₆-Generation, the four lines #2-9-4-9, #2-9-6-30, #16-12-6-14 and #16-12-10-18 were analysed and all further experiments were done with these lines. A final PCR for the deletion on gDNA and the *bar* gene in the T-DNA was performed (Fig 9).

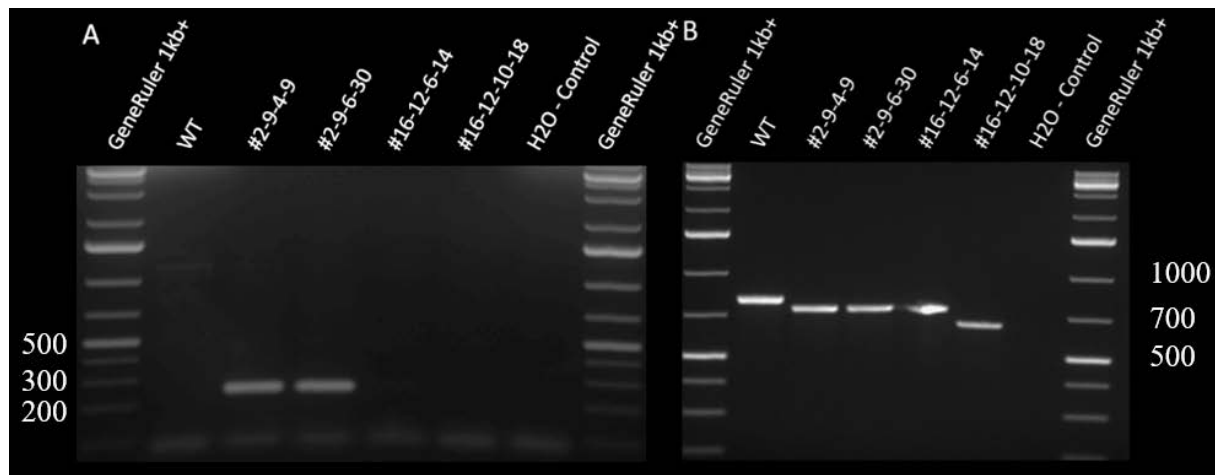


Figure 9: Final PCR based screening for the T₆-Generation to identify the *BdGSL3* genotype and the presence of T-DNA

WT = wild-type PCR product on Bd21 gDNA. The used DNA Marker is the GeneRuler 1kb+ supplied by ThermoFisher Scientific, numbers are indicating size in bp. **A)** Gel electrophoresis of PCR products on the BAR Gene. Primers used were TH81/TH82 (Tab. 4). The samples #2-9-4-9 and #2-9-6-30 showed a PCR product which indicates the presence of the T-DNA containing the selection marker cassette. The wild-type (WT) and the two lines #16-12-6-14 and #16-12-10-18 showed no amplified product. This indicates the loss of the selection marker *hpt* and presumably the T-DNA. **B)** Agarose gel electrophoresis of the screening PCR. The wild-type (WT) product has the expected size of 798 bp for the used primers TH57/TH56. The four lines tested had a homozygotic background with a smaller PCR product, whereas the lines #2-9-4-9, #2-9-6-30 and #16-12-6-14 have the same size and the line #16-12-10-18 a larger bigger deletion compared to the other three lines.

The final analysis of the sixth generation aimed to identify the genomic state of *BdGSL3* and the existence of the selection marker *bar*. Two different PCRs were performed on gDNA from leaves of five weeks old plants. The amplified products were separated via agarose gel electrophoresis and are presented here (Fig. 9). From the gDNA of the two lines #2-9-4-9 and #2-9-6-30, a product was amplified in the expected size of 246 bp. This implies the existence of the amplified region from the *bar* gene (Fig. 9 A). The wild-type and the two lines #16-12-6-14 and #16-12-10-18 showed no PCR product, indicating the loss of the desired region from the *bar* gene (Fig. 9 A). For the PCR on *bar* the primers TH81 and TH 82 were used (Table 4). To validate the genomic background of *BdGSL3*, a last screening PCR was performed. The resulting PCR products were separated on agarose gel electrophoresis (Fig. 9 B). All four genome edited lines showed a homozygotic deletion in the *BdGSL3* gene (Fig. 9 B). The amplified products from the lines #2-9-4-9, #2-9-6-30 and #16-12-6-14 showed an equal size and are distinct smaller than the wild-type. The line #16-12-10-18 showed a considerably larger deletion in the PCR product compared to the three other lines (Fig. 9 B). The wild-type size allele was not present in all four genome edited lines, indicating disruption of both allele copies and homozygous, stable genetic background in the plants. Based on the assessment of the smaller products, the three lines #2-9-4-9, #2-9-6-30 and #16-12-6-14 should have lost

approximately 50 bp in the target region (Fig. 9 B). While the line #16-12-10-18 should have at least doubled the amount of deleted bps, estimating at 100-120 bp (Fig. 9 B).

To identify the changes in *BdGSL3* precisely, sequencing of the target region was performed for the lines #2-9-4-9, #2-9-6-30, #16-12-6-14 and #16-12-10-18. For this in-depth analysis, PCR products amplified with the Q5 High-Fidelity DNA Polymerase were prepared for sequencing. The preparation was done with a clean-up kit on the excised bands from an agarose gel electrophoresis. The resulting sequences and chromatograms were *in silico* analysed and a sequence alignment with the MAFFT-Algorithm in Benchling revealed the exact position and number of deleted bases and possible integrations (Fig. 10). For the two lines, #2-9-4-9 and #2-9-6-30, two identical deletions between the first two targets with a loss of 67 bp and a cysteine integration at position 513 were present (Fig. 10). The line #16-12-6-14 had an equal deletion of 65 bps in the same region and the same integration of a cysteine (Fig. 10). Additionally, this line had a second integration at position 557, resulting in a stop codon (Fig. 10). For the last line, #16-12-10-18 a considerably different change in the gene is present. At position 366, an exchange from cysteine to guanine happened and at the first target, an 11 bp deletion was identified (Fig. 10). Between the second and fourth target 145 bps are excised from the gene and two additional bp exchanges happened (Fig. 10). At the position 591, adenine is changed to tyrosine and at position 592 another adenine is changed into a guanine (Fig. 10).

To visualise the effect of the described changes in the CDS of *BdGSL3* on the protein sequence, a sequence alignment of the new protein sequences was done in Benchling, using the Clustal Omega algorithm (Fig. 11). As expected, the lines #2-9-4-9 and #2-9-6-30 had identical changes on the AAs sequence, resulting in a possible 1770 AA long protein, missing several amino acids in the n-terminal region (Fig. 11). Furthermore, several amino acids changed in this region compared to the wild-type (Fig. 11). The line #16-12-10-18 translated also into a smaller protein with 1740 AAs compared to the wild-type 1792 AAs. This line had also several amino acid changes flanking the deletion, which partly are in the predicted FKS1 sub domain (Fig. 11). Only line #16-12-6-14 had an induced stop codon after 148 AA, which lead to a sequence of 148 AAs in the ORF (Fig. 11).



Figure 10: Sequence alignment of sequenced PCR products compared to the *BdGSL3* gDNA reference

The Sequence alignment was performed with the MAFFT-Algorithm V.7 (Standley and Katoh 2013) and the reference sequence was taken from GeneBank LOC100843972 (BRADI_2g50140). The blue annotations in front of the targets are the PAM sites; the green annotations indicate the sgRNA targets. The blue annotation indicates the FKS1 subunit domain. The targets are all in the same region between 370 and 560 bp of the gene.



Figure 11: Sequence alignment of the expected protein sequences of *BdGSL3* with the wild-type protein as reference

The sequence alignment was computed with Clustal omega (Sievers et al. 2011) mapped to the reference wild-type protein sequence (XP_010232338). The green annotations indicate the region where the sgRNA binds on the DNA, the annotations are solely for orientation. The blue annotation indicates the FKS1 subunit domain of the protein. The deletions are upstream of the FKS1 subunit domain, whereas for line #16-12-6-14 the resulting stop codon is upstream of the FKS1 subunit domain.

To identify the impact of the described amino acid changes on possible motifs in the genome edited region, a motif prediction search was performed. The results of this motif search are transferred into a table for all lines and the wild-type (Table 20). In the Bd21 wild-type sequence at the genome editing region four motifs were predicted (Table 20). An asparagine glycosylation site at position 139 to 142, an amidation site from aa 158 to aa 161, a myristylation site at position 163 to 168 and a tyrosine phosphorylation site ranging from position 193 to 201 (Table 20).

Table 19: Predicted Motifs for BdGSL3 at the genome edited region of the protein

Line	Start aa	End aa	Motif	Missing / Added
Wild-type	139	142	ASN_Glycosylation	
Wild-type	158	161	Amidation	
Wild-type	163	168	Myristyl	
Wild-type	193	201	Tyr_Phosphatase	
#2-9-4-9	139	142	ASN_Glycosylation	Missing
#2-9-4-9	158	161	Amidation	Missing
#2-9-4-9	163	168	Myristyl	Missing
#2-9-6-30	139	142	ASN_Glycosylation	Missing
#2-9-6-30	158	161	Amidation	Missing
#2-9-6-30	163	168	Myristyl	Missing
#16-12-6-14	139	142	ASN_Glycosylation	Missing
#16-12-6-14	148	148	Stop Codon	Added
#16-12-6-14	158	161	Amidation	Missing
#16-12-6-14	163	168	Myristyl	Missing
#16-12-10-18	139	142	ASN_Glycosylation	Missing
#16-12-10-18	158	161	Amidation	Missing
#16-12-10-18	163	168	Myristyl	Missing
#16-12-10-18	193	201	Tyr_Phosphatase	Missing

The motif search for all four genome edited lines revealed changes in the predicted motifs at the amino acid region of BdGSL3. The lines #2-9-4-9 and #2-9-6-30 have identical changes in this region. Both lines are missing a predicted asparagin glycosylation site (ASN_Glycolysation), an amidation site and an n-myristoylation (Myristyl) site compared to the wild-type motif prediction (Table 20). The line #16-12-6-14 is missing the ASN_Glycolysation site and due to the stop codon, the rest of the protein (Table 20 & Fig. 11). The line #16-12-10-18 is missing the same motifs as the first two lines, but additionally between position 193 and 201 a predicted tyrosine phosphatase site is missing (Table 20).

To identify possible off-site targets a search with the online-tool Cas-OFFinder was performed. Two off-site targets with three mismatches and for each target another four hits were chosen (Table Supplement 2).

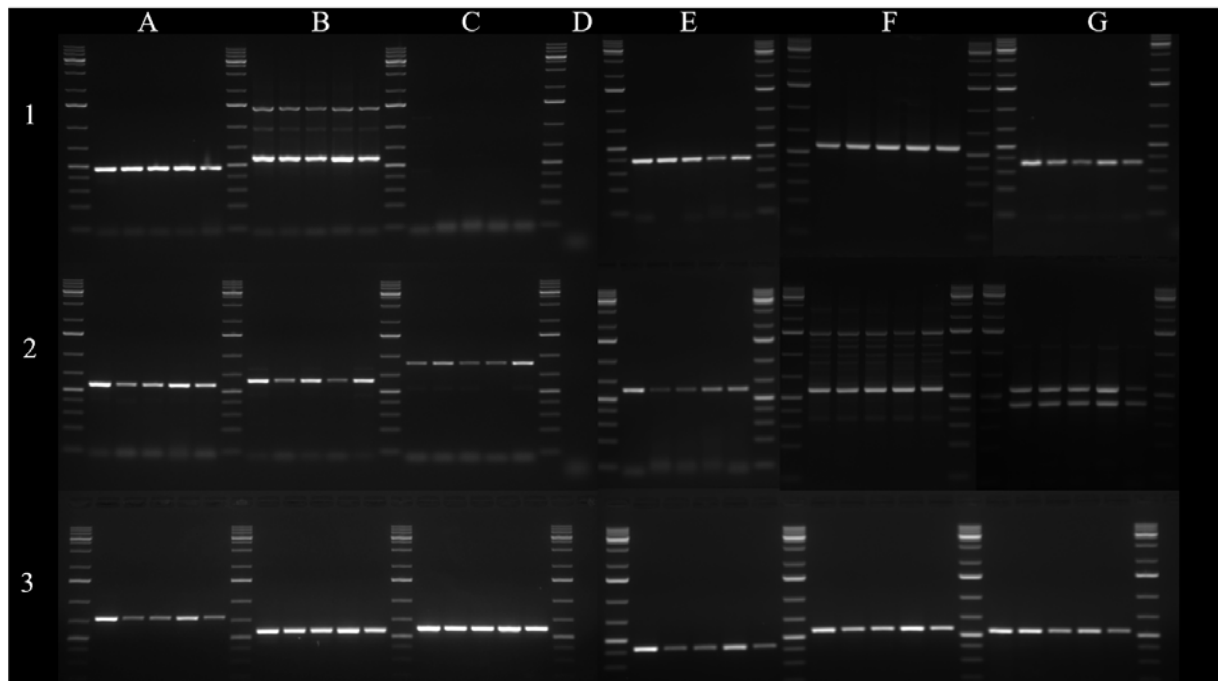


Figure 12: Off-Site target screening for the identified mismatching regions in the genome of Bd21

Sample loading for each off-site target PCR is identical in the following order: Marker, wild-type, #2-9-4-9, #2-9-6-30, #16-12-6-14 and #16-12-10-18 followed by the marker. The used Marker is the GeneRuler 1kb+ supplied by ThermoFisher Scientific. The negative controls are in D1 and D2. A detailed overview of the used primers is in the primer table (Table 4 + Table S. 1) and the identified off-site target regions in the supplement (Table S. 2). No differences in product sizes was detected for any off-site target checked compared to the wild-type. The target C1 (Table S. 2) showed no amplification for the wild-type and the four mutants. For the targets in B1, F2 and G2 (Table S. 2) a specific product could not be amplified even after several attempts. However, the PCR product sizes are identical for all four lines and the wild-type.

The PCR screening to reveal possible insertions or deletions (indels) at off-site targets showed no changes at the chosen off-site targets (Fig. 12). The loading order for each off-site target is as follows: Marker, wild-type, #2-9-4-9, #2-9-6-30, #16-12-6-14, #16-12-10-18 and marker. The marker used for the agarose gel electrophoresis is the GeneRuler 1kb+ from ThermoFisher Scientific. The corresponding off-site targets are listed in the supplement (Tab. S. 2). Negative Controls with the used primers showed no product (Fig. 8, D1 and D2). It is noteworthy, that for one off-site target no amplification was possible (Fig. 8, C1). For three off-site targets, the PCR yielded several products additionally to the desired product (Fig. 8, B1, F2, G2). It was not possible to amplify a single product in the desired size. However, comparing the separated bands from each genome edited line with the wild-type reveals no differences, indicating no indels (Fig. 8, B1, F2, G2).

3.3 Phenotyping of four genome edited *B. distachyon* lines

To identify possible impacts from the genome editing on the genotyped plant lines, a phenotyping of growth and overall look was performed. Plants were measured weekly over a period of eight weeks to gather growth data (Fig. 13). Every week photos were taken to visualise a possible difference in the overall appearance of the plant lines compared to the wild-type.

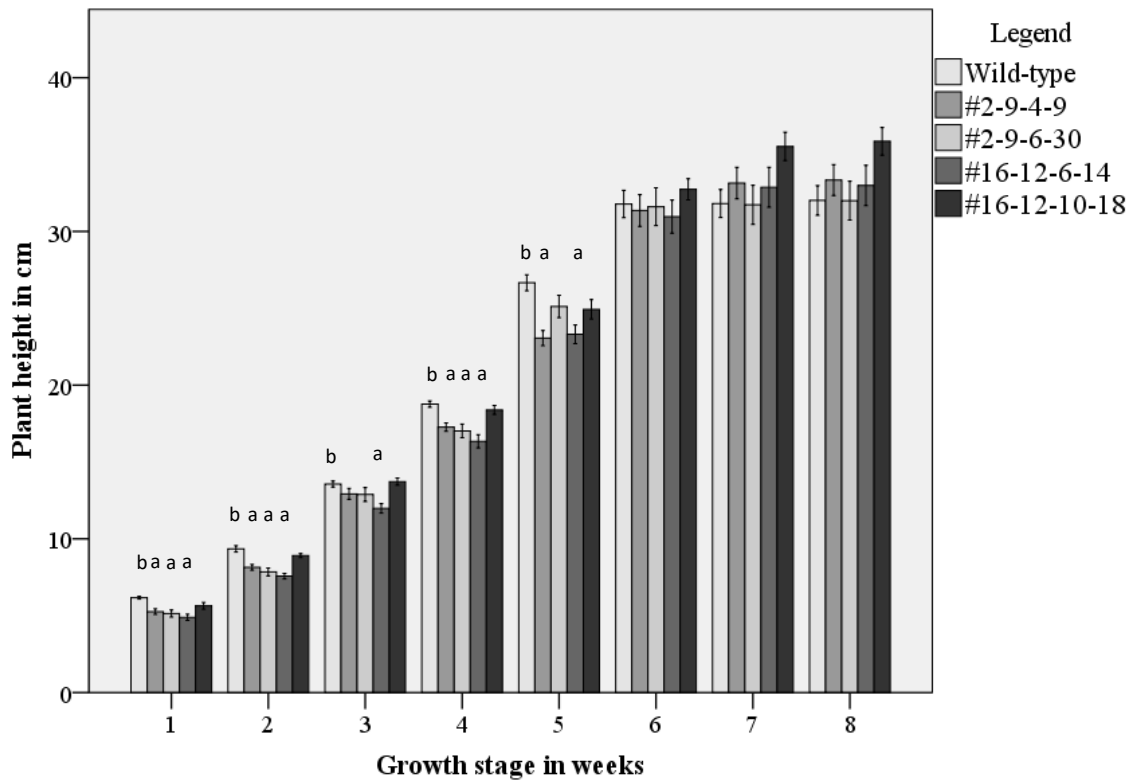


Figure 13: Growth of *B. distachyon* wild-type and the four genome edited lines for an eight weeks life cycle

The height of *B. distachyon* plants was measured for eight weeks and visualised. The mean height of each line is presented; the error bars are indicating the standard error of mean. To test for statistical differences, the data for the weeks one and two were tested with a one-way ANOVA coupled with the Bonferroni post-hoc test and the remaining data sets with a non-parametric Kruskal-Wallis test with Bonferroni correction (Table S. 4 + 5). A significant difference $p < 0.05$ is indicated with a. During the first five weeks, a growth deficiency could be observed. In the first two weeks, this difference was significant for three of the four lines. At the third week only the line #16-12-6-14 was significant shorter than the wild-type. In week four, again the three lines #2-9-4-9, #2-9-6-30 and #16-12-6-14 show a significant growth deficiency compared to the wild-type. In the fifth week, this significance was only present for the lines #2-9-4-9 and #16-12-6-14. After the fifth week no significant difference in growth was observed.

A closer look into the growth of the four genome edited lines compared to the wild-type reveals differences (Fig. 13). In the first week, the height of the wild-type was 6.2 cm, whereas the line #2-9-4-9 was only 5.3 cm tall (Fig. 13 & Tab. S. 3). The lines #2-9-6-30, #16-12-6-14 and #16-12-10-18 were 5.1 cm, 4.9cm and respectively 5.6 cm tall (Fig. 13 + Tab. S. 3).

The reduced height was significant for the lines #2-9-4-9, 2-9-6-30 and 16-12-6-14 (Fig. 13 & Tab. S. 3). This was also present in the second week, where the wild-type grew to a mean of 9.4 cm, the line #2-9-4-9 to 8.1 cm, line #2-9-6-30 to 7.8 cm, #16-12-6-14 was 7.6 cm tall and line #16-12-6-18 8.9 cm (Fig. 13 & Tab. S. 3). The difference was again significant for the three genome edited lines (Fig. 13 & Tab. S. 3). At the third week only #16-12-6-14 with 12 cm height was significantly different to the wild-type with 13.6 cm (Fig. 13 & Tab. S. 3). However, this changed again in the fourth week, which resembles the first two weeks (Fig. 13). After the fifth week, the gap diminishes and at the sixth week, the growth stopped for the wild-type and line #2-9-6-30 (Fig. 13). At the last time point observed after eight weeks, the wild-type and #2-9-6-30 reached a height of 32 cm (Fig. 13 & Tab. S. 3). The lines #2-9-4-9, #16-12-6-14 and #16-12-10-18 reached 33 cm and 35.9 cm (Fig. 13 & Tab. S. 3). The statistical analysis for the last time point revealed no significant differences (Tab. S. 4). Interestingly, the difference for the observed period is split into two phases. The first phase can be considered as a lagging phase, where the vegetative growth was behind the wild-type. In the second phase, the four genome edited lines closed this gap and partially surpassed the wild-type to a certain degree.

For a general overview of the plant appearances under controlled environment, pictures were taken at different time points during their lifecycle (Fig. 14). The photographed time points were two weeks (Fig. 14 A), five weeks (Fig. 14 B) and eight weeks (Fig. 14 C). In these time points the early vegetative phase is presented after two weeks. The switch from vegetative to a reproductive phase is present around the fifth week and illustrated (Fig. 14 B). To get an overview of the reproductive phase the eight weeks age was chosen since the flowering was completed and seeds were formed. Additionally, the senescence started at this age (Fig. 14 C).

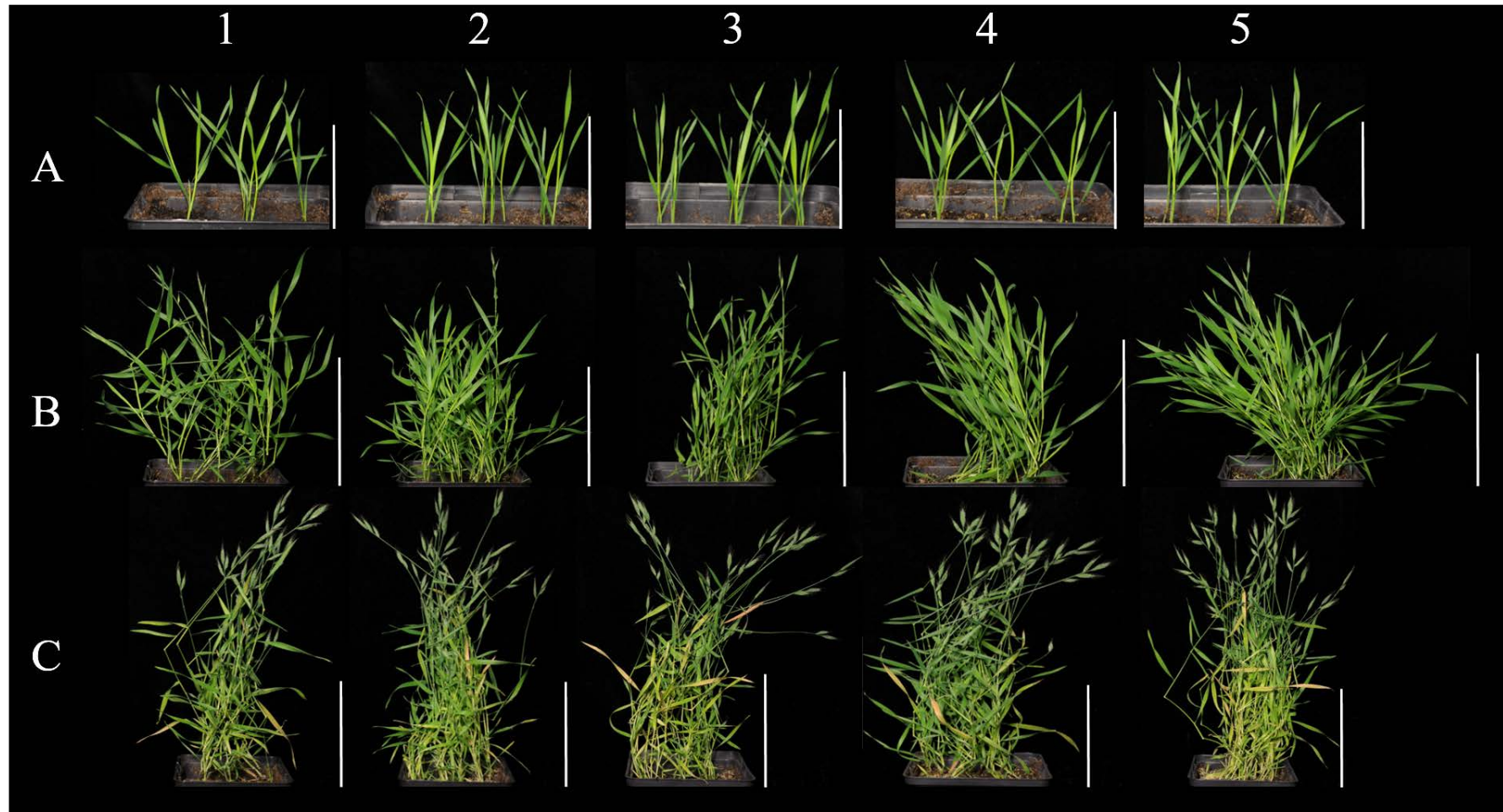


Figure 14: Overview of different growth stages for *B. distachyon* wild-type Bd21 and the four genome edited lines

The columns numbered from one to five are in the following order: 1: wild-type, 2: #2-9-4-9, 3: #2-9-6-30, 4: #16-12-6-14 and 5: #16-12-10-18. The scale bars indicate for row **A** 5 cm and for the rows **B** and **C** 10 cm. **A)** Two weeks old plants are shown. The four genome edited lines showed a slight reduced growth compared to the wild-type but no major differences or defects in growth, leaves or hypocotyl compared to the wild-type were present. **B)** Five weeks old plants are shown. When comparing the four genome edited lines to the wild-type the differences are only minor. The wild-type and the two lines #2-9-4-9 and #2-9-6-30 already shifted from vegetative growth to early reproductive stage in their life cycle. The wild-type is slightly ahead compared to the four genome edited lines, which are lagging in spikelet formation. The two lines #16-12-6-14 and #16-12-10-18 did not formed reproductive organs at this age. **C)** After eight weeks, there was no difference observable. Spikelet formation was completed for all observed lines and senescence started. No differences in this stage was observable.

At the early vegetative phase at two weeks, the genome edited lines were similar to the wild-type (Fig. 14 A). The plants were still in leaf forming state and the stem growth did not started. During the end of the vegetative phase, roughly after five weeks, the plants started to form the reproductive organs, but stem growth was still present (Fig. 14 B & Fig. 13). Here, the four genome edited lines seemed a little bit behind when compared to the wild-type which at this time point had already slightly bigger spikelets. The two lines #2-9-4-9 (Fig. 14 B 2) and #2-9-6-30 (Fig. 14 B 3) were closer to the wild-type (Fig. 14 B 1) than the two other genome edited lines (Fig. 14 B 4 & B 5). The vegetative growth ended after six to seven weeks (Fig. 13), and when compared with the wild-type all genome edited lines showed a comparable phenotype (Fig. 14 C 1-5). The plants blossomed and seeds were formed, the age dependent senescence at the end of the *B. distachyon* life cycle started (Fig. 14 C1-5). At this stage, no abnormalities were observed (Fig. 14 C 1-5).

In summary, BdGSL3 disruption had a slight impact on the genome edited *B. distachyon* lines compared to the wild-type Bd21 genotype. There was a growth difference with a lagging-phase in the early vegetative stage, that transformed after five weeks in a slightly longer vegetative growth with three of four genome edited lines surpassing the wild-type in height (Fig. 13). When comparing the overall phenotype of the wild-type and the four genome edited lines, no major differences or abnormalities could be observed. The overall life cycle of *B. distachyon* was not altered by the genome editing of *BdGSL3* (Fig. 14).

3.4 Infection analysis of genome edited plants

To study the role of BdGSL3 in plant defence, infections with the wheat pathogen *F. graminearum* were performed. For the analysis of those infections, three different time points are crucial. 1) 14 days post inoculation (dpi) to evaluate the infection on a phenotypical level for a longer period. 2) 7 dpi to evaluate a possible difference in the pace of host colonisation of *F. graminearum* and microscopic analysis. 3) 3 dpi to examine the forming of callose depositions in the infected spikelet rachis area on microscopic level.

To monitor the infection with *F. graminearum* 8/1 and the disease phenotype of the FHB, the Disease Score was evaluated from infected spikelets at 14 dpi (Fig. 15).

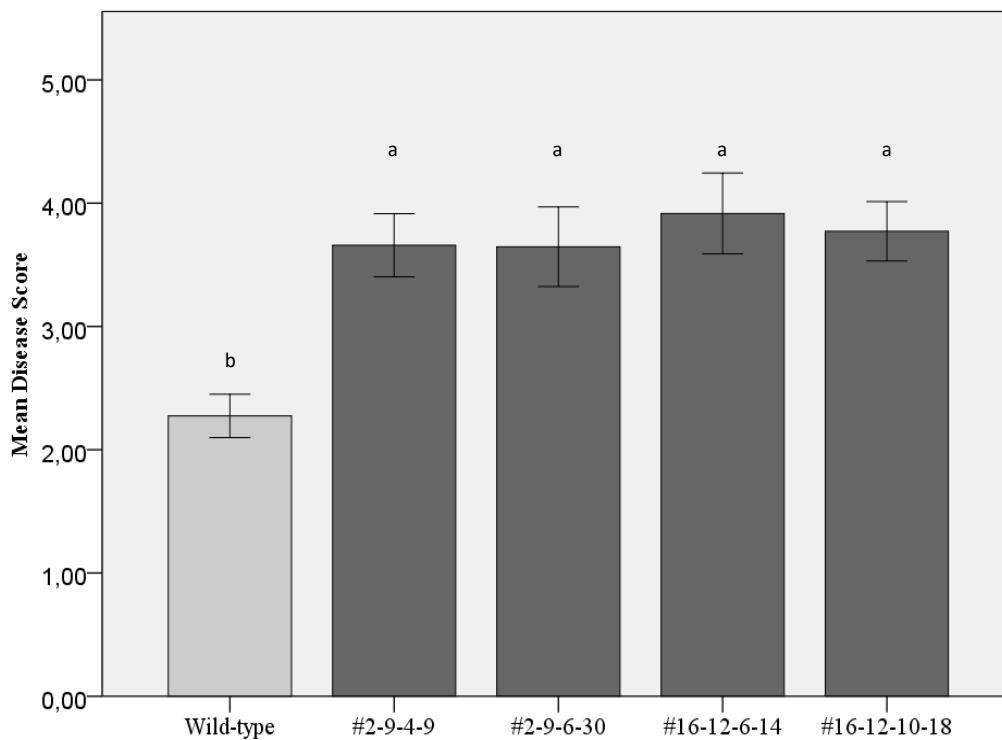


Figure 15: Disease Score mediated evaluation of *F. graminearum* 8/1 infection in *B. distachyon* at 14 dpi

Inoculated *B. distachyon* spikelets were evaluated 14 dpi with *F. graminearum* 8/1. The wild-type (WT) shows a disease score of 2.3, the line #2-9-4-9 reached a score of 3.7, #2-9-6-30 scores 3.6, #16-12-6-14 showed the highest score with 3.9 and #16-12-10-18 achieved a Disease Score of 3.6. The error bars indicate the standard error of mean. A one-way ANOVA was performed with a Dunnett T3 Post-Hoc test. Statistical differences to the wild-type are indicated with a. All four lines reached significant higher Disease Scores than the WT. $n_{(WT)}=20$; $n_{(\#2-9-4-9)}=44$; $n_{(\#2-9-6-30)}=41$; $n_{(\#16-12-6-14)}=42$; $n_{(\#16-12-10-18)}=46$.

The 14 dpi disease scoring revealed a difference between the wild-type and the four genome edited lines. After 14 days, the wild-type showed a Disease Score of 2.3 (Fig. 15 & Tab. S. 10). For the four genome edited lines the Disease Score was significantly higher (Fig. 15 & Tab. S. 11). The line #2-9-4-9 had a mean Disease Score of 3.7 (Fig. 15 & Tab. S. 10).

For the line #2-9-6-30, the mean Disease Score was at 3.6, which was close to the score of #2-9-4-9 (Fig. 15 & Tab. S. 10). The line #16-12-6-14 had the highest mean Disease Score with 3.9, compared with all the other tested lines, and the line #16-12-10-18 scored a mean Disease Score of 3.6 (Fig. 15 & Tab. S. 10). At 14 dpi all four genome edited lines showed a more severe disease resulting in a higher Disease Score compared to the wild-type. The FHB disease is present in more than three florets (Fig. 15). The strongest score was observed for the line #16-12-6-14 after 14 dpi (Fig. 15).

To test whether the FHB disease is significantly stronger in the genome edited lines than in the wild-type, a one-way ANOVA followed by a Dunnett T3 Post-Hoc test was performed (Table S. 11). The one-way ANOVA revealed significant differences for all four lines compared to the wild-type. The lines #2-9-4-9, #16-12-6-14 and #16-12-10-18 were highly significant with a p value of 0.000 (Tab. S. 11). The line #2-9-6-30 is also highly significant; the p value for this line is at 0.004 (Tab. S. 11).

Based on the 14 dpi evaluation of the FHB disease in *B. distachyon* and the significant differences in the disease severity between the *B. distachyon* wild-type Bd21 and the four genome edited lines, further studies were performed. One follow up study was the evaluation of an earlier time point to identify whether the differences were present during already at earlier stages of the FHB disease or manifests only at the late 14 dpi stage. Therefore, 7 dpi infections were surveyed and the Disease Score evaluation was performed. Additionally, confocal laser scanning microscopy were performed on 7 dpi spikelets to identify possible differences in the infection and colonisation at this stage. Stereomicroscopic pictures were taken to visualise the macroscopic differences of the FHB disease between the wild-type and the four genome edited lines. The evaluated mean Disease Score after 7 days post inoculation with *F. graminearum* strain 8/1 is shown in figure 16.

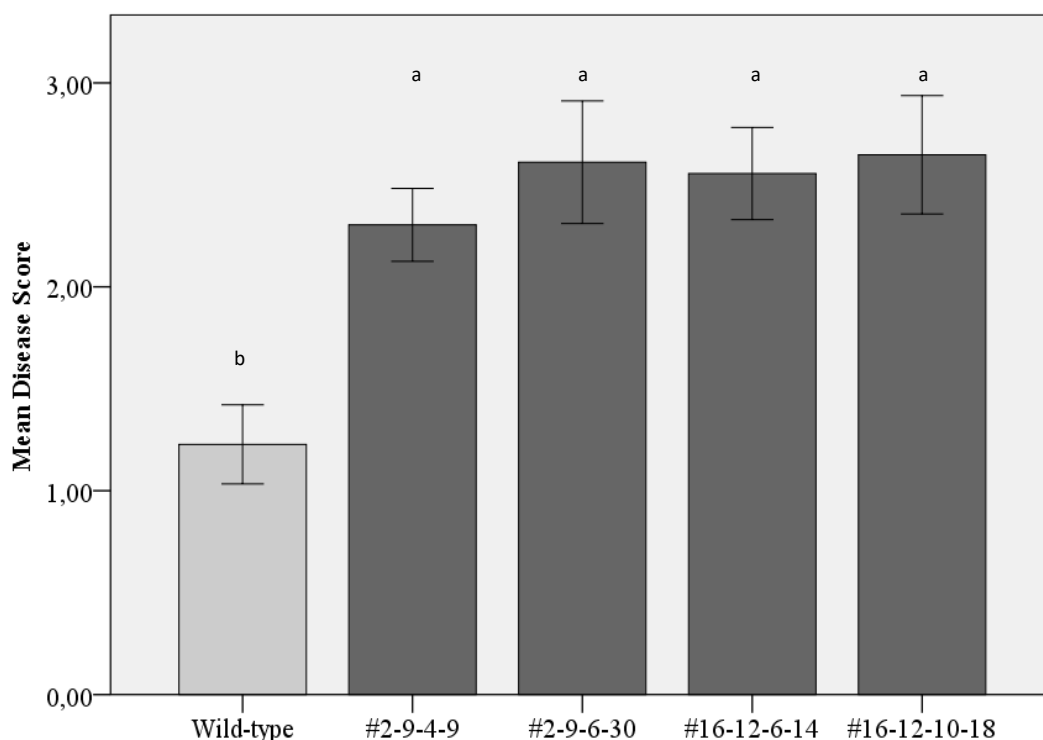


Figure 16: Evaluation of FHB Disease Score of *B. distachyon* spikelets at 7dpi with *F. graminearum* 8/1

Inoculated *B. distachyon* spikelets were evaluated at 7 dpi with *F. graminearum* and the Disease Score evaluated. The wild-type (WT) reached a mean Disease Score of 1.2, the four different lines reached a significantly higher Disease Score. The line #2-9-4-9 achieved a mean rating of 2.3, line #2-9-6-30 2.6, #16-12-6-14 2.55 and #16-12-10-18 the highest score with 2.65. The error bars indicate the standard error of mean. To test for significance, the non-parametric Kruskal-Wallis test followed by a Bonferroni correction was performed (Tab. S. 8 + 9). Significance is represented with a. All four genome edited lines reached a significant higher Disease Score rating than the wild-type (Tab. S 8 + 9). $n_{(WT)}=20$; $n_{(\#2-9-4-9)}=44$; $n_{(\#2-9-6-30)}=41$; $n_{(\#16-12-6-14)}=42$; $n_{(\#16-12-10-18)}=46$.

The evaluation of the 7 dpi state of FHB disease and the observed differences resembles the already described disease state at 14 dpi (Fig. 15 & Fig. 16). The wild-type is rated with a mean Disease Score of 1.2 after 7 dpi (Fig. 16 & Tab. S. 7). All four genome edited lines had a stronger infection resulting in a higher Disease Score (Fig. 16 & Tab. S. 7). The line #2-9-4-9 had the lowest Disease Score of all four lines, ranked with 2.3 (Fig. 16 & Tab. S. 7). The line #2-9-6-30 reached a mean Disease Score of 2.6, while the lines #16-12-6-14 and #16-12-10-18 scored at 2.55 and 2.65 respectively (Fig. 16 & Tab. S. 7). To test for significance between the wild-type and the genome edited lines a non-parametric Kruskal-Wallis test followed by a Bonferroni correction was performed (Table S. 9). The line #2-9-4-9 had an adjusted significance of 0.005, the line #2-9-6-30 scored 0.008, the line #16-12-6-14 and #16-12-10-18 scored 0.001 and 0.002 respectively (Tab. S 9).

For an overview of the infection at 7 dpi, longitudinal sections of infected spikelets were prepared. Pictures were taken with a stereo microscope and are presented (Fig. 17). The wild-type showed common symptoms of FHB in *B. distachyon*. The inoculated floret was completely necrotic and florets above started to show necrotic tissue (Fig. 17 A). The water control at this stage showed no symptoms of FHB (Fig. 17 F). The four genome edited lines exhibited a stronger FHB disease (Fig. 17 B – E). The line #2-9-4-9 had additionally to the fully necrotic inoculated floret necrosis symptoms in adjacent florets above. Two more florets were also necrotic. While the second one is fully necrotic, the third floret shows necrosis at the basal tissue (Fig. 17 B). Water control showed no symptoms of the FHB disease (Fig. 17G). This disease phenotype was also present for the line #2-9-6-30 (Fig. 17 C). The inoculated floret was fully necrotic, and two more florets showed large necrotic areas (Fig. 17 C). However, the water control showed no disease symptoms (Fig. 17 H). The FHB disease in the line #16-12-6-14 was also more severe compared to the wild-type (Fig. 17 D). The inoculated floret was completely necrotic, adjacent florets above showed large necrotic tissue (Fig. 17 D). However, the disease is comparable to the other genome edited lines. The water control showed no symptoms (Fig. 17 I). This condition was also present for the last line. The line #16-12-10-18 showed two necrotic florets and necrotic tissue on adjacent florets above (Fig. 17 E). Water control for this line showed no disease symptoms (Fig. 17 J).

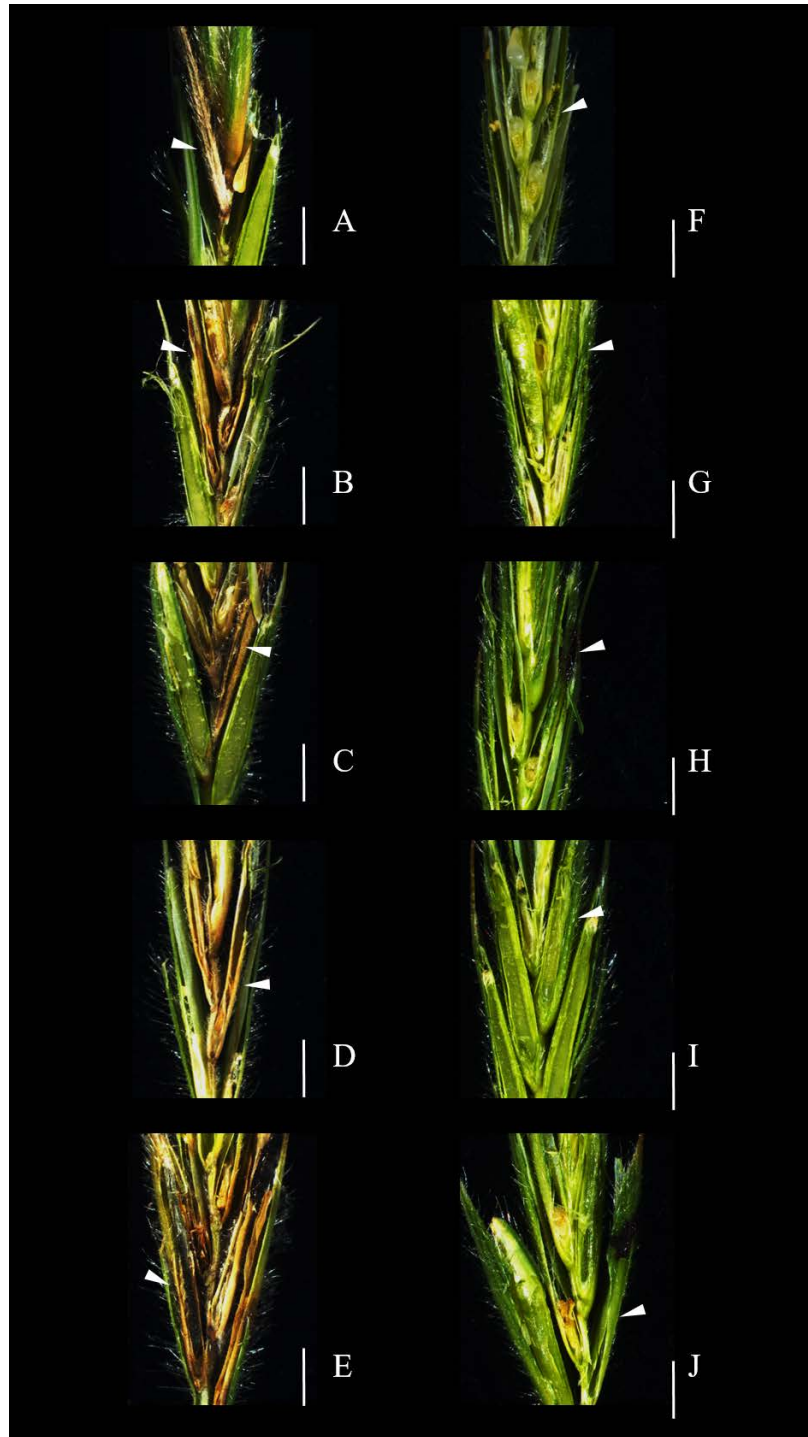


Figure 17: Overview of the *F. graminearum* mediated FHB disease at 7 dpi on the *B. distachyon* wild-type Bd21 and the four genome edited lines

The scale bar indicates 2mm, the white arrows indicate the inoculated floret. **A – E)** Spikelets at 7 dpi with *F. graminearum*. **F – J)** Water control at 7 dpi with upH₂O. In all five *B. distachyon* lines no necrosis or other symptoms of FHB was detected. **A)** The infection in the wild-type inbred line Bd21 revealed a fully necrotic inoculated floret. Adjacent florets above showed the beginning of necrosis. **B)** Infected spikelet of the genome edited line #2-9-4-9; two florets were fully necrotic; a third floret showed a large amount of necrotic tissue. **C)** In line #2-9-6-30 the inoculated floret was fully necrotic and two additional florets showed the FHB disease. **D)** The inoculated floret of line #16-12-6-14 was completely necrotic. The FHB disease is spreading throughout the spikelet and adjacent florets were necrotic too. **E)** Two florets were fully necrotic and two additional florets started to show necrosis in the basal parts of the florets. For line #16-12-10-18 the strongest disease symptoms were observed.

In addition to the stereo microscopic pictures, microscopy of the inoculated florets was performed. In Ethanol fixed longitudinal sections of inoculated spikelets were used to investigate in detail how the infection differs between the genome edited lines and the wild-type of *B. distachyon*.

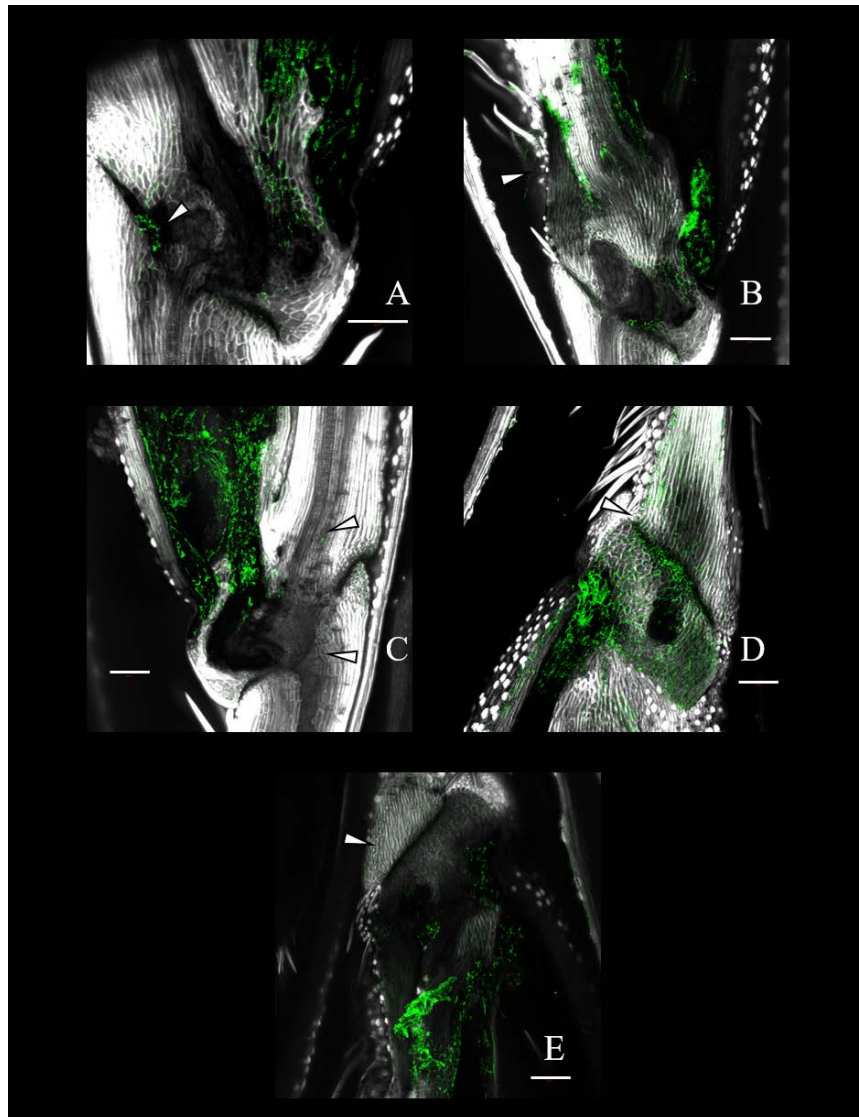


Figure 18: Confocal Laser Scanning Microscopy of inoculated *B. distachyon* florets at 7 dpi with *F. graminearum* strain 8/1

The scale bar in each picture indicates 100 μm . The fixed spikelets were stained with aniline blue shown in grey and the pathogenic fungus *F. graminearum* stained with WGA conjugated to Alexa Fluor 488 shown in green. **A)** Wild-type floret of *B. distachyon* Bd21. The pathogen started to grow through the rachis node but did not colonise adjacent tissue (arrow). **B)** The infection of the line #2-9-4-9 spread further. *F. graminearum* did not only penetrate the rachis node, but also started to infect the rachis and adjacent tissue (arrow). **C)** The line #2-9-6-30 showed less fungus in the adjacent tissue compared to #2-9-4-9; however, the amount of fungal tissue in the inoculated floret is higher. Spreading into the rachis of the above floret is indicated (arrow). **D)** The rachis node, the rachis and adjacent tissue is completely colonised by *F. graminearum* in the line #16-12-6-14 (arrow). **E)** Comparable to the other genome edited lines, in the line #16-12-10-18 the pathogen colonised the rachis node and is already in the adjacent rachis (arrow). Compared to the wild-type, in all four genome edited lines fungal tissue was detected beyond the rachis node in adjacent tissue and the rachis compared to the wild-type.

The microscopy of the inoculated florets supports the already existing data at 7 dpi. In the wild-type floret, the pathogen was detected at the rachis node and started with penetration of the rachis node (Fig. 18 A). In the four genome edited lines, *F. graminearum* penetrated the rachis node and was detected in adjacent tissue colonising the rachis and the rest of the spikelet (Fig. 18 B - E). In the line #2-9-4-9 the pathogen colonised the rachis node and the rachis above the inoculated floret (Fig. 18 B). This was also observed for the line #2-9-6-30. *F. graminearum* was also able to penetrate the rachis node and colonise the rachis of floret above (Fig. 18 C). This phenotype was also observable for the lines #16-12-6-14 and #16-12-10-18. In both lines, *F. graminearum* colonised the rachis node and the adjacent rachis of the spikelet (Fig. 18 D + E).

In conclusion, the 7 dpi state of the FHB disease in *B. distachyon* showed differences in the macroscopic observation of the disease and the microscopic observation of the infection. The disease symptoms were more severe in the genome edited lines (Fig. 15 + Fig. 16). On microscopic level, this difference is not that distinct, the fungus was in all tested lines and the wild-type able to colonise the rachis node (Fig. 18). However, it was possible to detect *F. graminearum* in the rachis of spikelets from the genome edited lines but not in the wild-type (Fig. 18 B – E). To study the influence of callose formation and the role of BdGSL3 in the FHB disease response the forming of callose depositions after 3 dpi were examined. Confocal Laser Scanning Microscopy of inoculated *B. distachyon* spikelets were performed to visualise the callose forming in response to the *F. graminearum* 8/1 infection (Fig. 19).

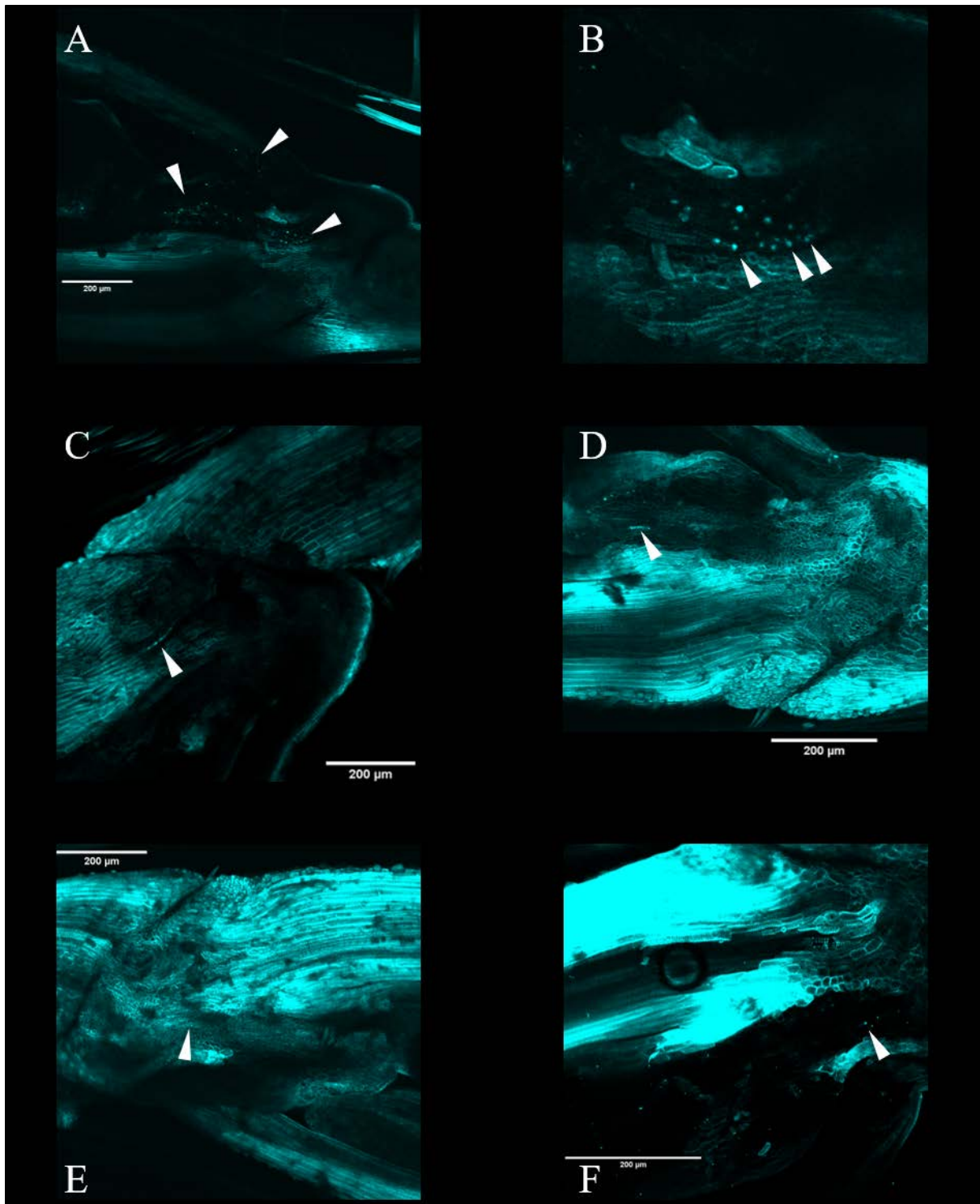


Figure 19: Callose depositions in spikelets of *B. distachyon* 3 dpi with *F. graminearum* 8/1

Pictures of inoculated *B. distachyon* florets 3 dpi inoculated with *F. graminearum*, stained with aniline blue. Scale Bar indicates 200 µm. **A)** Wild-type 3 dpi spikelet showed the forming of callose depositions as response to the *F. graminearum* infection. The white arrows indicate callose depositions in the inoculated floret and the rachis node. **B)** Closer look of the wild-type callose depositions in the rachis node marked in **A**. **C)** For the line #2-9-4-9 only rarely callose depositions were found. The arrow indicates some callose depositions. **D)** At the inoculated floret of the line #2-9-6-30 some callose depositions were observed (arrow). **E)** For the line #16-12-6-14 nearly no callose depositions were found. Some minor depositions are indicated close to the rachis node (arrow). **F)** The line #16-12-10-18 responded with only scattered small callose depositions close to the rachis node (arrow). Overall, the response was weaker for all four genome edited lines compared to the wild-type.

The microscopy of the 3 dpi samples revealed a reduced amount of callose depositions after inoculation with *F. graminearum*. The wild-type showed several callose depositions at the infected floret and rachis node (Fig. 19 A+B), whereas the genome edited lines revealed less callose depositions (Fig. 19 C - F). The line #2-9-4-9 showed some depositions at the inoculated floret (Fig. 19 C). This was also the case for the line #2-9-6-30 with occasional callose depositions in the floret (Fig. 19 D). The line #16-12-6-14 hardly had any callose depositions at the inoculated floret or the rachis node (Fig. 19 E). Only reduced amounts of scattered callose depositions were detected for the line #16-12-10-18 (Fig. 19 F).

For a better overview about the callose response in inoculated florets, a relative quantification was carried out to reveal and quantify the observed differences (Fig. 20).

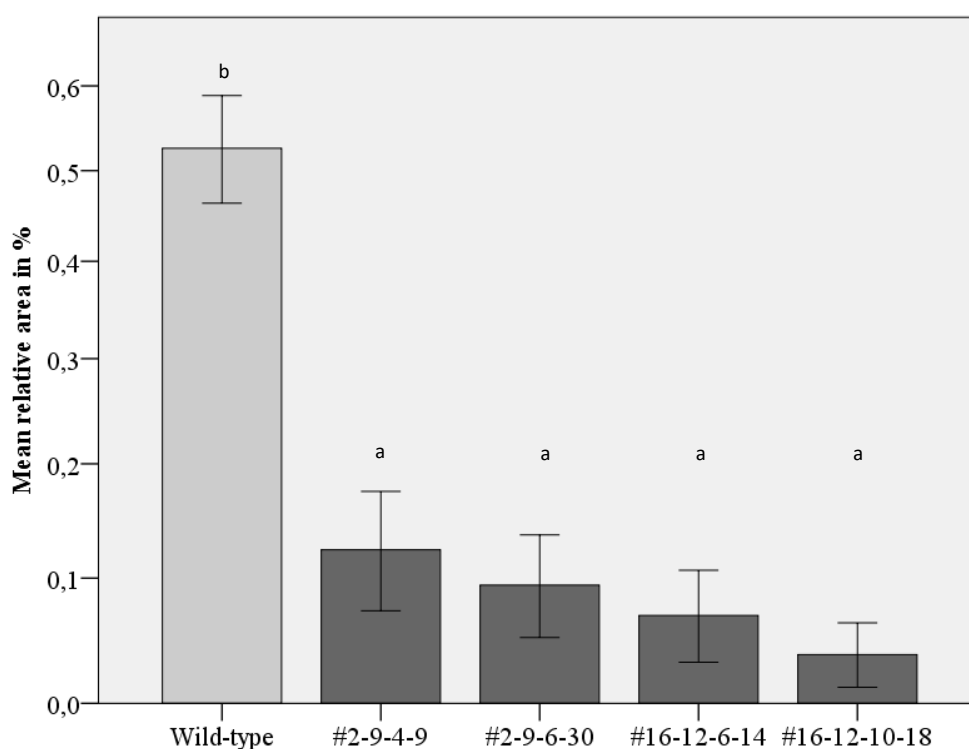


Figure 20: Mean relative area of callose depositions in 3 dpi spikelets of *Brachypodium distachyon*

This bar chart presents the mean relative area covered of callose depositions in inoculated *B. distachyon* spikelets at 3 dpi with *F. graminearum*. The mean area of callose deposition is shown in percentage of the whole basal floret area. The error bars indicate the standard error of mean. To test for significance, the non-parametric Kruskal-Wallis test was performed followed by a Bonferroni correction, significance is shown with an a (Tab. S. 13). The wild-type (WT) had a mean area of 0.53 % covered with callose depositions. The genome edited lines have significant less callose depositions, in the line #2-9-4-9 only 0.12 % are covered. Line #16-12-6-14 and line #16-12-10-18 had 0.07 % and 0.04 % relative callose area respectively. $n_{(WT)} = 10$; $n_{(\#2-9-4-9)} = 10$; $n_{(\#2-9-6-30)} = 10$; $n_{(\#16-12-6-14)} = 9$; $n_{(\#16-12-10-18)} = 10$.

When compared to the wild-type, the four genome edited lines responded with an reduced amount of callose in the inoculated spikelet at 3 dpi (Fig. 19 + Fig. 20). The wild-type had 0.53 % of the area covered with callose depositions, while the line #2-9-4-9 only 0.12 % (Fig. 20). The line #2-9-6-30 had an even lower amount of callose, covering only 0.9 % of the measured area (Fig. 20). The other two genome edited lines #16-12-6-14 and #16-12-10-18 had a callose coverage of 0.07 % and 0.04 % respectively (Fig. 20). The area covered with callose depositions was highly reduced in the four genome edited lines. This supports the already presented results of the infection at 14 dpi and 7 dpi, which showed a more severe FHB disease in these lines compared to the wild-type. The significance value for the line #2-9-4-9 was 0.011, the line #2-9-6-30 had a significance of 0.008 while the lines #16-12-6-14 and #16-12-10-18 had a significance of 0.001 and 0.000 respectively (Table S. 13).

Infection studies of *B. distachyon* spikelets revealed significant differences between the wild-type and the four genome edited lines. It was shown, that the FHB disease is more severe in the genome edited lines during different stages of the disease (Fig. 15 + Fig. 16). At the late stage of 14 dpi, the spikelets of the four genome edited lines are significant stronger infested with *F. graminearum* compared to the wild-type (Fig. 15). This was also the case at the earlier 7 dpi time point of the FHB disease evaluation (Fig. 16) Stereo microscopic photographs revealed differences in the infection and the formation of necrotic tissue (Fig. 17). Confocal Laser Scanning Microscopy revealed a faster colonisation of the rachis and rachis node by *F. graminearum* in the four genome edited lines compared to the wild-type (Fig. 18). To reveal the cause of these differences, an analysis of callose depositions at 3 dpi was performed (Fig. 19 + Fig. 20). This analysis quantified the area of callose depositions in relation to the floret rachis node. It was revealed that in all four genome edited lines significant less callose is formed at this state of the FHB disease compared to the Bd21 wild-type (Fig. 20).

3.5 Wounding and pathogen induced callose response in leaves of *B. distachyon*

To study the callose mediated stress response in leaves, wounding assays and infections with the necrotrophic leaf pathogen *Parastagonospora nodorum* SN15 were performed. Confocal Laser Scanning Microscopic was used to visualise the wounded and inoculated leaves of *B. distachyon* wild-type and the four genome edited lines.

Wounding was performed on leaves of *B. distachyon* after inflicting of mechanical damage to the leaves. Two different time points were selected, and the fixed leaves were stained with aniline blue to visualise callose around the wounded tissue.

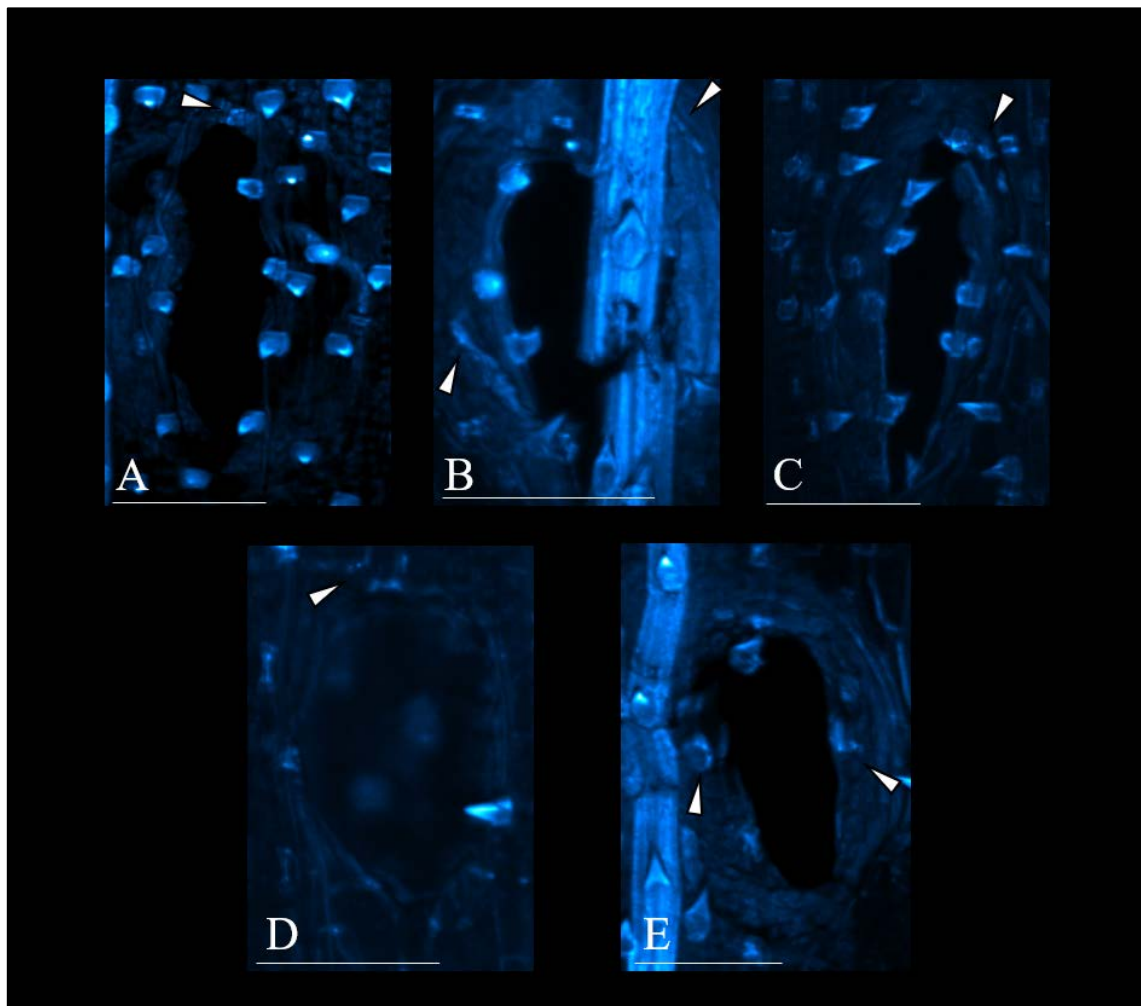


Figure 21: Wounding induced callose depositions in *B. distachyon* leaves six hours after wounding

Scale bar equals 100 μ m. **A)** Wild-type leaf with minor callose depositions (arrow). **B)** Line #2-9-4-9 responded with some callose depositions adjacent to the wounded tissue (arrow). **C)** #2-9-6-30 showed also only scarce callose at the surrounding cells. **D)** Callose formation adjacent to the wound in line #16-12-6-14 (arrow). **E)** #16-12-10-18 responds with little callose depositions at the wound (arrow). Overall, the response in the wild-type and all four genome edited lines did not differ and was rather weak.

The microscopy of wounded leaves at the 6 h time point revealed for all examined lines a comparable callose response (Fig. 21). In the wild-type minor callose depositions were found in adjacent cells to the wound (Fig. 21 A). This was also the case for the genome edited lines. The line #2-9-4-9 showed callose forming around the wound to seal the damaged tissue (Fig. 21 B). This induced callose for wound sealing was also detected in the line #2-9-6-30 (Fig. 21 C) and the last two genome edited lines #16-12-6-14 (Fig. 21 D) and #16-12-10-18 (Fig. 21 E). The callose response in all examined *B. distachyon* lines was rather weak at this early time point. This weak response at the six-hour time point did not gave much enlightenment for the role of BdGSL3 in wounding related stress response and callose formation in leaves. Therefore, a later time point needed to be examined, to reveal possible influence of BdGSL3 on wound sealing in leaves.

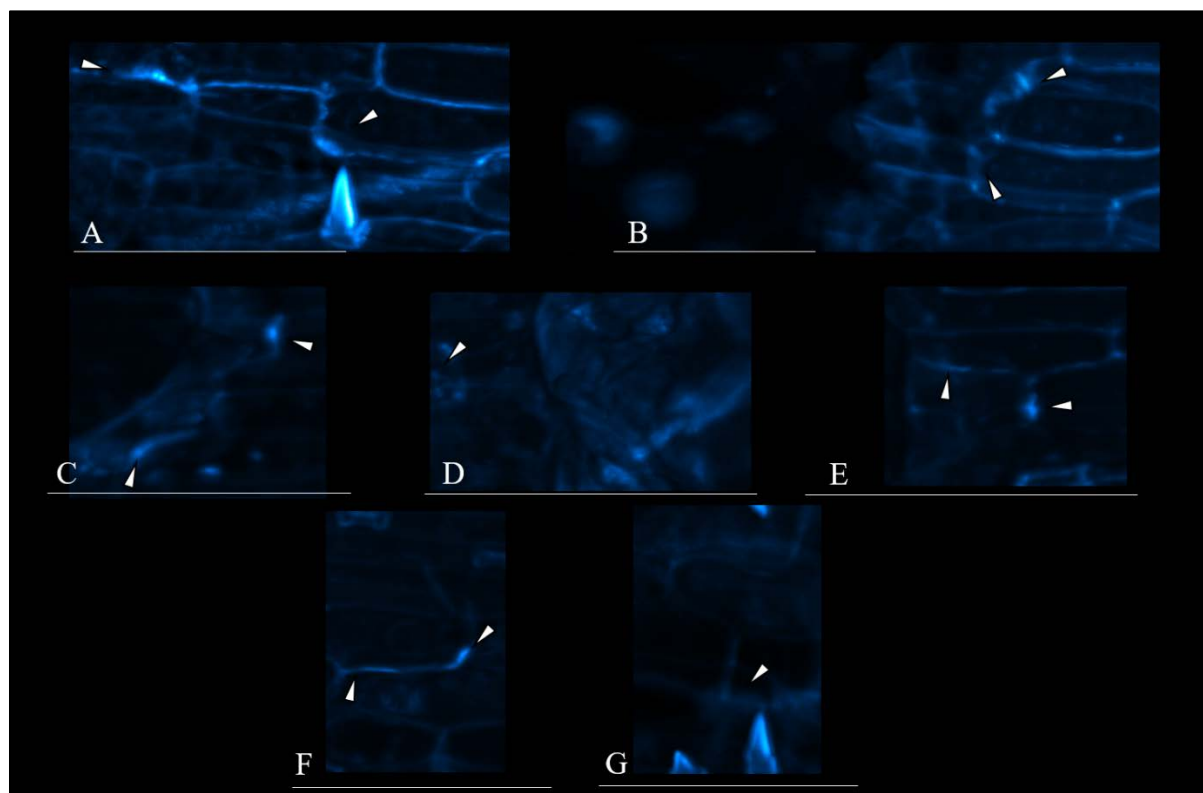


Figure 22: Wounding induced stress response and callose forming of *B. distachyon* leaves 16 hours after wounding

Scale bar equals 100 μ m. **A)** Wild-type responses with moderate callose in the cell walls close to the wound. The callose thickens at some cell walls (arrows). **B)** The line #2-9-4-9 response was weaker compared to the wild-type. Callose was scattered at cell walls of adjacent cells to the wound (arrows). **C)** Line #2-9-6-30 responded to the wounding after 16 hours with the formation of callose. Compared to the wild-type, this response was weaker (arrows). **D+E)** For the line #16-12-6-14 the response to wounding was unvarying compared to the other genome edited lines (arrows). **F+G)** The line #16-12-10-18 showed only minor callose depositions after 16 h (arrow). This is comparable to the other four lines and a weaker response compared to the wild-type. In general, the genome edited lines also responded with callose 16 h after wounding, however the reaction was weaker than in the wild-type.

The imaging of leaves 16 hours after wounding revealed some differences to the earlier time point (Fig. 21 & Fig. 22). After 16 hours, the callose response in the four genome edited lines was slightly weaker compared to the wild-type (Fig. 22). The wild-type responded with callose in the adjacent cells to the wounded tissue as a barrier and wound sealing, indicated by the arrows (Fig. 22 A).

The genome edited lines show a different response compared to the wild-type. The line #2-9-4-9 showed a weaker callose response around the artificial inflicted wounds (Fig. 22 B). Line #2-9-6-30 had a quite similar response like the line #2-9-4-9 and showed some callose forming in the cell wall of adjacent cells indicated by the arrow (Fig. 22 C). The other two lines showed a similar phenotype in the microscopic image. The line #16-12-6-14 showed only some scattered callose depositions in the surrounding cells indicated by the arrows (Fig. 22 D + E). For the line #16-12-10-18 there was also only a weak reaction observed via microscopy (Fig. 22 F+G). Some callose was formed close to the wounding incident, but the response was not on the wild-type level. Overall, the callose response after wounding is relatively weak, but the genome edited lines showed a weaker response compared to the wild-type at 16 hours after wounding. To better visualise the difference, a quantification of mean relative area of callose depositions at the wounding area was evaluated.

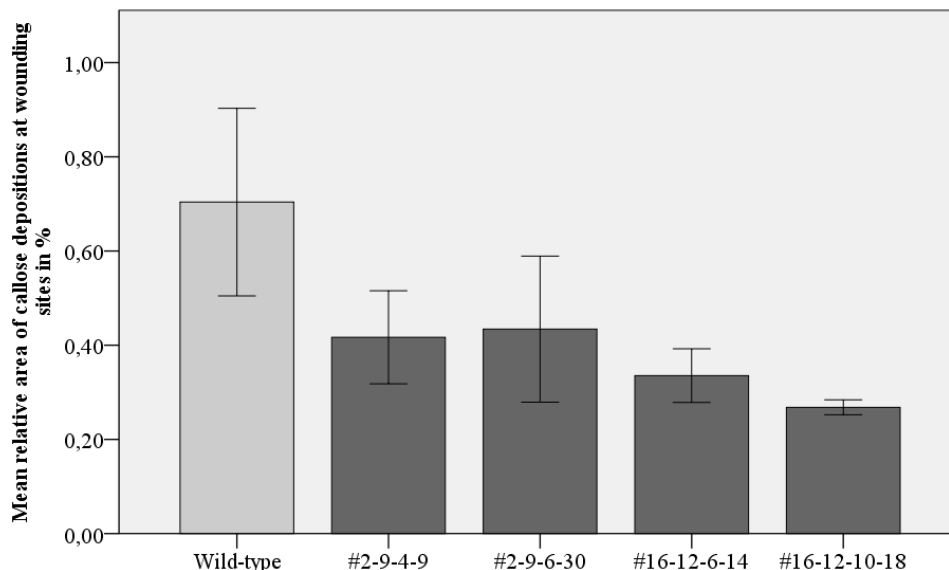


Figure 23: Mean relative area of callose depositions at wounded tissue 16 hours after wounding

The mean area of callose depositions around the wounding sites were quantified 16 hours past wounding. The mean area is shown in percentage to the wounded area. The error bars equal the standard error of mean. A non-parametric Kruskal-Wallis test was used to identify significant differences (Tab. S. 29). No significance was detected between the wild-type and each of the four genome edited lines. However, a clear indication for a reduced callose response is revealed. The wild-type formed callose equalling 0.7 % of the area. All four genome edited lines accumulate less callose, the line #2-9-4-9 had a coverage of 0.42 %, #2-9-6-30 0.43 %, the line #16-12-6-14 0.34 % and the line #16-12-10-18 only 0.27 %. $n_{(WT)}=4$; $n_{(\#2-9-4-9)}=7$; $n_{(\#2-9-6-30)}=4$; $n_{(\#16-12-6-14)}=5$; $n_{(\#16-12-10-18)}=4$.

The mean area of callose depositions at wounds 16 hours after wounding were quantified and are presented here (Fig. 23). The wild-type accumulated 0.7 % (Tab. S. 28) while the four genome edited lines showed a trend to accumulate less callose in comparison (Fig. 23). The line #2-9-4-9 only covered 0.42 % of the area with callose, the line #2-9-6-3 0.43 % while the two lines #16-12-6-14 and #16-12-10-18 covered 0.34 % and 0.27 % respectively (Fig. 23 + Tab. S. 28). A statistical analysis should reveal possible significant differences between the wild-type and each of the four genome edited lines. However, the non-parametric Kruskal-Wallis test found no significant differences (Tab. S. 29).

The callose response after abiotic wounding stress revealed only minor differences between the wild-type and the four genome edited lines. However, the main interest lies in the callose response to biotic stress. Therefore, a biotic stress like a pathogen infection should be observed. In the host pathogen interaction, many different interactions on molecular levels are in place that can affect the stress response on various ways. Therefore, infection with the necrotrophic leaf pathogen *Parastagonospora nodorum* strain SN15 were performed on leaves of the *B. distachyon* wild-type line Bd21 and the four genome edited lines. Confocal Laser Scanning Microscopy with inoculated leaves was done to visualise the pathogen induced stress response of *B. distachyon*.

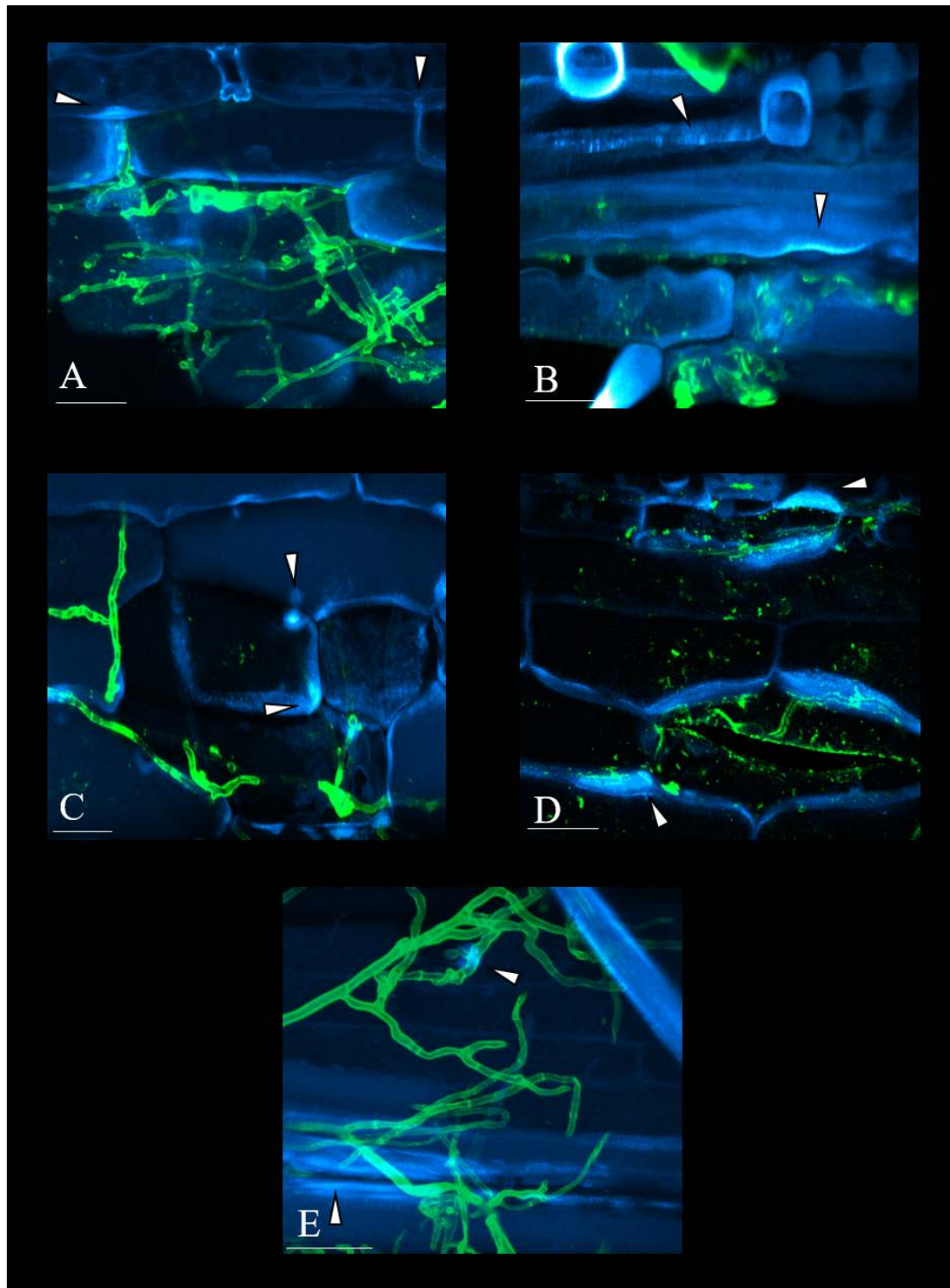


Figure 24: Confocal Laser Scanning Microscopy of *P. nodorum* strain SN15 infection on *B. distachyon* leaves 7 days post inoculation

Scale bar equals 20 μm . The fungus is stained with WGA-AF488. The microscopy of *B. distachyon* leaves at 7 dpi with *P. nodorum* revealed a callose response to the fungus in infected and adjacent cells. **A)** Wild-type reaction to *P. nodorum* revealed callose depositions in cells adjacent to fungal hyphae (arrows). **B)** The line #2-9-4-9 also responded with callose depositions in cells close to the colonising hyphae. **C)** Callose depositions were detected adjacent to infecting hyphae in leaves of the line #2-9-6-30. The response is comparable to the wild-type and the other genome edited lines. **D)** Line #16-12-6-14 responded like the wild-type with callose depositions close to fungal hyphae (arrows). **E)** The response to infecting hyphae in the line #16-12-10-18 was comparable to the other lines. Callose was detected adjacent to infecting hyphae (arrows).

Confocal Laser Scanning Microscopy performed on inoculated leaves 7 days post inoculation with *P. nodorum* revealed no differences between the wild-type Bd21 and the four genome edited lines (Fig. 24). The wild-type responded with several callose depositions adjacent to fungal hyphae as some form of barrier or fortification against the infecting pathogen (Fig. 24 A). This was also observed in the four genome edited lines. The line #2-9-4-9 showed callose barriers and several scattered callose depositions adjacent to infected cells and hyphae (Fig. 24 B). For the line #2-9-6-30, the pathogen induced stress response was quite similar (Fig. 24 C). Several callose depositions directly next to the infecting hyphae were detected (Fig. 24 C, arrows). Callose adjacent to hyphae from *P. nodorum* was also detected in line #16-12-6-14 (Fig. 24 D). At the cell membranes adjacent to the hyphae, callose depositions were detected via CLSM (Fig. 24 D, arrows). A similar response was also observed for the line #16-12-10-18 (Fig. 24 E). Callose depositions at cell membranes adjacent to infected cells or fungal hyphae were detected (Fig. 24 E, arrows). Overall, the stress induced response to *P. nodorum* SN15 infection in the wild-type and the four genome edited lines were comparable (Fig. 24).

3.6 qPCR analysis of the *Brachypodium distachyon* GSL Gene family

To study the influence of the genome editing performed on *BdGSL3* in *B. distachyon* on the GSL gene family, transcriptional analysis on different tissues were performed. With the aid of the Roche[®] Real-Time Ready system qPCRs on all 11 members of the *GSL* gene family were performed. Since the role of *BdGSL3* has not been fully disclosed, loss of function might have an impact on the transcription level of other *BdGSL* genes, e.g. an up- or down-regulation to maintain the observed normal plant development. Therefore, an expression analysis of three major organs, leaves, stem and spikelets was performed to reveal possible differences.

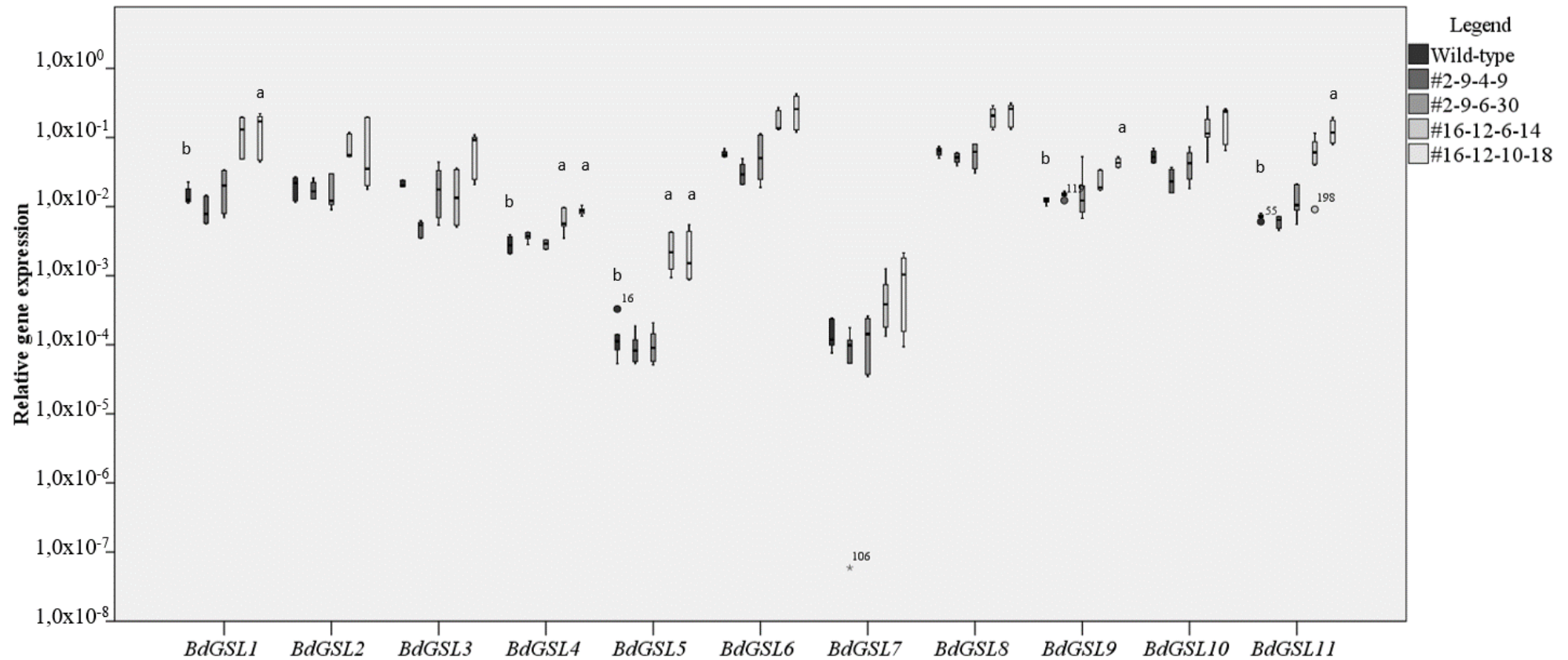


Figure 25: Relative gene expression of *BdGSL* gene family in leaves of three weeks old *B. distachyon* plants

For each tested line three biological replicates were analysed with two technical replicates each. To reveal significant differences between the wild-type and the four genome edited lines a pairwise non-parametric Kruskal-Wallis test was performed with Bonferroni correction for multiple tests (Tab. S. 16). Significance is indicated with a. Circles indicate outliers; asterisks indicate extreme outliers and the numbers the corresponding data point. The gene expression is shown in relation to the housekeeping gene *UBIQUITIN-1* of *B. distachyon*. For *BdGSL1* a statistically significant difference was found for line #16-12-10-18 compared to the wild-type. In *BdGSL4* and *BdGSL5*, a statistically significant difference was found for the lines #16-12-6-14 and #16-12-10-18. In *BdGSL9* and *BdGSL11*, the line #16-12-10-18 shows a significant difference compared to the wild-type. Further transcriptional differences are present for *BdGSL2*, *BdGSL6*, *BdGSL8* and *BdGSL10*. The two genome edited lines #16-12-6-14 and #16-12-10-18 showed a higher expression of these genes compared to the wild-type. For *BdGSL3* two lines showed a difference compared to the wild-type, whereas #2-9-4-9 showed a reduced expression and #16-12-10-18 a higher expression.

The transcriptional analysis of the *BdGSL* gene family expression in leaves revealed minor differences throughout the expression for two lines (Fig. 25). Significant differences in the expression levels of the genome edited lines were found in *BdGSL1* (Tab. S. 16). *BdGSL1* was significantly upregulated in the line #16-12-10-18 compared to the wild-type (Fig. 25). The other line #16-12-6-14 showed an indicated upregulation which was not significant compared to the wild-type. *BdGSL4* and *BdGSL5* were both significantly upregulated in the lines #16-12-6-14 and #16-12-10-18 compared to the wild-type (Fig. 25). Furthermore, *BdGSL9* and *BdGSL11* were significantly upregulated for the line #16-12-10-18 (Fig. 25). Further upregulations for the genes *BdGSL2*, *BdGSL6*, *BdGSL8* and *BdGSL10* in both lines were found. However, these differences were not significant and only indications for some differences (Table S. 16).

The other two genome edited lines, #2-9-4-9 and #2-9-6-30 showed no noticeable differences in the gene expression throughout the whole gene family except for *BdGSL3* in the line #2-9-4-9. The expression for the modified gene *BdGSL3* was affected in two lines. The expression of *BdGSL3* was reduced in #2-9-4-9, the two lines #2-9-6-30 and #16-12-6-14 had no differences compared to the wild-type. Opposite to the *BdGSL3* expression in #2-9-4-9, the line #16-12-10-18 had a stronger expression compared to the wild-type (Fig. 25). Overall, the expression in leaves indicated minor differences in the expression of some members of the GSL gene family. There were some significant transcriptional differences for the line #16-12-10-18 but most genes weren't affected.

To reveal possible differences in expression of GSL genes a qPCR was performed. The whole gene family of *GSL* genes were analysed and the expression normalized with the housekeeping gene *UBIQUITIN-1*. The relative expression is presented here (Fig. 26).

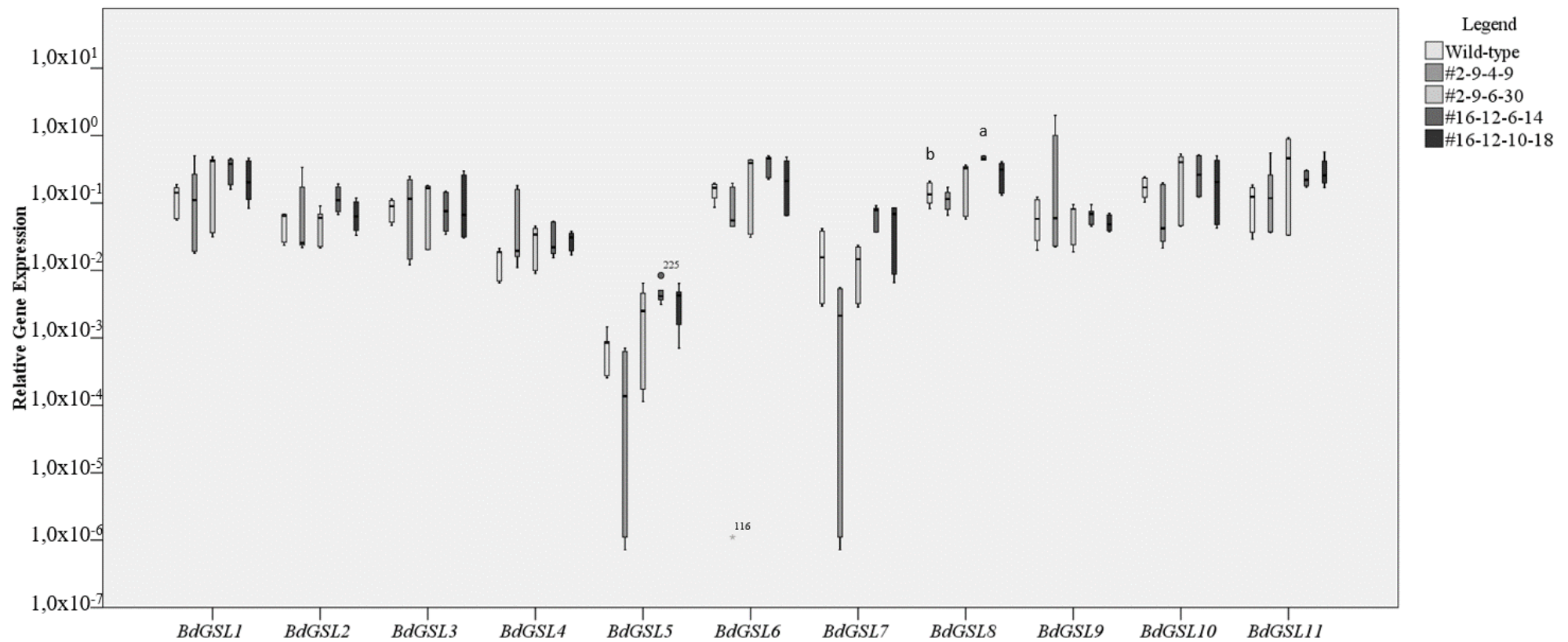


Figure 26: Gene expression of *BdGSL* gene family in stem tissue of five weeks old *B. distachyon* plants

For each tested line three biological replicates were analysed with two technical replicates each. To reveal significant differences between the wild-type and the four genome edited lines a pairwise non-parametric Kruskal-Wallis test was performed with Bonferroni correction for multiple tests (Tab. S. 19). Significance is indicated with a. Circles indicate outliers; asterisks indicate extreme outliers and the numbers the corresponding data point. The gene expression is shown in relation to the housekeeping gene *UBIQUITIN-1* of *B. distachyon*. The only significant difference in expression was found for *BdGSL8* in the line #16-12-6-14, which was upregulated compared to the wild-type. All other member of the gene family showed no significant differences to the wild-type in any of the four genome edited lines. Some indications for possible differences were found for the two genes *BdGSL5* and *BdGSL7* in the line #2-9-4-9 indicating a downregulation for both genes. An upregulation for *BdGSL5* is indicated for the other three genome edited lines compared to the wild-type and #2-9-4-9. The *BdGSL4* expression for all four genome edited lines compared to the wild-type is slightly higher. For the mutated gene *BdGSL3* no transcriptional difference in stem tissue of five weeks old plants is observed.

The qPCR expression analysis for the *GSL* gene family in *B. distachyon* stem tissue of five weeks old plants revealed only minor differences in the expression throughout the whole gene family (Fig. 26). To test for statistically significant differences the non-parametric Kruskal-Wallis test with Bonferroni correction was performed (Table S. 19). The statistical analysis revealed a significant upregulation of *BdGSL8* for the line #16-12-6-14 (Table S. 19). All other genes for the genome edited lines showed no significant differences (Fig. 26 + Tab. S. 19). However, there are some differences indicated in the expression of *BdGSL4* for the four genome edited lines. All lines showed a minor upregulation compared to the wild-type (Fig. 26). The two genes *BdGSL5* and *BdGSL7* showed an indication for a minor downregulation in #2-9-4-9. The *BdGSL5* expression showed an indicated upregulation three genome edited lines (Fig. 26). However, this was not the case for *BdGSL7*. *BdGSL11* showed also some indication of an upregulation in the lines #-2-9-6-30, #16-12-6-14 and #16-12-10-18 compared to the wild-type and #2-9-4-9.

In general, there were not many differences to the wild-type for the four genome edited lines in the expression of the *GSL* gene family in stem tissue of five weeks old *B. distachyon* plants. The only significant change in expression levels was found for *BdGSL8* in the line #16-12-6-14. All other genes were comparable to the wild-type.

Since the major concept of this study was to investigate the role of *BdGSL3* in disease resistance to FHB, a disease located in the spikelets of *B. distachyon* this highly important tissue directly involved in the defence reaction was investigated. A transcriptional analysis of the *BdGSL* gene family in spikelets was performed to reveal possible transcriptional differences. The acquired data were analysed and the gene expression was calculated in relation to the *B. distachyon* housekeeping gene *UBIQUITIN-1* to compare the wild-type expression level to the expression levels of the four genome edited lines.



Figure 27: *BdGSL* gene family expression in spikelets of *B. distachyon* during anthesis

For each tested line three biological replicates were analysed with two technical replicates each. To reveal significant differences between the wild-type and the four genome edited lines a pairwise non-parametric Kruskal-Wallis test was performed with Bonferroni correction for multiple tests (Tab. S. 22). Significance is indicated with a. Circles indicate outliers and the numbers the corresponding data point. The gene expression is shown in relation to the housekeeping gene *UBIQUITIN-1* of *B. distachyon*. Significant differences in expression are found for *BdGSL1*, *BdGSL3* and *BdGSL5*. In *BdGSL1* the line #2-9-4-9 shows a significant reduced expression compared to the wild-type. For *BdGSL3*, the line #16-12-6-14 showed a significant reduced expression. For *BdGSL3* the line #16-12-6-14 had a significant lower expression compared to the wild-type. Other differences, which are not statistical different, can be observed for *BdGSL1* where the other three lines also show a lower expression. This could also be observed for *BdGSL2* and *BdGSL11*. For *BdGSL3* the line #2-9-4-9 and the line #16-12-10-18 showed a reduced expression compared to the wild-type.

The qPCR analysis performed on spikelets of *B. distachyon* revealed some minor differences throughout the gene family with some exceptions. To test for statistically significant differences, the non-parametric Kruskal-Wallis test was performed with a Bonferroni correction for multiple comparisons (Table S. 22). A detailed descriptive statistic is supplied in the supplement (Table S. 20). For *BdGSL1* a significant difference between the wild-type (0.93) and the line #2-9-4-9 (0.29) was revealed. The other three genome edited lines have a reduced expression level compared to the wild-type (#2-9-6-30; 0.40, #16-12-6-14; 0.53, #16-12-10-18; 0.51), but no significance was found. The gene *BdGSL2* showed no significance for any genome edited lines, but all four lines show a reduced expression level.

The mutated gene, *BdGSL3* showed a significant lower expression for the line #16-12-6-14 compared to the wild-type. The line #2-9-4-9 showed also a reduced expression but not significantly. The lines #2-9-6-30 and #16-12-10-18 both had a comparable expression like the wild-type. For *BdGSL4* no difference in expression could be observed but for *BdGSL5* a significantly reduced expression for the line #2-9-4-9 was observable. The other three lines had no significant difference in expression but an indication for a lower expression for the lines #2-9-6-30 and #16-12-6-14 was observed (Fig. 27). For *BdGSL6*, *BdGSL7* and *BdGSL8* no significant differences were observed and no indications for any differences were found, except for the expression of *BdGSL7*. The *BdGSL7* expression was largely spread for the line #2-9-4-9. The *BdGSL9* expression did not differ from the wild-type to any genome edited line. However, the *BdGSL10* expression showed a tendency for a reduced expression in the genome edited lines compared to the wild-type expression level. However, there was no significance for this difference. For the gene *BdGSL11* a lower expression but not statistically significant for all four genome edited lines is revealed.

3.7 Analysis of pathogen responsive genes of *B. distachyon* and virulence genes of *F. graminearum* after inoculation

To investigate possible differences in the expression of PR genes after inoculation with *F. graminearum* a qPCR expression study was performed on cDNA synthesised from RNA of inoculated spikelets two days post inoculation. The expression at this early time point of the five different PR genes *PR1*, *PR2*, *BdMAPKKK*, *Chit8* and *UGT74f2* was analysed. The PR genes *PR1*, *PR2* and *BdMAPKKK* were already described as involved in *F. graminearum* defence of *B. distachyon* based on homology of barley (Blümke et al. 2015). *Chit8* and *UGT74f2* were identified in transcriptome analysis in *B. distachyon* and wheat during FHB disease (Powell et al. 2017).

The analysis of the genes *PR1*, *BdMAPKK1*, *Chit8* and *UGT74f2* showed no differences in expression characteristics compared to the wild-type (Table S. 23). Only *PR2* showed differences in the four genome edited lines compared to the wild-type (Fig. 28).

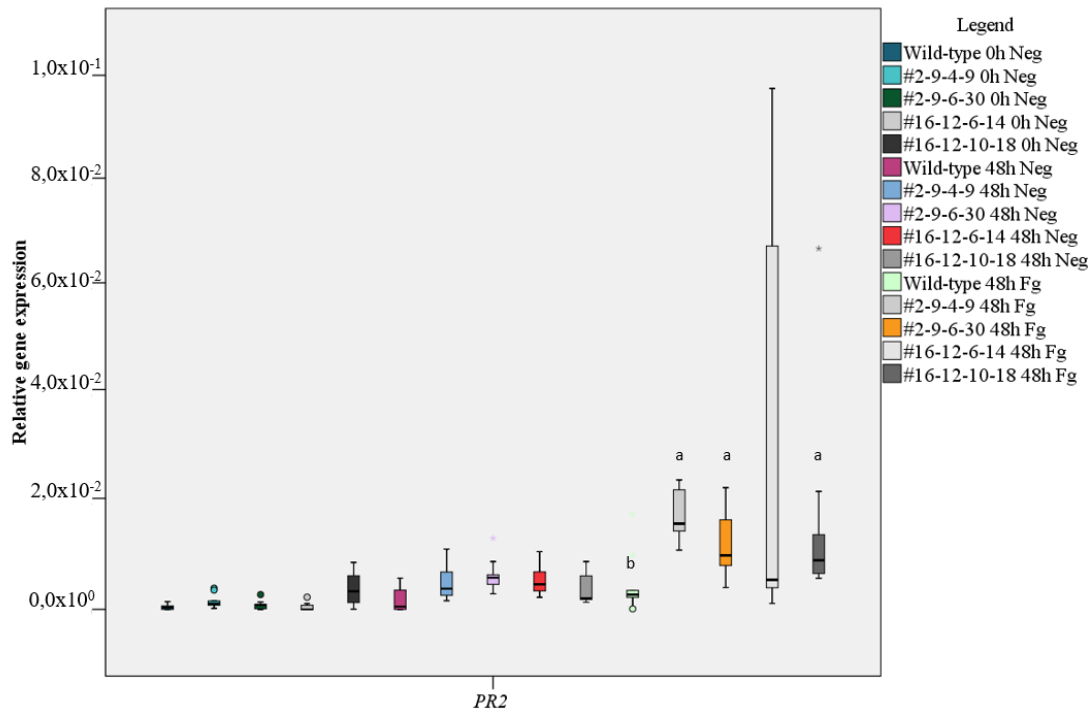


Figure 28: Relative gene expression of the pathogen responsive gene *PR2* at 0 dpi and 2 dpi in spikelets of *B. distachyon*

For each tested line three biological replicates were analysed with three technical replicates each. To reveal significant differences between the wild-type and the four genome edited lines a pairwise non-parametric Kruskal-Wallis test was performed with Bonferroni correction for multiple tests (Tab. S. 25). Significance is indicated with a. Circles indicate outliers and asterisks indicate extreme outliers. Neg indicates the negative control inoculated with upH₂O. Relative gene expression to the housekeeping genes *actin* and *UBC-18*. At this early time point, there was a significant upregulation observed for *PR2* in the three genome edited lines #2-9-4-9, #2-9-6-30 and #16-12-10-18. The expression of *PR2* was also upregulated in the line #16-12-6-14 but no statistical significance was observed.

At 0 dpi, water controls of all tested lines showed only low *PR2* expression levels which were not significantly different. After 2dpi, the expression is higher than the 0dpi state, but no difference between the wild-type and the four genome edited lines was observed (Fig.28). At 2 dpi with *F. graminearum* strain 8/1 (Fig. 28, 48h Fg) the wild-type still shows the same expression level as in the negative controls. The four genome edited lines showed a sig. higher expression of *PR2* to the 2dpi wild-type inoculated with *F. graminearum* (Tab. S. 25). For the three lines #2-9-4-9 (0.000), #2-9-6-30 (0.011) and #16-12-10-18 (0.010) a significant difference to the wild-type *PR2* expression could be observed. The line #16-12-6-14 (0.307) was not significantly upregulated. There were no statistical differences in distribution between the 2dpi with *F. graminearum* and the respectively negative controls (Tab. S. 25).

F. graminearum makes use of the two virulence genes *fgl1* and *tri5* for infection of *B. distachyon*. Therefore, it was interesting to examine if there are differences in the virulence gene expression during infection of the four genome edited lines compared to the wild-type. A qPCR analysis was performed at 2 dpi to reveal possible differences. The expression was set into relation to the two *F. graminearum* housekeeping genes *ACTIN* and *TUBULIN* and is presented here (Fig. 29).

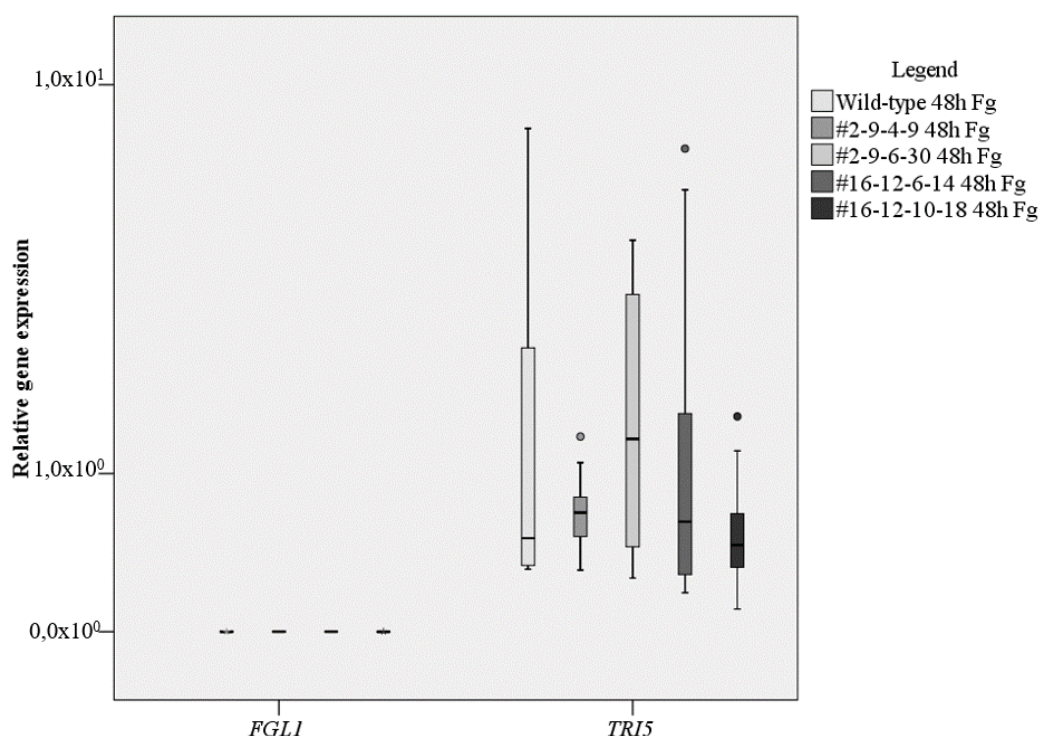


Figure 29: Relative gene expression for the two fungal virulence genes *fgl1* and *tri5* in 2dpi spikelets

For each tested fungal virulence gene three biological replicates were analysed with three technical replicates each. To reveal significant differences between the wild-type and the four genome edited lines a non-parametric Kruskal-Wallis test was performed with Bonferroni correction for multiple tests (Tab. S. 27). Significance is indicated with a. Circles indicate outliers. The expression of each virulence gene is relative to the two reference Genes *ACTIN* and *TUBULIN* from *F. graminearum*. For *fgl1* no expression could be found in the wild-type. Only in the four genome edited lines an expression was found for this virulence gene. The *tri5* expression was observed in the wild-type and all four genome edited lines. There was no difference in the *tri5* expression observed.

Expression of *FGL1* was detected at 2 dpi in the four genome edited lines. However, in the wild-type samples, no expression of *FGL1* could be detected (Fig. 29). The expression of the other *F. graminearum* virulence gene, *TRI5*, was detected at 2 dpi in the wild-type and all four genome edited lines. However, no significant differences in the expression of *TRI5* was observed between the wild-type and the four genome edited lines. No expression of *FGL1* and *TRI5* was detected in the negative controls and at the 0 dpi stage. (Tab. S. 26).

4. Discussion

4.1 Genome editing as new breeding technology for crops

4.1.1 CRISPR/Cas9 in *Brachypodium distachyon* and prospects for plant breeding

Brachypodium distachyon is a well-known and described model plant for crops such as wheat or barley, which unifies the features *A. thaliana* has for dicotyledons and gives researcher a tool closely relative to crops (Brkljacic et al. 2011; Vogel et al. 2006b). The transformation of *Brachypodium distachyon* with a CRISPR/Cas9 construct was successful. The screening of the plants regenerated after transformation already showed an activity of the construct (Fig. 7). Some lines showed already multiple bands after the screening PCR indicating a form of mosaicism, where different cells have different genomic background due to later activity of the endonuclease construct. This form of mosaicism was also detected in genome edited embryos of mice and tomato (Mianné et al. 2017; Ueta et al. 2017). Research shows, that infiltration with *A. tumefaciens* in *A. thaliana* and tobacco showed activity of the transformed construct (Jiang et al. 2013). Cell bombardment of embryos from maize, agrobacterium-mediated transformation of sorghum embryos and the transformation of rice protoplasts also showed activity of CRISPR/Cas9 constructs in these tissues (Jiang et al. 2013; Svtashev et al. 2016). Therefore, it is highly likely that activity of CRISPR/Cas9 is also present in transformed *Brachypodium distachyon* callus from isolated embryos which was already shown for rice (Endo et al. 2014).

When compared with the literature from CRISPR/Cas9 mediated genome editing in other plants (Jiang et al. 2013; Svtashev et al. 2016), and recent work with CRISPR/Cas9 mediated genome editing in *Brachypodium distachyon* (Qin et al. 2019), this work provides additional evidence for the applicability of CRISPR/Cas9 mediated genome editing in *Brachypodium distachyon*. This enables new prospects for future research in *B. distachyon*, which could be transferred to relative crops like wheat or barley. Due to the features of *B. distachyon* the small genome, the genetically affinity to wheat and barley, the diploid genome which enables fast breeding and the outcrossing of T-DNA and its short life cycle (Brkljacic et al. 2011; Ozdemir et al. 2008; Vogel and Bragg 2009; Vogel et al. 2006b), non-transgenic specific genomic analyses can be performed. Positive traits resulting from those studies then enable an easy transfer to crops like wheat, barley or rice. Evidence for these approaches in crops is already published. Li et al. (2015) could show that the overexpression of an UDP-glycosyltransferase from barley increased DON detoxification in wheat.

And the overexpression of the wheat *Lr34* gene in barley increased resistance against multiple fungal pathogens (Risk et al. 2013). However, both approaches were transgenic, but showed that interspecies identification of possible resistance targets can be transferred into the desired crop.

4.1.2 CRISPR/Cas9 in *Brachypodium distachyon* a look into the major concern of unspecific off-site mutations

The constant expression of the *Cas9* in plants containing the T-DNA and the constant expression of our sgRNAs might lead to off target mutations. In human systems, these off-site mutations are already well studied and research shows that these off-site mutations have highly reduced frequencies (Cradick et al. 2013; Kucsu et al. 2014; Lin et al. 2014). In plants, the specificity of *Cas9* is not that well studied and the differences in off-site events can range from plant species to plant species (Peterson et al. 2016; Svitashchev et al. 2016). An in-depth analysis of sgRNA in humans revealed that position and number of mismatching nucleotides play a key role. Mismatches in the 3' region or at least three mismatching nucleotides in the sgRNA reduced off-site mutation rates to negligible numbers (Fu et al. 2013; Hsu et al. 2013; Pattanayak et al. 2013). Therefore, the four genome edited lines were checked via PCR analysis for major deletions in possible off-target regions. A screening for off-targets was performed with the help of the Cas-OFFinder in the *B. distachyon* genome (Bae et al. 2014). The screening revealed no differences in size of the amplified off-target region between the wild-type and the four genome edited lines. Considering the amount of mismatching nucleotides and the region of mismatches in the sgRNAs, the probability of severe mutations in the off-target regions is relatively low (Fu et al. 2013; Hsu et al. 2013; Pattanayak et al. 2013). A closer look into some possible phenotypes of possible off-target mutations supports this statement.

For example, the off-site target A1 (Table S. 2) encodes for the predicted *Brachypodium distachyon* *COP9 SIGNALOSOME COMPLEX SUBUNIT 2* (*CSN2*; BRADI_2g10780). Research for the COP9 signalosome reveals that these complexes play a major role in regulation of cullin-RING ligase of ubiquitin E3 complexes (Wei et al. 2008). A knockout of the corresponding *CSN2* gene in *Arabidopsis thaliana* led to a severe photomorphogenic phenotype with brown leaves and an impaired cullin derubylation (Gusmaroli et al. 2007). Comparing the phenotype from *Arabidopsis thaliana* (Gusmaroli et al. 2007) with the generated plants in this work, and the fact that CSNs are highly conserved (Wei et al. 2008), it is highly unlikely that there is a loss of function mutation for the four genome edited lines present.

Another possible off- target was the *Brachypodium distachyon* *LOB DOMAIN-CONTAINING PROTEIN 37* (BRADI_1g22920). A BLAST search in the *Arabidopsis thaliana* genome revealed high homology to *LATERAL ORGAN BOUNDARIES 37* (LBD37). LBD37 is also known as *ASYMMETRIC LEAVES2 LIKE 39* (ASL39), and part of a plant specific gene family important for forming of simple leaves (Iwakawa et al. 2007; Matsumura et al. 2009; Shuai et al. 2002). Research regarding the phenotype of different expression levels of ASL39 homologs in rice and *A. thaliana* reveals that possible differences in expression have a severe impact on leaf formation (Albinsky et al. 2010; Matsumura et al. 2009). The knock-out of a single ASL gene in *Arabidopsis thaliana* lead to crumpled small leaves, a comparable phenotype was observed in rice, and could be connected especially to ASL39 (Albinsky et al. 2010; Matsumura et al. 2009). Considering the generated mutants analysed in this work did not show any impact on leaf formation and leaf forms, a loss of function or overexpression mutation in this off-site target can also be considered as unlikely.

The possible off-site target C1 (Table S. 2) is annotated as a predicted *Brachypodium distachyon* *LEUKOTRIENE A-4 HYDROLASE HOMOLOG* (LKH; BRADI_1g03860). LKH plays a major role in the inflammatory response via converting leukotriene A to the active form leukotriene B (Rådmark et al. 1984). However, in plants the role of LKH is still unknown. Some research on loss of function T-DNA insertion lines revealed no observable phenotype (Voisin 2008). Regarding the important role of leukotrienes in response to biotic stress, a loss of function mutation in this case is highly unlikely. In humans and animals, leukotriene plays a major role in an immediate hypersensitivity (Samuelsson et al. 1987). Any form of hypersensitivity or immediate response to the *Fusarium graminearum* inoculation was not observed during this work.

Taking into account that position and amount of mismatches plays a key role in the off-site target activity of Cas9 (Anderson et al. 2015; Fu et al. 2013; Hsu et al. 2013), and the severe impact of off-site target mutations on the plants, it is highly unlikely that off-site target mutations happened in those four genome edited lines. However, only a genome sequencing and mapping to the reference genome of Bd21 would provide an unambiguously answer.

4.2 The loss of function of BdGSL3 and the possible role in *Brachypodium distachyon*

4.2.1 CRISPR/Cas9 mediated loss of function mutants of BdGSL3

The target for genome editing in *Brachypodium distachyon* was the gene *GLUCAN SYNTHASE LIKE 3* (*BdGSL3*; Bradi_2g50140). A phylogenetic analysis with DNA sequences of glucan synthases from *Brachypodium distachyon*, *Oryza sativa* and *Arabidopsis thaliana* revealed a high homology to the stress induced callose synthase *POWDERY MILDEW RESISTANT 4* (*PMR4*; *AtGSL5*) (Blümke 2013). Therefore, it was interesting to see if it is possible to generate a knockout or loss-of-function mutant of this relative gene in *B. distachyon* and get insight into the role of this gene in a model plant for monocotyledons. The PCR based screening revealed three different deletions in the gene of interest when compared to wild-type. A PCR screen for T-DNA insertion via initial *Agrobacterium*-mediated transformation revealed on gDNA level that two lines lost the T-DNA as amplification of the resistance marker *bar* was not detectable, whereas the other two genome edited lines still contained the T-DNA. Sequencing of the target region revealed major changes in amino acids in the target region, and a stop codon insertion with frame shift for the line #16-12-6-14. Studies on *PMR4* indicated, that the catalytic active region for callose synthesis is located in the central, cytosolic loop between N- and C-terminal domains containing multiple transmembrane helices (Sode 2015). Further research on callose synthases suggested that large complexes would be formed (Brownfield et al. 2009; Li et al. 2003; Østergaard et al. 2002), which are associated with several proteins for activity and regulatory function like sucrose synthases providing UDP-glucose or annexin proteins which are needed for the activating Ca^{2+} intake (Amor et al. 1995; Andrawis et al. 1993; Hong et al. 2001b). In *Arabidopsis thaliana* research also revealed that, a UDP-glycosyltransferase is associated with *GLUCAN SYNTHASE LIKE 6* (*AtGSL6*) which is regulated by the Rho-like GTPase *ROP1*, similar to the already known regulation in *Saccharomyces cerevisiae* (Hong et al. 2001a; Qadota et al. 1996; Verma 2001; Verma and Hong 2001). More research about the regulation of *PMR4* revealed that phosphorylation plays a major role. The phosphorylation and dephosphorylation of specific sites is necessary for transport and activity of *PMR4* (Sode 2015). Therefore, a motif analysis was performed at the area around the sgRNA targets to identify possible sites of modification. The search for possible motifs revealed the absence of three post-translational regulatory motifs. For all four lines an amidation site, an asparagine glycosylation site and an N-myristoylation site were missing.

Amidation is a modification, which changes the carboxyl group of a peptide to an amide group (Kumar et al. 2014). This change has major effects on peptides; in general, it makes the peptide more stable to physiological pH changes and less prone to proteolytic activity (Kumar et al. 2014).

Asparagine glycosylation is responsible for protein folding and stability, biosynthetic quality control, intracellular traffic, physiological activity of proteins and functions as a multifunctional signal (Hebert and Molinari 2007; Olden et al. 1982; Shrimal et al. 2015). Research indicates that glycosylation is a regulator for protein folding and functions as a quality control (Daniels et al. 2003; Hammond et al. 1994; Helenius 1994; Ruddon et al. 1987; Sousa and Parodi 1995). Interestingly, also the activity of proteins is dependent on glycosylation (Asano et al. 1991; Branza-Nichita et al. 2000; Zheng et al. 1994). In plants these processes are also present (Rayon et al. 1998), one example is the regulation of cleavage from glycopeptides for maturation and transport of CONCANAVALLIN A (Bowles et al. 1986; Chrispeels et al. 1986; Faye and Chrispeels 1987). Glycosylation and de-glycosylation are important for proper protein function and signalling (Berger et al. 1995; Ceriotti et al. 1998; Rayon et al. 1998).

N-myristoylation is a co-translational process referring to the covalent, irreversible attachment of myristate to the target site (Johnson et al. 1994; Olson and Spizz 1986; Wilcox et al. 1987). N-myristoylation has different effects on proteins. In some cases, N-myristoylation enables the transport to the mitochondrial membrane from the endoplasmic reticulum (Borgese et al. 1996; Zha et al. 2000), or is required for proper targeting and binding to the plasmamembrane (Cross et al. 1984; Kamps et al. 1985; Song et al. 1996; Song et al. 1997). Also N-myristoylation could increase the stability of proteins, shown for cardiolipin and phosphatic acid-binding protein in humans (Maeda et al. 2018). The importance for plasma membrane targeting was also found in *Arabidopsis thaliana* (Batistič et al. 2008). In tobacco Saito et al. (2018) could shown that the N-myristoylation on calcium dependent kinases is required for plasma membrane sorting. The regulatory impact of N-myristoylation has even impact on whole pathways, shown in *A. thaliana* (Pierre et al. 2007). N-myristoylation could play a key role in the partitioning of proteins into the aqueous phase and transient interaction with membranes (Peitzsch and McLaughlin 1993; Shahinian and Silvius 1995; Silvius and l'Heureux 1994). An impaired ability to attach and detach from the plasmamembrane for CalS could have severe effects on proper protein function. The transport in vesicle to the penetration site for PMR4 is already described, and impaired transportation led to delayed and weaker callose depositions in the cell (Ellinger et al. 2013; Sode 2015).

When comparing the stress related phenotypes of all four genome edited lines, all lines have a similar impaired formation of callose after wounding in leaves and *F. graminearum* infection in spikelets. Since the line #16-12-6-14 has a stop codon in the ORF of *BdGSL3* coupled with a frameshift mutation it is likely that no proper protein is generated by the plant. Since the loss of the described predicted motifs have also a severe effect on the stability and folding of proteins it can be assumed, that in all four genome edited lines no *BdGSL3* is processed. However, it would be necessary to falsify this assumption by protein isolation. A general protein isolation and a specific protein isolation for plasma membrane-associated proteins followed by a western blot with antibodies specific to the N-terminal region of *BdGSL3* could be used to clarify the assumed absence.

4.2.2 Vegetative phenotype of genome edited *Brachypodium distachyon* plants

From research in *Arabidopsis thaliana* and the loss of function of the stress induced callose synthase *PMR4*, an earlier senescence due to upregulated salicylic acid, might also happen in *Brachypodium distachyon* (Nishimura et al. 2003). However, when comparing the four genome edited lines examined in this work with the wild-type after eight weeks, there was no difference in senescence observable. Experiments with RNAi constructs and knock downs of the callose synthases *HvGSL6* and *HvGSL7* revealed also no impaired phenotypes in the appearance (Chowdhury et al. 2016). This indicates that senescence and the salicylic acid phenotype of *PMR4* is not present in *Brachypodium distachyon* and other monocotyledons. Furthermore, it can be assumed that the T-DNA integration for the lines #2-9-4-9 and #2-9-6-30 had no severe impact on the life cycle of *Brachypodium distachyon*. A detailed look into the growth during the observed eight weeks reveals an interesting difference between the four lines and the wild-type. While the genome edited lines lagged in height in the early vegetative state, they surpassed the wild-type in later stages of the life cycle. This might be an interesting hint supporting the current hypothesis that the acquired stress response, which increases the fitness of plants, came with the trade-off of reduced growth and other agronomical traits (Kempel et al. 2011; Walters and Heil 2007). Research suggest that R genes but most dominantly changes in plant hormonal levels for jasmonic acid and salicylic acid have severe impact on growth (Heil and Baldwin 2002; Meldau et al. 2012; Tian et al. 2003). However, callose papillae are considered as a basal plant defence, and distinct pathways and PAMPs are responsible for this response (Luna et al. 2011; Stone and Clarke 1992). Nevertheless, currently there is no evidence that the acquired fitness of callose responses have a negative impact on plant growth.

The research in barley indicates no observable phenotype, and the PMR4 mutant in *A. thaliana* showed an increased hypersensitive response and salicylic acid, which negatively affects plant growth (Chowdhury et al. 2016; Meldau et al. 2012; Nishimura et al. 2003). This hypersensitive response was linked to upregulations of known salicylic acid induced genes or marker genes like the PR genes of the classes 1, 2, 3 and 5 (Nishimura et al. 2003). These transcriptional differences of PR genes were not observed and are discussed in chapter 4.2.6.

This study has revealed that disruption of the callose synthase *BdGSL3* did not affected major development of *Brachypodium distachyon*. However, small differences in growth between the early and the late life cycle compared to the wild-type were observed. This might be an interesting hint whether the acquired fitness from stress induced callose synthases might have a small growth deficit as trade-off. Current research indicates that the acquired plant defence comes with trade-offs in growth (Kempel et al. 2011; Walters and Heil 2007). This is majorly due to changes in hormone levels, like jasmonic acid or salicylic acid (Heil and Baldwin 2002; Meldau et al. 2012). Since research in barley with a predicted stress induced callose synthase homologue found no observable phenotype and based on the presented data, it is not clear, whether *BdGSL3* has an impact on hormonal regulation and therefore causes the observed phenotype or simply the missing function of the protein is the reason. Future research on the mutants should focus on detections in possible differences of plant hormonal levels to detect possible connections between *BdGSL3* and the regulation of plant hormones like jasmonic acid or salicylic acid.

4.2.3 Is *BdGSL3* responsible for the formation of callose depositions after infection of *Fusarium graminearum* in spikelets?

To reveal whether *BdGSL3* is responsible for callose depositions after inoculation of spikelets with *Fusarium graminearum*, infection studies were performed. The general suitability of *Brachypodium distachyon* as host for *F. graminearum* with the development of typical FHB symptoms was previously confirmed by Peraldi et al. (2011), specific interaction between the *F. graminearum* strain 8/1 and the used inbred line Bd21 by Blümke (2013). A correlation between callose depositions at the rachis node of infected *B. distachyon* florets and an increased resistance to *F. graminearum* was described by Blümke (2013). Furthermore, the resistance to *F. graminearum* could be increased in *B. distachyon* and the resistance *Blumeria graminis* f. sp. *hordei* in barley due to overexpression of *PMR4* (Blümke 2013; Blümke et al. 2013).

Evaluation of inoculated spikelets was done with the established Disease Score at 14 dpi and 7 dpi (Blümke 2013). Results for the wild-type were comparable to the already existing data of Bd21 (Blümke 2013). However, the Disease Score of all four genome edited lines with *BdGSL3* disruption was significant higher compared to wild-type. Stereomicroscopy of inoculated spikelets revealed the severe causes of the FHB disease and microscopy of inoculated spikelets showed a faster colonisation of *F. graminearum* in all four genome edited lines. This indicates a crucial role for *BdGSL3* in the pathogen-related stress response in spikelets of *B. distachyon*. The role of callose as an early blockade or attempt to slow down the infection is still debated (Voigt 2014). To get a better understanding of the influence of callose as response to the pathogen, inoculated spikelets at the early stage at 3 dpi were used to measure the amount of callose depositions compared to the wild-type. Confocal Laser Scanning Microscopy revealed a statistically significant difference in the relative callose area in spikelets at 3 dpi. Research on *Fusarium graminearum* infections in *Brachypodium distachyon* supports the hypothesis that callose depositions are involved in reducing the infection (Blümke 2013). The overexpression of *PMR4* from *Arabidopsis thaliana* in *Brachypodium distachyon* results in a significant higher amount of callose depositions at 3 dpi compared to the wild-type. This resulted in a reduced infection rating of Disease Score (Blümke 2013). An even stronger induced Type II resistance could be observed when *BdGSL3* was constitutive overexpressed in *B. distachyon* (unpublished data).

The importance of callose depositions to *F. graminearum* infection was shown in wheat by Blümke et al. (2014). The $\Delta fgl1$ *F. graminearum* strain could not suppress the callose biosynthesis due to the absence of free fatty acids (Blümke et al. 2014). In the presence of free fatty acids, the callose synthesis was suppressed resulting in a successful colonisation. However, the *fgl1* deficient strain could not suppress the callose biosynthesis and callose depositions were detected (Blümke et al. 2014; Voigt et al. 2005). These callose depositions supported containment of the pathogen in the inoculated floret preventing further colonisation (Blümke et al. 2014; Voigt et al. 2005). This was also observed in wheat, where papillae were formed in cell walls adjacent to hyphae after *Fusarium* infection in resistant wheat cultivars (Kang and Buchenauer 2000; Kang et al. 2008). The formation of a papillae was observed in proximity and distant to the fungal hyphae (Kang and Buchenauer 2000). Since callose is often associated in these papillae (Aist 1976; Stone and Clarke 1992) a functional callose response is a key part of the plant defence and type II resistance to *Fusarium* infection.

A similar observation in *B. distachyon* and the interaction with *F. graminearum* was possible. In the absence of callose depositions, the FHB disease was significantly stronger and the fungus was detected in the rachis node and rachis of the spikelet. This correlates with the studies of Kang and Buchenauer (2000) and Blümke et al. (2014). Both revealed the importance of callose depositions and papillae for resistance. Screening of different wheat cultivars regarding their susceptibility of callose synthases inhibition to free fatty acids gave further insights (Ellinger et al. 2014b). Ellinger et al. (2014b) revealed a correlation between the inhibition of callose biosynthesis through free fatty acids and the severity of FHB disease symptoms. In barley, the homolog *GSLs HvGSL6* and *HvGSL7* are connected to a FHB resistance QTL (Zhu et al. 1999a). Furthermore, it seems that barley has a natural stronger type II resistance to *F. graminearum* (Zhu et al. 1999b). An in depth analysis of *F. graminearum* infection between wheat and barley performed by Jansen et al. (2005) revealed a similar phenotype in barley compared to the $\Delta fgl1$ *F. graminearum* infection in wheat. The pathogen was not able to penetrate the rachis node and was contained in the inoculated spikelet (Blümke et al. 2014; Jansen et al. 2005). However, Jansen et al. (2005) did not observed any cell wall thickenings or papillae at *F. graminearum* infection but did not directly look for callose depositions in the rachis and rachis node as described in wheat (Blümke et al. 2014).

4.2.4 BdGSL3 as a universal answer to stress in *Brachypodium distachyon*?

In the previous chapter, it is discussed whether BdGSL3 is needed for the stress response to *Fusarium graminearum* infection, and it is concluded that BdGSL3 plays a major role in the response to *F. graminearum* infection in spikelets. In *A. thaliana*, it seems that PMR4 is responsible for callose forming after different stresses and pollen tube formation with AtGSL1 (Enns et al. 2005; Jacobs et al. 2003; Nishimura et al. 2003). However, in *Brachypodium distachyon* this is not clear, and the evidence suggests a key difference between *A. thaliana* and *B. distachyon* since the disruption of *BdGSL3* had no impaired vegetative phenotype.

In leaves, the callose response to wounding could be observed, and transcriptional studies indicate that *BdGSL2* and *BdGSL3* were upregulated 3 and 6 hours after wounding (Blümke 2013). It was possible to show a callose response after non-host infection with *Golovinomyces cichoracearum* by Blümke (2013). Wounding experiments were done with the wild-type and the four genome edited lines for the two time points 6 hours and 16 hours. However, no differences in the forming of callose depositions at 6 hours past wounding were detected. Possible changes to this wounding assay could be a different method to generate wounds. The used needles were inflicting rather big wounds and smaller wounds in higher frequencies could

induce a stronger callose formation. A possible other method to quantify the callose after wounding could be the use of a fluorescence-based assay which does not require microscopy. Additionally, CLSM with a fluorescent protein tagged BdGSL3 could enable a time-resolved visualisation of BdGSL3 after wounding.

Since the expression patterns of *BdGSL2* and *BdGSL3* after wounding revealed the highest expression after six hours (Blümke 2013), a later time point should be observed to make sure that the expressed mRNAs were translated into proteins. The wild-type response was comparable to already published data when comparing the 12 hour data with the 16 hour data presented here (Blümke 2013). However, the four genome edited lines showed a reduced coverage of callose adjacent to the inflicted wounds. Based on the transcriptional information from former work, and the reduced but not complete absence of callose observed in the disrupted mutants it can be concluded that BdGSL3 is not solely responsible for callose depositions after wounding in leaves and a combination of BdGSL2 and BdGSL3 might be responsible (Blümke 2013).

To get more insight into the role of BdGSL3 and stress responses in leaves, infections with the necrotrophic fungus *Parastagonospora nodorum* strain SN15 were done. Analysis of these infections showed for all four disrupted mutants and the wild-type a callose response adjacent to the infecting pathogen. This undermines the conclusion drawn out of the abiotic wounding stress response. BdGSL3 is not solely responsible for callose related stress response in leaves. Chowdhury et al. (2016) suggests an involvement of HvGSL6, a barley orthologue to BdGSL2, in stress response to *Blumeria graminis* f. sp. *Hordei*. Analysis of dsRNAi plants for the two CalS *HvGSL6* and *HvGSL7*, which is the orthologue to BdGSL3, suggests that HvGSL6 is involved in the forming of callose depositions after powdery mildew infection of *Blumeria graminis* f. sp. *Hordei* (Chowdhury et al. 2016). Furthermore, the knock-down of *HvGSL7* showed no significant difference in the amount of papillae with reduced callose depositions, even though they were slightly increased (Chowdhury et al. 2016). Transcriptional analysis in barley showed an upregulation of *HvGSL6* after inoculation with powdery mildew, which reached highest expression after 12 h post inoculation. Interestingly, *HvGSL7* showed a downregulation in expression (Chowdhury et al. 2016). In the untreated control, *HvGSL7* was downregulated in the first 8 hours but the expression of *HvGSL7* recovers. In the inoculated plants, this downregulation was persistent in all examined time points (Chowdhury et al. 2016). When comparing the transcript levels of both *HvGSLs*, *HvGSL7* transcript is more abundant at 0 hours compared to the relative low amounts of *HvGSL6* (Chowdhury et al. 2016), which

endorse the expression data already known about *HvGSLs* (Schober et al. 2009). This is somewhat contradictory to previous work in rice where the callose synthase genes *OsGSL2* (orthologue of *BdGSL2*) but not *OsGSL3* (orthologue of *BdGSL3*) revealed stable expression in different organs (Yamaguchi et al. 2006). However, after inoculation of rice with *Nilaparvata lugens*, a herbivore pathogen ingesting nutrients from rice phloem sap, the expression of *OsGSL3* changes (Hao et al. 2008). After 3 hours past inoculation the expression of *OsGSL3* increases until 6 h (Hao et al. 2008). Between 6 and 12 hours after inoculation the expression is downregulated but expression of *OsGSL3* increases again after 12 hours until 48 hours (Hao et al. 2008). Interestingly, the early expression change at 3 hours was higher for the more resistant cultivar B5 compared to the susceptible cultivar TN1 (Hao et al. 2008). The two other glucan synthases tested were *OsGSL1* and *OsGSL5*. *OsGSL1* is the orthologue to *AtGSL8* while *OsGSL5* is the orthologue to *AtGSL2* (Yamaguchi et al. 2006). *AtGSL8* is involved in the regulation of plasmodesmata closure due to defined callose deposition (Fernández-Calvino et al. 2011; Guseman et al. 2010; Han et al. 2014). And *AtGSL2* and its orthologue in *Nicotiana glauca* are involved in pollen tube growth and germination (Becker et al. 2003; Doblin et al. 2001; Nishikawa et al. 2005). The early upregulation of *OsGSL3* after inoculation with an herbivore indicates a stress-induced callose synthase, since it is not heavily expressed during vegetative conditions (Hao et al. 2008; Yamaguchi et al. 2006). While the two other genes *OsGSL1* and *OsGSL5* are linked to CalS responsible for developmental functions. Based on the described expression characteristics of *HvGSL7* and *OsGSL3* combined with the results from *F. graminearum* infections, there is good evidence that *BdGSL3* is a stress induced CalS; however, it is not as universal in its functions as PMR4 in *A. thaliana*.

4.2.5 The genome editing and loss of function of BdGSL3 and its impact on transcriptional level to the callose synthase gene family in *Brachypodium distachyon*

To investigate the impact of the genome editing on transcriptional level throughout the whole gene family of 1,3- β -glucan synthases in *Brachypodium distachyon*, a qPCR-based analysis was performed. The RealTime ready Custom Panel from Roche enabled a high throughput system to screen the whole gene family in 96 well plates. With this aid, it was possible to screen different organs, the leaves of three weeks old plants, the stems of five weeks old plants and the spikelets of six weeks old plants.

Interestingly, the *GSL* gene family expression in all three tissues was on different levels, while the expression in leaves was the lowest and in spikelets the highest. This observation is comparable to expression studies with another glucan synthase family, the cellulose synthase and cellulose synthase-like (*CESA/CSL*) in rice (Wang et al. 2010). The expression for the whole *CESA* family was the lowest in the flag leaves (Wang et al. 2010). Interestingly, opposed to the *GSL* expression, the highest *CESA* expression was found in stem tissue followed by the spikelet (Wang et al. 2010). However, the question if the genome editing event had any influence on the transcription of any member of the *GSL* family in *Brachypodium distachyon* needs to be addressed. The expression of all *BdGSLs* except for *BdGSL3* was upregulated in #16-12-6-14 and #16-12-10-18 compared to the wild-type. The *BdGSL* gene family expression was on wild-type level for the other two disrupted lines #2-9-4-9 and #2-9-6-30. Since all four genome edited lines did not differ in their vegetative phenotype and the examined stress related callose responses, it is hard to find any evidence for a transcriptional regulation of *BdGSL3* on other *BdGSLs*. It is notable, that both lines #2-9-4-9 and #2-9-6-30 still contain the T-DNA as discussed earlier. This might still have an impact on cellular processes, since the *Cas9* and sgRNAs are still expressed and the *Cas9* is translated and could be active. However, the literature and the results presented in this work indicate that stable transgenic CRISPR/*Cas9* plants have no severe impairments in looks or cellular processes (Belhaj et al. 2013; Osakabe et al. 2016; Zhou et al. 2017; Zhu et al. 2016). Furthermore, when comparing the leaf data with the data obtained from stem and spikelets, this distinctive upregulation is not found throughout the *GSL* gene family. Interestingly, this aberrant expression characteristic of *BdGSL3* is not observed in leaves. The *BdGSL3* was only in line #16-12-10-18 upregulated, while line #2-9-4-9 shows a lower expression. Therefore, the expression of *BdGSL3* did not had any impact on the expression of other *BdGSLs*.

A closer look into the stem expression reveals a downregulation of *BdGSL5* and *BdGSL7* for #2-9-4-9, while for *BdGSL5* the other three lines have a slightly higher expression. For *BdGSL7*, only the lines #16-12-6-14 and #16-12-10-18 had this shift. The role of *BdGSL5* in *Brachypodium distachyon* is still unclear. Phylogenetic analysis by Blümke (2013) revealed a close homology to *AtGSL2* also known as CALLOSE SYNTHASE 5 (CalS5). In *A. thaliana*, the role of CalS 5 is already well studied. CalS 5 is required for proper pollen wall formation and patterning during micro gametogenesis but not for the pollen tube growth (Dong et al. 2005; Huang et al. 2013; Nishikawa et al. 2005). Work with the rice orthologue *OsGSL5* in rice further confirm the importance of this callose synthase for reproduction. A knockout and RNAi experiment revealed that *OsGSL5* is important for the primary cell wall of microspores (Shi et al. 2014). However, there were no noticeable differences in male fertility or reproduction for the genome edited lines, hence it is highly unlikely that the downregulation or upregulation had any effect in these four lines. The orthologues of *BdGSL7* in *A. thaliana* and rice are *AtGSL12* (CalS 3) and *OsGSL7* respectively (Blümke 2013). In *A. thaliana*, CalS 3 plays an important role in the regulation of plasmodesmata which plays an important role in symplastic signalling for plant development (Sevilem et al. 2013; Vatén et al. 2011; Wu et al. 2016). However, the role in monocots for this CalS is not that well understood. Homology to *BdGSL7* was identified for rice, sorghum and barley (Chowdhury et al. 2016). In *Triticum durum*, Terracciano et al. (2013) found the orthologue in the set marker *ubw22*, an important marker for the leaf rust QTL LF14a. Research on transcription of the *HvGSL* gene family revealed, that *HvGSL5*, the homolog callose synthase to *BdGSL7*, has higher expression levels in the first leave base, early florals, floral anthesis and the 3 days old coleoptile (Schober et al. 2009). Structural expression analysis of roots showed highest expression at the root tip and the adjacent tissue (Schober et al. 2009). Combining the expression data from barley with the data from *A. thaliana*, this might hint to a similar role of *BdGSL7* in *B. distachyon* (Vatén et al. 2011; Zhu et al. 2016). Since there are no major phenotypical abnormalities, as described in chapter 4.2.2, it is arguable that there is any major impact from the transcriptional differences on the phenotype of *B. distachyon*. Even though there are some indications for up- or down-regulation of specific *GSL* family genes, the associated phenotypes from the literature, as far as the data supports, were not observed during this work. This raises the question, whether this kind of transcriptional analysis is even a reliable tool for statements in complex organisms. Many other regulatory pathways, posttranslational modification and other mechanisms as hormones or transcript transport play also key roles in development, therefore minor regulatory differences in expression of members of a gene family like the *GSL* family, might not have an impact on the plant's phenotype.

4.2.6 How does the plant respond to the absence of callose after inoculation with *Fusarium graminearum* on transcriptional level?

The existence of pathogen responsive (PR) genes were first described in the 70s of the last century and were grouped into ten different classes (Gianinazzi 1970; Kombrink and Somssich 1997; Van Loon and Van Kammen 1970). To get an overview about a set of PR genes, the expression of *PR1.3*, *PR2*, *BdMAPKKK*, *BdChit8* and *BdUGT74f2* was analysed (Blümke et al. 2015; Powell et al. 2017).

Members from the *PR1* gene family are associated with salicylic acid and function as a marker for salicylic acid related plant defence in dicotyledons (Friedrich et al. 1996; Uknes et al. 1992). However, there is some evidence that this might not be the case in monocotyledons. Kouzai et al. (2016) could show that *PR1.3* was more likely to be suppressed after treatment with jasmonic acid, salicylic acid or ethylene. In wheat two member of the *PR1* gene family were identified but had no salicylic acid response (Molina et al. 1999). Nevertheless, genes of this group were shown to be upregulated after inoculation with *Fusarium graminearum*, *Claviceps purpurea* or the Panicum Mosaic Virus (PMV) in *B. distachyon* indicating its suitability as PR gene (Blümke et al. 2015; Kind et al. 2018; Mandadi and Scholthof 2012). Interestingly, *PR1-3*, was shown to be upregulated after *F. graminearum* and *Claviceps purpurea* infection (Blümke et al. 2015; Kind et al. 2018). However, there was no difference in the expression between the wild-type and the four genome edited lines at the examined time point. This might be explained with the early time point used in this work compared to 7 dpi for *F. graminearum* infection by Blümke et al. (2015) and the late 5 dpi time point for the *C. purpurea* infection by Kind et al. (2018).

The second chosen PR gene was *PR2*. *PR2* is a predicted secreted glycoside hydrolase type 17, found only in mature organs, localizing at the plasma membrane of mature leaves with a high homology to the rice gene Os01g71380 and the wheat expressed sequence tag (EST) AK331482 (Douché et al. 2013; Zhang et al. 2010c). Other research links the homology to a putative glucan endo-1,3- β -d-glucosidase, *WGLUC5* (CAI64809) of wheat (Pós 2010). In wheat, *WGLUC5* was upregulated after infection with the leaf rust causing pathogen *Puccinia recondita* f.sp. *tritici* (Pós 2010). *PR2* was upregulated in *Brachypodium distachyon* after infection with PMV, *Fusarium graminearum* and *Claviceps purpurea* (Blümke et al. 2015; Kind et al. 2018; Mandadi and Scholthof 2012). In Barley, a member of the *PR2* gene family was upregulated after *Blumeria graminis* f.sp. *hordei* and *Fusarium graminearum* infection (Boddu et al. 2006; Gregersen et al. 1997).

Studies in wheat revealed, that *PR2* has the highest expression 36 to 48 hpi with *Fusarium graminearum*, but expression was additionally detected in controls without inoculation (Pritsch et al. 2000). Expression studies revealed that *PR2* is upregulated after *F. graminearum* infection, and previous research hints that *PR2* is connected with increased resistance in wheat (Kang et al. 2003; Zhou et al. 2005). This upregulation was also observed via qPCR in this work. It was possible to detect *PR2* at 48 hpi, interestingly more abundant in the four genome edited lines compared to the wild-type. This upregulation is quite interesting because it might be a substitution mechanism to cope with the loss of callose depositions after inoculation or due to the faster *F. graminearum* progress in infection of the spikelets. Research in wheat with an overexpression of the barley *PR2* member revealed an increased resistance to *Fusarium graminearum* (Mackintosh et al. 2007), which might be an hint for the substitution idea to cope with the loss of callose depositions.

Transcriptome analysis from *Brachypodium distachyon* and wheat revealed an upregulation of *BdChit8* and *BdUGT74f2* (Powell et al. 2017). Further information regarding *BdChit8* are from a search for secreted proteins, where *BdChit8* was found as a secreted endochitinase, specially secreted in mature leaves, basal and apical internodes (Douché et al. 2013). A large meta-analysis of wheat QTL regions revealed, that the wheat homolog to *BdChit8*, Ta.30501.1, is part of a meta-QTL (MQTL), responding to heat and drought stress and involved in carbon isotope discrimination, harvest index, kernel number, maturity, spike weight and water status (Acuña-Galindo et al. 2015). But most interestingly, this wheat homolog was analysed after *Fusarium graminearum* inoculation in wheat, and the expression study showed that 24 hpi an upregulation was found compared to a *tri5* deficient *F. graminearum* strain (Foroud et al. 2012). At the used 48 hpi time point in this work, an upregulation was not detected. It is questionable, whether *BdChit8* is upregulated this early or rather later upregulated. In the work done in wheat with *tri5* deficient mutants, the upregulation is not significant, and the transcriptome analysis found the described upregulation in *Brachypodium distachyon* and in wheat at a much later time points after 7 dpi (Foroud et al. 2012; Powell et al. 2017). A further hint regarding the activity and expression time point of this chitinase is the classification. With the help of PLAZA (Van Bel et al. 2017; Vandepoele et al. 2013), a bioinformatic database, bioinformatic predictions classify *BdChit8* as a member of the glycoside hydrolase family 19, which consists of class I, II and IV chitinases (Henrissat 1991). Research on these chitinase classes revealed highly constitutive expression in different tissue (Hamel and Bellemare 1995; Lawton et al. 1994; Neale et al. 1990; Robinson et al. 1997; Samac et al. 1990; van Buuren et al. 1992). However, there is some evidence that chitinases of these classes are upregulated after inoculation with

pathogens, between 3 to 10 dpi (Samac and Shah 1991; van Buuren et al. 1992). Therefore, the used 2 dpi time point might be too early to observe shifts in expression, and a later time point, for example 7 dpi, should be analysed. *BdUGT74f2* was chosen because of its major role in the detoxification of DON (Schweiger et al. 2013). The already mentioned transcriptome analysis of FHB in *B. distachyon* and wheat by Powell et al. (2017) revealed an upregulation of *BdUGT74f2* after 7 dpi in *B. distachyon*. In wheat no homologues were described, and a recent overexpression of *BdUGT74f2* in wheat confers to a Type II resistance (Gatti et al. 2019; Powell et al. 2017). Again, later stages of the infection were surveyed compared to the used 2 dpi time point in this work which explains the lack of transcription in this work. However, Schweiger et al. (2013) investigated earlier time points, and the expression of *BdUGT74f2* was upregulated already after 24 hpi of *F. graminearum* strain PH-1, and responsiveness to DON was shown as soon as 3 hours after treatment. It is noteworthy, that the inoculation of *B. distachyon* with PH-1 in our lab revealed an existing Type II resistance, it was never observed that PH-1 was able to penetrate the rachis node of the inoculated spikelet compared to the 8/1 strain of *F. graminearum* (unpublished data). Therefore, the comparison between our 2 dpi time point, which showed no differences in expression, and the time points of PH-1 inoculated spikelets is problematic, since the reason for the Type II resistance in Bd21 to PH-1 is not known yet.

The last interesting PR gene, the *BdMAPKKK* is a mitogen-activated protein kinase kinase (MAPKK); MAPKKs are part of the MAPK Pathway, which are highly conserved not only in plants but in all lifeforms (Ichimura et al. 2002; Widmann et al. 1999). MAPK-Pathways play a decisive role in several different development pathways, like auxin related developmental events, in different stress response pathways, oxidative stress, cold or drought stress (Jia et al. 2016; Jonak et al. 1996; Kovtun et al. 2000; Li et al. 2017; Raz and Fluhr 1993). They also play essential roles in plant defence pathways, with recent research indicating an essential role in the ETI ROS Burst (Jalmi and Sinha 2016; Jia et al. 2016; Lang et al. 2017; Yoshioka et al. 2016). However, at the early 2 dpi time point, no differential expression could be detected. Since the chosen MAPKKK is not really researched, not much is known regarding its function in *B. distachyon*. It was shown, that after 7dpi with *F. graminearum* strain 8/1 in *B. distachyon* an upregulation was observed, interestingly DON seems to not be the cause of this upregulation (Blümke et al. 2015).

In conclusion, the early time point at 2dpi with *F. graminearum* revealed some interesting transcriptional results. Even though, the genes *PR1.3*, *BdChit8*, *BdUGT74f2* and *BdMAPKKK* showed no differences in expression, the gene *PR2* was upregulated in the four genome edited lines compared to the wild-type. The early time point was chosen, because of three key factors: 1. Upregulation of *BdGSL3* was detected 3 hours after wounding and callose detection after 12 h. 2. Callose depositions after non-host inoculation with *G. cichoracearum* were detected after 6 hours. 3. The callose depositions after *F. graminearum* inoculations were detected after 3 dpi (Blümke 2013). Therefore, it was interesting to investigate the early response of described PR genes in the *BdGSL3* disrupted lines. The reasons for the *PR2* upregulation are only hypothetical as there might be several explanations. For example, possible phytohormonal changes in the cell, a back-up system of plant defence, where the early upregulation of *PR2* might be induced by absence of functional *BdGSL3* or callose depositions. A third possibility is the faster *F. graminearum* infection in the four *BdGSL3* disrupted lines. However, for definitive answers, further analyses must be done regarding phytohormonal levels and the possible regulation of *PR2*, which is still unknown.

In this context it is noteworthy, that phytohormones play a key regulatory role in response to biotrophic and necrotrophic pathogens (Creelman and Mullet 1997; Durner et al. 1997; Feys and Parker 2000; Uknes et al. 1992). Even though the *BdGSL3* disruption of the four genome edited lines might not have any impact on the vegetative phytohormone regulations, an impact on biotic stress response might be possible. The two major phytohormones in plant defence are salicylic acid and jasmonic acid which are antagonistic to each other and the induction of one alleviates the other (Feys and Parker 2000; Kunkel and Brooks 2002). A general model for this interplay was proposed by Robert-Seilaniantz et al. (2007) in which the jasmonic acid pathway results in resistance to necrotrophic pathogens (Creelman and Mullet 1997) but results in susceptibility to biotrophic pathogens which was the opposite for the salicylic acid pathway (Durner et al. 1997). However, this model is based majorly on research in dicotyledons and their PR gene responses. In monocotyledons there is contradictory work. The basic jasmonic acid pathway as response to necrotrophic pathogens in monocotyledons could be shown by Desmond et al. (2005) with *F. pseudograminearum* in wheat. However, contradictory work in the regulation of PR-genes was found in monocotyledons compared to dicotyledons. In rice Agrawal et al. (2000) could identify a *PR1* gene, *OsPR1a*, which is induced by several phytohormones especially jasmonic acid and salicylic acid after wounding. In rice Mei et al. (2006) described the upregulation of several PR genes and *PR1b* in detail to jasmonic acid.

The *B. distachyon* gene *PR1.3* was not upregulated by salicylic or jasmonic acid treatment (Kouzai et al. 2016). Additionally, in wheat two genes of the *PR1* gene family were identified, which did not respond to activators of systemic acquired resistance (Molina et al. 1999). Ding et al. (2016) evaluated the salicylic acid and jasmonic acid response of different PR genes in wheat. And the wheat *PR1.1* gene was induced by salicylic acid and jasmonic acid, which was contradictory to previous research (Ding et al. 2016; Lu et al. 2005). These differences compared to the research reported from dicotyledons indicates differences in the plant defence responses of monocotyledons and dicotyledons. The jasmonic acid pathway is still responsible for necrotrophic pathogens, however the PR gene classes regulated by jasmonic acid and salicylic acid might differ compared to the proposed PR gene classes from dicotyledons. It would be highly interesting, if there are changes in the phytohormonal levels in the four *BdGSL3* disrupted mutants compared to the wild-type and how these changes might affect the defence pathway. Possible future experiments could be the measurement of phytohormones at different infection time points. Maybe the use of MALDI imaging to reveal possible hot spots or gradients in the spikelet could be used. Huang et al. (2016) used this technique to visualise endogenous metabolites in leaves of *Cayratia japonica*.

Since in the host-pathogen interaction two organisms are involved, it was interesting to examine if the absence of *BdGSL3* had any influence on the pathogen *Fusarium graminearum* and its virulence gene expression. Therefore, the two already identified virulence genes *fgl1* and *tri5* were analysed via qPCR at 2 dpi. *Tri5* is part of a gene cluster in *Fusarium graminearum* responsible for the trichothecene production (Alexander et al. 2009; Brown et al. 2004; Hohn et al. 1998; Ward et al. 2002). Research early identified that *tri5* plays an essential role in the pathway for DON production, and loss of function mutants were impaired in infection and particularly colonisation through the rachis (Bai et al. 2002; Jansen et al. 2005; Maier et al. 2006; Proctor et al. 1995; Proctor et al. 1997). Further research could identify infection structures with an active *tri5* promoter (Boenisch and Schäfer 2011). Expression and promoter studies revealed an upregulation of *tri5* at early infection stages (Doohan et al. 1999; Hallen-Adams et al. 2011; Ilgen et al. 2009; Voigt et al. 2007). And a detailed analysis of DON distribution in wheat spikes showed as early as 4 dpi DON around the inoculated floret (Savard et al. 2000). This was also observed in this work. In the wild-type and the four genome edited lines the *tri5* expression was present at 2 dpi. This fits with the described *tri5* expression for the infection from literature and the current model for *F. graminearum* infection. Furthermore, this confirms, that callose depositions have no effect on the expression of *tri5*, and the expression of *tri5* and DON production is not needed to overcome callose depositions at the rachis.

Studies with knock-out mutants of *fgl1* and overexpression mutants revealed the importance of the secreted lipase FGL1 for the infection and colonisation of wheat spikes (Salomon et al. 2012; Voigt et al. 2005). These results clearly indicate, that *fgl1* is a *F. graminearum* virulence gene, and further research indicated four other secreted lipases, which could be involved in the infection cycle of *F. graminearum* or might play a role in host specificity (Nguyen et al. 2010). It has to be noted, that earlier research already revealed the inhibition of callose synthesis through free fatty acids (Kauss and Jeblick 1986a). Inoculation studies on wheat with a $\Delta fgl1$ *F. graminearum* strain revealed, that the pathogen was impaired in infecting wheat and more callose in vascular tissue was detected (Blümke et al. 2014; Voigt et al. 2005). Infection studies on *B. distachyon* with the $\Delta fgl1$ strain revealed, that there was no difference in the disease course until 7 dpi, where the $\Delta fgl1$ deficient strain was concealed in the inoculated spikelet (Blümke et al. 2015).

The expression of *fgl1* after 2 dpi was lacking in the wild-type, but present in the four genome edited lines. Which leads to two questions, why there is no *fgl1* expression in the inoculated wild-type plants, and is *fgl1* the reason for the missing callose depositions. This might be a possible explanation, however, the reason why *fgl1* is only present in the four genome edited lines is not explicable. If we assume, that *B. distachyon* has two stress induced callose synthase with BdGSL2 and BdGSL3, which the data and literature suggests, this might explain both results and could build a model (Blümke 2013; Chowdhury et al. 2016).

4.2.7 A prospect on BdGSL2 and BdGSL3 and their role in *B. distachyon*

In barley and *B. distachyon* two possible CalS could be involved in stress response. This was suggested in barley for powdery mildew infection and HvGSL6 by Chowdhury et al. (2016) and in *B. distachyon* for BdGSL3 and the *F. graminearum* infection in spikelets in this work. Since barley and *B. distachyon* both have two possible stress-induced CalS with high homology (Chowdhury et al. 2016), this might be an evolutionary adaption to different pathogen stress or a adaption to effectors or defence suppressors. Maybe BdGSL2 and HvGSL6 are specialised on defence reactions to biotrophic pathogens, as shown for barley (Chowdhury et al. 2016), while HvGSL7 and BdGSL3 are specialised in defence reactions on necrotrophic pathogens infecting the reproductive organs, which was shown in this work for *B. distachyon*. One possible reason for the existence of two CalS could be the susceptibility to free fatty acids shown in wheat (Blümke et al. 2015; Ellinger et al. 2014b) and an adaption by barley and *B. distachyon* could be the acquisition of a second CalS.

To study this interesting possibility, CRISP/Cas9 mediated disruptions for *BdGSL2* and *HvGSL7* should be generated and examined. Further, a double disruption of *BdGSL2* and *BdGSL3* could be generated. The generated plants then could be analysed in response to pathogen stress to decipher the roles of both CalS and possible regulatory pathways. If future experiments reveal this proposed specialisation, the next step would be to find specific differences in the sequence, which might be used as breeding targets in crops. Another model could be the specification of *BdGSL2* or *BdGSL3* to biotrophic or necrotrophic pathogens because of effectors or suppressing metabolites. This could be a reason why after *F. graminearum* infection, even in the *BdGSL3* disrupted lines a small amount of callose is detected. *BdGSL2* and *BdGSL3* are both recruited when the pathogen is infecting the plant. However, *BdGSL3* might be resistant to the free fatty acids; a study on different wheat cultivars indicates that there is a link between more resistant wheat cultivars to *F. graminearum* infection and the callose biosynthesis resistance to free fatty acids (Ellinger et al. 2014b). Whereas *BdGSL2* might be susceptible to the free fatty acids, the absence of *BdGSL3* leads to the recruitment of *BdGSL2* at the infection sites, which then gets inhibited by free fatty acids. Further evidence for this model comes from the ortholog of *BdGSL3* in *Oryza sativa*, which was upregulated after inoculation with a herbivore feeding from the phloem sap, and the free fatty acids suppressed callose depositions in vascular tissue of wheat (Blümke et al. 2014; Ellinger et al. 2014b; Hao et al. 2008). Since this model is only a hypothetical model, follow up studies must be performed to falsify this hypothesis. Possible follow up studies could be infection studies with the $\Delta fgl1$ *F. graminearum* strain in the *BdGSL3* disrupted lines. If the $\Delta fgl1$ can colonise the spikelet, no free fatty acid inhibition on *BdGSL2* occurs. However, if the $\Delta fgl1$ strain is still contained in the inoculated floret, microscopy should reveal if callose deposition are formed. This would support this model and could give new insight into targets for plant breeding. It would also be highly interesting if a double disruption of *BdGSL2* and *BdGSL3* in *Brachypodium distachyon* is possible and the resulting phenotype.

4.3 The role of callose in plant defence

Even though the role of callose in the papillae formation is still debated (Voigt 2014), it is shown that callose might help in plant defence in wheat and *B. distachyon* (Blümke 2013; Blümke et al. 2014; Ellinger et al. 2014b; Kang and Buchenauer 2000). In addition, this work further supports the evidence from former research. The genome editing of *BdGSL3* results in higher infections at 14 dpi and 7 dpi. It was shown that in the four genome edited lines the amount of callose in the inoculated floret at 3 dpi is significantly reduced compared to the wild-type. Therefore, not only the importance of callose for type II resistance and plant defence in *Brachypodium distachyon* is shown, but also the role of *BdGSL3* in this scenario is apparent. *BdGSL3* is important for the formation of callose depositions after infection with *Fusarium graminearum* in spikelets and helps in plant defence. Since papillae formation is an early response of plant defence (Jones and Dangl 2006), callose might be just a first line of defence until other plant defence responses are activated. In wild-type *A. thaliana* the callose depositions at penetration sites are not enough to prevent penetration of adopted powdery mildews but are sufficient to prevent penetration by the non-host *B. graminis* f. sp. *hordei* (Ellinger et al. 2013; Jacobs et al. 2003). The overexpression of *PMR4* resulted in earlier and bigger callose depositions after powdery mildew infection, indicating that timing and size of callose papillae are key factors for successful plant defence to biotrophic pathogens (Ellinger et al. 2013). Super resolution microscopy performed by Eggert et al. (2014) with *PMR4* overexpression lines revealed bigger callose depositions at penetration sites which had a stronger cellulose/callose network in the plant cell wall and callose on the other side of the cell wall compared to the *A. thaliana* wild-type. It is reported that 1,3- β -glucans can have a gel like structure in acidic pH conditions (Harada et al. 1968; Saitô et al. 1979). It is possible, that this gel like structure could be some sort of barrier for fungal effectors or metabolites preventing these compounds from entering the plant cell. This might also explain the observed phenotype in this work and former work with overexpression of *BdGSL3* and *PMR4* in *B. distachyon* and the phenotype of the $\Delta fgl1$ strain in wheat (Blümke 2013; Blümke et al. 2014; Voigt et al. 2005; Voigt et al. 2007). The absence of callose depositions in wheat and *B. distachyon* results in an increased susceptibility to *F. graminearum* (Blümke et al. 2014). However, when the plant is able to form callose depositions in the inoculated spikelet, an increased resistance is observed (Blümke 2013; Blümke et al. 2014). Voigt et al. (2007) could detect an increased amount of DON in spikelets infected with the $\Delta fgl1$ strain which might be a response to cope with the callose depositions discovered by Blümke et al. (2014). This would also explain the FHB disease phenotype observed in this work. In the absence of callose, DON can infiltrate cells and

tissues without any form of barrier preparing the tissue for infection. To test this hypothesis of one possible role of callose in plant defence the use of MALDI (McDonnell and Heeren 2007) or desorption electrospray ionisation (DESI) (Takáts et al. 2004) imaging could be used. Both technologies enable high resolution visualisation of compounds with coupled mass spectrometry (McDonnell and Heeren 2007; Takáts et al. 2004). In this specific case, cross sections of inoculated spikelets from wheat or *B. distachyon* could be used. Inoculation with the $\Delta fgl1$ deficient strain in wheat, and the use of wild-type and the *BdGSL3* disrupted lines from *B. distachyon* could deliver new insights into the role of callose depositions to the *F. graminearum* infection and the proposed function as a sealing barrier.

4.4 Conclusion

In summary during this work, a novel understanding of callose synthesis as pathogen associated stress response is presented and the usability of modern technologies could be shown. It was possible to reveal, that the genome editing method CRISPR/Cas9 is working in the model plant *Brachypodium distachyon*. The screening of transgenic plants revealed mutations in the genome. The data suggests that the endonuclease was already active in the homozygotic callus tissue used for agrobacteria-mediated transformation in single lines. Other lines had a mosaicism genotype, indicating the activity of the endonuclease construct during plant regeneration. Two lines lost the T-DNA but kept the identified mutations. This supports the usability of this modern method as a new tool for specific breeding of crops. Furthermore, it was possible to show that no major negative impact was observed in the mutated plant lines. This further supports the usability of CRISPR/Cas9 as a new breeding tool, since a major problem of classic mutagenesis breeding is the outcrossing of the unwanted genes.

With the aid of the CRISPR/Cas9 mediated genome editing, it was possible to induce severe deletions in the DNA sequence predicted stress-induced 1,3- β -glucan synthase *BdGSL3*. Analysis of the induced mutations in *BdGSL3* revealed several deletions and changes of amino acids and a frameshift mutation with stop codon in one of the analysed plant lines. This enabled further characterization of *BdGSL3* and its possible role in *B. distachyon*. On the general vegetative phenotype, the disrupted *BdGSL3* had no major impact. The life cycle was not altered, no severe impairments were observed in the formation of leaves, elongation of the plant stem or the formation and maturity of spikelets and seeds. However, the plant growth was altered slightly resulting in a minor slower elongation in the early life cycle, which diminished after five weeks.

The impact of non-functional BdGSL3 on the expression of all members of the GSL gene family was also examined. With the aid of the probe based Real-Time Ready system from Roche® it was possible to screen the expression throughout the three major aboveground organs of plants. It was possible to observe some minor differences in the expression of single members of the *GSL* family, and their possible roles from other plant species, but the impact of these expression differences was not observed. Therefore, it is highly likely that BdGSL3 in *Brachypodium distachyon* is not involved in general development processes.

Since callose depositions are often common stress responses, either to abiotic or biotic stress, different kind of stresses in different tissues were provoked and analysed. Abiotic wounding stress in leaves showed no clear difference between the wild-type and the four genome edited lines, and the inoculation with the necrotrophic fungus *Stagonospora nodorum* showed no differences in the callose response in all examined lines. However, the inoculation with the FHB causing pathogen *Fusarium graminearum* and the analysis of the infection revealed the importance of BdGSL3 in plant defence. Infection assays revealed a stronger FHB disease in all four genome edited lines compared to the wild-type at two different time points of the disease. Furthermore, the analysis of the early infection deciphered the role of BdGSL3. The four genome edited plant lines had a significantly reduced callose response to the *F. graminearum* infection. These results fit well into the current knowledge regarding the role of callose depositions in crops as a plant defence mechanism. Other research already revealed the importance of callose depositions for plant defence and the mechanism of *Fusarium graminearum* in suppressing callose depositions for a successful colonisation of the host plant. Further overexpression experiments with callose synthases led to a stronger callose response and a weaker disease course. Therefore, it is highly likely that BdGSL3 is responsible for the biotic stress related callose depositions in infected spikelets to repel the infecting pathogen.

This is further backed with expression studies on PR genes and virulence genes, which revealed a higher expression of *PR2* in the four genome edited lines compared to the wild-type and the expression of the *F. graminearum* virulence gene *fgl1*. A new hypothetical model for the role of BdGSL3 and BdGSL2 was drawn which incorporates the current research on both glucan synthases. There are some indications, that *B. distachyon* evolved two stress related glucan synthases, with either different organ specificity or as an evolutionary adaptation to pathogens. BdGSL3 seems to be dominantly active in the rachis nodes and rachis of spikelets, and fungal *fgl1*, which is suppressing callose depositions in wheat, is not working with BdGSL3. However, the absence of presumably active BdGSL3 might result in the recruitment of BdGSL2, which

is susceptible to *fgl1*, which is then expressed by *F. graminearum* to suppress the forming of callose depositions. In the end, this work revealed new insights in the plant response to the necrotrophic pathogenic fungus *F. graminearum* and opens new interesting questions for future research in the host-pathogen interaction.

5. Abstract

Since the last century, scientists around the globe have warned of the upcoming challenges for humanity. Climate change is affecting us not solely by more frequent catastrophes, melting glaciers, changes to ecosystems or rising temperatures. The indirect effects resulting from these climate changes might even be more severe. The threats on food safety and security is high, and phytopathogens play a major role. In western countries, the agriculture can adopt and fight those threats, but for small farmer in developing countries, these threats are alarming. Moreover, the human population is projected to reach 9.8 billion at the year 2050 and the food production need to increase by 40 %. However, already many pathogens, like *Fusarium graminearum*, *Parastagonospora nodorum* or *Magnaporthe grisea* are causing high yield losses. With the upcoming changes to the climate, these losses might even increase and the traditional agriculture and breeding might not be able to cope with these challenges. Therefore, new breeding technologies must be introduced in plant breeding and new possible targets for plant breeding must be studied. One of these targets might be the stress related formation of callose depositions. The importance of callose as a stress response to several biotic and abiotic stresses is long time known and previous work in *A. thaliana* revealed the possibility of the stress induced callose synthase *AtGSL5* as a new breeding target. Therefore, it was necessary to identify a possible stress induced callose synthase in *B. distachyon* a model plant for crops. With the aid of CRISPR/Cas9-mediated genome editing it was possible to generate plants with an impaired *BdGSL3* locus. The impaired *BdGSL3* locus caused no observable phenotype in the general appearance of *B. distachyon* for the analysed mutants compared to the wild-type. Furthermore, the mutants showed no severe deficiency in growth or senescence which might be assumed based on the data from *A. thaliana*. On transcriptional level throughout the whole *GSL* gene family, some minor changes in the transcription were observed, however these had no impact on the associated function of the involved GSLs leading to the conclusion, that *BdGSL3* has a stress related function in *B. distachyon*.

To study the stress related role of *BdGSL3*, several stresses were induced and the callose mediated responses were examined. After wounding of leaves, no difference in an early time point was observed but in a later time point, a slightly reduced callose response was observed. However, the infection with the necrotrophic leaf pathogen *P. nodorum* did not differ in the callose formation to infecting hyphae. To study the callose response to *F. graminearum* and the impact on the FHB disease, infections were evaluated after 14 dpi and 7 dpi.

At both evaluated time points in all examined mutants the disease was more present compared to the wild type. This was further backed by microscopy of inoculated florets at 7 dpi revealing a faster colonisation of the rachis node and the rachis tissue in all four genome edited lines. To reveal the reason behind this difference in the disease process, the early time point of 3 dpi was examined and the amount of callose in the inoculated florets was quantified. This evaluation revealed an almost complete loss of callose formation in the four genome edited lines compared to the wild type. QPCR experiments on PR-genes revealed a significant increase in *PR2* expression in the genome edited lines, indicating a possible compensation mechanism. It was further possible to detect the presence of *FGL1*, a *F. graminearum* virulence gene, in all four genome edited lines but not in the wild type.

In the end it was shown, that modern genome editing techniques could be easily applied to the monocotyledon model grass *Brachypodium distachyon* in example of the 1,3- β -glucan synthase BdGSL3. The role of BdGSL3 in *B. distachyon* could be identified leading to the conclusion that BdGSL3 is indeed a stress related callose synthase. Its primary role lies in the formation of callose depositions after *F. graminearum* infection to reduce the FHB symptoms and slow down the infection of *F. graminearum*. A secondary role could be the formation of wound induced callose to seal the tissue around wounds, but this might only be a minor function and the data is not clear.

6. Zusammenfassung

Schon seit dem letzten Jahrhundert warnen Wissenschaftler vor den Folgen und Herausforderungen des menschengemachten Klimawandels. Mögliche Folgen des Klimawandels sind eine erhöhte Anzahl an Naturkatastrophen, schmelzende Gletscher, steigende Temperaturen und schwerwiegende Veränderungen von Ökosystemen. Diese Folgen können jedoch zu indirekten Folgen führen, die weitaus schwerwiegender sind. Die Gefahr, dass die Nahrungsproduktion und Qualität nicht mehr zu halten sind, ist groß. Auch wenn in westlichen Ländern diese Probleme nicht so bedeutend sind, da der Einsatz von Chemikalien, modernen Agrartechnologien und ein großes Repertoire an Sorten diese Probleme vermindert, ist die Gefahr bedeutend für Bauern in Entwicklungsländern. Diese haben nicht den Zugriff auf moderne Technologien für die Landwirtschaft und müssen auf ihre verfügbaren Sorten zurückgreifen. Noch bedeutender wird diese Problemsituation mit einem Blick auf die Zukunft, die Menschheit soll auf 9,8 Milliarden Menschen bis 2050 anwachsen. Um diese Bevölkerungsexpansion weiterhin zu ernähren, muss die Landwirtschaft ihre Produktion um mindestens 40 % steigern. Viele Pflanzenkrankheitserreger sind jedoch heute schon schwerwiegende Probleme für die Landwirtschaft, so sorgen die Erreger *Fusarium graminearum*, *Parastagonospora nodorum* oder *Magnaporthe grisea* für bedeutende Ernteverluste bei wichtigen Feldfrüchten wie Weizen oder Reis. Durch die bevorstehenden Klimaveränderungen ist es zu erwarten, dass gerade pilzliche Pflanzenkrankheitserreger eine noch bedeutendere Rolle spielen könnten. Die klassischen Züchtungsmethoden könnten für den steigenden Druck auf die Landwirtschaft durch Pathogenbefall keine passenden Antworten mehr finden oder zu langsam sein, daher sind neue Züchtungsmethoden nötig. Einhergehend mit neuen Züchtungsmethoden ist auch die Identifizierung von neuen Zielen für die Züchtung, eines dieser Ziele wären Callosesynthesen. Arbeiten an der Stress-induzierten Callosesynthase AtGSL5 zeigten bereits die Möglichkeiten mit modernen Technologien die Pflanzenabwehr zu stärken. Um dies auch auf Gräser zu übertragen, sollte eine mögliche stress induzierte Callosesynthase in *Brachypodium distachyon* identifiziert und ihre Rolle in der Pathogenabwehr charakterisiert werden. Durch Zuhilfenahme des jüngsten Vertreters der *genome editing* Verfahren, dem CRISPR/Cas9 vermitteltem *genome editing*, sollte *BdGSL3* untersucht werden. Es war möglich, eine Gendisruption mit CRISPR/Cas9 zu induzieren, welche keine phänotypischen Auswirkungen auf die Pflanzen zu haben scheint. Es wurden keine Auffälligkeiten beim Wachstum entdeckt und auch während der Beobachtung des Lebenszyklus von *B. distachyon* konnten keine Auffälligkeiten beobachtet werden.

Auf transkriptioneller Ebene sollte die Auswirkung der Mutationen auf die restliche *GSL* Genfamilie studiert werden. Es konnten zwar in verschiedenen Organen vereinzelte Änderungen in der Genexpression beobachtet werden, jedoch konnte keiner der mit diesen Callosesynthesen assoziierten Phänotypen beobachtet werden. Es lässt sich darauf schließen, dass BdGSL3 keinen Einfluss auf die Pflanzenentwicklung hat, jedoch vielleicht regulativ auf die Expression anderer Callosesynthesen wirkt.

Um den Einfluss von Stress auf die Aktivität und Aufgaben von BdGSL3 zu untersuchen, wurden verschiedene abiotische und biotische Stresssituationen hervorgerufen und analysiert. Verwundungen der Blätter wurden zu unterschiedlichen Zeitpunkten analysiert, um den Callose vermittelten Wundverschluss zu untersuchen. Es konnten jedoch keine Auffälligkeiten zum frühen Zeitpunkt beobachtet werden und zum späten Zeitpunkt waren die Unterschiede nicht signifikant, jedoch mit einer deutlichen Tendenz zu einer geringeren Callosemenge bei Verwundung. Ein weiterer Stress auf Blättern wurde durch den nekrotrophen Pilz *Parastagonospora nodorum* ausgelöst, jedoch konnte auch hier keine relevanten Unterschiede in der Calloseantwort beobachtet werden. Um den Einfluss von BdGSL3 auf die Fusariose zu untersuchen, wurden Infektionen mit dem Auslöser der Fusariose, *Fusarium graminearum* analysiert. Zu den Zeitpunkten 14- und 7-Tage nach Inokulation konnte ein deutlich stärkerer Krankheitsverlauf für alle vier mutierten Linien im Vergleich zum Wild-typ beobachtet werden. Diese Beobachtung konnte durch Mikroskopie unterstützt werden, die beim frühen Zeitpunkt aufzeigte, dass *F. graminearum* bereits den Rachisknoten befallen hat und in die Rachis des Ährchen eingedrungen ist. Um die Ursache für diesen stärkeren Krankheitsverlauf zu begründen, wurden Aufnahmen von inokulierten Blüten drei Tage nach der Inokulation mikroskopiert. Es konnte gezeigt werden, dass im Vergleich zum Wild-typ alle mutierten Linien deutlich weniger Callose aufweisen was die Ursache für den stärkeren Krankheitsverlauf zu sein scheint. Um mögliche Auswirkungen auf die Expression von PR-Genen zu untersuchen, wurden *qPCR*-Experimente durchgeführt. Hier konnte beobachtet werden, dass die vier genomeditierten Linien eine signifikant höhere *PR2* Expression aufweisen. Das spricht für einen Versuch den stärkeren Befall mit anderen Abwehrmechanismen zu kompensieren. Es war außerdem möglich in diesen Linien die Expression eines *F. graminearum* Virulenzgen, der Lipase *FGL1*, zu detektieren. Zusammenfassend war es möglich mittels *CRISPR/Cas9* eine Mutation in *B. distachyon* zu induzieren, die einen Verlust der Aktivität von BdGSL3 zur Folge hatte. BdGSL3 scheint nicht für die generelle Pflanzenentwicklung benötigt zu werden. Die Hauptaufgabe von BdGSL3 scheint jedoch in der Stressantwort zu liegen, wobei die Hauptaufgabe in der Verteidigungsantwort nach *F. graminearum* Infektion zu liegen scheint.

7. References

- Ablazov A, Tombuloglu H (2016) Genome-wide identification of the mildew resistance locus O (MLO) gene family in novel cereal model species *Brachypodium distachyon* European journal of plant pathology 145:239-253
- Acuña-Galindo MA, Mason RE, Subramanian NK, Hays DB (2015) Meta-Analysis of Wheat QTL Regions Associated with Adaptation to Drought and Heat Stress Crop Science 55:477-492 doi:10.2135/cropsci2013.11.0793
- Agrawal GK, Jwa N-S, Rakwal R (2000) A Novel Rice (*Oryza sativa* L.) Acidic PR1 Gene Highly Responsive to Cut, Phytohormones, and Protein Phosphatase Inhibitors Biochemical and Biophysical Research Communications 274:157-165 doi:<https://doi.org/10.1006/bbrc.2000.3114>
- Aist JR (1976) Papillae and Related Wound Plugs of Plant Cells Annual Review of Phytopathology 14:145-163 doi:10.1146/annurev.py.14.090176.001045
- Alazem M, Lin NS (2015) Roles of plant hormones in the regulation of host–virus interactions Molecular plant pathology 16:529-540
- Albinsky D et al. (2010) Metabolomic Screening Applied to Rice FOX Arabidopsis Lines Leads to the Identification of a Gene-Changing Nitrogen Metabolism Molecular Plant 3:125-142 doi:<https://doi.org/10.1093/mp/ssp069>
- Alexander NJ, Proctor RH, McCormick SP (2009) Genes, gene clusters, and biosynthesis of trichothecenes and fumonisins in *Fusarium* Toxin Reviews 28:198-215 doi:10.1080/15569540903092142
- Ali MA, Abbas A, Kreil DP, Bohlmann H (2013) Overexpression of the transcription factor RAP2. 6 leads to enhanced callose deposition in syncytia and enhanced resistance against the beet cyst nematode *Heterodera schachtii* in Arabidopsis roots BMC plant biology 13:47
- Alves SC, Worland B, Thole V, Snape JW, Bevan MW, Vain P (2009) A protocol for Agrobacterium-mediated transformation of *Brachypodium distachyon* community standard line Bd21 Nature protocols 4:638
- Amor Y, Haigler CH, Johnson S, Wainscott M, Delmer DP (1995) A membrane-associated form of sucrose synthase and its potential role in synthesis of cellulose and callose in plants Proceedings of the National Academy of Sciences 92:9353-9357
- Anders C, Niewoehner O, Duerst A, Jinek M (2014) Structural basis of PAM-dependent target DNA recognition by the Cas9 endonuclease Nature 513:569 doi:10.1038/nature13579
<https://www.nature.com/articles/nature13579#supplementary-information>
- Anderson CT, Carroll A, Akhmetova L, Somerville C (2010) Real-Time Imaging of Cellulose Reorientation during Cell Wall Expansion in Arabidopsis Roots Plant Physiology 152:787-796 doi:10.1104/pp.109.150128
- Anderson EM et al. (2015) Systematic analysis of CRISPR–Cas9 mismatch tolerance reveals low levels of off-target activity Journal of Biotechnology 211:56-65 doi:<https://doi.org/10.1016/j.jbiotec.2015.06.427>
- Andrawis A, Solomon M, Delmer DP (1993) Cotton fiber annexins: a potential role in the regulation of callose synthase The Plant Journal 3:763-772
- Arseniuk E, Góral T, Sowa W, Czembor1 H, Krysiak H, Scharen A (1998) Transmission of *Stagonospora nodorum* and *Fusarium* spp. on triticale and wheat seed and the effect of seedborne *Stagonospora nodorum* on disease severity under field conditions Journal of Phytopathology 146:339-345
- Asano T et al. (1991) The role of N-glycosylation of GLUT1 for glucose transport activity Journal of Biological Chemistry 266:24632-24636
- Aspinall GOaK, G. (1957) The structure of callose from the grape vine. Chemistry and Industry, London.

- Axtell MJ, Staskawicz BJ (2003) Initiation of RPS2-specified disease resistance in *Arabidopsis* is coupled to the AvrRpt2-directed elimination of RIN4 Cell 112:369-377
- Ayliffe M, Singh D, Park R, Moscou M, Pryor T (2013) Infection of *Brachypodium distachyon* with selected grass rust pathogens Molecular plant-microbe interactions 26:946-957
- Babla P, Draper J, Davey MR, Lynch PT (1995) Plant regeneration and micropropagation of *Brachypodium distachyon* Plant Cell, Tissue and Organ Culture 42:97-107
doi:10.1007/BF00037687
- Bae K-H et al. (2003) Human zinc fingers as building blocks in the construction of artificial transcription factors Nature biotechnology 21:275
- Bae S, Park J, Kim J-S (2014) Cas-OFFinder: a fast and versatile algorithm that searches for potential off-target sites of Cas9 RNA-guided endonucleases Bioinformatics 30:1473-1475
doi:10.1093/bioinformatics/btu048
- Bai GH, Desjardins AE, Plattner RD (2002) Deoxynivalenol-nonproducing *Fusarium graminearum* Causes Initial Infection, but does not Cause Disease Spread in Wheat Spikes Mycopathologia 153:91-98 doi:10.1023/A:1014419323550
- Baltrus DA et al. (2011) Dynamic evolution of pathogenicity revealed by sequencing and comparative genomics of 19 *Pseudomonas syringae* isolates PLoS pathogens 7:e1002132
- Bari R, Jones JD (2009) Role of plant hormones in plant defence responses Plant molecular biology 69:473-488
- Barrangou R, Doudna JA (2016) Applications of CRISPR technologies in research and beyond Nature biotechnology 34:933
- Barrangou R, Horvath P (2012) CRISPR: New Horizons in Phage Resistance and Strain Identification Annual Review of Food Science and Technology 3:143-162 doi:10.1146/annurev-food-022811-101134
- Barratt DHP et al. (2011) Callose Synthase GSL7 Is Necessary for Normal Phloem Transport and Inflorescence Growth in *Arabidopsis* Plant Physiology 155:328-341
doi:10.1104/pp.110.166330
- Bathgate J, Loughman R (2001) Ascospores are a source of inoculum of *Phaeosphaeria nodorum*, *P. avenaria* f. sp. *avenaria* and *Mycosphaerella graminicola* in Western Australia Australasian Plant Pathology 30:317-322
- Batistič O, Sorek N, Schültke S, Yalovsky S, Kudla J (2008) Dual Fatty Acyl Modification Determines the Localization and Plasma Membrane Targeting of CBL/CIPK Ca^{2+} Signaling Complexes in *Arabidopsis* The Plant Cell 20:1346-1362 doi:10.1105/tpc.108.058123
- Bebber DP, Gurr SJ (2015) Crop-destroying fungal and oomycete pathogens challenge food security Fungal Genetics and Biology 74:62-64 doi:<https://doi.org/10.1016/j.fgb.2014.10.012>
- Becker JD, Boavida LC, Carneiro J, Haury M, Feijó JA (2003) Transcriptional Profiling of *Arabidopsis* Tissues Reveals the Unique Characteristics of the Pollen Transcriptome Plant Physiology 133:713-725 doi:10.1104/pp.103.028241
- Belhaj K, Chaparro-Garcia A, Kamoun S, Nekrasov V (2013) Plant genome editing made easy: targeted mutagenesis in model and crop plants using the CRISPR/Cas system Plant Methods 9:39 doi:10.1186/1746-4811-9-39
- Bender KW, Snedden WA (2013) Calmodulin-Related Proteins Step Out from the Shadow of Their Namesake Plant Physiology 163:486-495 doi:10.1104/pp.113.221069
- Benschop JJ, Mohammed S, O'Flaherty M, Heck AJR, Slijper M, Menke FLH (2007) Quantitative Phosphoproteomics of Early Elicitor Signaling in *Arabidopsis* Molecular & Cellular Proteomics 6:1198-1214 doi:10.1074/mcp.M600429-MCP200
- Berger S, Menudier A, Julien R, Karamanos Y (1995) Do de-N-glycosylation enzymes have an important role in plant cells? Biochimie 77:751-760
- Bernoux M et al. (2011) Structural and functional analysis of a plant resistance protein TIR domain reveals interfaces for self-association, signaling, and autoregulation Cell host & microbe 9:200-211
- Berry DJ (2019) Historiographies of Plant Breeding and Agriculture
- Bessueille L, Sindt N, Guichardant M, Djerbi S, Teeri TT, Bulone V (2009) Plasma membrane microdomains from hybrid aspen cells are involved in cell wall polysaccharide biosynthesis Biochemical Journal 420:93 doi:10.1042/BJ20082117

- Bhathal J, Loughman R, Speijers J (2003) Yield reduction in wheat in relation to leaf disease from yellow (tan) spot and septoria nodorum blotch *European Journal of Plant Pathology* 109:435-443
- Bibikova M, Carroll D, Segal DJ, Trautman JK, Smith J, Kim Y-G, Chandrasegaran S (2001) Stimulation of homologous recombination through targeted cleavage by chimeric nucleases *Molecular and cellular biology* 21:289-297
- Bird PM, Ride JP (1981) The resistance of wheat to *Septoria nodorum*: fungal development in relation to host lignification *Physiological Plant Pathology* 19:289-IN283
doi:[https://doi.org/10.1016/S0048-4059\(81\)80063-X](https://doi.org/10.1016/S0048-4059(81)80063-X)
- Blume B, Nürnberger T, Nass N, Scheel D (2000) Receptor-mediated increase in cytoplasmic free calcium required for activation of pathogen defense in parsley *The Plant Cell* 12:1425-1440
- Blümke A (2013) Induktion der Resistenz gegenüber dem Weizenpathogen *Fusarium graminearum* durch gezielte Zellwandveränderungen in *Brachypodium distachyon*
- Blümke A et al. (2014) Secreted Fungal Effector Lipase Releases Free Fatty Acids to Inhibit Innate Immunity-Related Callose Formation during Wheat Head Infection *Plant Physiology* 165:346-358 doi:10.1104/pp.114.236737
- Blümke A, Sode B, Ellinger D, Voigt CA (2015) Reduced susceptibility to *Fusarium* head blight in *Brachypodium distachyon* through priming with the *Fusarium* mycotoxin deoxynivalenol *Molecular Plant Pathology* 16:472-483 doi:10.1111/mpp.12203
- Blümke A, Somerville SC, Voigt CA (2013) Transient expression of the <i>Arabidopsis thaliana</i> callose synthase PMR4 increases penetration resistance to powdery mildew in barley *Advances in Bioscience and Biotechnology* 04:810-813 doi:10.4236/abb.2013.48106
- Boch J, Bonas U (2010) *Xanthomonas* AvrBs3 family-type III effectors: discovery and function *Annual review of phytopathology* 48:419-436
- Boch J et al. (2009) Breaking the Code of DNA Binding Specificity of TAL-Type III Effectors *Science* 326:1509-1512 doi:10.1126/science.1178811
- Boddu J, Cho S, Kruger WM, Muehlbauer GJ (2006) Transcriptome Analysis of the Barley-*Fusarium graminearum* Interaction *Molecular Plant-Microbe Interactions* 19:407-417
doi:10.1094/mpmi-19-0407
- Boenisch MJ, Schäfer W (2011) *Fusarium graminearum* forms mycotoxin producing infection structures on wheat *BMC Plant Biology* 11:110 doi:10.1186/1471-2229-11-110
- Boller T (1995) Chemoperception of microbial signals in plant cells *Annual review of plant biology* 46:189-214
- Boller T, Felix G (2009) A Renaissance of Elicitors: Perception of Microbe-Associated Molecular Patterns and Danger Signals by Pattern-Recognition Receptors *Annual Review of Plant Biology* 60:379-406 doi:10.1146/annurev.arplant.57.032905.105346
- Bolotin A, Quinquis B, Sorokin A, Ehrlich SD (2005) Clustered regularly interspaced short palindrome repeats (CRISPRs) have spacers of extrachromosomal origin *Microbiology* 151:2551-2561 doi:<https://doi.org/10.1099/mic.0.28048-0>
- Bondy-Denomy J, Pawluk A, Maxwell KL, Davidson AR (2013) Bacteriophage genes that inactivate the CRISPR/Cas bacterial immune system *Nature* 493:429
- Borgese N, Aggularo D, Carrera P, Pietrini G, Bassetti M (1996) A role for N-myristoylation in protein targeting: NADH-cytochrome b5 reductase requires myristic acid for association with outer mitochondrial but not ER membranes *The Journal of Cell Biology* 135:1501-1513
doi:10.1083/jcb.135.6.1501
- Bormann J, Boenisch MJ, Brückner E, Firat D, Schäfer W (2014) The adenylyl cyclase plays a regulatory role in the morphogenetic switch from vegetative to pathogenic lifestyle of *Fusarium graminearum* on wheat *PLoS one* 9:e91135
- Bos JI et al. (2010) *Phytophthora infestans* effector AVR3a is essential for virulence and manipulates plant immunity by stabilizing host E3 ligase CMPG1 *Proceedings of the National Academy of Sciences* 107:9909-9914
- Bos JI et al. (2006) The C-terminal half of *Phytophthora infestans* RXLR effector AVR3a is sufficient to trigger R3a-mediated hypersensitivity and suppress INF1-induced cell death in *Nicotiana benthamiana* *The Plant Journal* 48:165-176

- Botha C, Matsiliza B, Bornman C (2004) Reduction in transport in wheat (*Triticum aestivum*) is caused by sustained phloem feeding by the Russian wheat aphid (*Diuraphis noxia*) South African Journal of Botany 70:249-254
- Botha CEJ, Cross RHM, van Bel AJE, Peter CI (2000) Phloem loading in the sucrose-export-defective (SXD-1) mutant maize is limited by callose deposition at plasmodesmata in bundle sheath—vascular parenchyma interface Protoplasma 214:65-72 doi:10.1007/BF02524263
- Bowles DJ, Marcus SE, Pappin D, Findlay J, Eliopoulos E, Maycox PR, Burgess J (1986) Posttranslational processing of concanavalin A precursors in jackbean cotyledons The Journal of cell biology 102:1284-1297
- Braam J, Davis RW (1990) Rain-, wind-, and touch-induced expression of calmodulin and calmodulin-related genes in Arabidopsis Cell 60:357-364
- Bradshaw JE (2016) Plant breeding: past, present and future. Springer,
- Bragg JN, Anderton A, Nieu R, Vogel JP (2015) Brachypodium distachyon. In: Agrobacterium Protocols. Springer, pp 17-33
- Bragg JN et al. (2012) Generation and characterization of the Western Regional Research Center Brachypodium T-DNA insertional mutant collection PloS one 7:e41916
- Branza-Nichita N et al. (2000) Mutations at critical N-glycosylation sites reduce tyrosinase activity by altering folding and quality control Journal of Biological Chemistry 275:8169-8175
- Breen S, Williams SJ, Winterberg B, Kobe B, Solomon PS (2016) Wheat PR-1 proteins are targeted by necrotrophic pathogen effector proteins The Plant Journal 88:13-25
- Brito SSB, Cunha APMA, Cunningham CC, Alvalá RC, Marengo JA, Carvalho MA (2018) Frequency, duration and severity of drought in the Semiarid Northeast Brazil region International Journal of Climatology 38:517-529 doi:10.1002/joc.5225
- Britt AB (1999) Molecular genetics of DNA repair in higher plants Trends in Plant Science 4:20-25 doi:[https://doi.org/10.1016/S1360-1385\(98\)01355-7](https://doi.org/10.1016/S1360-1385(98)01355-7)
- Brkljacic J et al. (2011) Brachypodium as a model for the grasses: today and the future Plant Physiology 157:3-13
- Brouns SJ et al. (2008) Small CRISPR RNAs guide antiviral defense in prokaryotes Science 321:960-964
- Brown DW, Dyer RB, McCormick SP, Kendra DF, Plattner RD (2004) Functional demarcation of the Fusarium core trichothecene gene cluster Fungal Genetics and Biology 41:454-462 doi:<https://doi.org/10.1016/j.fgb.2003.12.002>
- Brown NA, Urban M, Van De Meene AM, Hammond-Kosack KE (2010) The infection biology of Fusarium graminearum: Defining the pathways of spikelet to spikelet colonisation in wheat ears Fungal biology 114:555-571
- Brownfield L, Doblin M, Fincher GB, Bacic A (2009) Biochemical and molecular properties of biosynthetic enzymes for (1, 3)- β -glucans in embryophytes, chlorophytes and rhodophytes. In: Chemistry, Biochemistry, and Biology of 1-3 Beta Glucans and Related Polysaccharides. Elsevier, pp 283-326
- Budman J, Chu G (2005) Processing of DNA for nonhomologous end-joining by cell-free extract Embo j 24:849-860 doi:10.1038/sj.emboj.7600563
- Busse-Wicher M et al. (2014) The pattern of xylan acetylation suggests xylan may interact with cellulose microfibrils as a twofold helical screw in the secondary plant cell wall of Arabidopsis thaliana The Plant Journal 79:492-506
- Cao Y, Liang Y, Tanaka K, Nguyen CT, Jedrzejczak RP, Joachimiak A, Stacey G (2014) The kinase LYK5 is a major chitin receptor in Arabidopsis and forms a chitin-induced complex with related kinase CERK1 Elife 3:e03766
- Carlile A, Bindschedler L, Bailey A, Bowyer P, Clarkson J, Cooper RM (2000) Characterization of SNP1, a cell wall-degrading trypsin, produced during infection by Stagonospora nodorum Molecular plant-microbe interactions 13:538-550
- Carpita NC, Gibeaut DM (1993) Structural models of primary cell walls in flowering plants: consistency of molecular structure with the physical properties of the walls during growth The Plant Journal 3:1-30 doi:10.1111/j.1365-3113.1993.tb00007.x
- CARVER TLW, GRIFFITHS E (1981) Relationship between powdery mildew infection, green leaf area and grain yield of barley Annals of Applied Biology 99:255-266 doi:doi:10.1111/j.1744-7348.1981.tb04794.x

- Caryl AP, Jones GH, Franklin FCH (2003) Dissecting plant meiosis using *Arabidopsis thaliana* mutants *Journal of Experimental Botany* 54:25-38
- Catalan P, Kellogg EA, Olmstead RG (1997) Phylogeny of Poaceae subfamily Pooideae based on chloroplast *ndhF* gene sequences *Molecular phylogenetics and evolution* 8:150-166 doi:10.1006/mpev.1997.0416
- Catalan P, López-Álvarez D, Díaz-Pérez A, Sancho R, López-Herránz ML (2016) Phylogeny and Evolution of the Genus *Brachypodium*. In: Vogel JP (ed) *Genetics and Genomics of Brachypodium*. Springer International Publishing, Cham, pp 9-38. doi:10.1007/7397_2015_17
- Catalan P et al. (2012) Evolution and taxonomic split of the model grass *Brachypodium distachyon* *Annals of botany* 109:385-405 doi:10.1093/aob/mcr294
- Cerioti A, Duranti M, Bollini R (1998) Effects of N-glycosylation on the folding and structure of plant proteins *Journal of Experimental Botany* 49:1091-1103
- Chawade A, Alexandersson E, Bengtsson T, Andreasson E, Levander F (2016) Targeted Proteomics Approach for Precision Plant Breeding *Journal of Proteome Research* 15:638-646 doi:10.1021/acs.jproteome.5b01061
- Chen X-Y et al. (2009) The *Arabidopsis* Callose Synthase Gene *GSL8* Is Required for Cytokinesis and Cell Patterning *Plant Physiology* 150:105-113 doi:10.1104/pp.108.133918
- Chinchilla D et al. (2007) A flagellin-induced complex of the receptor FLS2 and BAK1 initiates plant defence *Nature* 448:497
- Chisholm ST, Coaker G, Day B, Staskawicz BJ (2006) Host-microbe interactions: shaping the evolution of the plant immune response *Cell* 124:803-814
- Choo Y, Klug A (1994) Toward a code for the interactions of zinc fingers with DNA: selection of randomized fingers displayed on phage *Proceedings of the National Academy of Sciences* 91:11163-11167
- Chooi Y-H, Muria-Gonzalez MJ, Solomon PS (2014) A genome-wide survey of the secondary metabolite biosynthesis genes in the wheat pathogen *Parastagonospora nodorum* *Mycology* 5:192-206 doi:10.1080/21501203.2014.928386
- Chowdhury J et al. (2016) Down-regulation of the glucan synthase-like 6 gene (*HvGsl6*) in barley leads to decreased callose accumulation and increased cell wall penetration by *Blumeria graminis* f. sp. *hordei* *New Phytologist* 212:434-443 doi:10.1111/nph.14086
- Chrispeels M, Hartl PM, Sturm A, Faye L (1986) Characterization of the endoplasmic reticulum-associated precursor of concanavalin A. Partial amino acid sequence and lectin activity *Journal of Biological Chemistry* 261:10021-10024
- Christian M et al. (2010) Targeting DNA double-strand breaks with TAL effector nucleases *Genetics* 186:757-761
- Christiansen P, Andersen CH, Didion T, Folling M, Nielsen KK (2005) A rapid and efficient transformation protocol for the grass *Brachypodium distachyon* *Plant cell reports* 23:751-758 doi:10.1007/s00299-004-0889-5
- Chu VT, Weber T, Wefers B, Wurst W, Sander S, Rajewsky K, Kühn R (2015) Increasing the efficiency of homology-directed repair for CRISPR-Cas9-induced precise gene editing in mammalian cells *Nature Biotechnology* 33:543 doi:10.1038/nbt.3198
- <https://www.nature.com/articles/nbt.3198#supplementary-information>
- Cohen P (1988) Review Lecture: Protein phosphorylation and hormone action *Proceedings of the Royal Society of London Series B Biological Sciences* 234:115-144 doi:10.1098/rspb.1988.0040
- Collard Bertrand CY, Mackill David J (2008) Marker-assisted selection: an approach for precision plant breeding in the twenty-first century *Philosophical Transactions of the Royal Society B: Biological Sciences* 363:557-572 doi:10.1098/rstb.2007.2170
- Collier SM, Moffett P (2009) NB-LRRs work a “bait and switch” on pathogens *Trends in plant science* 14:521-529
- Cong L, Zhou R, Kuo Y-c, Cunniff M, Zhang F (2012) Comprehensive interrogation of natural TALE DNA-binding modules and transcriptional repressor domains *Nature Communications* 3:968 doi:10.1038/ncomms1962
- <https://www.nature.com/articles/ncomms1962#supplementary-information>

- Conner RL, Kuzyk AD, Su H (2003) Impact of powdery mildew on the yield of soft white spring wheat cultivars *Canadian Journal of Plant Science* 83:725-728 doi:10.4141/P03-043
- Cosgrove DJ (2014) Re-constructing our models of cellulose and primary cell wall assembly *Current opinion in plant biology* 22:122-131 doi:10.1016/j.pbi.2014.11.001
- Cradick TJ, Fine EJ, Antico CJ, Bao G (2013) CRISPR/Cas9 systems targeting β -globin and CCR5 genes have substantial off-target activity *Nucleic Acids Research* 41:9584-9592 doi:10.1093/nar/gkt714
- Creelman RA, Mullet JE (1997) Biosynthesis and action of jasmonates in plants *Annual review of plant biology* 48:355-381
- Cross FR, Garber EA, Pellman D, Hanafusa H (1984) A short sequence in the p60src N terminus is required for p60src myristylation and membrane association and for cell transformation *Molecular and Cellular Biology* 4:1834-1842 doi:10.1128/mcb.4.9.1834
- Cui X, Shin H, Song C, Laosinchai W, Amano Y, Brown MR (2001) A putative plant homolog of the yeast β -1, 3-glucan synthase subunit FKS1 from cotton (*Gossypium hirsutum* L.) fibers *Planta* 213:223-230
- Cunfer BM, Ueng PP (1999) Taxonomy and identification of *Septoria* and *Stagonospora* species on small-grain cereals *Annual review of phytopathology* 37:267-284
- Currier HB (1957) CALLOSE SUBSTANCE IN PLANT CELLS *American Journal of Botany* 44:478-488 doi:10.1002/j.1537-2197.1957.tb10567.x
- Currier HB, Strugger S (1956) Aniline blue and fluorescence microscopy of callose in bulb scales of *Allium cepa* L *Protoplasma* 45:552-559 doi:10.1007/BF01252676
- D'Ovidio R, Mattei B, Roberti S, Bellincampi D (2004) Polygalacturonases, polygalacturonase-inhibiting proteins and pectic oligomers in plant-pathogen interactions *Biochimica et Biophysica Acta (BBA) - Proteins and Proteomics* 1696:237-244 doi:<https://doi.org/10.1016/j.bbapap.2003.08.012>
- Dalmay M et al. (2013) A TILLING platform for functional genomics in *Brachypodium distachyon* *PLoS one* 8:e65503
- Dangl JL, Horvath DM, Staskawicz BJ (2013) Pivoting the Plant Immune System from Dissection to Deployment *Science* 341:746-751 doi:10.1126/science.1236011
- Dangl JL, Jones JD (2001) Plant pathogens and integrated defence responses to infection *nature* 411:826
- Daniels R, Kurowski B, Johnson AE, Hebert DN (2003) N-Linked Glycans Direct the Cotranslational Folding Pathway of Influenza Hemagglutinin *Molecular Cell* 11:79-90 doi:[https://doi.org/10.1016/S1097-2765\(02\)00821-3](https://doi.org/10.1016/S1097-2765(02)00821-3)
- Dekazos ED, Worley J (1967) Induction of callose formation by bruising and aging of red tart cherries *Journal of Food Science* 32:287-289
- Delmer D, Potikha T (1997) Structures and functions of annexins in plants *Cellular and Molecular Life Sciences CMLS* 53:546-553
- Deltcheva E et al. (2011) CRISPR RNA maturation by trans-encoded small RNA and host factor RNase III *Nature* 471:602-607 doi:10.1038/nature09886
- Deng D et al. (2012) Structural Basis for Sequence-Specific Recognition of DNA by TAL Effectors *Science* 335:720-723 doi:10.1126/science.1215670
- Desmond OJ, Edgar CI, Manners JM, Maclean DJ, Schenk PM, Kazan K (2005) Methyl jasmonate induced gene expression in wheat delays symptom development by the crown rot pathogen *Fusarium pseudograminearum* *Physiological and Molecular Plant Pathology* 67:171-179 doi:<https://doi.org/10.1016/j.pmpp.2005.12.007>
- Desta ZA, Ortiz R (2014) Genomic selection: genome-wide prediction in plant improvement *Trends in Plant Science* 19:592-601 doi:10.1016/j.tplants.2014.05.006
- Ding L-N, Yang G-X, Yang R-Y, Cao J, Zhou Y (2016) Investigating interactions of salicylic acid and jasmonic acid signaling pathways in monocots wheat *Physiological and Molecular Plant Pathology* 93:67-74 doi:<https://doi.org/10.1016/j.pmpp.2016.01.002>
- Ding S-Y, Zhao S, Zeng Y (2014) Size, shape, and arrangement of native cellulose fibrils in maize cell walls *Cellulose* 21:863-871
- Diotallevi F, Mulder B (2007) The cellulose synthase complex: a polymerization driven supramolecular motor *Biophysical Journal* 92:2666-2673

- Doblin MS, De Melis L, Newbigin E, Basic A, Read SM (2001) Pollen Tubes of *Nicotiana glauca* Express Two Genes from Different β -Glucan Synthase Families Plant Physiology 125:2040-2052 doi:10.1104/pp.125.4.2040
- Dodds PN, Rathjen JP (2010) Plant immunity: towards an integrated view of plant–pathogen interactions Nature Reviews Genetics 11:539
- Döll S, Dänicke S (2011) The Fusarium toxins deoxynivalenol (DON) and zearalenone (ZON) in animal feeding Preventive Veterinary Medicine 102:132-145 doi:<https://doi.org/10.1016/j.prevetmed.2011.04.008>
- Dong X, Hong Z, Sivaramakrishnan M, Mahfouz M, Verma DPS (2005) Callose synthase (CalS5) is required for exine formation during microgametogenesis and for pollen viability in Arabidopsis The Plant Journal 42:315-328 doi:10.1111/j.1365-3113.2005.02379.x
- Doohan FM, Weston G, Rezanoor HN, Parry DW, Nicholson P (1999) Development and Use of a Reverse Transcription-PCR Assay To Study Expression of *Tri5* by *Fusarium* Species In Vitro and In Planta Applied and Environmental Microbiology 65:3850-3854
- Douché T et al. (2013) Brachypodium distachyon as a model plant toward improved biofuel crops: Search for secreted proteins involved in biogenesis and disassembly of cell wall polymers PROTEOMICS 13:2438-2454 doi:10.1002/pmic.201200507
- Doudna JA, Charpentier E (2014) The new frontier of genome engineering with CRISPR-Cas9 Science 346:1258096
- Draper J, Mur LA, Jenkins G, Ghosh-Biswas GC, Bablak P, Hasterok R, Routledge AP (2001) Brachypodium distachyon. A new model system for functional genomics in grasses Plant physiology 127:1539-1555
- Dreier B, Beerli RR, Segal DJ, Flippin JD, Barbas CF (2001) Development of zinc finger domains for recognition of the 5'-ANN-3' family of DNA sequences and their use in the construction of artificial transcription factors Journal of Biological Chemistry 276:29466-29478
- Dreier B et al. (2005) Development of zinc finger domains for recognition of the 5'-CNN-3' family DNA sequences and their use in the construction of artificial transcription factors Journal of Biological Chemistry 280:35588-35597
- Durner J, Shah J, Klessig DF (1997) Salicylic acid and disease resistance in plants Trends in plant science 2:266-274
- Edwards D, Batley J, Snowdon RJ (2013) Accessing complex crop genomes with next-generation sequencing Theoretical and Applied Genetics 126:1-11
- Eggert D, Naumann M, Reimer R, Voigt CA (2014) Nanoscale glucan polymer network causes pathogen resistance Scientific reports 4:4159
- Eitas TK, Dangel JL (2010) NB-LRR proteins: pairs, pieces, perception, partners, and pathways Current Opinion in Plant Biology 13:472-477 doi:<https://doi.org/10.1016/j.pbi.2010.04.007>
- Ellinger D et al. (2014a) Interaction of the Arabidopsis GTPase RabA4c with its effector PMR4 results in complete penetration resistance to powdery mildew Plant Cell 26:3185-3200 doi:10.1105/tpc.114.127779
- Ellinger D et al. (2013) Elevated early callose deposition results in complete penetration resistance to powdery mildew in Arabidopsis Plant Physiol 161:1433-1444 doi:10.1104/pp.112.211011
- Ellinger D, Sode B, Falter C, Voigt CA (2014b) Resistance of callose synthase activity to free fatty acid inhibition as an indicator of Fusarium head blight resistance in wheat Plant Signal Behav 9:e28982 doi:10.4161/psb.28982
- Endo M, Mikami M, Toki S (2014) Multigene Knockout Utilizing Off-Target Mutations of the CRISPR/Cas9 System in Rice Plant and Cell Physiology 56:41-47 doi:10.1093/pcp/pcu154
- Enns LC, Kanaoka MM, Torii KU, Comai L, Okada K, Cleland RE (2005) Two callose synthases, GSL1 and GSL5, play an essential and redundant role in plant and pollen development and in fertility Plant Molecular Biology 58:333-349 doi:10.1007/s11103-005-4526-7
- Erda L, Wei X, Hui J, Yinlong X, Yue L, Liping B, Liyong X (2005) Climate change impacts on crop yield and quality with CO₂ fertilization in China Philosophical Transactions of the Royal Society B: Biological Sciences 360:2149-2154 doi:10.1098/rstb.2005.1743
- Erwig J, Ghareeb H, Kopischke M, Hacke R, Matei A, Petutschnig E, Lipka V (2017) Chitin-induced and CHITIN ELICITOR RECEPTOR KINASE1 (CERK1) phosphorylation-dependent

- endocytosis of *Arabidopsis thaliana* LYSIN MOTIF-CONTAINING RECEPTOR-LIKE KINASE5 (LYK5) *New Phytologist* 215:382-396
- Eticha D, Thé C, Welcker C, Narro L, Staß A, Horst WJ (2005) Aluminium-induced callose formation in root apices: inheritance and selection trait for adaptation of tropical maize to acid soils *Field Crops Research* 93:252-263 doi:<https://doi.org/10.1016/j.fcr.2004.10.004>
- Falter C, Voigt CA (2014) Comparative Cellular Analysis of Pathogenic Fungi with a Disease Incidence in *Brachypodium distachyon* and *Miscanthus x giganteus* *BioEnergy Research* 7:958-973 doi:10.1007/s12155-014-9439-3
- Falter C et al. (2015) Glucanocellulosic ethanol: the undiscovered biofuel potential in energy crops and marine biomass *Scientific Reports* 5:13722 doi:10.1038/srep13722
- <https://www.nature.com/articles/srep13722#supplementary-information>
- Faye L, Chrispeels MJ (1987) Transport and processing of the glycosylated precursor of concanavalin A in jack-bean *Planta* 170:217-224
- Fears R, Aro E-M, Pais MS, ter Meulen V (2014) How should we tackle the global risks to plant health? *Trends in Plant Science* 19:206-208 doi:10.1016/j.tplants.2014.02.010
- Felix G, Duran JD, Volko S, Boller T (1999) Plants have a sensitive perception system for the most conserved domain of bacterial flagellin *The Plant journal : for cell and molecular biology* 18:265-276 doi:10.1046/j.1365-313x.1999.00265.x
- Fernandes AN et al. (2011) Nanostructure of cellulose microfibrils in spruce wood *Proceedings of the National Academy of Sciences* 108:E1195-E1203
- Fernández-Calvino L, Faulkner C, Maule A (2011) Plasmodesmata as active conduits for virus cell-to-cell movement *Recent Advances in Plant Virology*:47-74
- Fernie AR, Schauer N (2009) Metabolomics-assisted breeding: a viable option for crop improvement? *Trends in Genetics* 25:39-48 doi:10.1016/j.tig.2008.10.010
- Feys BJ, Parker JE (2000) Interplay of signaling pathways in plant disease resistance *Trends in genetics* 16:449-455
- Figueroa M, Alderman S, Garvin DF, Pfender WF (2013) Infection of *Brachypodium distachyon* by formae speciales of *Puccinia graminis*: early infection events and host-pathogen incompatibility *PloS one* 8:e56857
- Figueroa M, Hammond-Kosack KE, Solomon PS (2018) A review of wheat diseases—a field perspective *Molecular Plant Pathology* 19:1523-1536 doi:10.1111/mpp.12618
- Fillinger S, Elad Y (2016) *Botrytis: The Fungus, the Pathogen and Its Management in Agricultural Systems*. Springer,
- Fitzgerald TL et al. (2015) *Brachypodium* as an emerging model for cereal–pathogen interactions *Annals of botany* 115:717-731
- Flors V, Ton J, Van Doorn R, Jakab G, García-Agustín P, Mauch-Mani B (2008) Interplay between JA, SA and ABA signalling during basal and induced resistance against *Pseudomonas syringae* and *Alternaria brassicicola* *The Plant Journal* 54:81-92
- Fones H, Gurr S (2015) The impact of *Septoria tritici* Blotch disease on wheat: An EU perspective *Fungal Genetics and Biology* 79:3-7 doi:<https://doi.org/10.1016/j.fgb.2015.04.004>
- Foroud NA, Ouellet T, Laroche A, Oosterveen B, Jordan MC, Ellis BE, Eudes F (2012) Differential transcriptome analyses of three wheat genotypes reveal different host response pathways associated with *Fusarium* head blight and trichothecene resistance *Plant Pathology* 61:296-314 doi:10.1111/j.1365-3059.2011.02512.x
- Fridborg I, Grainger J, Page A, Coleman M, Findlay K, Angell S (2003) TIP, A Novel Host Factor Linking Callose Degradation with the Cell-to-Cell Movement of Potato virus X *Molecular Plant-Microbe Interactions* 16:132-140 doi:10.1094/MPMI.2003.16.2.132
- Fried G, Chauvel B, Reynaud P, Sache I (2017) Decreases in Crop Production by Non-native Weeds, Pests, and Pathogens. In: Vilà M, Hulme PE (eds) *Impact of Biological Invasions on Ecosystem Services*. Springer International Publishing, Cham, pp 83-101. doi:10.1007/978-3-319-45121-3_6
- Friedrich L et al. (1996) A benzothiadiazole derivative induces systemic acquired resistance in tobacco *The Plant Journal* 10:61-70
- Frye CA, Innes RW (1998) An *Arabidopsis* Mutant with Enhanced Resistance to Powdery Mildew *The Plant Cell* 10:947-956 doi:10.1105/tpc.10.6.947

- Fu Y, Foden JA, Khayter C, Maeder ML, Reyon D, Joung JK, Sander JD (2013) High-frequency off-target mutagenesis induced by CRISPR-Cas nucleases in human cells *Nature Biotechnology* 31:822 doi:10.1038/nbt.2623
- <https://www.nature.com/articles/nbt.2623#supplementary-information>
- Fu Y, Sander JD, Reyon D, Cascio VM, Joung JK (2014) Improving CRISPR-Cas nuclease specificity using truncated guide RNAs *Nature Biotechnology* 32:279 doi:10.1038/nbt.2808
- <https://www.nature.com/articles/nbt.2808#supplementary-information>
- Fujisaki K et al. (2015) Rice Exo70 interacts with a fungal effector, AVR-Pii, and is required for AVR-Pii-triggered immunity *The Plant Journal* 83:875-887 doi:10.1111/tpj.12934
- Gaj T, Gersbach CA, Barbas CF (2013) ZFN, TALEN, and CRISPR/Cas-based methods for genome engineering *Trends in Biotechnology* 31:397-405
doi:<https://doi.org/10.1016/j.tibtech.2013.04.004>
- Gao Y et al. (2015) Identification and Characterization of the SnTox6-Snn6 Interaction in the *Parastagonospora nodorum*–Wheat Pathosystem *Molecular Plant-Microbe Interactions* 28:615-625 doi:10.1094/MPMI-12-14-0396-R
- Garcia-Arenal F, Sagasta EM (1977) Callose deposition and phytoalexin accumulation in *Botrytis cinerea*-infected bean (*Phaseolus vulgaris*) *Plant Science Letters* 10:305-312
doi:[https://doi.org/10.1016/0304-4211\(77\)90054-2](https://doi.org/10.1016/0304-4211(77)90054-2)
- Garneau JE et al. (2010) The CRISPR/Cas bacterial immune system cleaves bacteriophage and plasmid DNA *Nature* 468:67
- Garvin DF (2007) Brachypodium: a new monocot model plant system emerges *Journal of the Science of Food and Agriculture* 87:1177-1179
- Gasiunas G, Barrangou R, Horvath P, Siksnys V (2012) Cas9-crRNA ribonucleoprotein complex mediates specific DNA cleavage for adaptive immunity in bacteria *Proc Natl Acad Sci U S A* 109:E2579-2586 doi:10.1073/pnas.1208507109
- Gatti M (2017) Detoxification of mycotoxins as a source of resistance to Fusarium Head blight: from *Brachypodium distachyon* to *Triticum aestivum*. Paris Saclay
- Gatti M, Cambon F, Tassy C, Macadre C, Guerard F, Langin T, Dufresne M (2019) The *Brachypodium distachyon* UGT Bradi5gUGT03300 confers type II fusarium head blight resistance in wheat *Plant Pathology* 68:334-343 doi:10.1111/ppa.12941
- Ghorbal M, Gorman M, Macpherson CR, Martins RM, Scherf A, Lopez-Rubio J-J (2014) Genome editing in the human malaria parasite *Plasmodium falciparum* using the CRISPR-Cas9 system *Nature Biotechnology* 32:819 doi:10.1038/nbt.2925
- <https://www.nature.com/articles/nbt.2925#supplementary-information>
- Gianinazzi S (1970) Hypersensibilite aux virus, temperature et proteines solubles chez le *Nicotiana xanthi* nc Apparition de nouvelles macromolecules lors de la repression de la synthese virale *CR Acad Sci (Paris)* 270:2383-2386
- Gill US, Serrani-Yarce JC, Lee H-K, Mysore KS (2018) Tissue culture (somatic embryogenesis)-induced Tnt1 retrotransposon-based mutagenesis in *Brachypodium distachyon*. In: *Brachypodium Genomics*. Springer, pp 57-63
- Gill US, Uppalapati SR, Nakashima J, Mysore KS (2015) Characterization of *Brachypodium distachyon* as a nonhost model against switchgrass rust pathogen *Puccinia emaculata* *BMC plant biology* 15:113
- Gimenez-Ibanez S, Hann DR, Ntoukakis V, Petutschnig E, Lipka V, Rathjen JP (2009) AvrPtoB targets the LysM receptor kinase CERK1 to promote bacterial virulence on plants *Current biology* 19:423-429
- Godde JS, Bickerton A (2006) The repetitive DNA elements called CRISPRs and their associated genes: evidence of horizontal transfer among prokaryotes *Journal of Molecular evolution* 62:718-729
- Göhre V et al. (2008) Plant pattern-recognition receptor FLS2 is directed for degradation by the bacterial ubiquitin ligase AvrPtoB *Current biology* 18:1824-1832
- Gómez-Gómez L, Bauer Z, Boller T (2001) Both the extracellular leucine-rich repeat domain and the kinase activity of FLS2 are required for flagellin binding and signaling in *Arabidopsis* *The Plant Cell* 13:1155-1163

- Gómez-Gómez L, Boller T (2000) FLS2: an LRR receptor-like kinase involved in the perception of the bacterial elicitor flagellin in *Arabidopsis* Molecular cell 5:1003-1011
- Gómez-Gómez L, Felix G, Boller T (1999) A single locus determines sensitivity to bacterial flagellin in *Arabidopsis thaliana* The Plant Journal 18:277-284
- Gonneau M, Desprez T, Guillot A, Vernhettes S, Höfte H (2014) Catalytic subunit stoichiometry within the cellulose synthase complex Plant physiology 166:1709-1712
- Gorbunova V, Levy AA (1999) How plants make ends meet: DNA double-strand break repair Trends in plant science 4:263-269
- Goss EM et al. (2014) The Irish potato famine pathogen *Phytophthora infestans* originated in central Mexico rather than the Andes Proceedings of the National Academy of Sciences 111:8791-8796
- GOSWAMI RS, KISTLER HC (2004) Heading for disaster: *Fusarium graminearum* on cereal crops Molecular Plant Pathology 5:515-525 doi:doi:10.1111/j.1364-3703.2004.00252.x
- Grant SR, Fisher EJ, Chang JH, Mole BM, Dangl JL (2006) Subterfuge and manipulation: type III effector proteins of phytopathogenic bacteria Annu Rev Microbiol 60:425-449
- Gregersen PL, Thordal-Christensen H, Förster H, Collinge DB (1997) Differential gene transcript accumulation in barley leaf epidermis and mesophyll in response to attack by *Blumeria graminis* f.sp. *hordei* (syn. *Erysiphe graminis* f.sp. *hordei*) Physiological and Molecular Plant Pathology 51:85-97 doi:<https://doi.org/10.1006/pmpp.1997.0108>
- Griffey CA, Das MK, Stromberg EL (1993) Effectiveness of adult-plant resistance in reducing grain yield loss to powdery mildew in winter wheat Plant Disease 77:618-622 doi:10.1094/PD-77-0618
- Groß F, Durner J, Gaupels F (2013) Nitric oxide, antioxidants and prooxidants in plant defence responses Frontiers in Plant Science 4:419
- Group GPW et al. (2001) Phylogeny and subfamilial classification of the grasses (Poaceae) Annals of the Missouri Botanical Garden:373-457
- Guseman JM et al. (2010) Dysregulation of cell-to-cell connectivity and stomatal patterning by loss-of-function mutation in *Arabidopsis* CHORUS (*GLUCAN SYNTHASE-LIKE 8*) Development 137:1731-1741 doi:10.1242/dev.049197
- Gusmaroli G, Figueroa P, Serino G, Deng XW (2007) Role of the MPN Subunits in COP9 Signalosome Assembly and Activity, and Their Regulatory Interaction with *Arabidopsis* Cullin3-Based E3 Ligases The Plant Cell 19:564-581 doi:10.1105/tpc.106.047571
- Haas BJ et al. (2009) Genome sequence and analysis of the Irish potato famine pathogen *Phytophthora infestans* Nature 461:393
- Haft DH, Selengut J, Mongodin EF, Nelson KE (2005) A Guild of 45 CRISPR-Associated (Cas) Protein Families and Multiple CRISPR/Cas Subtypes Exist in Prokaryotic Genomes PLOS Computational Biology 1:e60 doi:10.1371/journal.pcbi.0010060
- Hallen-Adams HE, Wenner N, Kuldau GA, Trail F (2011) Deoxynivalenol Biosynthesis-Related Gene Expression During Wheat Kernel Colonization by *Fusarium graminearum* Phytopathology 101:1091-1096 doi:10.1094/phyto-01-11-0023
- Hamel F, Bellemare G (1995) Characterization of a class I chitinase gene and of wound-inducible, root and flower-specific chitinase expression in *Brassica napus* Biochimica et Biophysica Acta (BBA) - Gene Structure and Expression 1263:212-220 doi:[https://doi.org/10.1016/0167-4781\(95\)00099-3](https://doi.org/10.1016/0167-4781(95)00099-3)
- Hammond-Kosack KE, Jones J (1996) Resistance gene-dependent plant defense responses The Plant Cell 8:1773
- Hammond C, Braakman I, Helenius A (1994) Role of N-linked oligosaccharide recognition, glucose trimming, and calnexin in glycoprotein folding and quality control Proceedings of the National Academy of Sciences 91:913-917 doi:10.1073/pnas.91.3.913
- Han W, Liang C, Jiang B, Ma W, Zhang Y (2016) Major Natural Disasters in China, 1985–2014: Occurrence and Damages International Journal of Environmental Research and Public Health 13 doi:10.3390/ijerph13111118
- Han X et al. (2014) Auxin-Callose-Mediated Plasmodesmal Gating Is Essential for Tropic Auxin Gradient Formation and Signaling Developmental Cell 28:132-146 doi:<https://doi.org/10.1016/j.devcel.2013.12.008>

- Hao P et al. (2008) Herbivore-induced callose deposition on the sieve plates of rice: an important mechanism for host resistance *Plant physiology* 146:1810-1820
- Harada T, Misaki A, Saito H (1968) Curdlan: A bacterial gel-forming β -1, 3-glucan *Archives of Biochemistry and Biophysics* 124:292-298 doi:[https://doi.org/10.1016/0003-9861\(68\)90330-5](https://doi.org/10.1016/0003-9861(68)90330-5)
- Hau J, Muller M, Pagni M (2007) HitKeeper, a generic software package for hit list management *Source Code for Biology and Medicine* 2:2
- Hauck P, Thilmoney R, He SY (2003) A *Pseudomonas syringae* type III effector suppresses cell wall-based extracellular defense in susceptible *Arabidopsis* plants *Proceedings of the National Academy of Sciences* 100:8577-8582
- Have At, Mulder W, Visser J, van Kan JAL (1998) The Endopolygalacturonase Gene Bcpg1 Is Required for Full Virulence of *Botrytis cinerea* *Molecular Plant-Microbe Interactions* 11:1009-1016 doi:10.1094/MPMI.1998.11.10.1009
- Hayafune M et al. (2014) Chitin-induced activation of immune signaling by the rice receptor CEBiP relies on a unique sandwich-type dimerization *Proceedings of the National Academy of Sciences* 111:E404-E413
- Hayashi T, Read S, Bussell J, Thelen M, Lin F-C, Brown R, Delmer D (1987) UDP-glucose:(1 \rightarrow 3)- β -glucan synthases from mung bean and cotton: differential effects of Ca²⁺ and Mg²⁺ on enzyme properties and on macromolecular structure of the glucan product *Plant physiology* 83:1054-1062
- Hebert DN, Molinari M (2007) In and Out of the ER: Protein Folding, Quality Control, Degradation, and Related Human Diseases *Physiological Reviews* 87:1377-1408 doi:10.1152/physrev.00050.2006
- Heese A et al. (2007) The receptor-like kinase SERK3/BAK1 is a central regulator of innate immunity in plants *Proceedings of the National Academy of Sciences* 104:12217-12222
- Heil M, Baldwin IT (2002) Fitness costs of induced resistance: emerging experimental support for a slippery concept *Trends in Plant Science* 7:61-67 doi:[https://doi.org/10.1016/S1360-1385\(01\)02186-0](https://doi.org/10.1016/S1360-1385(01)02186-0)
- Helenius A (1994) How N-linked oligosaccharides affect glycoprotein folding in the endoplasmic reticulum *Molecular Biology of the Cell* 5:253-265 doi:10.1091/mbc.5.3.253
- Henrissat B (1991) A classification of glycosyl hydrolases based on amino acid sequence similarities *Biochem J* 280 (Pt 2):309-316 doi:10.1042/bj2800309
- Hill JL, Hammudi MB, Tien M (2014) The *Arabidopsis* cellulose synthase complex: a proposed hexamer of CESA trimers in an equimolar stoichiometry *The Plant Cell* 26:4834-4842
- Hofmann J, Youssef-Banora M, de Almeida-Engler J, Grundler FM (2010) The role of callose deposition along plasmodesmata in nematode feeding sites *Molecular Plant-Microbe Interactions* 23:549-557
- Hohn TM, McCormick SP, Alexander NJ, Desjardins AE, Proctor RH (1998) Function and Biosynthesis of Trichothecenes Produced by *Fusarium* Species. In: Kohmoto K, Yoder OC (eds) *Molecular Genetics of Host-Specific Toxins in Plant Disease: Proceedings of the 3rd Tottori International Symposium on Host-Specific Toxins*, Daisen, Tottori, Japan, August 24–29, 1997. Springer Netherlands, Dordrecht, pp 17-24. doi:10.1007/978-94-011-5218-1_2
- Hong SY, Park JH, Cho SH, Yang MS, Park CM (2011) Phenological growth stages of *Brachypodium distachyon*: codification and description *Weed Research* 51:612-620 doi:10.1111/j.1365-3180.2011.00877.x
- Hong Z, Delauney AJ, Verma DPS (2001a) A cell plate-specific callose synthase and its interaction with phragmoplastin *The Plant Cell* 13:755-768
- Hong Z, Zhang Z, Olson JM, Verma DPS (2001b) A Novel UDP-Glucose Transferase Is Part of the Callose Synthase Complex and Interacts with Phragmoplastin at the Forming Cell Plate *The Plant Cell* 13:769-779 doi:10.1105/tpc.13.4.769
- Horst W, Püschel A-K, Schmohl N (1997) Induction of callose formation is a sensitive marker for genotypic aluminium sensitivity in maize *Plant and Soil* 192:23-30
- Horvath P, Barrangou R (2010) CRISPR/Cas, the immune system of bacteria and archaea *Science* 327:167-170
- Hsia MM et al. (2017) Sequencing and functional validation of the JGI *Brachypodium distachyon* T-DNA collection *The Plant Journal* 91:361-370

- Hsu PD et al. (2013) DNA targeting specificity of RNA-guided Cas9 nucleases *Nature Biotechnology* 31:827 doi:10.1038/nbt.2647
- <https://www.nature.com/articles/nbt.2647#supplementary-information>
- Huang L, Tang X, Zhang W, Jiang R, Chen D, Zhang J, Zhong H (2016) Imaging of Endogenous Metabolites of Plant Leaves by Mass Spectrometry Based on Laser Activated Electron Tunneling *Scientific Reports* 6:24164 doi:10.1038/srep24164
- Huang LS, Doherty HK, Herskowitz I (2005) The Smk1p MAP kinase negatively regulates Gsc2p, a 1, 3- β -glucan synthase, during spore wall morphogenesis in *Saccharomyces cerevisiae* *Proceedings of the National Academy of Sciences* 102:12431-12436
- Huang X-Y et al. (2013) CYCLIN-DEPENDENT KINASE G1 Is Associated with the Spliceosome to Regulate *CALLOSE SYNTHASE5* Splicing and Pollen Wall Formation in *Arabidopsis* *The Plant Cell* 25:637-648 doi:10.1105/tpc.112.107896
- Huber SC (2007) Exploring the role of protein phosphorylation in plants: from signalling to metabolism *Biochemical Society Transactions* 35:28-32 doi:10.1042/bst0350028
- Hunter T (1995) Protein kinases and phosphatases: The Yin and Yang of protein phosphorylation and signaling *Cell* 80:225-236 doi:[https://doi.org/10.1016/0092-8674\(95\)90405-0](https://doi.org/10.1016/0092-8674(95)90405-0)
- Hussey RS, Mims CW, Westcott SW (1992) Immunocytochemical localization of callose in root cortical cells parasitized by the ring nematode *Criconemella xenoplax* *Protoplasma* 171:1-6 doi:10.1007/BF01379274
- Hwang WY et al. (2013) Efficient genome editing in zebrafish using a CRISPR-Cas system *Nature Biotechnology* 31:227 doi:10.1038/nbt.2501
- <https://www.nature.com/articles/nbt.2501#supplementary-information>
- Iakoucheva LM, Radivojac P, Brown CJ, O'Connor TR, Sikes JG, Obradovic Z, Dunker AK (2004) The importance of intrinsic disorder for protein phosphorylation *Nucleic Acids Research* 32:1037-1049 doi:10.1093/nar/gkh253
- Ichimura K et al. (2002) Mitogen-activated protein kinase cascades in plants: a new nomenclature *Trends in Plant Science* 7:301-308 doi:[https://doi.org/10.1016/S1360-1385\(02\)02302-6](https://doi.org/10.1016/S1360-1385(02)02302-6)
- Iglesias VA, Meins Jr F (2000) Movement of plant viruses is delayed in a β -1,3-glucanase-deficient mutant showing a reduced plasmodesmatal size exclusion limit and enhanced callose deposition *The Plant Journal* 21:157-166 doi:10.1046/j.1365-3113x.2000.00658.x
- Ilgen P, Haderl B, Maier FJ, Schäfer W (2009) Developing Kernel and Rachis Node Induce the Tricothecene Pathway of *Fusarium graminearum* During Wheat Head Infection *Molecular Plant-Microbe Interactions* 22:899-908 doi:10.1094/MPMI-22-8-0899
- Initiative IB (2010) Genome sequencing and analysis of the model grass *Brachypodium distachyon* *Nature* 463:763
- Inoue SB et al. (1995) Characterization and gene cloning of 1, 3- β -d-glucan synthase from *Saccharomyces cerevisiae* *European journal of biochemistry* 231:845-854
- Ishino Y, Shinagawa H, Makino K, Amemura M, Nakata A (1987) Nucleotide sequence of the iap gene, responsible for alkaline phosphatase isozyme conversion in *Escherichia coli*, and identification of the gene product *Journal of bacteriology* 169:5429-5433 doi:10.1128/jb.169.12.5429-5433.1987
- Israel HW, Wilson RG, Aist JR, Kunoh H (1980) Cell wall appositions and plant disease resistance: Acoustic microscopy of papillae that block fungal ingress *Proceedings of the National Academy of Sciences* 77:2046-2049 doi:10.1073/pnas.77.4.2046
- Iswanto ABB, Kim J-Y (2017) Lipid Raft, Regulator of Plasmodesmal Callose Homeostasis *Plants* 6 doi:10.3390/plants6020015
- Ito Y, Nishizawa-Yokoi A, Endo M, Mikami M, Toki S (2015) CRISPR/Cas9-mediated mutagenesis of the RIN locus that regulates tomato fruit ripening *Biochemical and Biophysical Research Communications* 467:76-82 doi:<https://doi.org/10.1016/j.bbrc.2015.09.117>
- Iwakawa H et al. (2007) Expression of the *ASYMMETRIC LEAVES2* gene in the adaxial domain of *Arabidopsis* leaves represses cell proliferation in this domain and is critical for the development of properly expanded leaves *The Plant Journal* 51:173-184

- Jach G et al. (1995) Enhanced quantitative resistance against fungal disease by combinatorial expression of different barley antifungal proteins in transgenic tobacco *The Plant Journal* 8:97-109
- Jacobs AK, Lipka V, Burton RA, Panstruga R, Strizhov N, Schulze-Lefert P, Fincher GB (2003) An *Arabidopsis* callose synthase, *GSL5*, is required for wound and papillary callose formation *The Plant Cell* 15:2503-2513
- Jaffe MJ, Telewski FW (1984) Thigmomorphogenesis: Callose and Ethylene in the Hardening of Mechanically Stressed Plants. In: Timmermann BN, Steelink C, Loewus FA (eds) *Phytochemical Adaptations to Stress*. Springer US, Boston, MA, pp 79-95. doi:10.1007/978-1-4684-1206-2_4
- Jain D, Khurana JP (2018) Role of Pathogenesis-Related (PR) Proteins in Plant Defense Mechanism. In: Singh A, Singh IK (eds) *Molecular Aspects of Plant-Pathogen Interaction*. Springer Singapore, Singapore, pp 265-281. doi:10.1007/978-981-10-7371-7_12
- Jalmi SK, Sinha AK (2016) Functional involvement of a mitogen activated protein kinase module, OsMKK3-OsMPK7-OsWRK30 in mediating resistance against *Xanthomonas oryzae* in rice *Scientific reports* 6:37974
- Jamieson AC, Kim S-H, Wells JA (1994) In vitro selection of zinc fingers with altered DNA-binding specificity *Biochemistry* 33:5689-5695
- Jansen C, von Wettstein D, Schäfer W, Kogel K-H, Felk A, Maier FJ (2005) Infection patterns in barley and wheat spikes inoculated with wild-type and trichodiene synthase gene disrupted *Fusarium graminearum* *Proceedings of the National Academy of Sciences of the United States of America* 102:16892-16897 doi:10.1073/pnas.0508467102
- Jansen R, Embden JD, Gaastra W, Schouls LM (2002) Identification of genes that are associated with DNA repeats in prokaryotes *Mol Microbiol* 43:1565-1575 doi:10.1046/j.1365-2958.2002.02839.x
- Jers C, Soufi B, Grangeasse C, Deutscher J, Mijakovic I (2008) Phosphoproteomics in bacteria: towards a systemic understanding of bacterial phosphorylation networks *Expert Review of Proteomics* 5:619-627 doi:10.1586/14789450.5.4.619
- Jeworutzki E et al. (2010) Early signaling through the *Arabidopsis* pattern recognition receptors FLS2 and EFR involves Ca^{2+} -associated opening of plasma membrane anion channels *The Plant Journal* 62:367-378
- Jia W et al. (2016) Mitogen-Activated Protein Kinase Cascade MKK7-MPK6 Plays Important Roles in Plant Development and Regulates Shoot Branching by Phosphorylating PIN1 in *Arabidopsis* *PLOS Biology* 14:e1002550 doi:10.1371/journal.pbio.1002550
- Jia Y, McAdams SA, Bryan GT, Hershey HP, Valent B (2000) Direct interaction of resistance gene and avirulence gene products confers rice blast resistance *The EMBO journal* 19:4004-4014
- Jiang F, Doudna JA (2017) CRISPR–Cas9 Structures and Mechanisms *Annual Review of Biophysics* 46:505-529 doi:10.1146/annurev-biophys-062215-010822
- Jiang W, Zhou H, Bi H, Fromm M, Yang B, Weeks DP (2013) Demonstration of CRISPR/Cas9/sgRNA-mediated targeted gene modification in *Arabidopsis*, tobacco, sorghum and rice *Nucleic Acids Research* 41:e188-e188 doi:10.1093/nar/gkt780
- Jiao Y et al. (2009) A transcriptome atlas of rice cell types uncovers cellular, functional and developmental hierarchies *Nature genetics* 41:258
- Jinek M, Chylinski K, Fonfara I, Hauer M, Doudna JA, Charpentier E (2012) A programmable dual-RNA-guided DNA endonuclease in adaptive bacterial immunity *Science* 337:816-821 doi:10.1126/science.1225829
- Jinek M et al. (2014a) Structures of Cas9 endonucleases reveal RNA-mediated conformational activation *Science* 343:1247997
- Jinek M et al. (2014b) Structures of Cas9 Endonucleases Reveal RNA-Mediated Conformational Activation *Science* 343:1247997 doi:10.1126/science.1247997
- Johnson DR, Bhatnagar RS, Knoll LJ, Gordon JI (1994) Genetic and biochemical studies of protein N-myristoylation *Annual review of biochemistry* 63:869-914
- Johnson JW, Baenziger PS, Yamazaki WT, Smith RT (1979) Effects of Powdery Mildew on Yield and Quality of Isogenic Lines of ‘Chancellor’ Wheat *Crop Science* 19:349-352 doi:10.2135/cropsci1979.0011183X001900030018x

- Jonak C, Kiegerl S, Ligterink W, Barker PJ, Huskisson NS, Hirt H (1996) Stress signaling in plants: a mitogen-activated protein kinase pathway is activated by cold and drought Proceedings of the National Academy of Sciences 93:11274-11279 doi:10.1073/pnas.93.20.11274
- Jones G, Armstrong S, Caryl A, Franklin F (2003) Meiotic chromosome synapsis and recombination in *Arabidopsis thaliana*; an integration of cytological and molecular approaches Chromosome Research 11:205-215
- Jones JDG, Dangl JL (2006) The plant immune system Nature 444:323 doi:10.1038/nature05286
- Jongedijk E et al. (1995) Synergistic activity of chitinases and β -1, 3-glucanases enhances fungal resistance in transgenic tomato plants Euphytica 85:173-180
- Jørgensen IH (1992) Discovery, characterization and exploitation of Mlo powdery mildew resistance in barley Euphytica 63:141-152
- Jorns AC, Hecht-Buchholz C, Wissemeier AH (1991) Aluminium-induced callose formation in root tips of Norway spruce (*Picea abies* (L.) Karst.) Zeitschrift für Pflanzenernährung und Bodenkunde 154:349-353
- Jorin-Novo JV et al. (2009) Plant proteomics update (2007–2008): second-generation proteomic techniques, an appropriate experimental design, and data analysis to fulfill MIAPE standards, increase plant proteome coverage and expand biological knowledge Journal of proteomics 72:285-314
- Junier T, Pagni M (2000) Dotlet: diagonal plots in a Web browser Bioinformatics 16:178-179
- Junier T, Pagni M, Bucher P (2001) mmsearch: a motif arrangement language and search program Bioinformatics 17:1234-1235
- Kaku H et al. (2006) Plant cells recognize chitin fragments for defense signaling through a plasma membrane receptor Proceedings of the National Academy of Sciences 103:11086-11091
- Kammerhofer N et al. (2015) Role of stress-related hormones in plant defence during early infection of the cyst nematode *Heterodera schachtii* in *Arabidopsis* New Phytologist 207:778-789
- Kamps MP, Buss JE, Sefton BM (1985) Mutation of NH₂-terminal glycine of p60src prevents both myristoylation and morphological transformation Proceedings of the National Academy of Sciences 82:4625-4628 doi:10.1073/pnas.82.14.4625
- Kang Z, Buchenauer H (2000) Ultrastructural and immunocytochemical investigation of pathogen development and host responses in resistant and susceptible wheat spikes infected by *Fusarium culmorum* Physiological and Molecular Plant Pathology 57:255-268 doi:<https://doi.org/10.1006/pmpp.2000.0305>
- Kang Z, Buchenauer H, Huang L, Han Q, Zhang H (2008) Cytological and immunocytochemical studies on responses of wheat spikes of the resistant Chinese cv. Sumai 3 and the susceptible cv. Xiaoyan 22 to infection by *Fusarium graminearum* European Journal of Plant Pathology 120:383-396 doi:10.1007/s10658-007-9230-9
- Kang Z, Huang L, Buchenauer H (2003) Subcellular localization of chitinase and β -1,3-glucanase in compatible and incompatible interactions between wheat and *Puccinia striiformis* f. sp. tritici / Subzelluläre Lokalisation der Chitinase und β -1,3-Glukanase in einer kompatiblen und inkompatiblen Interaktion von Weizen und *Puccinia striiformis* f. sp. tritici Zeitschrift für Pflanzenkrankheiten und Pflanzenschutz / Journal of Plant Diseases and Protection 110:170-183
- Karjalainen R, Lounatmaa K (1986) Ultrastructure of penetration and colonization of wheat leaves by *Septoria nodorum* Physiological and molecular plant pathology 29:263-270
- Kartusch R (2003) On the mechanism of callose synthesis induction by metal ions in onion epidermal cells Protoplasma 220:219-225
- Kauss H (1989) Fluorometric Measurement of Callose and Other 1,3- β -Glucans. In: Linskens H-F, Jackson JF (eds) Plant Fibers. Springer Berlin Heidelberg, Berlin, Heidelberg, pp 127-137. doi:10.1007/978-3-642-83349-6_7
- Kauss H (1996) Callose synthesis Membranes : specialized functions in plants:77-92
- Kauss H, Jeblick W (1986a) Influence of Free Fatty Acids, Lysophosphatidylcholine, Platelet-Activating Factor, Acylcarnitine, and Echinocandin B on 1,3- β -D-Glucan Synthase and Callose Synthesis Plant Physiology 80:7-13 doi:10.1104/pp.80.1.7
- Kauss H, Jeblick W (1986b) Synergistic activation of 1,3- β -D-glucan synthase by Ca²⁺ and polyamines Plant Science 43:103-107 doi:[https://doi.org/10.1016/0168-9452\(86\)90149-4](https://doi.org/10.1016/0168-9452(86)90149-4)

- Kauss H, Köhle H, Jeblick W (1983) Proteolytic activation and stimulation by Ca²⁺ of glucan synthase from soybean cells FEBS letters 158:84-88
- Kauss H, Waldmann T, Quader H (1990) Ca²⁺ as a signal in the induction of callose synthesis. In: Signal perception and transduction in higher plants. Springer, pp 117-131
- Kay S, Bonas U (2009) How Xanthomonas type III effectors manipulate the host plant Current opinion in microbiology 12:37-43
- Kay S, Hahn S, Marois E, Wieduwild R, Bonas U (2009) Detailed analysis of the DNA recognition motifs of the Xanthomonas type III effectors AvrBs3 and AvrBs3Δrep16 The Plant Journal 59:859-871
- Keegstra K (2010) Plant cell walls Plant physiology 154:483-486
- Keeney S (2001) Mechanism and control of meiotic recombination initiation Current topics in developmental biology 52:1-53
- Kempel A, Schädler M, Chrobok T, Fischer M, van Kleunen M (2011) Tradeoffs associated with constitutive and induced plant resistance against herbivory Proceedings of the National Academy of Sciences 108:5685-5689 doi:10.1073/pnas.1016508108
- Kempema LA, Cui X, Holzer FM, Walling LL (2007) Arabidopsis transcriptome changes in response to phloem-feeding silverleaf whitefly nymphs. Similarities and distinctions in responses to aphids Plant Physiology 143:849-865
- Khan MMH, Bryceson I, Kolivras KN, Faruque F, Rahman MM, Haque U (2015) Natural disasters and land-use/land-cover change in the southwest coastal areas of Bangladesh Regional Environmental Change 15:241-250 doi:10.1007/s10113-014-0642-8
- Kim Y-G, Cha J, Chandrasegaran S (1996) Hybrid restriction enzymes: zinc finger fusions to Fok I cleavage domain Proceedings of the National Academy of Sciences 93:1156-1160
- Kim Y-G, Chandrasegaran S (1994) Chimeric restriction endonuclease Proceedings of the National Academy of Sciences 91:883-887
- Kim Y-G, Smith J, Durgesha M, Chandrasegaran S (1998) Chimeric restriction enzyme: Gal4 fusion to FokI cleavage domain Biological chemistry 379:489-496
- Kim Y et al. (2013) A library of TAL effector nucleases spanning the human genome Nature Biotechnology 31:251 doi:10.1038/nbt.2517
- <https://www.nature.com/articles/nbt.2517#supplementary-information>
- Kind S, Schurack S, Hinsch J, Tudzynski P (2018) Brachypodium distachyon as alternative model host system for the ergot fungus Claviceps purpurea Molecular Plant Pathology 19:1005-1011 doi:10.1111/mpp.12563
- Koeck M, Hardham AR, Dodds PN (2011) The role of effectors of biotrophic and hemibiotrophic fungi in infection Cellular microbiology 13:1849-1857
- Kombrink E, Somssich IE (1997) Pathogenesis-Related Proteins and Plant Defense. In: Carroll GC, Tudzynski P (eds) Plant Relationships: Part A. Springer Berlin Heidelberg, Berlin, Heidelberg, pp 107-128. doi:10.1007/978-3-662-10370-8_7
- Koncz C, Schell J (1986) The promoter of T L-DNA gene 5 controls the tissue-specific expression of chimaeric genes carried by a novel type of Agrobacterium binary vector Molecular and General Genetics MGG 204:383-396
- Koo SC et al. (2009) The calmodulin-binding transcription factor OsCBT suppresses defense responses to pathogens in rice Molecules and cells 27:563-570
- Kõressaar T, Lepamets M, Kaplinski L, Raime K, Andreson R, Remm M (2018) Primer3_masker: integrating masking of template sequence with primer design software Bioinformatics 34:1937-1938 doi:10.1093/bioinformatics/bty036
- Koressaar T, Remm M (2007) Enhancements and modifications of primer design program Primer3 Bioinformatics 23:1289-1291 doi:10.1093/bioinformatics/btm091
- Kourelis J, van der Hoorn RAL (2018) Defended to the Nines: 25 Years of Resistance Gene Cloning Identifies Nine Mechanisms for R Protein Function The Plant Cell 30:285-299 doi:10.1105/tpc.17.00579
- Kouzai Y et al. (2016) Expression profiling of marker genes responsive to the defence-associated phytohormones salicylic acid, jasmonic acid and ethylene in Brachypodium distachyon BMC Plant Biology 16:59 doi:10.1186/s12870-016-0749-9

- Kouzai Y et al. (2014) CEBiP is the major chitin oligomer-binding protein in rice and plays a main role in the perception of chitin oligomers *Plant Mol Biol* 84:519-528 doi:10.1007/s11103-013-0149-6
- Kovtun Y, Chiu W-L, Tena G, Sheen J (2000) Functional analysis of oxidative stress-activated mitogen-activated protein kinase cascade in plants *Proceedings of the National Academy of Sciences* 97:2940-2945 doi:10.1073/pnas.97.6.2940
- Krogh A, Larsson B, von Heijne G, Sonnhammer ELL (2001) Predicting transmembrane protein topology with a hidden markov model: application to complete genomes *Journal of Molecular Biology* 305:567-580 doi:<https://doi.org/10.1006/jmbi.2000.4315>
- Kroh M, Knuiman B (1982) Ultrastructure of cell wall and plugs of tobacco pollen tubes after chemical extraction of polysaccharides *Planta* 154:241-250 doi:10.1007/BF00387870
- Krupinsky J (1989) Variability in *Septoria musiva* in aggressiveness *Phytopathology* 79:413-416
- Kumar D, Eipper BA, Mains RE (2014) Amidation☆. In: *Reference Module in Biomedical Sciences*. Elsevier. doi:<https://doi.org/10.1016/B978-0-12-801238-3.04040-X>
- Kunkel BN, Brooks DM (2002) Cross talk between signaling pathways in pathogen defense *Current opinion in plant biology* 5:325-331
- Kuscu C, Arslan S, Singh R, Thorpe J, Adli M (2014) Genome-wide analysis reveals characteristics of off-target sites bound by the Cas9 endonuclease *Nature Biotechnology* 32:677 doi:10.1038/nbt.2916
- <https://www.nature.com/articles/nbt.2916#supplementary-information>
- Kushalappa AC, Gunnaiah R (2013) Metabolo-proteomics to discover plant biotic stress resistance genes *Trends in Plant Science* 18:522-531 doi:<https://doi.org/10.1016/j.tplants.2013.05.002>
- KUŚNIERCZYK A, Winge P, JØRSTAD TS, TROCZYŃSKA J, Rossiter JT, Bones AM (2008) Towards global understanding of plant defence against aphids—timing and dynamics of early *Arabidopsis* defence responses to cabbage aphid (*Brevicoryne brassicae*) attack *Plant, cell & environment* 31:1097-1115
- Lang J, Genot B, Hirt H, Colcombet J (2017) Constitutive activity of the *Arabidopsis* MAP Kinase 3 confers resistance to *Pseudomonas syringae* and drives robust immune responses *Plant Signaling & Behavior* 12:e1356533 doi:10.1080/15592324.2017.1356533
- Laohavisit A, Davies JM (2011) Annexins *New Phytologist* 189:40-53
- Lawton KA, Beck J, Potter S, Ward E, Ryals J (1994) Regulation of Cucumber Class III Chitinase Gene Expression
- Leach J, Lang B, Yoder O (1982) Methods for selection of mutants and in vitro culture of *Cochliobolus heterostrophus* *Microbiology* 128:1719-1729
- Leba L-J, Cheval C, Ortiz-Martín I, Ranty B, Beuzón CR, Galaud J-P, Aldon D (2012) CML9, an *Arabidopsis* calmodulin-like protein, contributes to plant innate immunity through a flagellin-dependent signalling pathway *The Plant Journal* 71:976-989 doi:10.1111/j.1365-3113.2012.05045.x
- Lecourieux D, Ranjeva R, Pugin A (2006) Calcium in plant defence-signalling pathways *New Phytologist* 171:249-269
- Lee JS, Kallehauge TB, Pedersen LE, Kildegaard HF (2015) Site-specific integration in CHO cells mediated by CRISPR/Cas9 and homology-directed DNA repair pathway *Scientific Reports* 5:8572 doi:10.1038/srep08572
- <https://www.nature.com/articles/srep08572#supplementary-information>
- Lehtinen U (1993) Plant cell wall degrading enzymes of *Septoria nodorum* *Physiological and Molecular Plant Pathology* 43:121-134
- Lennon KA, Lord EM (2000) In vivo pollen tube cell of *Arabidopsis thaliana* I. Tube cell cytoplasm and wall *Protoplasma* 214:45-56 doi:10.1007/BF02524261
- Li H, Lin Y, Heath RM, Zhu MX, Yang Z (1999) Control of Pollen Tube Tip Growth by a Rop GTPase-Dependent Pathway That Leads to Tip-Localized Calcium Influx *The Plant Cell* 11:1731-1742 doi:10.1105/tpc.11.9.1731
- Li J, Burton RA, Harvey AJ, Hrmova M, Wardak AZ, Stone BA, Fincher GB (2003) Biochemical evidence linking a putative callose synthase gene with (1→3)-β-d-glucan biosynthesis in barley *Plant Molecular Biology* 53:213-225 doi:10.1023/B:PLAN.0000009289.50285.52

- Li K et al. (2017) AIK1, A Mitogen-Activated Protein Kinase, Modulates Absciscic Acid Responses through the MKK5-MPK6 Kinase Cascade *Plant Physiology* 173:1391-1408
doi:10.1104/pp.16.01386
- Li L et al. (2014) The FLS2-associated kinase BIK1 directly phosphorylates the NADPH oxidase RbohD to control plant immunity *Cell host & microbe* 15:329-338
- Li R et al. (2018) Multiplexed CRISPR/Cas9-mediated metabolic engineering of γ -aminobutyric acid levels in *Solanum lycopersicum* *Plant Biotechnology Journal* 16:415-427
doi:10.1111/pbi.12781
- Li T, Liu B, Spalding MH, Weeks DP, Yang B (2012) High-efficiency TALEN-based gene editing produces disease-resistant rice *Nature Biotechnology* 30:390 doi:10.1038/nbt.2199
<https://www.nature.com/articles/nbt.2199#supplementary-information>
- Li X, Lin H, Zhang W, Zou Y, Zhang J, Tang X, Zhou J-M (2005) Flagellin induces innate immunity in nonhost interactions that is suppressed by *Pseudomonas syringae* effectors *Proceedings of the National Academy of Sciences* 102:12990-12995
- Li X et al. (2015) Transgenic Wheat Expressing a Barley UDP-Glucosyltransferase Detoxifies Deoxynivalenol and Provides High Levels of Resistance to *Fusarium graminearum* *Molecular Plant-Microbe Interactions* 28:1237-1246 doi:10.1094/MPMI-03-15-0062-R
- Liang F, Han M, Romanienko PJ, Jasin M (1998) Homology-directed repair is a major double-strand break repair pathway in mammalian cells *Proceedings of the National Academy of Sciences* 95:5172-5177 doi:10.1073/pnas.95.9.5172
- Lieber MR, Ma Y, Pannicke U, Schwarz K (2003) Mechanism and regulation of human non-homologous DNA end-joining *Nature Reviews Molecular Cell Biology* 4:712-720
doi:10.1038/nrm1202
- Lin Y et al. (2014) CRISPR/Cas9 systems have off-target activity with insertions or deletions between target DNA and guide RNA sequences *Nucleic Acids Research* 42:7473-7485
doi:10.1093/nar/gku402
- Lionetti V (2015) PECTOPLATE: the simultaneous phenotyping of pectin methylesterases, pectinases, and oligogalacturonides in plants during biotic stresses *Frontiers in Plant Science* 6:331
- Liu J, Du H, Ding X, Zhou Y, Xie P, Wu J (2017) Mechanisms of callose deposition in rice regulated by exogenous abscisic acid and its involvement in rice resistance to *Nilaparvata lugens* Stål (Hemiptera: Delphacidae) *Pest Management Science* 73:2559-2568 doi:10.1002/ps.4655
- Liu T et al. (2012) Chitin-induced dimerization activates a plant immune receptor *Science* 336:1160-1164
- Liu Z et al. (2016) SnTox1, a *Parastagonospora nodorum* necrotrophic effector, is a dual-function protein that facilitates infection while protecting from wheat-produced chitinases *New Phytologist* 211:1052-1064
- Lloyd A, Plaisier CL, Carroll D, Drews GN (2005) Targeted mutagenesis using zinc-finger nucleases in *Arabidopsis* *Proceedings of the National Academy of Sciences* 102:2232-2237
- Lobell DB, Field CB (2007) Global scale climate-crop yield relationships and the impacts of recent warming *Environmental Research Letters* 2:014002 doi:10.1088/1748-9326/2/1/014002
- Lu S, Faris JD, Sherwood R, Friesen TL, Edwards MC (2014) A dimeric PR-1-type pathogenesis-related protein interacts with ToxA and potentially mediates ToxA-induced necrosis in sensitive wheat *Molecular plant pathology* 15:650-663
- Lu T et al. (2010) Function annotation of the rice transcriptome at single-nucleotide resolution by RNA-seq *Genome research* 20:1238-1249
- Lu Z-X, Gaudet D, Puchalski B, Despins T, Frick M, Laroche A (2005) Inducers of resistance reduce common bunt infection in wheat seedlings while differentially regulating defence-gene expression *Physiological and Molecular Plant Pathology* 67:138-148
- Lukasik E, Takken FL (2009) STANDING strong, resistance proteins instigators of plant defence *Current opinion in plant biology* 12:427-436
- Luna E, Pastor V, Robert J, Flors V, Mauch-Mani B, Ton J (2011) Callose Deposition: A Multifaceted Plant Defense Response *Molecular Plant-Microbe Interactions* 24:183-193 doi:10.1094/mpmi-07-10-0149

- Lusser M, Parisi C, Plan D, Rodríguez-Cerezo E (2012) Deployment of new biotechnologies in plant breeding *Nature Biotechnology* 30:231 doi:10.1038/nbt.2142
<https://www.nature.com/articles/nbt.2142#supplementary-information>
- MacInnes J, Fogelman R (1923) Wheat Scab in Minnesota
- Mackey D, Belkhadir Y, Alonso JM, Ecker JR, Dangl JL (2003) Arabidopsis RIN4 is a target of the type III virulence effector AvrRpt2 and modulates RPS2-mediated resistance *Cell* 112:379-389
- Mackintosh CA et al. (2007) Overexpression of defense response genes in transgenic wheat enhances resistance to Fusarium head blight *Plant cell reports* 26:479-488 doi:10.1007/s00299-006-0265-8
- Madgwick JW, West JS, White RP, Semenov MA, Townsend JA, Turner JA, Fitt BDL (2011) Impacts of climate change on wheat anthesis and fusarium ear blight in the UK *European Journal of Plant Pathology* 130:117-131 doi:10.1007/s10658-010-9739-1
- Maeda A, Uchida M, Nishikawa S, Nishino T, Konishi H (2018) Role of N-myristoylation in stability and subcellular localization of the CLPABP protein *Biochemical and Biophysical Research Communications* 495:1249-1256 doi:<https://doi.org/10.1016/j.bbrc.2017.11.112>
- Maekawa T, Kufer TA, Schulze-Lefert P (2011) NLR functions in plant and animal immune systems: so far and yet so close *Nature Immunology* 12:817 doi:10.1038/ni.2083
- Maier FJ et al. (2006) Involvement of trichothecenes in fusarioses of wheat, barley and maize evaluated by gene disruption of the trichodiene synthase (Tri5) gene in three field isolates of different chemotype and virulence *Molecular Plant Pathology* 7:449-461 doi:10.1111/j.1364-3703.2006.00351.x
- Mak AN-S, Bradley P, Cernadas RA, Bogdanove AJ, Stoddard BL (2012) The Crystal Structure of TAL Effector PthXo1 Bound to Its DNA Target *Science* 335:716-719 doi:10.1126/science.1216211
- Makarova KS, Aravind L, Grishin NV, Rogozin IB, Koonin EV (2002) A DNA repair system specific for thermophilic Archaea and bacteria predicted by genomic context analysis *Nucleic Acids Research* 30:482-496 doi:10.1093/nar/30.2.482
- Makarova KS, Grishin NV, Shabalina SA, Wolf YI, Koonin EV (2006) A putative RNA-interference-based immune system in prokaryotes: computational analysis of the predicted enzymatic machinery, functional analogies with eukaryotic RNAi, and hypothetical mechanisms of action *Biology direct* 1:7
- Malamy J, Carr JP, Klessig DF, Raskin I (1990) Salicylic acid: a likely endogenous signal in the resistance response of tobacco to viral infection *Science* 250:1002-1004
- Mandadi KK, Scholthof K-BG (2012) Characterization of a Viral Synergism in the Monocot *Brachypodium distachyon* Reveals Distinctly Altered Host Molecular Processes Associated with Disease *Plant Physiology* 160:1432-1452 doi:10.1104/pp.112.204362
- Markell S, Franc L (2003) Fusarium head blight inoculum: species prevalence and Gibberella zeae spore type *Plant disease* 87:814-820
- Martins PM, Merfa MV, Takita MA, De Souza AA (2018) Persistence in phytopathogenic bacteria: do we know enough? *Frontiers in microbiology* 9
- Mashimo T, Takizawa A, Voigt B, Yoshimi K, Hiai H, Kuramoto T, Serikawa T (2010) Generation of knockout rats with X-linked severe combined immunodeficiency (X-SCID) using zinc-finger nucleases *PloS one* 5:e8870
- Matano M et al. (2015) Modeling colorectal cancer using CRISPR-Cas9-mediated engineering of human intestinal organoids *Nature Medicine* 21:256 doi:10.1038/nm.3802
<https://www.nature.com/articles/nm.3802#supplementary-information>
- Matny ON (2015) Fusarium head blight and crown rot on wheat & barley: losses and health risks *Adv Plants Agric Res* 2:10.15406
- Matsumura Y, Iwakawa H, Machida Y, Machida C (2009) Characterization of genes in the ASYMMETRIC LEAVES2/LATERAL ORGAN BOUNDARIES (AS2/LOB) family in *Arabidopsis thaliana*, and functional and molecular comparisons between AS2 and other family members *The Plant Journal* 58:525-537 doi:10.1111/j.1365-313X.2009.03797.x

- Mauritz R, Mouritzen P, Pfundheller H, Tolstrup N, Lomholt C (2005) Universal ProbeLibrary Set: One Transcriptome-One Kit BIOCHEMICA-MANNHEIM- 2:22
- McCann MC et al. (2001) Approaches to understanding the functional architecture of the plant cell wall *Phytochemistry* 57:811-821
- McCormack E, Tsai Y-C, Braam J (2005) Handling calcium signaling: Arabidopsis CaMs and CMLs *Trends in Plant Science* 10:383-389 doi:<https://doi.org/10.1016/j.tplants.2005.07.001>
- McDonnell LA, Heeren RMA (2007) Imaging mass spectrometry *Mass Spectrometry Reviews* 26:606-643 doi:10.1002/mas.20124
- McFarlane HE, Döring A, Persson S (2014) The cell biology of cellulose synthesis *Annual review of plant biology* 65:69-94
- McMullen MP, Stack RW (2008) Fusarium head blight (scab) of small grains
- McNairn RB (1972) Phloem translocation and heat-induced callose formation in field-grown *Gossypium hirsutum* L *Plant physiology* 50:366-370
- Mei C, Qi M, Sheng G, Yang Y (2006) Inducible Overexpression of a Rice Allene Oxide Synthase Gene Increases the Endogenous Jasmonic Acid Level, PR Gene Expression, and Host Resistance to Fungal Infection *Molecular Plant-Microbe Interactions* 19:1127-1137 doi:10.1094/MPMI-19-1127
- Meldau S, Ullman-Zeunert L, Govind G, Bartram S, Baldwin IT (2012) MAPK-dependent JA and SA signalling in *Nicotiana attenuata* affects plant growth and fitness during competition with conspecifics *BMC Plant Biology* 12:213 doi:10.1186/1471-2229-12-213
- Mianné J et al. (2017) Analysing the outcome of CRISPR-aided genome editing in embryos: Screening, genotyping and quality control *Methods* 121-122:68-76 doi:<https://doi.org/10.1016/j.ymeth.2017.03.016>
- Miedaner T, Reinbrecht C, Schilling AG (2000) Association among aggressiveness, fungal colonization, and mycotoxin production of 26 isolates of *Fusarium graminearum* in winter rye head blight/Beziehung zwischen Aggressivität, Myzelwachstum und Mykotoxinproduktion von 26 *Fusarium-graminearum*-Isolaten bei der Ährenfusariose des Winterroggens *Zeitschrift für Pflanzenkrankheiten und Pflanzenschutz/Journal of Plant Diseases and Protection*:124-134
- Miller JC et al. (2010) A TALE nuclease architecture for efficient genome editing *Nature Biotechnology* 29:143 doi:10.1038/nbt.1755
- <https://www.nature.com/articles/nbt.1755#supplementary-information>
- Miller SS, Chabot DM, Ouellet T, Harris LJ, Fedak G (2004) Use of a *Fusarium graminearum* strain transformed with green fluorescent protein to study infection in wheat (*Triticum aestivum*) *Canadian Journal of Plant Pathology* 26:453-463
- Miya A et al. (2007) CERK1, a LysM receptor kinase, is essential for chitin elicitor signaling in *Arabidopsis* *Proceedings of the National Academy of Sciences* 104:19613-19618
- Mojica FJM, Díez-Villaseñor C, Soria E, Juez G (2000) Biological significance of a family of regularly spaced repeats in the genomes of Archaea, Bacteria and mitochondria *Molecular Microbiology* 36:244-246 doi:10.1046/j.1365-2958.2000.01838.x
- Mojica FJM, Díez-Villaseñor Cs, García-Martínez J, Soria E (2005) Intervening Sequences of Regularly Spaced Prokaryotic Repeats Derive from Foreign Genetic Elements *Journal of Molecular Evolution* 60:174-182 doi:10.1007/s00239-004-0046-3
- Molina A, Görlach J, Volrath S, Ryals J (1999) Wheat Genes Encoding Two Types of PR-1 Proteins Are Pathogen Inducible, but Do Not Respond to Activators of Systemic Acquired Resistance *Molecular Plant-Microbe Interactions* 12:53-58 doi:10.1094/mpmi.1999.12.1.53
- Monaghan J, Zipfel C (2012) Plant pattern recognition receptor complexes at the plasma membrane *Current Opinion in Plant Biology* 15:349-357 doi:<https://doi.org/10.1016/j.pbi.2012.05.006>
- Monsigny M, Roche A-C, Sene C, Maget-Dana R, Delmotte F (1980) Sugar-Lectin Interactions: How Does Wheat-Germ Agglutinin Bind Sialoglycoconjugates? *European Journal of Biochemistry* 104:147-153 doi:10.1111/j.1432-1033.1980.tb04410.x
- Moore JK, Haber JE (1996) Cell cycle and genetic requirements of two pathways of nonhomologous end-joining repair of double-strand breaks in *Saccharomyces cerevisiae* *Mol Cell Biol* 16:2164-2173 doi:10.1128/mcb.16.5.2164
- Moore JW, Loake GJ, Spoel SH (2011) Transcription dynamics in plant immunity *The Plant Cell* 23:2809-2820

- Moore KE (1978) Barrier-zone formation in wounded stems of sweetgum *Canadian Journal of Forest Research* 8:389-397 doi:10.1139/x78-058
- Morrell PL, Buckler ES, Ross-Ibarra J (2012) Crop genomics: advances and applications *Nature Reviews Genetics* 13:85
- Morrow DL, Lucas WJ (1986) (1→3)- β -D-glucan synthase from sugar beet: I. isolation and solubilization *Plant physiology* 81:171-176
- Moscou MJ, Bogdanove AJ (2009) A Simple Cipher Governs DNA Recognition by TAL Effectors *Science* 326:1501-1501 doi:10.1126/science.1178817
- Mucyn TS, Clemente A, Andriotis VM, Balmuth AL, Oldroyd GE, Staskawicz BJ, Rathjen JP (2006) The tomato NBARC-LRR protein Prf interacts with Pto kinase in vivo to regulate specific plant immunity *The Plant Cell* 18:2792-2806
- Mudge K, Janick J, Scofield S, Goldschmidt EE. doi:doi:10.1002/9780470593776.ch9
- Mur LA et al. (2011) Exploiting the Brachypodium Tool Box in cereal and grass research *New Phytologist* 191:334-347
- Murray GM, Brennan JP (2009) Estimating disease losses to the Australian wheat industry *Australasian Plant Pathology* 38:558-570
- Myers JH, Sarfraz RM (2017) Impacts of insect herbivores on plant populations *Annual review of entomology* 62:207-230
- Nagel R, Elliott A, Masel A, Birch RG, Manners JM (1990) Electroporation of binary Ti plasmid vector into *Agrobacterium tumefaciens* and *Agrobacterium rhizogenes* *FEMS Microbiology Letters* 67:325-328 doi:10.1111/j.1574-6968.1990.tb04041.x
- Nardozi JD, Lott K, Cingolani G (2010) Phosphorylation meets nuclear import: a review *Cell Communication and Signaling* 8:32 doi:10.1186/1478-811X-8-32
- Neale AD et al. (1990) Chitinase, beta-1,3-glucanase, osmotin, and extensin are expressed in tobacco explants during flower formation *The Plant Cell* 2:673-684 doi:10.1105/tpc.2.7.673
- Newman RH, Hill SJ, Harris PJ (2013) Wide-angle x-ray scattering and solid-state nuclear magnetic resonance data combined to test models for cellulose microfibrils in mung bean cell walls *Plant physiology* 163:1558-1567
- Nguyen LN, Dao TT, Živković T, Fehrholz M, Schäfer W, Salomon S (2010) Enzymatic properties and expression patterns of five extracellular lipases of *Fusarium graminearum* in vitro *Enzyme and Microbial Technology* 46:479-486 doi:<https://doi.org/10.1016/j.enzmictec.2010.02.005>
- Nishikawa S-i, Zinkl GM, Swanson RJ, Maruyama D, Preuss D (2005) Callose (β -1,3 glucan) is essential for *Arabidopsis* pollen wall patterning, but not tube growth *BMC Plant Biology* 5:22 doi:10.1186/1471-2229-5-22
- Nishimura MT, Stein M, Hou B-H, Vogel JP, Edwards H, Somerville SC (2003) Loss of a Callose Synthase Results in Salicylic Acid-Dependent Disease Resistance *Science* 301:969-972 doi:10.1126/science.1086716
- Nühse TS, Bottrill AR, Jones AME, Peck SC (2007) Quantitative phosphoproteomic analysis of plasma membrane proteins reveals regulatory mechanisms of plant innate immune responses *The Plant Journal* 51:931-940 doi:10.1111/j.1365-313X.2007.03192.x
- O'Neill M, Albersheim P, Darvill A (1990) 12 - The Pectic Polysaccharides of Primary Cell Walls. In: Dey PM (ed) *Methods in Plant Biochemistry*, vol 2. Academic Press, pp 415-441. doi:<https://doi.org/10.1016/B978-0-12-461012-5.50018-5>
- O'Driscoll A, Doohan F, Mullins E (2015) Exploring the utility of *Brachypodium distachyon* as a model pathosystem for the wheat pathogen *Zymoseptoria tritici* *BMC research notes* 8:132
- O'Neill MA, York WS (2003) The composition and structure of plant primary cell walls *The plant cell wall*:1-54
- Ochoa-Villarreal M, Aispuro-Hernández E, Vargas-Arispuro I, Martínez-Téllez MÁ (2012) Plant cell wall polymers: function, structure and biological activity of their derivatives *Polymerization* 4:63-86
- Oerke EC (2006) Crop losses to pests *The Journal of Agricultural Science* 144:31-43 doi:10.1017/S0021859605005708
- Ogasawara Y et al. (2008) Synergistic activation of the *Arabidopsis* NADPH oxidase AtrbohD by Ca^{2+} and phosphorylation *Journal of Biological Chemistry* 283:8885-8892

- Olden K, Parent JB, White SL (1982) Carbohydrate moieties of glycoproteins a re-evaluation of their function *Biochimica et Biophysica Acta (BBA) - Reviews on Biomembranes* 650:209-232 doi:[https://doi.org/10.1016/0304-4157\(82\)90017-X](https://doi.org/10.1016/0304-4157(82)90017-X)
- Oliver RP, Friesen TL, Faris JD, Solomon PS (2011) *Stagonospora nodorum*: From Pathology to Genomics and Host Resistance *Annual Review of Phytopathology* 50:23-43 doi:10.1146/annurev-phyto-081211-173019
- Olson EN, Spizz G (1986) Fatty acylation of cellular proteins. Temporal and subcellular differences between palmitate and myristate acylation *Journal of Biological Chemistry* 261:2458-2466
- Osakabe Y, Watanabe T, Sugano SS, Ueta R, Ishihara R, Shinozaki K, Osakabe K (2016) Optimization of CRISPR/Cas9 genome editing to modify abiotic stress responses in plants *Scientific Reports* 6:26685 doi:10.1038/srep26685
<https://www.nature.com/articles/srep26685#supplementary-information>
- Osbourn A, Scott P, Caten C (1986) The effects of host passaging on the adaptation of *Septoria nodorum* to wheat or barley *Plant pathology* 35:135-145
- Østergaard L, Petersen M, Mattsson O, Mundy J (2002) An *Arabidopsis* callose synthase *Plant Molecular Biology* 49:559-566 doi:10.1023/A:1015558231400
- Ozdemir BS, Hernandez P, Filiz E, Budak H (2008) *Brachypodium* genomics *International Journal of Plant Genomics* 2008
- Pabo CO, Peisach E, Grant RA (2001) Design and selection of novel Cys2His2 zinc finger proteins *Annual review of biochemistry* 70:313-340
- Păcurar DI, Thordal-Christensen H, Nielsen KK, Lenk I (2008) A high-throughput *Agrobacterium*-mediated transformation system for the grass model species *Brachypodium distachyon* *L Transgenic research* 17:965-975
- Pagni M, Ioannidis V, Cerutti L, Zahn-Zabal M, Jongeneel CV, Falquet L (2004) MyHits: a new interactive resource for protein annotation and domain identification *Nucleic Acids Research* 32:W332-335
- Pagni M et al. (2007) MyHits: improvements to an interactive resource for analyzing protein sequences *Nucleic Acids Research* 35:W433-437
- Pagni M, Iseli C, Junier T, Falquet L, Jongeneel V, Bucher P (2001) trEST, trGEN and Hits: access to databases of predicted protein sequences *Nucleic Acids Research* 29:148-151
- Palazzini J, Fumero V, Yerkovich N, Barros G, Cuniberti M, Chulze S (2015) Correlation between *Fusarium graminearum* and deoxynivalenol during the 2012/13 wheat *Fusarium* head blight outbreak in Argentina *Cereal research communications* 43:627-637
- Pallotta M, Graham R, Langridge P, Sparrow D, Barker S (2000) RFLP mapping of manganese efficiency in barley *Theoretical and Applied Genetics* 101:1100-1108
- Panchuk-Voloshina N et al. (1999) Alexa Dyes, a Series of New Fluorescent Dyes that Yield Exceptionally Bright, Photostable Conjugates *Journal of Histochemistry & Cytochemistry* 47:1179-1188 doi:10.1177/002215549904700910
- Paquet D et al. (2016) Efficient introduction of specific homozygous and heterozygous mutations using CRISPR/Cas9 *Nature* 533:125 doi:10.1038/nature17664
<https://www.nature.com/articles/nature17664#supplementary-information>
- Parker D et al. (2008) Rice blast infection of *Brachypodium distachyon* as a model system to study dynamic host/pathogen interactions *Nature Protocols* 3:435
- Parry D, Jenkinson P, McLeod L (1995) *Fusarium* ear blight (scab) in small grain cereals—a review *Plant pathology* 44:207-238
- Pattanayak V, Lin S, Guilinger JP, Ma E, Doudna JA, Liu DR (2013) High-throughput profiling of off-target DNA cleavage reveals RNA-programmed Cas9 nuclease specificity *Nature Biotechnology* 31:839 doi:10.1038/nbt.2673
<https://www.nature.com/articles/nbt.2673#supplementary-information>
- Pavletich NP, Pabo CO (1991) Zinc finger-DNA recognition: crystal structure of a Zif268-DNA complex at 2.1 Å *Science* 252:809-817
- Peitzsch RM, McLaughlin S (1993) Binding of acylated peptides and fatty acids to phospholipid vesicles: pertinence to myristoylated proteins *Biochemistry* 32:10436-10443

- Peraldi A, Beccari G, Steed A, Nicholson P (2011) Brachypodium distachyon: a new pathosystem to study Fusarium head blight and other Fusarium diseases of wheat BMC Plant Biology 11:100 doi:10.1186/1471-2229-11-100
- Perez-Rodriguez R, Haitjema C, Huang Q, Nam KH, Bernardis S, Ke A, DeLisa MP (2011) Envelope stress is a trigger of CRISPR RNA-mediated DNA silencing in Escherichia coli Molecular microbiology 79:584-599
- Peterson BA, Haak DC, Nishimura MT, Teixeira PJPL, James SR, Dangl JL, Nimchuk ZL (2016) Genome-Wide Assessment of Efficiency and Specificity in CRISPR/Cas9 Mediated Multiple Site Targeting in Arabidopsis PloS one 11:e0162169 doi:10.1371/journal.pone.0162169
- Peterson CA, Rauser WE (1979) Callose deposition and photoassimilate export in Phaseolus vulgaris exposed to excess cobalt, nickel, and zinc Plant Physiology 63:1170-1174
- Petes TD, Malone RE, Symington LS (1991) 8 Recombination in Yeast Cold Spring Harbor Monograph Archive 21:407-521
- Pfaffl MW (2001) A new mathematical model for relative quantification in real-time RT-PCR Nucleic acids research 29:e45-e45
- Pierre M, Traverso JA, Boisson B, Domenichini S, Bouchez D, Giglione C, Meinel T (2007) N-Myristoylation Regulates the SnRK1 Pathway in Arabidopsis The Plant Cell 19:2804-2821 doi:10.1105/tpc.107.051870
- Pieterse CMJ, van Loon LC (1999) Salicylic acid-independent plant defence pathways Trends in Plant Science 4:52-58 doi:[https://doi.org/10.1016/S1360-1385\(98\)01364-8](https://doi.org/10.1016/S1360-1385(98)01364-8)
- Porteus MH, Baltimore D (2003) Chimeric nucleases stimulate gene targeting in human cells Science 300:763-763
- Pós V (2010)
- Leaf rust and cadmium-induced changes in the protein pattern of the apoplast of wheat and barley. Budapesti Corvinus Egyetem
- Pourcel C, Salvignol G, Vergnaud G (2005) CRISPR elements in Yersinia pestis acquire new repeats by preferential uptake of bacteriophage DNA, and provide additional tools for evolutionary studies Microbiology 151:653-663
- Powell JJ et al. (2017) Transcriptome analysis of Brachypodium during fungal pathogen infection reveals both shared and distinct defense responses with wheat Scientific Reports 7:17212 doi:10.1038/s41598-017-17454-3
- Pritsch C, Muehlbauer GJ, Bushnell WR, Somers DA, Vance CP (2000) Fungal Development and Induction of Defense Response Genes During Early Infection of Wheat Spikes by Fusarium graminearum Molecular Plant-Microbe Interactions 13:159-169 doi:10.1094/mpmi.2000.13.2.159
- Pritsch C, Vance CP, Bushnell WR, Somers DA, Hohn TM, Muehlbauer GJ (2001) Systemic expression of defense response genes in wheat spikes as a response to Fusarium graminearum infection Physiological and Molecular Plant Pathology 58:1-12 doi:<https://doi.org/10.1006/pmpp.2000.0308>
- Proctor RH, Hohn TM, McCormick SP (1995) Reduced virulence of Gibberella zeae caused by disruption of a trichothecene toxin biosynthetic gene MPMI-Molecular Plant Microbe Interactions 8:593-601
- Proctor RH, Hohn TM, McCormick SP (1997) Restoration of wild-type virulence to Tri5 disruption mutants of Gibberella zeae via gene reversion and mutant complementation Microbiology 143:2583-2591
- Puchta H (2004) The repair of double-strand breaks in plants: mechanisms and consequences for genome evolution Journal of Experimental Botany 56:1-14 doi:10.1093/jxb/eri025
- Qadota H et al. (1996) Identification of yeast Rho1p GTPase as a regulatory subunit of 1, 3-β-glucan synthase Science 272:279-281
- Qin R, Hirano Y, Brunner I (2007) Exudation of organic acid anions from poplar roots after exposure to Al, Cu and Zn Tree physiology 27:313-320
- Qin Z et al. (2019) Divergent roles of FT-like 9 in flowering transition under different day lengths in Brachypodium distachyon Nature Communications 10:812 doi:10.1038/s41467-019-08785-y
- Quaedvlieg W et al. (2013) Sizing up Septoria Studies in mycology 75:307-390 doi:10.3114/sim0017

- Rabbinge R, Jorritsma ITM, Schans J (1985) Damage components of powdery mildew in winter wheat Netherlands Journal of Plant Pathology 91:235-247 doi:10.1007/bf01997967
- Radford JE, Vesik M, Overall RL (1998) Callose deposition at plasmodesmata Protoplasma 201:30-37 doi:10.1007/BF01280708
- Rådmark O, Shimizu T, Jörnvall H, Samuelsson B (1984) Leukotriene A4 hydrolase in human leukocytes. Purification and properties Journal of Biological Chemistry 259:12339-12345
- Raffaele S et al. (2010) Genome Evolution Following Host Jumps in the Irish Potato Famine Pathogen Lineage Science 330:1540-1543 doi:10.1126/science.1193070
- Ran FA et al. (2013) Double Nicking by RNA-Guided CRISPR Cas9 for Enhanced Genome Editing Specificity Cell 154:1380-1389 doi:<https://doi.org/10.1016/j.cell.2013.08.021>
- Ranf S, Eschen-Lippold L, Pecher P, Lee J, Scheel D (2011) Interplay between calcium signalling and early signalling elements during defence responses to microbe-or damage-associated molecular patterns The Plant Journal 68:100-113
- Rayon C, Lerouge P, Faye L (1998) The protein N-glycosylation in plants Journal of Experimental Botany 49:1463-1472
- Raz V, Fluhr R (1993) Ethylene Signal Is Transduced via Protein Phosphorylation Events in Plants The Plant Cell 5:523-530 doi:10.1105/tpc.5.5.523
- Rebar EJ, Pabo CO (1994) Zinc finger phage: affinity selection of fingers with new DNA-binding specificities Science 263:671-673
- Ride JP, Pearce RB (1979) Lignification and papilla formation at sites of attempted penetration of wheat leaves by non-pathogenic fungi Physiological Plant Pathology 15:79-92 doi:[https://doi.org/10.1016/0048-4059\(79\)90041-9](https://doi.org/10.1016/0048-4059(79)90041-9)
- Ridley BL, O'Neill MA, Mohnen D (2001) Pectins: structure, biosynthesis, and oligogalacturonide-related signaling Phytochemistry 57:929-967 doi:[https://doi.org/10.1016/S0031-9422\(01\)00113-3](https://doi.org/10.1016/S0031-9422(01)00113-3)
- Rincón M, Gonzales RA (1992) Aluminum partitioning in intact roots of aluminum-tolerant and aluminum-sensitive wheat (*Triticum aestivum* L.) cultivars Plant Physiology 99:1021-1028
- Riou C, Freyssinet G, Fevre M (1991) Production of Cell Wall-Degrading Enzymes by the Phytopathogenic Fungus *Sclerotinia sclerotiorum* Applied and Environmental Microbiology 57:1478-1484
- Risk JM et al. (2013) The wheat Lr34 gene provides resistance against multiple fungal pathogens in barley Plant Biotechnology Journal 11:847-854 doi:10.1111/pbi.12077
- Robert-Seilanianz A, Navarro L, Bari R, Jones JDG (2007) Pathological hormone imbalances Current Opinion in Plant Biology 10:372-379 doi:<https://doi.org/10.1016/j.pbi.2007.06.003>
- Robertson IH (1981) Chromosome numbers in *Brachypodium Beauv.* (Gramineae) Genetica 56:55-60
- Robinson SP, Jacobs AK, Dry IB (1997) A Class IV Chitinase Is Highly Expressed in Grape Berries during Ripening Plant Physiology 114:771-778 doi:10.1104/pp.114.3.771
- Römer P et al. (2010) Promoter elements of rice susceptibility genes are bound and activated by specific TAL effectors from the bacterial blight pathogen, *Xanthomonas oryzae* pv. *oryzae* New Phytologist 187:1048-1057
- ROUTLEDGE AP, SHELLEY G, SMITH JV, Talbot NJ, Draper J, Mur LA (2004) Magnaporthe grisea interactions with the model grass *Brachypodium distachyon* closely resemble those with rice (*Oryza sativa*) Molecular Plant Pathology 5:253-265
- Ruan Y-L, Xu S-M, White R, Furbank RT (2004) Genotypic and Developmental Evidence for the Role of Plasmodesmatal Regulation in Cotton Fiber Elongation Mediated by Callose Turnover Plant Physiology 136:4104-4113 doi:10.1104/pp.104.051540
- Ruddon RW, Krzesicki R, Norton S, Beebe JS, Peters B, Perini F (1987) Detection of a glycosylated, incompletely folded form of chorionic gonadotropin beta subunit that is a precursor of hormone assembly in trophoblastic cells Journal of Biological Chemistry 262:12533-12540
- Rueden CT, Schindelin J, Hiner MC, DeZonia BE, Walter AE, Arena ET, Eliceiri KW (2017) ImageJ2: ImageJ for the next generation of scientific image data BMC bioinformatics 18:529
- Saitô H, Ohki T, Sasaki T (1979) A ¹³C-nuclear magnetic resonance study of polysaccharide gels. Molecular architecture in the gels consisting of fungal, branched (1 → 3)-β-d-glucans (lentinan and schizophyllan) as manifested by conformational changes induced by sodium hydroxide Carbohydrate Research 74:227-240 doi:[https://doi.org/10.1016/S0008-6215\(00\)84779-5](https://doi.org/10.1016/S0008-6215(00)84779-5)

- Saito S et al. (2018) N-myristoylation and S-acylation are common modifications of Ca²⁺-regulated Arabidopsis kinases and are required for activation of the SLAC1 anion channel *New Phytologist* 218:1504-1521 doi:10.1111/nph.15053
- Salmond GPC (1994) SECRETION OF EXTRACELLULAR VIRULENCE FACTORS BY PLANT PATHOGENIC BACTERIA *Annual Review of Phytopathology* 32:181-200 doi:10.1146/annurev.py.32.090194.001145
- Salomon S, Gácsér A, Frerichmann S, Kröger C, Schäfer W, Voigt CA (2012) The secreted lipase FGL1 is sufficient to restore the initial infection step to the apathogenic *Fusarium graminearum* MAP kinase disruption mutant Δ gpmk1 *European Journal of Plant Pathology* 134:23-37 doi:10.1007/s10658-012-0017-2
- Samac DA, Hironaka CM, Yallaly PE, Shah DM (1990) Isolation and Characterization of the Genes Encoding Basic and Acidic Chitinase in *Arabidopsis thaliana* *Plant Physiology* 93:907-914 doi:10.1104/pp.93.3.907
- Samac DA, Shah DM (1991) Developmental and Pathogen-Induced Activation of the Arabidopsis Acidic Chitinase Promoter *The Plant Cell* 3:1063-1072 doi:10.1105/tpc.3.10.1063
- Samuelsson B, Dahlen S, Lindgren J, Rouzer C, Serhan C (1987) Leukotrienes and lipoxins: structures, biosynthesis, and biological effects *Science* 237:1171-1176 doi:10.1126/science.2820055
- Sánchez-León S, Gil-Humanes J, Ozuna CV, Giménez MJ, Sousa C, Voytas DF, Barro F (2018) Low-gluten, nontransgenic wheat engineered with CRISPR/Cas9 *Plant Biotechnology Journal* 16:902-910 doi:10.1111/pbi.12837
- Sancho R, Cantalapiedra CP, López-Alvarez D, Gordon SP, Vogel JP, Catalán P, Contreras-Moreira B (2018) Comparative plastome genomics and phylogenomics of *Brachypodium*: flowering time signatures, introgression and recombination in recently diverged ecotypes *New Phytologist* 218:1631-1644
- Sandoya GV, Buanafina MMdO (2014) Differential responses of *Brachypodium distachyon* genotypes to insect and fungal pathogens *Physiological and Molecular Plant Pathology* 85:53-64 doi:<https://doi.org/10.1016/j.pmpp.2014.01.001>
- Sarris Panagiotis F et al. (2015) A Plant Immune Receptor Detects Pathogen Effectors that Target WRKY Transcription Factors *Cell* 161:1089-1100 doi:<https://doi.org/10.1016/j.cell.2015.04.024>
- Saucet SB, Ma Y, Sarris PF, Furzer OJ, Sohn KH, Jones JDG (2015) Two linked pairs of Arabidopsis TNL resistance genes independently confer recognition of bacterial effector AvrRps4 *Nature Communications* 6:6338 doi:10.1038/ncomms7338
- <https://www.nature.com/articles/ncomms7338#supplementary-information>
- Savard ME, Sinha RC, Lloyd Seaman W, Fedak G (2000) Sequential distribution of the mycotoxin deoxynivalenol in wheat spikes after inoculation with *Fusarium graminearum* *Canadian Journal of Plant Pathology* 22:280-285 doi:10.1080/07060660009500476
- Savary S, Willocquet L, Pethybridge SJ, Esker P, McRoberts N, Nelson A (2019) The global burden of pathogens and pests on major food crops *Nature Ecology & Evolution* 3:430-439 doi:10.1038/s41559-018-0793-y
- Schaart JG, van de Wiel CCM, Lotz LAP, Smulders MJM (2016) Opportunities for Products of New Plant Breeding Techniques *Trends in Plant Science* 21:438-449 doi:<https://doi.org/10.1016/j.tplants.2015.11.006>
- Scheller HV, Ulvskov P (2010) Hemicelluloses *Annual review of plant biology* 61
- Schindelin J et al. (2012) Fiji: an open-source platform for biological-image analysis *Nature methods* 9:676
- Schippmann U (1991) Revision der europäischen Arten der Gattung *Brachypodium* Palisot de Beauvois (Poaceae). Geneve,
- Schlüpman H, Bacic A, Read SM (1993) A novel callose synthase from pollen tubes of *Nicotiana glauca* *Plant* 191:470-481
- Schmeitzl C et al. (2015) Identification and characterization of carboxylesterases from *brachypodium distachyon* deacetylating trichothecene mycotoxins *Toxins* 8:6
- Schmidhuber J, Tubiello FN (2007) Global food security under climate change *Proceedings of the National Academy of Sciences* 104:19703-19708 doi:10.1073/pnas.0701976104

- Schneider R, Hanak T, Persson S, Voigt CA (2016) Cellulose and callose synthesis and organization in focus, what's new? *Current Opinion in Plant Biology* 34:9-16
doi:<https://doi.org/10.1016/j.pbi.2016.07.007>
- Schober MS, Burton RA, Shirley NJ, Jacobs AK, Fincher GB (2009) Analysis of the (1,3)- β -d-glucan synthase gene family of barley *Phytochemistry* 70:713-720
doi:<https://doi.org/10.1016/j.phytochem.2009.04.002>
- Scholthof K-B, Irigoyen S, Catalan P, Mandadi K (2018) Brachypodium: A monocot grass model system for plant biology *The Plant Cell* 30:tpc.00083.02018 doi:10.1105/tpc.18.00083
- Schweiger W et al. (2013) Functional Characterization of Two Clusters of Brachypodium distachyon UDP-Glycosyltransferases Encoding Putative Deoxynivalenol Detoxification Genes *Molecular Plant-Microbe Interactions* 26:781-792 doi:10.1094/mpmi-08-12-0205-r
- Segal DJ et al. (2003) Evaluation of a modular strategy for the construction of novel polydactyl zinc finger DNA-binding proteins *Biochemistry* 42:2137-2148
- Segal DJ, Dreier B, Beerli RR, Barbas CF (1999) Toward controlling gene expression at will: selection and design of zinc finger domains recognizing each of the 5'-GNN-3' DNA target sequences *Proceedings of the National Academy of Sciences* 96:2758-2763
- Sevilem I, Miyashima S, Helariutta Y (2013) Cell-to-cell communication via plasmodesmata in vascular plants *Cell Adhesion & Migration* 7:27-32 doi:10.4161/cam.22126
- Seyran E, Craig W (2018) New Breeding Techniques and Their Possible Regulation *AgBioForum* 21:1-12
- Shah D, Bergstrom G, Ueng P (1995) Initiation of Septoria nodorum blotch epidemics in winter wheat by seedborne *Stagonospora nodorum* *Phytopathology* 85:452-457
- Shah DA, Bergstrom GC, Ueng PP (2001) Foci of stagonospora nodorum blotch in winter wheat before canopy development *Phytopathology* 91:642-647 doi:10.1094/phyto.2001.91.7.642
- Shahinian S, Silvius JR (1995) Doubly-lipid-modified protein sequence motifs exhibit long-lived anchorage to lipid bilayer membranes *Biochemistry* 34:3813-3822
- Shan L et al. (2008) Bacterial effectors target the common signaling partner BAK1 to disrupt multiple MAMP receptor-signaling complexes and impede plant immunity *Cell host & microbe* 4:17-27
- Shi X, Han X, Lu T-g (2016) Callose synthesis during reproductive development in monocotyledonous and dicotyledonous plants *Plant Signaling & Behavior* 11:e1062196 doi:10.1080/15592324.2015.1062196
- Shi X et al. (2014) GLUCAN SYNTHASE-LIKE 5 (GSL5) Plays an Essential Role in Male Fertility by Regulating Callose Metabolism During Microsporogenesis in Rice Plant and Cell Physiology 56:497-509 doi:10.1093/pcp/pcu193
- Shimizu T et al. (2010) Two LysM receptor molecules, CEBiP and OsCERK1, cooperatively regulate chitin elicitor signaling in rice *The Plant Journal* 64:204-214
- Shin H, Brown RM (1999) GTPase Activity and Biochemical Characterization of a Recombinant Cotton Fiber Annexin *Plant Physiology* 119:925-934 doi:10.1104/pp.119.3.925
- Shinya T et al. (2014) Selective regulation of the chitin-induced defense response by the A rabidopsis receptor-like cytoplasmic kinase PBL 27 *The Plant Journal* 79:56-66
- Shrimal S, Cherepanova NA, Gilmore R (2015) Cotranslational and posttranslational N-glycosylation of proteins in the endoplasmic reticulum *Seminars in Cell & Developmental Biology* 41:71-78 doi:<https://doi.org/10.1016/j.semcdb.2014.11.005>
- Shuai B, Reynaga-Pena CG, Springer PS (2002) The lateral organ boundaries gene defines a novel, plant-specific gene family *Plant physiology* 129:747-761
- Sierla M, Rahikainen M, Salojärvi J, Kangasjärvi J, Kangasjärvi S (2013) Apoplastic and chloroplastic redox signaling networks in plant stress responses *Antioxidants & redox signaling* 18:2220-2239
- Sievers F et al. (2011) Fast, scalable generation of high-quality protein multiple sequence alignments using Clustal Omega *Molecular systems biology* 7:539-539 doi:10.1038/msb.2011.75
- Sigrist CJA, Cerutti L, de Castro E, Langendijk-Genevaux PS, Bulliard V, Bairoch A, Hulo N (2010) PROSITE, a protein domain database for functional characterization and annotation *Nucleic Acids Research* 38:D161-D166
- Silvius JR, l'Heureux F (1994) Fluorometric evaluation of the affinities of isoprenylated peptides for lipid bilayers *Biochemistry* 33:3014-3022

- Singh RP et al. (2008) Will Stem Rust Destroy the World's Wheat Crop? In: Advances in Agronomy, vol 98. Academic Press, pp 271-309. doi:[https://doi.org/10.1016/S0065-2113\(08\)00205-8](https://doi.org/10.1016/S0065-2113(08)00205-8)
- Singh RP et al. (2016) Disease impact on wheat yield potential and prospects of genetic control Annual review of phytopathology 54:303-322
- Sivaguru M et al. (2000) Aluminum-induced 1 \rightarrow 3- β -d-glucan inhibits cell-to-cell trafficking of molecules through plasmodesmata. A new mechanism of aluminum toxicity in plants Plant physiology 124:991-1006
- Škalamera D, Heath MC (1995) Changes in the plant endomembrane system associated with callose synthesis during the interaction between cowpea (*Vigna unguiculata*) and the cowpea rust fungus (*Uromyces vignae*) Canadian Journal of Botany 73:1731-1738 doi:10.1139/b95-185
- Skou J-P, Jørgensen JH, Lilholt U (1984) Comparative studies on callose formation in powdery mildew compatible and incompatible barley Journal of Phytopathology 109:147-168
- Slaymaker IM, Gao L, Zetsche B, Scott DA, Yan WX, Zhang F (2016) Rationally engineered Cas9 nucleases with improved specificity Science 351:84-88 doi:10.1126/science.aad5227
- Sode B (2015) Phosphorylierung als Regulator in der stressinduzierten Callosebiosynthese in *Arabidopsis thaliana* (L.). Verlag nicht ermittelbar,
- Sogutmaz Ozdemir B, Budak H (2018) Application of Tissue Culture and Transformation Techniques in Model Species *Brachypodium distachyon*. In: Sablok G, Budak H, Ralph PJ (eds) *Brachypodium Genomics: Methods and Protocols*. Springer New York, New York, NY, pp 289-310. doi:10.1007/978-1-4939-7278-4_18
- Solomon PS, Lowe RGT, Tan K-C, Waters ODC, Oliver RP (2006) *Stagonospora nodorum*: cause of *stagonospora nodorum* blotch of wheat Molecular Plant Pathology 7:147-156 doi:10.1111/j.1364-3703.2006.00326.x
- Solomon PS, Tan K-C, Sanchez P, Cooper RM, Oliver RP (2004) The disruption of a $G\alpha$ subunit sheds new light on the pathogenicity of *Stagonospora nodorum* on wheat Molecular Plant-Microbe Interactions 17:456-466
- Somerville C et al. (2004) Toward a Systems Approach to Understanding Plant Cell Walls Science 306:2206-2211 doi:10.1126/science.1102765
- Somssich M, Khan GA, Persson S (2016) Cell Wall Heterogeneity in Root Development of *Arabidopsis* Frontiers in Plant Science 7:1242
- Song J, Hirschman J, Gunn K, Dohlman HG (1996) Regulation of membrane and subunit interactions by N-myristoylation of a G protein α subunit in yeast Journal of Biological Chemistry 271:20273-20283
- Song K, Sargiacomo M, Galbiati F, Parenti M, Lisanti M (1997) Targeting of a G alpha subunit (G_i1 alpha) and c-Src tyrosine kinase to caveolae membranes: clarifying the role of N-myristoylation Cellular and molecular biology (Noisy-le-Grand, France) 43:293-303
- Sousa M, Parodi AJ (1995) The molecular basis for the recognition of misfolded glycoproteins by the UDP-Glc: glycoprotein glucosyltransferase The EMBO journal 14:4196-4203
- Sperisen P, Iseli C, Pagni M, Stevenson BJ, Bucher P, Jongeneel CV (2004) trEMBL, trEST and trGEN: databases of predicted protein sequences Nucleic Acids Research 32:D509-511
- Sperisen P, Pagni M (2005) JACOP: A simple and robust method for the automated classification of protein sequences with modular architecture BMC Bioinformatics 6:216
- Srivastava V, Malm E, Sundqvist G, Bulone V (2013) Quantitative proteomics reveals that plasma membrane microdomains from poplar cell suspension cultures are enriched in markers of signal transduction, molecular transport, and callose biosynthesis Molecular & Cellular Proteomics 12:3874-3885
- Stack RW (2000) Return of an old problem: *Fusarium* head blight of small grains Plant health progress 1:19
- Standley DM, Katoh K (2013) MAFFT Multiple Sequence Alignment Software Version 7: Improvements in Performance and Usability Molecular Biology and Evolution 30:772-780 doi:10.1093/molbev/mst010
- Steer MW, Steer JM (1989) Pollen tube tip growth New Phytologist 111:323-358 doi:10.1111/j.1469-8137.1989.tb00697.x
- Sternberg SH, Redding S, Jinek M, Greene EC, Doudna JA (2014) DNA interrogation by the CRISPR RNA-guided endonuclease Cas9 Nature 507:62

- Stintzi A et al. (1993) Plant 'pathogenesis-related' proteins and their role in defense against pathogens *Biochimie* 75:687-706
- Stone BA (1992) Chemistry and physiology of higher plant (1-3)- β -glucans (callose) *Chemistry, and Biology of (1-3)- β -Glucans*
- Stone BA, Clarke AE (1992) Chemistry and Biology of 1, 3- β -Glucans. Intl Specialized Book Service Inc,
- Stone BA, Evans NA, Bonig I, Clarke AE (1984) The application of Sirofluor, a chemically defined fluorochrome from aniline blue for the histochemical detection of callose *Protoplasma* 122:191-195 doi:10.1007/BF01281696
- Streubel J, Blücher C, Landgraf A, Boch J (2012) TAL effector RVD specificities and efficiencies *Nature Biotechnology* 30:593-595 doi:10.1038/nbt.2304
- Sun Y et al. (2013) Structural basis for flg22-induced activation of the Arabidopsis FLS2-BAK1 immune complex *Science* 342:624-628
- Sutton J (1982) Epidemiology of wheat head blight and maize ear rot caused by *Fusarium graminearum* *Canadian journal of plant pathology* 4:195-209
- Svitashev S, Schwartz C, Lenderts B, Young JK, Mark Cigan A (2016) Genome editing in maize directed by CRISPR–Cas9 ribonucleoprotein complexes *Nature Communications* 7:13274 doi:10.1038/ncomms13274
- <https://www.nature.com/articles/ncomms13274#supplementary-information>
- Takáts Z, Wiseman JM, Gologan B, Cooks RG (2004) Mass Spectrometry Sampling Under Ambient Conditions with Desorption Electrospray Ionization *Science* 306:471-473 doi:10.1126/science.1104404
- Takken FL, Goverse A (2012) How to build a pathogen detector: structural basis of NB-LRR function *Current opinion in plant biology* 15:375-384
- Tan K-C, Waters ODC, Rybak K, Antoni E, Furuki E, Oliver RP (2014) Sensitivity to three *Parastagonospora nodorum* necrotrophic effectors in current Australian wheat cultivars and the presence of further fungal effectors *Crop and Pasture Science* 65:150-158 doi:<https://doi.org/10.1071/CP13443>
- Terns MP, Terns RM (2011) CRISPR-based adaptive immune systems *Current opinion in microbiology* 14:321-327
- Terracciano I et al. (2013) Development of COS-SNP and HRM markers for high-throughput and reliable haplotype-based detection of Lr14a in durum wheat (*Triticum durum* Desf.) *Theoretical and Applied Genetics* 126:1077-1101 doi:10.1007/s00122-012-2038-9
- Tester M, Langridge P (2010) Breeding Technologies to Increase Crop Production in a Changing World *Science* 327:818-822 doi:10.1126/science.1183700
- Thole V, Worland B, Wright J, Bevan MW, Vain P (2010) Distribution and characterization of more than 1000 T-DNA tags in the genome of *Brachypodium distachyon* community standard line Bd21 *Plant biotechnology journal* 8:734-747
- Thordal-Christensen H, Zhang Z, Wei Y, Collinge DB (1997) Subcellular localization of H₂O₂ in plants. H₂O₂ accumulation in papillae and hypersensitive response during the barley—powdery mildew interaction *The Plant Journal* 11:1187-1194
- Tian D, Traw MB, Chen JQ, Kreitman M, Bergelson J (2003) Fitness costs of R-gene-mediated resistance in *Arabidopsis thaliana* *Nature* 423:74-77 doi:10.1038/nature01588
- Tirlapur UK, Willemse M (1992) Changes in calcium and calmodulin levels during microsporogenesis, pollen development and germination in *Gasteria verrucosa* (Mill.) H. Duval *Sexual Plant Reproduction* 5:214-223
- Ton J, Mauch-Mani B (2004) β -amino-butyric acid-induced resistance against necrotrophic pathogens is based on ABA-dependent priming for callose *The Plant Journal* 38:119-130 doi:10.1111/j.1365-313X.2004.02028.x
- Torriani SFF, Melichar JPE, Mills C, Pain N, Sierotzki H, Courbot M (2015) *Zymoseptoria tritici*: A major threat to wheat production, integrated approaches to control *Fungal Genetics and Biology* 79:8-12 doi:<https://doi.org/10.1016/j.fgb.2015.04.010>
- Trail F, Xu H, Loranger R, Gadoury D (2002) Physiological and environmental aspects of ascospore discharge in *Gibberella zeae* (anamorph *Fusarium graminearum*) *Mycologia* 94:181-189

- Tsai SQ, Joung JK (2016) Defining and improving the genome-wide specificities of CRISPR–Cas9 nucleases *Nature Reviews Genetics* 17:300 doi:10.1038/nrg.2016.28
- Ueta R et al. (2017) Rapid breeding of parthenocarpic tomato plants using CRISPR/Cas9 *Scientific Reports* 7:507 doi:10.1038/s41598-017-00501-4
- Uknes S et al. (1992) Acquired resistance in *Arabidopsis* *The Plant Cell* 4:645-656 doi:10.1105/tpc.4.6.645
- Untergasser A, Cutcutache I, Koressaar T, Ye J, Faircloth BC, Remm M, Rozen SG (2012) Primer3—new capabilities and interfaces *Nucleic acids research* 40:e115-e115
- Urnov FD, Rebar EJ, Holmes MC, Zhang HS, Gregory PD (2010) Genome editing with engineered zinc finger nucleases *Nature Reviews Genetics* 11:636 doi:10.1038/nrg2842
- Vain P et al. (2008) Agrobacterium-mediated transformation of the temperate grass *Brachypodium distachyon* (genotype Bd21) for T-DNA insertional mutagenesis *Plant biotechnology journal* 6:236-245
- Van Bel M et al. (2017) PLAZA 4.0: an integrative resource for functional, evolutionary and comparative plant genomics *Nucleic acids research* 46:D1190-D1196
- van Buuren M, Neuhaus J-M, Shinshi H, Ryals J, Meins F (1992) The structure and regulation of homeologous tobacco endochitinase genes of *Nicotiana sylvestris* and *N. tomentosiformis* origin *Molecular and General Genetics MGG* 232:460-469 doi:10.1007/BF00266251
- van der Hoorn RA, Kamoun S (2008) From guard to decoy: a new model for perception of plant pathogen effectors *The Plant Cell* 20:2009-2017
- Van Loon L, Van Kammen A (1970) Polyacrylamide disc electrophoresis of the soluble leaf proteins from *Nicotiana tabacum* var. 'Samsun' and 'Samsun NN': II. Changes in protein constitution after infection with tobacco mosaic virus *Virology* 40:199-211
- Van Loon LC, Van Strien EA (1999) The families of pathogenesis-related proteins, their activities, and comparative analysis of PR-1 type proteins *Physiological and Molecular Plant Pathology* 55:85-97 doi:<https://doi.org/10.1006/pmpp.1999.0213>
- Vandepoele K et al. (2013) pico-PLAZA, a genome database of microbial photosynthetic eukaryotes *Environmental microbiology* 15:2147-2153
- Varshney RK, Graner A, Sorrells ME (2005) Genomics-assisted breeding for crop improvement *Trends in plant science* 10:621-630
- Vatén A et al. (2011) Callose Biosynthesis Regulates Symplastic Trafficking during Root Development *Developmental Cell* 21:1144-1155 doi:<https://doi.org/10.1016/j.devcel.2011.10.006>
- Verhage A, van Wees SC, Pieterse CM (2010) Plant immunity: it's the hormones talking, but what do they say? *Plant Physiology* 154:536-540
- Verma DPS (2001) Cytokinesis and building of the cell plate in plants *Annual review of plant biology* 52:751-784
- Verma DPS, Hong Z (2001) Plant callose synthase complexes *Plant molecular biology* 47:693-701
- Vogel J (2008) Unique aspects of the grass cell wall *Current opinion in plant biology* 11:301-307
- Vogel J, Bragg J (2009) *Brachypodium distachyon*, a new model for the Triticeae. In: *Genetics and Genomics of the Triticeae*. Springer, pp 427-449
- Vogel J, Hill T (2008) High-efficiency Agrobacterium-mediated transformation of *Brachypodium distachyon* inbred line Bd21-3 *Plant cell reports* 27:471-478
- Vogel JP, Garvin DF, Leong OM, Hayden DM (2006a) Agrobacterium-mediated transformation and inbred line development in the model grass *Brachypodium distachyon* *Plant Cell, Tissue and Organ Culture* 84:199-211
- Vogel JP et al. (2006b) EST sequencing and phylogenetic analysis of the model grass *Brachypodium distachyon* *Theor Appl Genet* 113:186-195 doi:10.1007/s00122-006-0285-3
- Vogel JP, Tuna M, Budak H, Huo N, Gu YQ, Steinwand MA (2009) Development of SSR markers and analysis of diversity in Turkish populations of *Brachypodium distachyon* *BMC Plant Biol* 9:88 doi:10.1186/1471-2229-9-88
- Voigt CA (2014) Callose-mediated resistance to pathogenic intruders in plant defense-related papillae *Frontiers in Plant Science* 5:168
- Voigt CA, Schäfer W, Salomon S (2005) A secreted lipase of *Fusarium graminearum* is a virulence factor required for infection of cereals *The Plant Journal* 42:364-375 doi:10.1111/j.1365-3113.2005.02377.x

- Voigt CA, von Scheidt B, Gácsér A, Kassner H, Lieberei R, Schäfer W, Salomon S (2007) Enhanced mycotoxin production of a lipase-deficient *Fusarium graminearum* mutant correlates to toxin-related gene expression *European Journal of Plant Pathology* 117:1-12 doi:10.1007/s10658-006-9063-y
- Voisin DF (2008) Biochemical and genetic responses in cuticular mutants. Universität zu Köln
- Vonarx EJ, Mitchell HL, Karthikeyan R, Chatterjee I, Kunz BA (1998) DNA repair in higher plants *Mutation Research/Fundamental and Molecular Mechanisms of Mutagenesis* 400:187-200
- Vorwerk S, Somerville S, Somerville C (2004) The role of plant cell wall polysaccharide composition in disease resistance *Trends in plant science* 9:203-209
- Vunsh R (2018) Methods for Functional Transgenics: Development of Highly Efficient Transformation Protocol in *Brachypodium* and Its Suitability for Advancing *Brachypodium* Transgenics. In: Sablok G, Budak H, Ralph PJ (eds) *Brachypodium Genomics: Methods and Protocols*. Springer New York, New York, NY, pp 101-117. doi:10.1007/978-1-4939-7278-4_9
- Walters D, Heil M (2007) Costs and trade-offs associated with induced resistance *Physiological and Molecular Plant Pathology* 71:3-17 doi:<https://doi.org/10.1016/j.pmpp.2007.09.008>
- Wan J, Tanaka K, Zhang X-C, Son GH, Brechenmacher L, Nguyen THN, Stacey G (2012) LYK4, a lysin motif receptor-like kinase, is important for chitin signaling and plant innate immunity in *Arabidopsis* *Plant physiology* 160:396-406
- Wang L et al. (2010) Expression profiling and integrative analysis of the CESA/CSL superfamily in rice *BMC plant biology* 10:282
- Wang Y, Cheng X, Shan Q, Zhang Y, Liu J, Gao C, Qiu J-L (2014) Simultaneous editing of three homoeoalleles in hexaploid bread wheat confers heritable resistance to powdery mildew *Nature Biotechnology* 32:947 doi:10.1038/nbt.2969
- <https://www.nature.com/articles/nbt.2969#supplementary-information>
- Ward TJ, Bielawski JP, Kistler HC, Sullivan E, O'Donnell K (2002) Ancestral polymorphism and adaptive evolution in the trichothecene mycotoxin gene cluster of phytopathogenic *Fusarium* *Proceedings of the National Academy of Sciences* 99:9278-9283 doi:10.1073/pnas.142307199
- Wei C, Liu J, Yu Z, Zhang B, Gao G, Jiao R (2013) TALEN or Cas9 – Rapid, Efficient and Specific Choices for Genome Modifications *Journal of Genetics and Genomics* 40:281-289 doi:<https://doi.org/10.1016/j.jgg.2013.03.013>
- Wei N, Serino G, Deng X-W (2008) The COP9 signalosome: more than a protease *Trends in Biochemical Sciences* 33:592-600 doi:<https://doi.org/10.1016/j.tibs.2008.09.004>
- West JS, Holdgate S, Townsend JA, Edwards SG, Jennings P, Fitt BDL (2012) Impacts of changing climate and agronomic factors on fusarium ear blight of wheat in the UK *Fungal Ecology* 5:53-61 doi:<https://doi.org/10.1016/j.funeco.2011.03.003>
- Weterings E, Chen DJ (2008) The endless tale of non-homologous end-joining *Cell Research* 18:114-124 doi:10.1038/cr.2008.3
- Widmann C, Gibson S, Jarpe MB, Johnson GL (1999) Mitogen-activated protein kinase: conservation of a three-kinase module from yeast to human *Physiological reviews* 79:143-180
- Wilcox C, Hu J, Olson E (1987) Acylation of proteins with myristic acid occurs cotranslationally *Science* 238:1275-1278 doi:10.1126/science.3685978
- Will T, van Bel AJ (2006) Physical and chemical interactions between aphids and plants *Journal of experimental botany* 57:729-737
- William Allwood J, Ellis DI, Heald JK, Goodacre R, Mur LAJ (2006) Metabolomic approaches reveal that phosphatidic and phosphatidyl glycerol phospholipids are major discriminatory non-polar metabolites in responses by *Brachypodium distachyon* to challenge by *Magnaporthe oryzae* *The Plant Journal* 46:351-368 doi:10.1111/j.1365-3113.2006.02692.x
- Williams EG, Knox RB, Kaul V, Rouse JL (1984) Post-pollination callose development in ovules of *Rhododendron* and *Ledum* (Ericaceae): zygote special wall *Journal of Cell Science* 69:127-135
- Williams JR, Jones DG (1973) Infection of grasses by *Septoria nodorum* and *S. tritici* *Transactions of the British Mycological Society* 60:355-358

- Williamson VM, Hussey RS (1996) Nematode pathogenesis and resistance in plants *The Plant cell* 8:1735-1745 doi:10.1105/tpc.8.10.1735
- Wilson TE, Lieber MR (1999) Efficient processing of DNA ends during yeast nonhomologous end joining. Evidence for a DNA polymerase beta (Pol4)-dependent pathway *The Journal of biological chemistry* 274:23599-23609 doi:10.1074/jbc.274.33.23599
- Wilson W, Dahl B, Nganje W (2018) Economic costs of fusarium head blight, scab and deoxynivalenol *World Mycotoxin Journal* 11:291-302
- Windels CE (2000) Economic and social impacts of Fusarium head blight: changing farms and rural communities in the Northern Great Plains *Phytopathology* 90:17-21
- Wissemeier A, Diening A, Hergenröder A, Horst W, Mix-Wagner G (1992) Callose formation as parameter for assessing genotypical plant tolerance of aluminium and manganese *Plant and Soil* 146:67-75
- Wissemeier A, Klotz F, Horst W (1987) Aluminium induced callose synthesis in roots of soybean (*Glycine max* L.) *Journal of Plant Physiology* 129:487-492
- Wolny E, Hasterok R (2009) Comparative cytogenetic analysis of the genomes of the model grass *Brachypodium distachyon* and its close relatives *Annals of botany* 104:873-881
- Wu S, O'Lexy R, Xu M, Sang Y, Chen X, Yu Q, Gallagher KL (2016) Symplastic signaling instructs cell division, cell expansion, and cell polarity in the ground tissue of *Arabidopsis thaliana* roots *Proceedings of the National Academy of Sciences* 113:11621-11626 doi:10.1073/pnas.1610358113
- Wu Y et al. (2013) Correction of a Genetic Disease in Mouse via Use of CRISPR-Cas9 *Cell Stem Cell* 13:659-662 doi:<https://doi.org/10.1016/j.stem.2013.10.016>
- Xiang T et al. (2008) *Pseudomonas syringae* effector AvrPto blocks innate immunity by targeting receptor kinases *Current biology* 18:74-80
- Xie B, Wang X, Zhu M, Zhang Z, Hong Z (2011) CalS7 encodes a callose synthase responsible for callose deposition in the phloem *The Plant Journal* 65:1-14 doi:10.1111/j.1365-3113.2010.04399.x
- Xing W et al. (2007) The structural basis for activation of plant immunity by bacterial effector protein AvrPto *Nature* 449:243
- Xu B et al. (2017) A calmodulin-like protein regulates plasmodesmal closure during bacterial immune responses *New Phytologist* 215:77-84 doi:10.1111/nph.14599
- Xu R et al. (2016) Rapid improvement of grain weight via highly efficient CRISPR/Cas9-mediated multiplex genome editing in rice *Journal of Genetics and Genomics* 43:529-532 doi:<https://doi.org/10.1016/j.jgg.2016.07.003>
- Xu X, Nicholson P (2009) Community ecology of fungal pathogens causing wheat head blight *Annual review of phytopathology* 47:83-103
- Xu Y, Chang P-FL, Liu D, Narasimhan ML, Raghothama KG, Hasegawa PM, Bressan RA (1994) Plant defense genes are synergistically induced by ethylene and methyl jasmonate *The Plant Cell* 6:1077-1085
- Xue H-Y, Ji L-J, Gao A-M, Liu P, He J-D, Lu X-J (2016) CRISPR-Cas9 for medical genetic screens: applications and future perspectives *Journal of medical genetics* 53:91-97
- Yamaguchi K et al. (2013) A receptor-like cytoplasmic kinase targeted by a plant pathogen effector is directly phosphorylated by the chitin receptor and mediates rice immunity *Cell host & microbe* 13:347-357
- Yamaguchi T, Hayashi T, Nakayama K, Koike S (2006) Expression Analysis of Genes for Callose Synthases and Rho-Type Small GTP-Binding Proteins That Are Related to Callose Synthesis in Rice Anther *Bioscience, Biotechnology, and Biochemistry* 70:639-645 doi:10.1271/bbb.70.639
- Yang Z-B, Eticha D, Albacete A, Rao IM, Roitsch T, Horst WJ (2012) Physiological and molecular analysis of the interaction between aluminium toxicity and drought stress in common bean (*Phaseolus vulgaris*) *Journal of Experimental Botany* 63:3109-3125 doi:10.1093/jxb/ers038
- Yoshioka H, Adachi H, Nakano T, Miyagawa N, Asai S, Ishihama N, Yoshioka M (2016) Hierarchical regulation of NADPH oxidase by protein kinases in plant immunity *Physiological and Molecular Plant Pathology* 95:20-26 doi:<https://doi.org/10.1016/j.pmpp.2016.03.004>
- Yu Q-h et al. (2017) CRISPR/Cas9-induced Targeted Mutagenesis and Gene Replacement to Generate Long-shelf Life Tomato Lines *Scientific Reports* 7:11874 doi:10.1038/s41598-017-12262-1

- Yun MH et al. (2006) Xanthan Induces Plant Susceptibility by Suppressing Callose Deposition Plant Physiology 141:178-187 doi:10.1104/pp.105.074542
- Zavaliev R, Ueki S, Epel BL, Citovsky V (2011) Biology of callose (β -1,3-glucan) turnover at plasmodesmata Protoplasma 248:117-130 doi:10.1007/s00709-010-0247-0
- Zeng L, Velásquez AC, Munkvold KR, Zhang J, Martin GB (2012) A tomato LysM receptor-like kinase promotes immunity and its kinase activity is inhibited by AvrPtoB The Plant Journal 69:92-103
- Zeyen R, Carver T, Lyngkjær MF (2002) Epidermal cell papillae. In: The powdery mildews. A comprehensive treatise. APS Press,
- Zha J, Weiler S, Oh KJ, Wei MC, Korsmeyer SJ (2000) Posttranslational N-Myristoylation of BID as a Molecular Switch for Targeting Mitochondria and Apoptosis Science 290:1761-1765 doi:10.1126/science.290.5497.1761
- Zhang F, Cong L, Lodato S, Kosuri S, Church GM, Arlotta P (2011) Efficient construction of sequence-specific TAL effectors for modulating mammalian transcription Nature Biotechnology 29:149 doi:10.1038/nbt.1775
- <https://www.nature.com/articles/nbt.1775#supplementary-information>
- Zhang F et al. (2010a) High frequency targeted mutagenesis in Arabidopsis thaliana using zinc finger nucleases Proceedings of the National Academy of Sciences 107:12028-12033
- Zhang F, Wen Y, Guo X (2014) CRISPR/Cas9 for genome editing: progress, implications and challenges Human molecular genetics 23:R40-R46
- Zhang J et al. (2010b) Receptor-like cytoplasmic kinases integrate signaling from multiple plant immune receptors and are targeted by a Pseudomonas syringae effector Cell host & microbe 7:290-301
- Zhang W et al. (2010c) Genetic Maps of Stem Rust Resistance Gene Sr35 in Diploid and Hexaploid Wheat Crop Science 50:2464-2474 doi:10.2135/cropsci2010.04.0202
- Zhang Y, Bai Y, Wu G, Zou S, Chen Y, Gao C, Tang D (2017) Simultaneous modification of three homoeologs of TaEDR1 by genome editing enhances powdery mildew resistance in wheat The Plant Journal 91:714-724 doi:10.1111/tpj.13599
- Zhang Y, Fan W, Kinkema M, Li X, Dong X (1999) Interaction of NPR1 with basic leucine zipper protein transcription factors that bind sequences required for salicylic acid induction of the PR-1 gene Proceedings of the National Academy of Sciences 96:6523-6528
- Zhao X, Wang Q, Jiao Y, Huang R, Deng Y, Wang H, Du X (2012) Identification of genes potentially related to biomineralization and immunity by transcriptome analysis of pearl sac in pearl oyster Pinctada martensii Marine biotechnology 14:730-739
- Zhao Z, Crespi VH, Kubicki JD, Cosgrove DJ, Zhong L (2014) Molecular dynamics simulation study of xyloglucan adsorption on cellulose surfaces: effects of surface hydrophobicity and side-chain variation Cellulose 21:1025-1039
- Zheng M, Fang H, Hakomori S-i (1994) Functional role of N-glycosylation in alpha 5 beta 1 integrin receptor. De-N-glycosylation induces dissociation or altered association of alpha 5 and beta 1 subunits and concomitant loss of fibronectin binding activity Journal of Biological Chemistry 269:12325-12331
- Zheng Z-L, Yang Z (2000) The Rop GTPase: an emerging signaling switch in plants Plant molecular biology 44:1-9
- Zhou J et al. (2017) CRISPR-Cas9 Based Genome Editing Reveals New Insights into MicroRNA Function and Regulation in Rice Frontiers in Plant Science 8 doi:10.3389/fpls.2017.01598
- Zhou W, Kolb FL, Riechers DE (2005) Identification of proteins induced or upregulated by Fusarium head blight infection in the spikes of hexaploid wheat (Triticum aestivum) Genome 48:770-780 doi:10.1139/g05-041
- Zhu H, Briceño G, Dovel R, Hayes PM, Liu BH, Liu CT, Ullrich SE (1999a) Molecular breeding for grain yield in barley: an evaluation of QTL effects in a spring barley cross Theoretical and Applied Genetics 98:772-779 doi:10.1007/s001220051134
- Zhu H et al. (1999b) Does function follow form? Principal QTLs for Fusarium head blight (FHB) resistance are coincident with QTLs for inflorescence traits and plant height in a doubled-haploid population of barley Theoretical and Applied Genetics 99:1221-1232 doi:10.1007/s001220051328

- Zhu J, Song N, Sun S, Yang W, Zhao H, Song W, Lai J (2016) Efficiency and Inheritance of Targeted Mutagenesis in Maize Using CRISPR-Cas9 *Journal of Genetics and Genomics* 43:25-36
doi:<https://doi.org/10.1016/j.jgg.2015.10.006>
- Zhu Q, Maher EA, Masoud S, Dixon RA, Lamb CJ (1994) Enhanced protection against fungal attack by constitutive co-expression of chitinase and glucanase genes in transgenic tobacco *Bio/technology* 12:807
- Zielinski RE (1998) CALMODULIN AND CALMODULIN-BINDING PROTEINS IN PLANTS *Annual Review of Plant Physiology and Plant Molecular Biology* 49:697-725
doi:10.1146/annurev.arplant.49.1.697
- Zinkernagel V, Riess F, Wendland M, Bartscherer H-C (1988) Infection structures of *Septoria nodorum* in leaves of susceptible wheat cultivars *Zeitschrift fuer Pflanzenkrankheiten und Pflanzenschutz* (Germany, FR)
- Zipfel C, Rathjen JP (2008) Plant immunity: AvrPto targets the frontline *Current biology* 18:R218-R220

8. Supplement

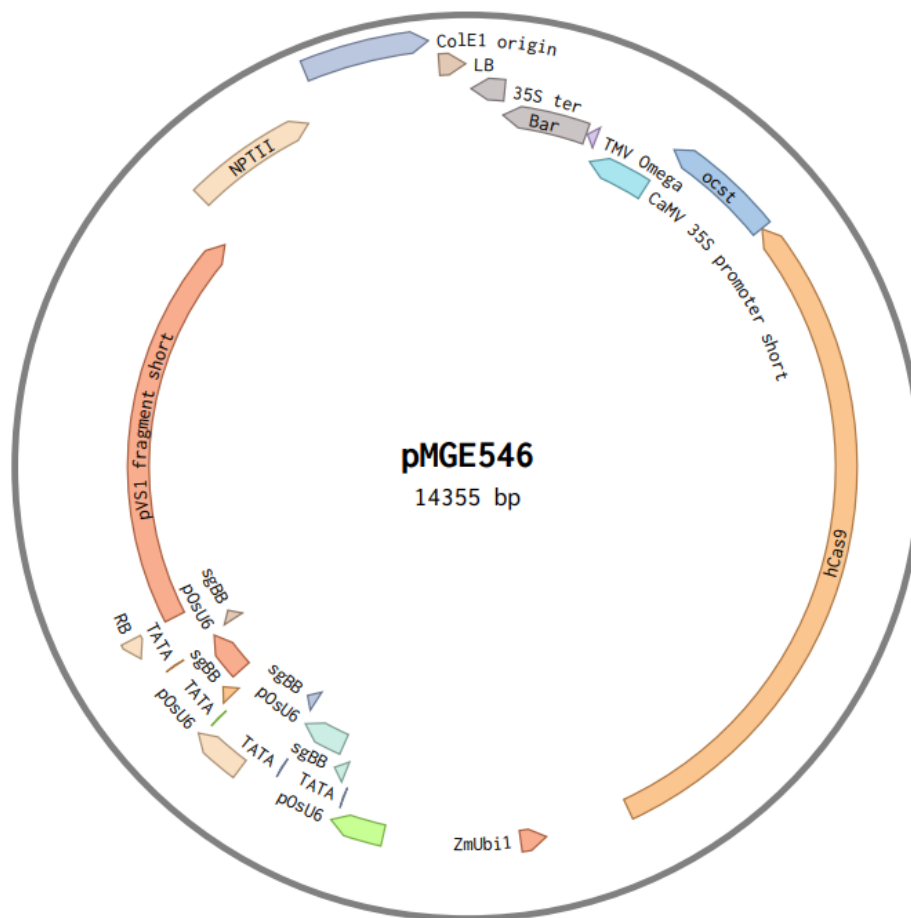


Figure Supplement 1: Binary vector pMGE546 used for Agrobacteria transformation and plant transformation

The binary vector pMGE546 contains a T-DNA enclosed by the right border (RB) and left border (LB). In the T-DNA four sgRNAs (sgBB) are under expression of the rice ubiquitin promoter (pOsU6). The *cas9* is under constitutive expression of the maize ubiquitin promoter (ZmUbi1), and the selection marker (*Bar/hptii*) is under constitutive expression of the *CALIFLOWER MOSAIC VIRUS PROMOTER 35S* (CaMV 35S). For bacterial replication a ColE1 origin is present and for selection the NPTII cassette is present for resistance to kanamycin. The plasmid is 14355 bp large.

Table Supplement 1: Primer overview and loading for the off-site target PCR Fig. 12

Lin	A	B	C	D	E	F	G
e							
1	TH89+TH9	TH91+TH9	TH93+TH9	H ₂ O-	TH107+TH	TH109+TH	TH111+TH
	0	2	4	Contr	108	110	112
				ol			
2	TH95+TH9	TH97+TH9	TH99+TH1	H ₂ O-	TH113+TH	TH115+TH	TH117+TH
	6	8	00	Contr	114	116	118
				ol			
3	TH101+TH	TH103+TH	TH105+TH	Empt	TH119+TH	TH121+TH	TH123+TH
	102	104	106	y	120	122	124

Legend: The Primer used for each PCR are indicated in the table. The H₂O-Control D 1 and D 2 consists of all Primers without template. The respective primer pair and Target can be concluded from the primer-table (Table X).

Table Supplement 2: Overview of the analysed off-site targets for the four sgRNA targets

Offsite-Targets

	Targets	Chromosome	Position	GL	Accession No.	Annotation
crRNA	CCCAGATTAGCAGGTACAAANGG	ENA CM000881 CM000881.3	9015840	A1	XM_003567251.4	PREDICTED: Brachypodium distachyon COP9 signalosome complex subunit 2 (LOC100836634), transcript variant X2, mRNA
DNA	CCaAaATaAGCAGGTACAAATGG					
crRNA	CTACTCCGTTCCCCGGGCCANGG	ENA CM000882 CM000882.3	26625064	B1		No Gene annotated
DNA	CTtCTCCGTTCCCgGGaCCAAGG					
crRNA	GGTGCGCGTACCTCGGCCAGNGG	ENA CM000880 CM000880.3	2590059	C1	XM_003563657.4	PREDICTED: Brachypodium distachyon leukotriene A-4 hydrolase homolog (LOC100828470), mRNA
DNA	GGTGcAgGgACCTCGGCCcGAGG					
crRNA	GGTGCGCGTACCTCGGCCAGNGG	ENA CM000880 CM000880.3	49674399	A2	XM_003557154.3	PREDICTED: Brachypodium distachyon early nodulin-93 (LOC100825538), mRNA
DNA	GccGCGCcTACCTCGaCCAGAGG					
crRNA	GGTGCGCGTACCTCGGCCAGNGG	ENA CM000880 CM000880.3	57507250	B2	XM_024461141.1	
DNA	GGTcCcCGTgCCTCcGCCAGTGG					
crRNA	GTGCGCGTACCTCGGCCAGNGG	ENA CM000880 CM000880.3	62912926	C2	XM_003561622.4	PREDICTED: Brachypodium distachyon probable leucine-rich repeat receptor-like protein kinase At5g49770 (LOC100841195), mRNA
DNA	GGTGCGCGTACCgtaCCAGGGG					
crRNA	CCCAGATTAGCAGGTACAAANGG	ENA CM000880 CM000880.3	16771279	A3	XM_014897740.2	PREDICTED: Brachypodium distachyon 3-oxoacyl-[acyl-carrier-protein] synthase II, chloroplastic (LOC100841004), mRNA
DNA	CCCAtATTAGtAGtTgCAAATGG					
crRNA	CCCAGATTAGCAGGTACAAANGG	ENA CM000880 CM000880.3	43887427	B3		
DNA	CCCAacTTtGCAGGaACAAAAGG					
crRNA	CCCAGATTAGCAGGTACAAANGG	ENA CM000881 CM000881.3	2484233	C3	XR_002963839.1	
DNA	aCCAaATTAGCAGGaAtAAAAAGG					
crRNA	CCCAGATTAGCAGGTACAAANGG				XM_003569230.4	

DNA	tCCAGAgTAaCAGGgACAAAAGG	ENA CM000881 CM000881.3	42334589	E1		
crRNA	CTACTCCGTTCCCCGGGCCANGG	ENA CM000880 CM000880.3	18432666	F1	XM_003562738.4	PREDICTED: Brachypodium distachyon LOB domain-containing protein 37 (LOC100829268), mRNA
DNA	aTACTCCGcTCCCCtGGCCgTGG					
crRNA	CTACTCCGTTCCCCGGGCCANGG	ENA CM000880 CM000880.3	70082764	G1		
DNA	CTACTtCcTTCtCCGGGCCgGGG					
crRNA	CTACTCCGTTCCCCGGGCCANGG	ENA CM000881 CM000881.3	2776488	E2	NC_016132.3	
DNA	CctCTCCGgTCgCCGGGCCACGG					
crRNA	CTACTCCGTTCCCCGGGCCANGG	ENA CM000881 CM000881.3	53379929	F2	XM_003564549.4	PREDICTED: Brachypodium distachyon uncharacterized LOC100846283 (LOC100846283), mRNA
DNA	CTgCaCCGTgtCCCGGGCCATGG					
crRNA	GGTCCCTGCGGATGTCAGGNGG	ENA CM000881 CM000881.3	18233853	G2	XM_003566025.3	PREDICTED: Brachypodium distachyon scarecrow-like protein 32 (LOC100842640), mRNA
DNA	AGGTCgCgGCGGAgGTaAGGCGG					
crRNA	AGGTCCCTGCGGATGTCAGGNGG	ENA CM000881 CM000881.3	37042889	E3		
DNA	tGtTCCCTGCcGATGTaAGGGGG					
crRNA	AGGTCCCTGCGGATGTCAGGNGG	ENA CM000882 CM000882.3	12438188	F3		
DNA	AGGTCCaacCGGATGaCAGGTGG					
crRNA	GGTCCCTGCGGATGTCAGGNGG	ENA CM000882 CM000882.3	12519421	G3		
DNA	AGGTgCCgGCGGATGTCgtGGGG					

Legend: GL indicates the position where this Target is loaded on the Gel in Figure 8.

Table Supplement 3: Descriptive statistics for the growth analysis of *B. distachyon* wild-type Bd21 and the four genome edited mutants

			Statistic	Std. Error		Statistic	Std. Error
Week1	Wild-type	Mean	6,1684	0,08821	Week2	9,3526	0,20766
		Median	6,1000			9,5000	
		Variance	0,148			0,819	
		Std. Deviation	0,38449			0,90515	
	#2-9-4-9	Mean	5,2615	0,17994		8,1462	0,18626
		Median	5,5000			8,2000	
		Variance	0,421			0,451	
		Std. Deviation	0,64877			0,67158	
	#2-9-6-30	Mean	5,1385	0,23137		7,8462	0,25334
		Median	5,1000			8,2000	
		Variance	0,696			0,834	
		Std. Deviation	0,83420			0,91343	
	#16-12-6-14	Mean	4,8909	0,20111		7,5727	0,17689
		Median	5,0000			7,6000	
		Variance	0,445			0,344	
		Std. Deviation	0,66702			0,58667	
	#16-12-10-18	Mean	5,6444	0,31407		8,7556	0,13240
		Median	5,6000			8,9000	
		Variance	0,888			0,158	
		Std. Deviation	0,94222			0,39721	
Week3	Wild-type	Mean	13,5684	0,19691	Week4	18,7684	0,20874
		Median	13,5000			18,6000	
		Variance	0,737			0,828	
		Std. Deviation	0,85833			0,90986	
	#2-9-4-9	Mean	12,9231	0,35737		17,2692	0,27605
		Median	13,5000			17,3000	
		Variance	1,660			0,991	
		Std. Deviation	1,28851			0,99531	
	#2-9-6-30	Mean	12,8846	0,45133		17,0231	0,44291
		Median	13,5000			16,8000	
		Variance	2,648			2,550	
		Std. Deviation	1,62729			1,59695	
	#16-12-6-14	Mean	11,9818	0,30743		16,3455	0,42882
		Median	11,9000			16,5000	
		Variance	1,040			2,023	
		Std. Deviation	1,01963			1,42223	
	#16-12-10-18	Mean	13,5556	0,31185		18,3889	0,29176
		Median	13,2000			18,4000	
		Variance	0,875			0,766	
		Std. Deviation	0,93556			0,87528	

Week5	Wild-type	Mean	26,6632	0,51991	Week6	31,7842	0,89139
		Median	26,6000			32,3000	
		Variance	5,136			15,097	
		Std. Deviation	2,26623			3,88548	
	#2-9-4-9	Mean	23,0615	0,48826		31,3615	1,03121
		Median	22,6000			31,5000	
		Variance	3,099			13,824	
		Std. Deviation	1,76046			3,71810	
	#2-9-6-30	Mean	25,1154	0,72668		31,6077	1,22686
		Median	25,9000			34,1000	
		Variance	6,865			19,567	
		Std. Deviation	2,62007			4,42351	
Week7	#16-12-6-14	Mean	23,3091	0,60595	Week8	30,9636	1,07824
		Median	23,5000			30,0000	
		Variance	4,039			12,789	
		Std. Deviation	2,00970			3,57611	
	#16-12-10-18	Mean	24,1333	0,63004		33,0222	0,97948
		Median	24,0000			34,1000	
		Variance	3,573			8,634	
		Std. Deviation	1,89011			2,93844	
	Wild-type	Mean	31,8158	0,91009		32,0158	0,97003
		Median	32,1000			32,6000	
		Variance	15,737			17,878	
		Std. Deviation	3,96698			4,22825	
Week8	#2-9-4-9	Mean	33,1462	1,02567	Week9	33,3385	1,00291
		Median	31,5000			31,7000	
		Variance	13,676			13,076	
		Std. Deviation	3,69811			3,61606	
	#2-9-6-30	Mean	31,7308	1,27246		32,0000	1,26019
		Median	33,5000			34,5000	
		Variance	21,049			20,645	
		Std. Deviation	4,58792			4,54368	
	#16-12-6-14	Mean	32,8727	1,30364		32,9909	1,30930
		Median	34,2000			34,2000	
		Variance	18,694			18,857	
		Std. Deviation	4,32368			4,34245	
Week9	#16-12-10-18	Mean	37,0556	0,93082	Week10	37,4111	0,86562
		Median	36,0000			37,1000	
		Variance	7,798			6,744	
		Std. Deviation	2,79245			2,59685	

Table Supplement 4: Multiple Comparisons for the first two weeks of growth data

					95% Confidence Interval		
		Mean Difference (I-J)	Std. Error	Sig.	Lower Bound	Upper Bound	
Week1	Wild-type	#2-9-4-9	,90688*	0,23784	0,003	0,2153	1,5984
		#2-9-6-30	1,02996*	0,23784	0,001	0,3384	1,7215
		#16-12-6-14	1,27751*	0,25035	0,000	0,5496	2,0054
		#16-12-10-18	0,52227	0,23784	0,317	-0,1693	1,2138
	#2-9-4-9	Wild-type	-,90688*	0,23784	0,003	-1,5984	-0,2153
		#2-9-6-30	0,12308	0,25918	1,000	-0,6305	0,8767
		#16-12-6-14	0,37063	0,27070	1,000	-0,4165	1,1577
		#16-12-10-18	-0,38462	0,25918	1,000	-1,1382	0,3690
	#2-9-6-30	Wild-type	-1,02996*	0,23784	0,001	-1,7215	-0,3384
		#2-9-4-9	-0,12308	0,25918	1,000	-0,8767	0,6305
		#16-12-6-14	0,24755	0,27070	1,000	-0,5395	1,0346
		#16-12-10-18	-0,50769	0,25918	0,545	-1,2613	0,2459
	#16-12-6-14	Wild-type	-1,27751*	0,25035	0,000	-2,0054	-0,5496
		#2-9-4-9	-0,37063	0,27070	1,000	-1,1577	0,4165
		#2-9-6-30	-0,24755	0,27070	1,000	-1,0346	0,5395
		#16-12-10-18	-0,75524	0,27070	0,069	-1,5423	0,0319
	#16-12-10-18	Wild-type	-0,52227	0,23784	0,317	-1,2138	0,1693
		#2-9-4-9	0,38462	0,25918	1,000	-0,3690	1,1382
		#2-9-6-30	0,50769	0,25918	0,545	-0,2459	1,2613
		#16-12-6-14	0,75524	0,27070	0,069	-0,0319	1,5423
Week2	Wild-type	#2-9-4-9	1,20648*	0,27131	0,000	0,4176	1,9953
		#2-9-6-30	1,50648*	0,27131	0,000	0,7176	2,2953
		#16-12-6-14	1,77990*	0,28558	0,000	0,9495	2,6103
		#16-12-10-18	0,44494	0,27131	1,000	-0,3439	1,2338
	#2-9-4-9	Wild-type	-1,20648*	0,27131	0,000	-1,9953	-0,4176
		#2-9-6-30	0,30000	0,29565	1,000	-0,5596	1,1596
		#16-12-6-14	0,57343	0,30880	0,679	-0,3244	1,4713
		#16-12-10-18	-0,76154	0,29565	0,123	-1,6212	0,0981
	#2-9-6-30	Wild-type	-1,50648*	0,27131	0,000	-2,2953	-0,7176
		#2-9-4-9	-0,30000	0,29565	1,000	-1,1596	0,5596
		#16-12-6-14	0,27343	0,30880	1,000	-0,6244	1,1713
		#16-12-10-18	-1,06154*	0,29565	0,006	-1,9212	-0,2019
	#16-12-6-14	Wild-type	-1,77990*	0,28558	0,000	-2,6103	-0,9495
		#2-9-4-9	-0,57343	0,30880	0,679	-1,4713	0,3244
		#2-9-6-30	-0,27343	0,30880	1,000	-1,1713	0,6244
		#16-12-10-18	-1,33497*	0,30880	0,001	-2,2328	-0,4371
#16-12-10-18	Wild-type	-0,44494	0,27131	1,000	-1,2338	0,3439	

#2-9-4-9	0,76154	0,29565	0,123	-0,0981	1,6212
#2-9-6-30	1,06154*	0,29565	0,006	0,2019	1,9212
#16-12-6-14	1,33497*	0,30880	0,001	0,4371	2,2328

*. The mean difference is significant at the 0.05 level.

Table Supplement 5: Hypothesis Test Summary for the growth data of *B. distachyon* and the four genome edited mutants

Null Hypothesis	Test	Sig.	Decision
The distribution of Week3 is the same.	Independent-Samples Kruskal-Wallis Test	0,008	Reject the null hypothesis.
The distribution of Week4 is the same.	Independent-Samples Kruskal-Wallis Test	0,000	Reject the null hypothesis.
The distribution of Week5 is the same.	Independent-Samples Kruskal-Wallis Test	0,001	Reject the null hypothesis.
The distribution of Week6 is the same.	Independent-Samples Kruskal-Wallis Test	0,869	Retain the null hypothesis.
The distribution of Week7 is the same.	Independent-Samples Kruskal-Wallis Test	0,191	Retain the null hypothesis.
The distribution of Week8 is the same.	Independent-Samples Kruskal-Wallis Test	0,138	Retain the null hypothesis.

Asymptotic significances are displayed. The significance level is ,050.

Table Supplement 6: Pairwise Comparisons for the weeks 3 to 5

Pairwise Comparisons of Week 3

Sample 1-Sample 2	Test Statistic	Std. Error	Std. Test Statistic	Sig.	Adj. Sig. ^a
#2-9-4-9-Wild-type	-7,287	7,215	-1,010	0,312	1,000
#2-9-6-30-Wild-type	-5,172	7,215	-0,717	0,473	1,000
#16-12-6-14-Wild-type	-23,529	7,594	-3,098	0,002	0,029
Wild-type-#16-12-10-18	4,713	7,215	0,653	0,514	1,000

Pairwise Comparisons of Week 4

#2-9-4-9-Wild-type	-21,826	6,800	-3,210	0,001	0,020
#2-9-6-30-Wild-type	-23,480	6,800	-3,453	0,001	0,008
#16-12-6-14-Wild-type	-32,301	7,158	-4,513	0,000	0,000
#16-12-10-18-Wild-type	-4,933	7,645	-0,645	0,519	1,000

Pairwise Comparisons of Week 5

Sample 1-Sample 2	Test Statistic	Std. Error	Std. Test Statistic	Sig.	Adj. Sig. ^a
#2-9-4-9-Wild-type	-27,733	7,219	-3,842	0,000	0,002
#2-9-6-30-Wild-type	-9,348	7,219	-1,295	0,195	1,000
#16-12-6-14-Wild-type	-25,533	7,599	-3,360	0,001	0,012
#16-12-10-18-Wild-type	-13,387	7,219	-1,854	0,064	0,955

Each row tests the null hypothesis that the Sample 1 and Sample 2 distributions are the same.

Asymptotic significances (2-sided tests) are displayed. The significance level is ,05.

a. Significance values have been adjusted by the Bonferroni correction for multiple tests.

Table Supplement 7: Descriptive statistics of 7 dpi infections of *B. distachyon* spikelets

		Statistic	Std. Error
Wild-type	Mean	1,2273	0,19386
	Median	1,0000	
	Variance	0,827	
	Std. Deviation	0,90931	
#2-9-4-9	Mean	2,3039	0,17882
	Median	2,0000	
	Variance	1,631	
	Std. Deviation	1,27702	
#2-9-6-30	Mean	2,6111	0,30063
	Median	2,0000	
	Variance	4,067	
	Std. Deviation	2,01666	
#16-12-6-14	Mean	2,5556	0,22598
	Median	2,5000	
	Variance	2,298	
	Std. Deviation	1,51591	
#16-12-10-18	Mean	2,6477	0,29016
	Median	2,0000	
	Variance	3,704	
	Std. Deviation	1,92469	

Table Supplement 8: Test for normal distribution of 7 dpi Disease Score data

Null Hypothesis			
Hypothesis	Test	Sig.	Decision
The distribution of DiseaseScore is the same across.	Independent-Samples Kruskal-Wallis Test	0,001	Reject the null hypothesis.
Asymptotic significances are displayed. The significance level is ,050.			

Table Supplement 9: Pairwise Comparisons of 7 dpi Disease Score between the Wild-type and four genome edited lines of *B. distachyon*

Sample 1- Test	Statistic	Std. Error	Sample 2- Test	Sig.	Adj. Sig. ^a
Wild-type-#2-9-4-9	-53,069	15,159	-3,501	0,000	0,005
Wild-type-#2-9-6-30	-51,756	15,461	-3,348	0,001	0,008
Wild-type-#16-12-6-14	-59,811	15,461	-3,869	0,000	0,001
Wild-type-#16-12-10-18	-57,261	15,518	-3,690	0,000	0,002

Each row tests the null hypothesis that the Sample 1 and Sample 2 distributions are the same.

Asymptotic significances (2-sided tests) are displayed. The significance level is ,05.

a. Significance values have been adjusted by the Bonferroni correction for multiple tests.

Table Supplement 10: Descriptive statistics for the 14 dpi Disease Score of infected *B. distachyon* spikelets

	Statistic	Std. Error
Wild-type	Mean	2,2750
	Median	2,0000
	Variance	0,618
	Std. Deviation	0,78598
#2-9-4-9	Mean	3,6591
	Median	3,5000
	Variance	2,881
	Std. Deviation	1,69737
#2-9-6-30	Mean	3,6463
	Median	3,0000
	Variance	4,278
	Std. Deviation	2,06834
#16-12-6-14	Mean	3,9167
	Median	4,0000
	Variance	4,511
	Std. Deviation	2,12395
#16-12-10-18	Mean	3,7717
	Median	3,5000
	Variance	2,675
	Std. Deviation	1,63540

Table Supplement 11: Statistical analysis with Dunnett T3 Post-Hoc for Disease Score of *B. distachyon* spikelets 14dpi with *F. graminearum* 8/1

		Mean Difference			95% Confidence Interval	
		(I-J)	Std. Error	Sig.	Lower Bound	Upper Bound
WT	#2-9-4-9	-1,38409 ^b	,31043	,000	-2,2834	-,4848
	#2-9-6-30	-1,37134 ^b	,36774	,004	-2,4400	-,3027
	#16-12-6-14	-1,64167 ^b	,37188	,000	-2,7217	-,5616
	#16-12-10-18	-1,49674 ^b	,29838	,000	-2,3605	-,6330

b. The mean difference is significant at the 0.05 level.

Table Supplement 12: Descriptive statistics for the relative area of callose depositions in rachis of *B. distachyon* spikelets 3 dpi

		Statistic	Std. Error
Wild-type	Mean	0,525782006500	0,0624503533896
	Median	0,567233759500	
	Variance	0,039	
	Std. Deviation	0,1974853573936	
#2-9-4-9	Mean	0,124001345600	0,0510135115622
	Median	0,064215879000	
	Variance	0,026	
	Std. Deviation	0,1613188879798	
#2-9-6-30	Mean	0,094085015333	0,0426825337123
	Median	0,044431397000	
	Variance	0,016	
	Std. Deviation	0,1280476011369	
#16-12-6-14	Mean	0,069209021400	0,0374210398881
	Median	0,000000000000	
	Variance	0,014	
	Std. Deviation	0,1183357184585	
#16-12-10-18	Mean	0,037738801000	0,0254729268483
	Median	0,000000000000	
	Variance	0,006	
	Std. Deviation	0,0805524675114	

Table Supplement 13: Pairwise Comparisons of relative area of callose depositions in rachis are of spikelets 3dpi

Samples	Test	Std. Error	Std.	Test	Adj. Sig. ^a
	Statistic		Statistic	Sig.	
#2-9-4-9 - WT ^b	19,700	6,051	3,256	,001	,011
#2-9-6-30 - WT ^b	20,878	6,217	3,358	,001	,008
#16-12-6-14 - WT ^b	23,500	6,051	3,884	,000	,001
#16-12-10-18 - WT ^b	26,700	6,051	4,412	,000	,000

Each row tests the null hypothesis that the Sample 1 and Sample 2 distributions are the same.

Asymptotic significances (2-sided tests) are displayed. The significance level is ,05.

a. Significance values have been adjusted by the Bonferroni correction for multiple tests.

b. Wild-type inbred line Bd21

Table Supplement 14: Descriptive statistics for the leaf qPCR of the BdGSL gene family

		Statistic	Std. Error			Statistic	Std. Error
BdGSL1	Wild-type	Mean	0,014767	BdGSL2	Mean	0,020083	0,0027356
		Median	0,012450		Median	0,021950	
		Variance	0,000		Variance	0,000	
		Std.	0,0045898		Std.	0,0067009	
		Deviation			Deviation		
	#2-9-4-9	Mean	0,009283	Mean	0,017833	0,0021194	
		Median	0,007800	Median	0,016550		
		Variance	0,000	Variance	0,000		
		Std.	0,0040410	Std.	0,0051914		
		Deviation		Deviation			
	#2-9-6-30	Mean	0,020400	Mean	0,017317	0,0040270	
		Median	0,020300	Median	0,012200		
		Variance	0,000	Variance	0,000		
		Std.	0,0117329	Std.	0,0098642		
		Deviation		Deviation			
	#16-12-6-14	Mean	0,125000	Mean	0,074517	0,0127428	
		Median	0,130300	Median	0,056000		
		Variance	0,004	Variance	0,001		
		Std.	0,0661812	Std.	0,0312134		
		Deviation		Deviation			
	#16-12-10-18	Mean	0,142317	Mean	0,083233	0,0356123	
		Median	0,170850	Median	0,035250		
		Variance	0,006	Variance	0,008		

		Std. Deviation	0,0773196		Std. Deviation	0,0872318	
BdGSL3	Wild-type	Mean	0,021167	0,0009010	Mean	0,002883	0,0003146
		Median	0,020000		Median	0,002750	
		Variance	0,000		Variance	0,000	
		Std. Deviation	0,0022070		Std. Deviation	0,0007705	
		Mean	0,005000	0,0004946	Mean	0,003700	0,0002160
	#2-9-4-9	Median	0,005400		Median	0,003750	
		Variance	0,000		Variance	0,000	
		Std. Deviation	0,0012116		Std. Deviation	0,0005292	
		Mean	0,020817	0,0061695	Mean	0,002883	0,0001662
		Median	0,017700		Median	0,002950	
	#2-9-6-30	Variance	0,000		Variance	0,000	
		Std. Deviation	0,0151120		Std. Deviation	0,0004070	
		Mean	0,017917	0,0056476	Mean	0,006567	0,0010433
		Median	0,013500		Median	0,005650	
		Variance	0,000		Variance	0,000	
	#16-12-6-14	Std. Deviation	0,0138336		Std. Deviation	0,0025555	
		Mean	0,073250	0,0162047	Mean	0,008667	0,0004447
		Median	0,092150		Median	0,008600	
		Variance	0,002		Variance	0,000	
		Std. Deviation	0,0396933		Std. Deviation	0,0010893	
Wild-type	Mean	0,000133	0,0000333	Mean	0,058033	0,0026919	
	Median	0,000100		Median	0,056200		
	Variance	0,000		Variance	0,000		
	Std. Deviation	0,0000816		Std. Deviation	0,0065938		
	Mean	0,000117	0,0000167	Mean	0,031783	0,0046394	
#2-9-4-9	Median	0,000100		Median	0,029350		
	Variance	0,000		Variance	0,000		
	Std. Deviation	0,0000408		Std. Deviation	0,0113641		
	Mean	0,000117	0,0000167	Mean	0,060983	0,0166284	
	Median	0,000100		Median	0,050350		
#2-9-6-30	Variance	0,000		Variance	0,002		
	Std. Deviation	0,0000408		Std. Deviation	0,0407312		
	Mean	0,002583	0,0006467	Mean	0,174683	0,0264544	
	Median	0,002450		Median	0,135850		

BdGSL7	#16-12-10-18	Variance	0,000		BdGSL8	Variance	0,004	
		Std.	0,0015842			Std.	0,0647997	
		Deviation				Deviation		
		Mean	0,002450	0,0007945		Mean	0,264083	0,0528216
		Median	0,001550			Median	0,257800	
		Variance	0,000			Variance	0,017	
	Wild-type	Std.	0,0019460			Std.	0,1293860	
		Deviation				Deviation		
		Mean	0,000133	0,0000211		Mean	0,063017	0,0035526
		Median	0,000100			Median	0,064500	
		Variance	0,000			Variance	0,000	
		Std.	0,0000516			Std.	0,0087020	
	#2-9-4-9	Deviation				Deviation		
		Mean	0,000100	0,0000258		Mean	0,050833	0,0034051
		Median	0,000100			Median	0,051500	
		Variance	0,000			Variance	0,000	
		Std.	0,0000632			Std.	0,0083407	
		Deviation				Deviation		
#2-9-6-30	Mean	0,000133	0,0000494	Mean	0,058233	0,0086779		
	Median	0,000150		Median	0,062100			
	Variance	0,000		Variance	0,000			
	Std.	0,0001211		Std.	0,0212565			
	Deviation			Deviation				
	Mean	0,000517	0,0001797	Mean	0,204950	0,0259678		
#16-12-6-14	Median	0,000400		Median	0,206750			
	Variance	0,000		Variance	0,004			
	Std.	0,0004401		Std.	0,0636078			
	Deviation			Deviation				
	Mean	0,001050	0,0003314	Mean	0,232850	0,0319067		
	Median	0,001050		Median	0,259900			
#16-12-10-18	Variance	0,000		Variance	0,006			
	Std.	0,0008118		Std.	0,0781550			
	Deviation			Deviation				
	Mean	0,012233	0,0004897	Mean	0,0540	0,00451		
	Median	0,012450		Median	0,0523			
	Variance	0,000		Variance	0,000			
BdGSL9	Wild-type	Std.	0,0011994		BdGSL10	Std.	0,01104	
		Deviation				Deviation		
		Mean	0,014850	0,0006163		Mean	0,0248	0,00370
		Median	0,015000			Median	0,0231	
		Variance	0,000			Variance	0,000	
		Std.	0,0015096			Std.	0,00907	
	#2-9-4-9	Deviation				Deviation		
		Mean	0,018667	0,0070381		Mean	0,0437	0,00840
		Median				Median		
		Variance				Variance		

	Median	0,012250		Median	0,0432
	Variance	0,000		Variance	0,000
	Std.			Std.	
	Deviation	0,0172397		Deviation	0,02058
	Mean	0,023467	0,0033314	Mean	0,1657 0,03522
#16-12-6-14	Median	0,019000		Median	0,1188
	Variance	0,000		Variance	0,007
	Std.			Std.	
	Deviation	0,0081603		Deviation	0,08626
	Mean	0,043600	0,0026715	Mean	0,1878 0,03695
#16-12-10-18	Median	0,042850		Median	0,2374
	Variance	0,000		Variance	0,008
	Std.			Std.	
	Deviation	0,0065437		Deviation	0,09050
	Mean	0,0071	0,00028		
Wild-type	Median	0,0072			
	Variance	0,000			
	Std.				
	Deviation	0,00069			
	Mean	0,0061	0,00047		
#2-9-4-9	Median	0,0065			
	Variance	0,000			
	Std.				
	Deviation	0,00114			
	Mean	0,0127	0,00272		
BdGSL11 #2-9-6-30	Median	0,0098			
	Variance	0,000			
	Std.				
	Deviation	0,00666			
	Mean	0,0730	0,01360		
#16-12-6-14	Median	0,0639			
	Variance	0,001			
	Std.				
	Deviation	0,03331			
	Mean	0,1282	0,01955		
#16-12-10-18	Median	0,1179			
	Variance	0,002			
	Std.				
	Deviation	0,048			

Table Supplement 15: Hypothesis Test Summary of leaf qPCR

	Null Hypothesis	Test	Sig.	Decision
1	The distribution of BdGSL1 is the same.	Independent-Samples Kruskal-Wallis Test	0,006	Reject the null hypothesis.
2	The distribution of BdGSL2 is the same.	Independent-Samples Kruskal-Wallis Test	0,030	Reject the null hypothesis.
3	The distribution of BdGSL3 is the same.	Independent-Samples Kruskal-Wallis Test	0,000	Reject the null hypothesis.
4	The distribution of BdGSL4 is the same.	Independent-Samples Kruskal-Wallis Test	0,004	Reject the null hypothesis.
5	The distribution of BdGSL5 is the same.	Independent-Samples Kruskal-Wallis Test	0,001	Reject the null hypothesis.
6	The distribution of BdGSL6 is the same.	Independent-Samples Kruskal-Wallis Test	0,002	Reject the null hypothesis.
7	The distribution of BdGSL7 is the same.	Independent-Samples Kruskal-Wallis Test	0,001	Reject the null hypothesis.
8	The distribution of BdGSL8 is the same.	Independent-Samples Kruskal-Wallis Test	0,003	Reject the null hypothesis.
9	The distribution of BdGSL9 is the same.	Independent-Samples Kruskal-Wallis Test	0,001	Reject the null hypothesis.
10	The distribution of BdGSL10 is the same.	Independent-Samples Kruskal-Wallis Test	0,002	Reject the null hypothesis.

11 The Independent- 0,001 Reject the null
 distribution of Samples hypothesis.
 BdGSL11 is Kruskal-
 the same. Wallis Test

Asymptotic significances are displayed. The significance level is ,050.

Table Supplement 16: Pairwise comparisons of leaf qPCR analysis

Pairwise Comparisons of BdGSL1						Pairwise Comparisons of BdGSL2					
Sample 1- Sample 2	Test Statistic	Std. Error	Std. Test Statistic	Test Sig.	Adj. Sig. ^a	Test Statistic	Std. Error	Std. Test Statistic	Test Sig.	Adj. Sig. ^a	
#2-9-4-9- Wild-type	5,833	7,083	0,824	0,410	1,000	2,500	7,082	0,353	0,724	1,000	
Wild-type- #2-9-6-30	-2,917	7,083	-0,412	0,680	1,000	4,667	7,082	0,659	0,510	1,000	
Wild-type- #16-12-6- 14	-12,333	6,134	-2,011	0,044	0,444	-12,083	6,133	-1,970	0,049	0,488	
Wild-type- #16-12- 10-18	-13,042	6,134	-2,126	0,033	0,335	-5,500	6,133	-0,897	0,370	1,000	
Pairwise Comparisons of BdGSL3						Pairwise Comparisons of BdGSL4					
Sample 1- Sample 2	Test Statistic	Std. Error	Std. Test Statistic	Test Sig.	Adj. Sig. ^a	Test Statistic	Std. Error	Std. Test Statistic	Test Sig.	Adj. Sig. ^a	
#2-9-4-9- Wild-type	17,333	7,082	2,448	0,014	0,144	-10,000	7,076	-1,413	0,158	1,000	
#2-9-6-30- Wild-type	3,250	7,082	0,459	0,646	1,000	0,000	7,076	0,000	1,000	1,000	
#16-12-6- 14-Wild- type	11,708	6,133	1,909	0,056	0,563	-12,625	6,128	-2,060	0,039	0,394	
Wild-type- #16-12- 10-18	-6,833	6,133	-1,114	0,265	1,000	-19,417	6,128	-3,169	0,002	0,015	
Pairwise Comparisons of BdGSL5						Pairwise Comparisons of BdGSL6					
Sample 1- Sample 2	Test Statistic	Std. Error	Std. Test Statistic	Test Sig.	Adj. Sig. ^a	Test Statistic	Std. Error	Std. Test Statistic	Test Sig.	Adj. Sig. ^a	
#2-9-4-9- Wild-type	0,500	6,791	0,074	0,941	1,000	12,583	7,082	1,777	0,076	0,756	
#2-9-6-30- Wild-type	0,500	6,791	0,074	0,941	1,000	4,000	7,082	0,565	0,572	1,000	
Wild-type- #16-12-6- 14	-16,625	5,881	-2,827	0,005	0,047	-6,417	6,133	-1,046	0,295	1,000	

Wild-type- #16-12- 10-18	-13,917	5,881	-2,366	0,018	0,180	-10,333	6,133	-1,685	0,092	0,920
--------------------------------	---------	-------	--------	-------	-------	---------	-------	--------	-------	-------

Pairwise Comparisons of BdGSL7						Pairwise Comparisons of BdGSL8				
Sample 1- Sample 2	Test Statistic	Std. Error	Std. Test Statistic	Test Sig.	Adj. Sig. ^a	Test Statistic	Std. Error	Std. Test Statistic	Test Sig.	Adj. Sig. ^a
#2-9-4-9- Wild-type	3,083	6,959	0,443	0,658	1,000	6,833	7,082	0,965	0,335	1,000
Wild-type- #2-9-6-30	-0,167	6,959	-0,024	0,981	1,000	2,833	7,082	0,400	0,689	1,000
Wild-type- #16-12-6- 14	-10,083	6,027	-1,673	0,094	0,943	-9,833	6,133	-1,603	0,109	1,000
Wild-type- #16-12- 10-18	-17,625	6,027	-2,925	0,003	0,034	-13,083	6,133	-2,133	0,033	0,329

Pairwise Comparisons of BdGSL9						Pairwise Comparisons of BdGSL10					
Sample 1- Sample 2	Test Statistic	Std. Error	Std. Test Statistic	Sig.	Adj. Sig. ^a	Test Statistic	Std. Error	Std. Test Statistic	Sig.	Adj. Sig. ^a	
Wild-type- #2-9-4-9	-6,167	7,082	-0,871	0,384	1,000	13,500	7,082	1,906	0,057	0,566	
Wild-type- #2-9-6-30	-5,167	7,082	-0,730	0,466	1,000	4,583	7,082	0,647	0,518	1,000	
Wild-type- #16-12-6- 14	-9,042	6,133	-1,474	0,140	1,000	-7,833	6,133	-1,277	0,202	1,000	
Wild-type- #16-12- 10-18	-23,208	6,133	-3,784	0,000	0,002	-7,625	6,133	-1,243	0,214	1,000	

Pairwise Comparisons of BdGSL11

Sample 1- Sample 2	Test Statistic	Std. Error	Std. Test Statistic	Test Sig.	Adj. Sig. ^a
#2-9-4-9- Wild-type	5,000	7,082	0,706	0,480	1,000
Wild-type- #2-9-6-30	-7,167	7,082	-1,012	0,312	1,000
Wild-type- #16-12-6- 14	-10,833	6,133	-1,766	0,077	0,773
Wild-type- #16-12- 10-18	-19,000	6,133	-3,098	0,002	0,019

Each row tests the null hypothesis that the Sample 1 and Sample 2 distributions are the same.

Asymptotic significances (2-sided tests) are displayed. The significance level is ,05.

a. Significance values have been adjusted by the Bonferroni correction for multiple tests.

Table Supplement 17: Descriptive statistics for the stem tissue qPCR analysis

		Statistic		Std. Error			Statistic	Std. Error
BdGSL1	Wild-type	Mean	0,126	0,023	BdGSL2	Mean	0,052	0,009
		Median	0,142			Median	0,064	
		Variance	0,003			Variance	0,000	
		Std.	0,056			Std.	0,021	
		Deviation				Deviation		
	#2-9-4-9	Mean	0,172	0,076		Mean	0,101	0,053
		Median	0,110			Median	0,026	
		Variance	0,035			Variance	0,017	
		Std.	0,186			Std.	0,131	
		Deviation				Deviation		
	#2-9-6-30	Mean	0,306	0,087		Mean	0,054	0,011
		Median	0,424			Median	0,060	
		Variance	0,045			Variance	0,001	
		Std.	0,212			Std.	0,027	
		Deviation				Deviation		
	#16-12-6-14	Mean	0,335	0,053		Mean	0,121	0,021
		Median	0,380			Median	0,110	
		Variance	0,017			Variance	0,003	
		Std.	0,129			Std.	0,051	
		Deviation				Deviation		
	#16-12-10-18	Mean	0,248	0,065		Mean	0,070	0,014
		Median	0,203			Median	0,063	
		Variance	0,025			Variance	0,001	
		Std.	0,159			Std.	0,034	
		Deviation				Deviation		
BdGSL3	Wild-type	Mean	0,084	0,012	BdGSL4	Mean	0,015	0,003
		Median	0,090			Median	0,019	
		Variance	0,001			Variance	0,000	
		Std.	0,029			Std.	0,007	
		Deviation				Deviation		
	#2-9-4-9	Mean	0,122	0,041		Mean	0,068	0,033
		Median	0,117			Median	0,020	
		Variance	0,010			Variance	0,006	
		Std.	0,100			Std.	0,080	
		Deviation				Deviation		

	#2-9-6-30	Mean	0,123	0,033		Mean	0,029	0,006
		Median	0,167			Median	0,034	
		Variance	0,006			Variance	0,000	
	#16-12-6-14	Std.	0,080			Std.	0,016	
		Deviation				Deviation		
		Mean	0,086	0,021		Mean	0,031	0,007
	#16-12-10-18	Median	0,076			Median	0,022	
		Variance	0,003			Variance	0,000	
		Std.	0,050			Std.	0,018	
BdGSL5	Wild-type	Deviation			BdGSL6	Deviation		
		Mean	0,001	0,000		Mean	0,155	0,018
		Median	0,001			Median	0,169	
		Variance	0,000			Variance	0,002	
		Std.	0,000			Std.	0,044	
		Deviation				Deviation		
	#2-9-4-9	Mean	0,000	0,000		Mean	0,087	0,032
		Median	0,000			Median	0,056	
		Variance	0,000			Variance	0,006	
		Std.	0,000			Std.	0,078	
		Deviation				Deviation		
	#2-9-6-30	Mean	0,003	0,001		Mean	0,288	0,081
		Median	0,003			Median	0,394	
		Variance	0,000			Variance	0,039	
		Std.	0,002			Std.	0,199	
		Deviation				Deviation		
	#16-12-6-14	Mean	0,005	0,001		Mean	0,392	0,052
		Median	0,004			Median	0,456	
		Variance	0,000			Variance	0,016	
		Std.	0,002			Std.	0,126	
		Deviation				Deviation		
	#16-12-10-18	Mean	0,004	0,001		Mean	0,243	0,072
		Median	0,004			Median	0,212	
		Variance	0,000			Variance	0,031	
		Std.	0,002			Std.	0,175	
		Deviation				Deviation		
BdGSL7	Wild-type	Mean	0,020	0,007	BdGSL8	Mean	0,143	0,021
		Median	0,016			Median	0,134	
		Variance	0,000			Variance	0,003	

		Std. Deviation	0,017		Std. Deviation	0,052	
	#2-9-4-9	Mean	0,003	0,001	Mean	0,116 0,016	
		Median	0,002		Median	0,116	
		Variance	0,000		Variance	0,002	
		Std. Deviation	0,002		Std. Deviation	0,040	
		#2-9-6-30	Mean	0,014	0,004	Mean	0,249 0,060
	Median		0,015		Median	0,329	
	Variance		0,000		Variance	0,022	
	Std. Deviation		0,009		Std. Deviation	0,147	
	#16-12-6-14		Mean	0,068	0,010	Mean	0,464 0,013
		Median	0,079		Median	0,454	
		Variance	0,001		Variance	0,001	
		Std. Deviation	0,024		Std. Deviation	0,031	
		#16-12-10-18	Mean	0,054	0,015	Mean	0,283 0,049
	Median		0,069		Median	0,313	
Variance	0,001			Variance	0,015		
Std. Deviation	0,037			Std. Deviation	0,121		
BdGSL9	Wild-type		Mean	0,066	0,017	BdGSL10	Mean
		Median	0,058		Median		0,171
		Variance	0,002		Variance		0,003
		Std. Deviation	0,042		Std. Deviation		0,058
		#2-9-4-9	Mean	0,529	0,334		Mean
	Median		0,061		Median		0,046
	Variance		0,669		Variance		0,007
	Std. Deviation		0,818		Std. Deviation		0,083
	#2-9-6-30		Mean	0,064	0,014		Mean
		Median	0,082		Median		0,403
		Variance	0,001		Variance		0,048
		Std. Deviation	0,033		Std. Deviation		0,219
		#16-12-6-14	Mean	0,067	0,007		Mean
	Median		0,069		Median		0,263
	Variance		0,000		Variance		0,030
Std. Deviation	0,018			Std. Deviation	0,175		
#16-12-10-18	Mean		0,052	0,006	Mean	0,238 0,078	
	Median	0,048		Median	0,205		

		Variance	0,000		Variance	0,036
		Std.	0,014		Std.	0,191
		Deviation			Deviation	
	BdGSL11	Wild-type	Mean	0,111	0,027	
			Median	0,124		
			Variance	0,004		
			Std.			
			Deviation	0,065		
		#2-9-4-9	Mean	0,187	0,080	
			Median	0,119		
			Variance	0,039		
			Std.			
			Deviation	0,196		
		#2-9-6-30	Mean	0,470	0,161	
			Median	0,462		
			Variance	0,156		
			Std.			
			Deviation	0,394		
		#16-12-6-14	Mean	0,234	0,024	
			Median	0,221		
			Variance	0,003		
			Std.			
			Deviation	0,058		
		#16-12-10-18	Mean	0,312	0,062	
			Median	0,257		
			Variance	0,023		
			Std.			
			Deviation	0,153		

Table Supplement 18: Test for normal distribution of Stem qPCR

	Null Hypothesis	Test	Sig.	Decision
1	The distribution of BdGSL1 is the same.	Independent-Samples Wallis Test	Kruskal- 0,240	Retain the null hypothesis.
2	The distribution of BdGSL2 is the same.	Independent-Samples Wallis Test	Kruskal- 0,103	Retain the null hypothesis.
3	The distribution of BdGSL3 is the same.	Independent-Samples Wallis Test	Kruskal- 0,970	Retain the null hypothesis.
4	The distribution of BdGSL4 is the same.	Independent-Samples Wallis Test	Kruskal- 0,386	Retain the null hypothesis.

5	The distribution of BdGSL5 is the same.	Independent-Samples Wallis Test	Kruskal-	0,002	Reject the null hypothesis.
6	The distribution of BdGSL6 is the same.	Independent-Samples Wallis Test	Kruskal-	0,010	Reject the null hypothesis.
7	The distribution of BdGSL7 is the same.	Independent-Samples Wallis Test	Kruskal-	0,001	Reject the null hypothesis.
8	The distribution of BdGSL8 is the same.	Independent-Samples Wallis Test	Kruskal-	0,001	Reject the null hypothesis.
9	The distribution of BdGSL9 is the same.	Independent-Samples Wallis Test	Kruskal-	0,871	Retain the null hypothesis.
10	The distribution of BdGSL10 is the same	Independent-Samples Wallis Test	Kruskal-	0,090	Retain the null hypothesis.
11	The distribution of BdGSL11 is the same.	Independent-Samples Wallis Test	Kruskal-	0,096	Retain the null hypothesis.

Asymptotic significances are displayed. The significance level is ,050.

Table Supplement 19: Pairwise comparison for the stem qPCR

Pairwise Comparisons of BdGSL5						Pairwise Comparisons of BdGSL6					
Sample 1- Sample 2	Test Statistic	Std. Error	Std. Test Statistic	Sig.	Adj. Sig. ^a	Sample 1- Sample 2	Test Statistic	Std. Error	Std. Test Statistic	Sig.	Adj. Sig. ^a
#2-9-4-9- Wild-type	6,250	5,079	1,231	0,218	1,000	#2-9-4-9- Wild-type	5,000	5,082	0,984	0,325	1,000
Wild-type- #2-9-6-30	-4,750	5,079	-0,935	0,350	1,000	Wild-type- #2-9-6-30	-4,083	5,082	-0,803	0,422	1,000
Wild-type- #16-12-10-18	-9,583	5,079	-1,887	0,059	0,592	Wild-type- #16-12-6-14	-12,750	5,082	-2,509	0,012	0,121
Wild-type- #16-12-6-14	-11,917	5,079	-2,346	0,019	0,190	Wild-type- #16-12-10-18	-4,833	5,082	-0,951	0,342	1,000
Pairwise Comparisons of BdGSL7						Pairwise Comparisons of BdGSL8					
Sample 1- Sample 2	Test Statistic	Std. Error	Std. Test Statistic	Sig.	Adj. Sig. ^a	Sample 1- Sample 2	Test Statistic	Std. Error	Std. Test Statistic	Sig.	Adj. Sig. ^a
#2-9-4-9- Wild-type	9,500	5,081	1,870	0,062	0,615	#2-9-4-9- Wild-type	2,250	5,082	0,443	0,658	1,000
#2-9-6-30- Wild-type	1,667	5,081	0,328	0,743	1,000	Wild-type- #2-9-6-30	-3,500	5,082	-0,689	0,491	1,000
Wild-type- #16-12-6-14	-10,000	5,081	-1,968	0,049	0,491	Wild-type- #16-12-6-14	-17,000	5,082	-3,345	0,001	0,008
Wild-type- #16-12-10-18	-7,000	5,081	-1,378	0,168	1,000	Wild-type- #16-12-10-18	-6,750	5,082	-1,328	0,184	1,000

Each row tests the null hypothesis that the Sample 1 and Sample 2 distributions are the same.

Asymptotic significances (2-sided tests) are displayed. The significance level is ,05.

a. Significance values have been adjusted by the Bonferroni correction for multiple tests.

Table Supplement 20: Descriptive statistic of spikelet qPCR for *B. distachyon* wild-type and the four genome edited lines for the spikelet qPCR

			Statistic	Std. Error				Statistic	Std. Error
BdGSL1	Wild-type	Mean	0,932600	0,2488296	BdGSL2	Mean	0,372950	0,0639322	
		Median	0,729850			Median	0,397800		
		Variance	0,371			Variance	0,025		
		Std.	0,6095055			Std.	0,1566013		
		Deviation				Deviation			
	#2-9-4-9	Mean	0,288717	0,0520556		Mean	0,164050	0,0255298	
		Median	0,223850			Median	0,176500		
		Variance	0,016			Variance	0,004		
		Std.	0,1275096			Std.	0,0625350		
		Deviation				Deviation			
	#2-9-6-30	Mean	0,457267	0,0214077		Mean	0,176950	0,0183756	
		Median	0,445950			Median	0,157700		
		Variance	0,003			Variance	0,002		
		Std.	0,0524380			Std.	0,0450108		
		Deviation				Deviation			
	#16-12-6-14	Mean	0,534433	0,0531509		Mean	0,271017	0,0192077	
		Median	0,582900			Median	0,257950		
		Variance	0,017			Variance	0,002		
		Std.	0,1301926			Std.	0,0470491		
		Deviation				Deviation			
	#16-12-10-18	Mean	0,505867	0,0469151		Mean	0,285450	0,0142802	
		Median	0,521250			Median	0,296350		
		Variance	0,013			Variance	0,001		
		Std.	0,1149180			Std.	0,0349792		
		Deviation				Deviation			
BdGSL3	Wild-type	Mean	0,263867	0,0323263	BdGSL4	Mean	0,026700	0,0042282	
		Median	0,259250			Median	0,030050		
		Variance	0,006			Variance	0,000		
		Std.	0,0791829			Std.	0,0103570		
		Deviation				Deviation			
	#2-9-4-9	Mean	0,148083	0,0068786		Mean	0,020067	0,0024467	
		Median	0,148700			Median	0,021950		
		Variance	0,000			Variance	0,000		
		Std.	0,0168490			Std.	0,0059932		
		Deviation				Deviation			
	#2-9-6-30	Mean	0,256117	0,0433660		Mean	0,015600	0,0021038	
		Median	0,202250			Median	0,013750		

		Variance	0,011		Variance	0,000			
		Std.	0,1062245		Std.	0,0051533			
		Deviation			Deviation				
		Mean	0,109633		0,0109547	Mean		0,031683	0,0024300
		Median	0,106650		Median	0,031200			
	#16-12-6-14	Variance	0,001	Variance	0,000				
		Std.	0,0268334	Std.	0,0059523				
		Deviation		Deviation					
		Mean	0,183850	0,0197813	Mean		0,028317	0,0007503	
		Median	0,195050	Median	0,027700				
	#16-12-10-18	Variance	0,002	Variance	0,000				
		Std.	0,0484542	Std.	0,0018378				
Deviation			Deviation						
Mean		0,059867	0,0168102	Mean	0,375833		0,0411599		
Median		0,046250	Median	0,399300					
BdGSL5	Wild-type	Variance	0,002	Variance	0,010				
		Std.	0,0411765	Std.	0,1008208				
		Deviation		Deviation					
		Mean	0,013033	0,0033567	Mean		0,241517	0,0152637	
		Median	0,008600	Median	0,221450				
	#2-9-4-9	Variance	0,000	Variance	0,001				
		Std.	0,0082221	Std.	0,0373883				
		Deviation		Deviation					
		Mean	0,020767	0,0020342	Mean		0,366117	0,0494557	
		Median	0,021200	Median	0,319800				
	#2-9-6-30	Variance	0,000	Variance	0,015				
		Std.	0,0049826	Std.	0,1211413				
Deviation			Deviation						
Mean		0,030150	0,0040200	Mean	0,483900		0,0434145		
Median		0,033500	Median	0,477050					
#16-12-6-14	Variance	0,000	Variance	0,011					
	Std.	0,0098470	Std.	0,1063434					
	Deviation		Deviation						
	Mean	0,046883	0,0015696	Mean		0,307717	0,0088057		
	Median	0,046050	Median	0,318600					
BdGSL7	Wild-type	Variance	0,000	Variance	0,000				
		Std.	0,0038447	Std.	0,0215695				
		Deviation		Deviation					
		Mean	0,347500	0,0489337	Mean		0,589850	0,0737381	
		Median	0,368700	Median	0,687800				
	#2-9-4-9	Variance	0,014	Variance	0,033				
		Std.	0,1198626	Std.	0,1806206				
		Deviation		Deviation					
		Mean	0,129483	0,0489661	Mean		0,394917	0,0220394	
		Median		Median					

		Median	0,095100		Median	0,393050		
		Variance	0,014		Variance	0,003		
		Std.	0,1199418		Std.	0,0539852		
		Deviation			Deviation			
	#2-9-6-30	Mean	0,159017	0,0336980	Mean	0,486567	0,0189256	
		Median	0,116850		Median	0,491950		
		Variance	0,007		Variance	0,002		
		Std.	0,0825428		Std.	0,0463580		
		Deviation			Deviation			
	#16-12-6-14	Mean	0,346633	0,0603955	Mean	0,687783	0,0360047	
		Median	0,410800		Median	0,671650		
		Variance	0,022		Variance	0,008		
		Std.	0,1479380		Std.	0,0881932		
		Deviation			Deviation			
	#16-12-10-18	Mean	0,450300	0,0298693	Mean	0,616317	0,0321948	
		Median	0,493100		Median	0,624250		
Variance		0,005		Variance	0,006			
Std.		0,0731646		Std.	0,0788609			
Deviation				Deviation				
BdGSL9	Wild-type	Mean	0,090900	0,0220441	BdGSL10	Mean	0,3753	0,05104
		Median	0,087600			Median	0,3653	
		Variance	0,003			Variance	0,016	
		Std.	0,0539969			Std.	0,12501	
		Deviation				Deviation		
	#2-9-4-9	Mean	0,048633	0,0041631		Mean	0,1830	0,04308
		Median	0,050600			Median	0,1266	
		Variance	0,000			Variance	0,011	
		Std.	0,0101974			Std.	0,10554	
		Deviation				Deviation		
	#2-9-6-30	Mean	0,044317	0,0044770		Mean	0,2402	0,02731
		Median	0,046600			Median	0,2458	
		Variance	0,000			Variance	0,004	
		Std.	0,0109664			Std.	0,06689	
		Deviation				Deviation		
	#16-12-6-14	Mean	0,078717	0,0039376		Mean	0,3655	0,04911
		Median	0,078650			Median	0,3904	
		Variance	0,000			Variance	0,014	
		Std.	0,0096452			Std.	0,12029	
		Deviation				Deviation		
#16-12-10-18	Mean	0,072617	0,0056555	Mean	0,2973	0,01821		
	Median	0,072050		Median	0,2943			
	Variance	0,000		Variance	0,002			
	Std.	0,0138531		Std.	0,04462			
	Deviation			Deviation				

BdGSL11	Wild-type	Mean	0,2700	0,04085
		Median	0,2280	
		Variance	0,010	
		Std. Deviation	0,10007	
	#2-9-4-9	Mean	0,1519	0,01844
		Median	0,1604	
		Variance	0,002	
		Std. Deviation	0,04516	
	#2-9-6-30	Mean	0,2041	0,01029
		Median	0,1992	
		Variance	0,001	
		Std. Deviation	0,02521	
	#16-12-6-14	Mean	0,2173	0,01026
		Median	0,2089	
		Variance	0,001	
		Std. Deviation	0,02513	
	#16-12-10-18	Mean	0,1609	0,00959
		Median	0,1606	
		Variance	0,001	
		Std. Deviation	0,02350	

Table Supplement 21: Test for normal distribution of spikelet qPCR

	Null Hypothesis	Test	Sig.	Decision
1	The distribution of BdGSL1 is the same.	Independent-Samples Kruskal-Wallis Test	0,039	Reject the null hypothesis.
2	The distribution of BdGSL2 is the same.	Independent-Samples Kruskal-Wallis Test	0,004	Reject the null hypothesis.
3	The distribution of BdGSL3 is the same.	Independent-Samples Kruskal-Wallis Test	0,001	Reject the null hypothesis.
4	The distribution of BdGSL4 is the same.	Independent-Samples Kruskal-Wallis Test	0,004	Reject the null hypothesis.
5	The distribution of BdGSL5 is the same.	Independent-Samples Kruskal-Wallis Test	0,001	Reject the null hypothesis.
6	The distribution of BdGSL6 is the same.	Independent-Samples Kruskal-Wallis Test	0,005	Reject the null hypothesis.
7	The distribution of BdGSL7 is the same.	Independent-Samples Kruskal-Wallis Test	0,002	Reject the null hypothesis.
8	The distribution of BdGSL8 is the same.	Independent-Samples Kruskal-Wallis Test	0,004	Reject the null hypothesis.
9	The distribution of BdGSL9 is the same.	Independent-Samples Kruskal-Wallis Test	0,011	Reject the null hypothesis.
10	The distribution of BdGSL10 is the same.	Independent-Samples Kruskal-Wallis Test	0,052	Retain the null hypothesis.

11 The Independent-
distribution of Samples
BdGSL11 is Kruskal-
the same. Wallis Test
0,005
Reject the null
hypothesis.

Asymptotic significances are displayed. The significance level is ,050.

Table Supplement 22: Pairwise comparisons of spikelet qPCR data

Pairwise Comparisons of BdGSL1							Pairwise Comparisons of BdGSL2						
Sample 1- Sample 2	Test Statistic	Std. Error	Std. Statistic	Test Statistic	Sig.	Adj. Sig. ^a	Sample 1- Sample 2	Test Statistic	Std. Error	Std. Statistic	Test Statistic	Sig.	Adj. Sig. ^a
#2-9-4-9- Wild-type	15,25	5,081	3,001		0,003	0,027	#2-9-4-9- Wild-type	14,167	5,082	2,788		0,005	0,053
#2-9-6-30- Wild-type	7,25	5,081	1,427		0,154	1	#2-9-6-30- Wild-type	13,833	5,082	2,722		0,006	0,065
#16-12-6- 14-Wild- type	3,417	5,081	0,672		0,501	1	#16-12-6- 14-Wild- type	2,917	5,082	0,574		0,566	1
#16-12-10- 18-Wild- type	5,333	5,081	1,05		0,294	1	#16-12-10- 18-Wild- type	0,75	5,082	0,148		0,883	1
Pairwise Comparisons of BdGSL3							Pairwise Comparisons of BdGSL4						
Sample 1- Sample 2	Test Statistic	Std. Error	Std. Statistic	Test Statistic	Sig.	Adj. Sig. ^a	Sample 1- Sample 2	Test Statistic	Std. Error	Std. Statistic	Test Statistic	Sig.	Adj. Sig. ^a
#2-9-4-9- Wild-type	12,917	5,081	2,542		0,011	0,11	#2-9-4-9- Wild-type	9,5	5,08	1,87		0,061	0,615
#2-9-6-30- Wild-type	1,583	5,081	0,312		0,755	1	#2-9-6-30- Wild-type	11,583	5,08	2,28		0,023	0,226
#16-12-6- 14-Wild- type	18,75	5,081	3,69		0	0,002	#16-12-6- 14 Wild-type	-4,083	5,08	-0,804		0,421	1
#16-12-10- 18-Wild- type	6,333	5,081	1,246		0,213	1	#16-12-10- 18	-1,583	5,08	-0,312		0,755	1
Pairwise Comparisons of BdGSL5							Pairwise Comparisons of BdGSL6						
Sample 1- Sample 2	Test Statistic	Std. Error	Std. Statistic	Test Statistic	Sig.	Adj. Sig. ^a	Sample 1- Sample 2	Test Statistic	Std. Error	Std. Statistic	Test Statistic	Sig.	Adj. Sig. ^a
#2-9-4-9- Wild-type	16,25	5,082	3,198		0,001	0,014	#2-9-4-9- Wild-type	11,75	5,082	2,312		0,021	0,208
#2-9-6-30- Wild-type	11,917	5,082	2,345		0,019	0,19	#2-9-6-30- Wild-type	0,667	5,082	0,131		0,896	1
#16-12-6- 14-Wild- type	7,25	5,082	1,427		0,154	1	#16-12-6- 14	-7,5	5,082	-1,476		0,14	1

Wild-type- #16-12-10- 18	-2,5	5,082	-0,492	0,623	1	#16-12-10- 18-Wild- type	3,417	5,082	0,672	0,501	1
Pairwise Comparisons of BdGSL7						Pairwise Comparisons of BdGSL8					
Sample 1- Sample 2	Test Statistic	Std. Error	Std. Statistic	Test Sig.	Adj. Sig. ^a	Sample 1- Sample 2	Test Statistic	Std. Error	Std. Statistic	Test Sig.	Adj. Sig. ^a
#2-9-4-9- Wild-type	11,5	5,082	2,263	0,024	0,236	#2-9-4-9- Wild-type	12,333	5,079	2,428	0,015	0,152
#2-9-6-30- Wild-type	9,833	5,082	1,935	0,053	0,53	#2-9-6-30- Wild-type	6,417	5,079	1,263	0,206	1
Wild-type- #16-12-6- 14	0	5,082	0	1	1	Wild-type- #16-12-6- 14	-5,667	5,079	-1,116	0,265	1
Wild-type- #16-12-10- 18	-6,333	5,082	-1,246	0,213	1	Wild-type- #16-12-10- 18	-1,417	5,079	-0,279	0,78	1
Pairwise Comparisons of BdGSL9						Pairwise Comparisons of BdGSL11					
Sample 1- Sample 2	Test Statistic	Std. Error	Std. Statistic	Test Sig.	Adj. Sig. ^a	Sample 1- Sample 2	Test Statistic	Std. Error	Std. Statistic	Test Sig.	Adj. Sig. ^a
#2-9-4-9- Wild-type	9,417	5,082	1,853	0,064	0,639	#2-9-4-9- Wild-type	13,083	5,082	2,574	0,01	0,1
#2-9-6-30- Wild-type	11,667	5,082	2,296	0,022	0,217	#2-9-6-30- Wild-type	4,083	5,082	0,803	0,422	1
Wild-type- #16-12-6- 14	-2,75	5,082	-0,541	0,588	1	Wild-type- #16-12-6- 14	-0,083	5,082	-0,016	0,987	1
Wild-type- #16-12-10- 18	-0,417	5,082	-0,082	0,935	1	#16-12-10- 18-Wild- type	14,167	5,082	2,788	0,005	0,053

Each row tests the null hypothesis that the Sample 1 and Sample 2 distributions are the same.

Asymptotic significances (2-sided tests) are displayed. The significance level is ,05.

a. Significance values have been adjusted by the Bonferroni correction for multiple tests.

Table Supplement 23: Descriptive statistics for pathogen responsive genes expression analysis.

		Statistic		Std. Error	Statistic		Std. Error	Statistic		Std. Error
PR2	WT 0h Neg	Mean	4,47E-04	1,52E-04	PR1	1,91E-11	1,73E-11	Chit8	1,03E+00	4,57E-01
		Median	3,37E-04			1,23E-13			4,86E-01	
		Variance	2,08E-07			2,71E-21			1,88E+00	
		Std. Deviation	4,56E-04			5,20E-11			1,37E+00	
	WT 48h Neg	Mean	1,60E-03	6,99E-04		1,25E-10	1,21E-10		1,13E+00	7,30E-01
		Median	4,87E-04			8,88E-16			4,13E-01	
		Variance	4,40E-06			1,32E-19			4,80E+00	
		Std. Deviation	2,10E-03			3,63E-10			2,19E+00	
	WT 48h Fg	Mean	4,59E-03	1,82E-03		7,75E-10	5,29E-10		3,82E-01	1,43E-01
		Median	2,63E-03			8,46E-11			2,62E-01	
		Variance	2,97E-05			2,52E-18			1,85E-01	
		Std. Deviation	5,45E-03			1,59E-09			4,30E-01	
	#2-9-4-9 0h Neg	Mean	1,46E-03	4,27E-04		8,13E-09	7,61E-09		1,00E-01	3,38E-02
		Median	1,01E-03			2,10E-11			6,96E-02	
		Variance	1,64E-06			5,22E-16			1,03E-02	
		Std. Deviation	1,28E-03			2,28E-08			1,01E-01	
	#2-9-4-9 48h Neg	Mean	4,73E-03	1,04E-03		7,72E-11	6,11E-11		1,40E-01	4,73E-02
		Median	3,71E-03			8,90E-12			1,19E-01	
		Variance	9,76E-06			3,36E-20			2,02E-02	
		Std. Deviation	3,12E-03			1,83E-10			1,42E-01	

	#2-9-4-9 48h Fg	Mean	1,67E-02	1,64E-03	1,54E-08	1,48E-08	1,14E-01	3,80E-02
		Median	1,54E-02		3,73E-10		3,37E-02	
		Variance	2,41E-05		1,98E-15		1,30E-02	
		Std. Deviation	4,91E-03		4,45E-08		1,14E-01	
	#2-9-6-30 0h Neg	Mean	7,82E-04	2,74E-04	1,51E-04	7,58E-05	3,09E-01	7,33E-02
		Median	7,80E-04		2,13E-09		2,80E-01	
		Variance	6,78E-07		5,17E-08		4,84E-02	
		Std. Deviation	8,23E-04		2,27E-04		2,20E-01	
	#2-9-6-30 48h Neg	Mean	6,17E-03	9,84E-04	6,95E-10	5,66E-10	1,78E-01	5,98E-02
		Median	5,68E-03		1,48E-11		8,11E-02	
		Variance	8,71E-06		2,89E-18		3,22E-02	
		Std. Deviation	2,95E-03		1,70E-09		1,79E-01	
	#2-9-6-30 48h Fg	Mean	1,16E-02	2,08E-03	1,46E-05	1,46E-05	1,49E-01	5,53E-02
		Median	9,69E-03		3,91E-11		4,00E-02	
		Variance	3,88E-05		1,93E-09		2,75E-02	
		Std. Deviation	6,23E-03		4,39E-05		1,66E-01	
	#16-12-6-14 0h Neg	Mean	4,92E-04	2,46E-04	1,92E-09	1,91E-09	1,94E+00	8,21E-01
		Median	2,27E-07		1,87E-12		4,97E-01	
		Variance	5,46E-07		3,30E-17		6,06E+00	
		Std. Deviation	7,39E-04		5,74E-09		2,46E+00	
	#16-12-6-14 48h Neg	Mean	5,28E-03	9,53E-04	9,92E-09	9,71E-09	9,65E-01	2,59E-01
		Median	4,47E-03		5,36E-11		5,30E-01	

		Variance	8,17E-06			8,48E-16		6,04E-01	
		Std. Deviation	2,86E-03			2,91E-08		7,77E-01	
	#16-12-6-14 48h Fg	Mean	2,83E-02	1,27E-02		6,39E-03	2,48E-03	1,03E+00	2,45E-01
		Median	5,28E-03			3,93E-03		7,07E-01	
		Variance	1,44E-03			5,54E-05		5,40E-01	
		Std. Deviation	3,80E-02			7,45E-03		7,35E-01	
	#16-12-10-18 0h Neg	Mean	3,39E-03	9,73E-04		1,34E-08	1,34E-08	4,57E+00	1,20E+00
		Median	3,22E-03			6,15E-16		5,22E+00	
		Variance	8,52E-06			1,61E-15		1,30E+01	
		Std. Deviation	2,92E-03			4,01E-08		3,61E+00	
	#16-12-10-18 48h Neg	Mean	3,74E-03	9,57E-04		3,07E-08	2,88E-08	4,20E-01	2,75E-02
		Median	1,92E-03			6,15E-13		3,98E-01	
		Variance	8,24E-06			7,47E-15		6,80E-03	
		Std. Deviation	2,87E-03			8,64E-08		8,25E-02	
	#16-12-10-18 48h Fg	Mean	1,64E-02	6,48E-03		7,64E-10	5,90E-10	5,88E-01	6,53E-02
		Median	8,79E-03			1,07E-15		6,01E-01	
		Variance	3,78E-04			3,14E-18		3,84E-02	
		Std. Deviation	1,94E-02			1,77E-09		1,96E-01	
UGT74f2	WT 0h Neg	Mean	1,14E-01	4,95E-02			Mean	1,42E-03	5,13E-04
		Median	6,56E-02			BDMAPKKKI	Median	1,07E-03	
		Variance	2,20E-02				Variance	2,37E-06	
		Std. Deviation	1,48E-01				Std. Deviation	1,54E-03	

	WT 48h Neg	Mean	3,37E-02	5,82E-03	Mean	1,18E-03	7,44E-04
		Median	3,06E-02		Median	5,05E-06	
		Variance	3,05E-04		Variance	4,99E-06	
		Std. Deviation	1,75E-02		Std. Deviation	2,23E-03	
	WT 48h Fg	Mean	9,68E-02	1,39E-02	Mean	5,12E-04	1,55E-04
		Median	7,86E-02		Median	3,78E-04	
		Variance	1,75E-03		Variance	2,17E-07	
		Std. Deviation	4,18E-02		Std. Deviation	4,66E-04	
	#2-9-4-9 0h Neg	Mean	8,89E-02	1,76E-02	Mean	5,17E-04	9,61E-05
		Median	7,28E-02		Median	4,08E-04	
		Variance	2,77E-03		Variance	8,31E-08	
		Std. Deviation	5,27E-02		Std. Deviation	2,88E-04	
	#2-9-4-9 48h Neg	Mean	7,66E-02	1,10E-02	Mean	7,22E-04	1,85E-04
		Median	7,18E-02		Median	6,42E-04	
		Variance	1,09E-03		Variance	3,08E-07	
		Std. Deviation	3,30E-02		Std. Deviation	5,55E-04	
	#2-9-4-9 48h Fg	Mean	7,17E-02	1,92E-02	Mean	1,46E-03	3,50E-04
		Median	5,79E-02		Median	9,50E-04	
		Variance	3,31E-03		Variance	1,10E-06	
		Std. Deviation	5,75E-02		Std. Deviation	1,05E-03	
	#2-9-6-30 0h Neg	Mean	2,54E-02	2,65E-03	Mean	1,12E-03	1,78E-04

		Median	2,23E-02		Median	1,24E-03	
		Variance	6,31E-05		Variance	2,87E-07	
		Std. Deviation	7,94E-03		Std. Deviation	5,35E-04	
	#2-9-6-30 48h Neg	Mean	2,74E-02	6,06E-03	Mean	8,02E-04	2,05E-04
		Median	2,56E-02		Median	6,49E-04	
		Variance	3,30E-04		Variance	3,78E-07	
		Std. Deviation	1,82E-02		Std. Deviation	6,15E-04	
		#2-9-6-30 48h Fg	Mean	1,81E-02	5,67E-03	Mean	4,11E-04
	Median		1,25E-02		Median	2,96E-04	
	Variance		2,89E-04		Variance	1,11E-07	
	Std. Deviation		1,70E-02		Std. Deviation	3,34E-04	
	#16-12-6-14 0h Neg		Mean	5,27E-02	1,39E-02	Mean	1,81E-03
		Median	3,98E-02		Median	1,74E-03	
		Variance	1,74E-03		Variance	1,50E-06	
		Std. Deviation	4,17E-02		Std. Deviation	1,23E-03	
		#16-12-6-14 48h Neg	Mean	9,63E-02	1,89E-02	Mean	7,45E-04
	Median		8,28E-02		Median	4,70E-04	
	Variance		3,23E-03		Variance	5,19E-07	
	Std. Deviation		5,68E-02		Std. Deviation	7,21E-04	
	#16-12-6-14 48h Fg		Mean	5,63E-01	3,06E-01	Mean	1,55E-03
Median		1,07E-01		Median	1,04E-03		

		Variance	8,43E-01		Variance	2,06E-06
		Std. Deviation	9,18E-01		Std. Deviation	1,43E-03
	#16-12-10-18 0h Neg	Mean	2,15E-01	6,78E-02	Mean	3,13E-03
		Median	1,84E-01		Median	1,87E-03
		Variance	4,13E-02		Variance	1,01E-05
		Std. Deviation	2,03E-01		Std. Deviation	3,18E-03
	#16-12-10-18 48h Neg	Mean	5,76E-02	9,25E-03	Mean	2,59E-03
		Median	5,15E-02		Median	2,17E-03
		Variance	7,70E-04		Variance	4,30E-06
		Std. Deviation	2,77E-02		Std. Deviation	2,07E-03
	#16-12-10-18 48h Fg	Mean	2,84E-01	4,92E-02	Mean	2,70E-03
		Median	2,22E-01		Median	3,19E-03
		Variance	2,18E-02		Variance	5,01E-06
		Std. Deviation	1,48E-01		Std. Deviation	2,24E-03

Table Supplement 24: Test for normal distribution of PR2 expression data

Null Hypothesis	Test	Sig.	Decision
1 The distribution of PR2 is the same across categories of L2.	Independent-Samples Kruskal-Wallis Test	,000	Reject the null hypothesis.

Asymptotic significances are displayed. The significance level is ,050.

Table Supplement 25: Pairwise Comparisons of PR2 expression analysis

Sample 1-Sample 2	Test Statistic	Std. Error	Std. Test Statistic	Sig.	Adj. Sig. ^a
WT 48h Neg-WT 48h Fg	27,722	18,437	1,504	0,133	1,000
WT 48h Neg-#16-12-6-14 48h Fg	55,611	18,437	3,016	0,003	0,307
WT 48h Neg-#2-9-6-30 48h Fg	72,056	18,437	3,908	0,000	0,011
WT 48h Neg-#16-12-10-18 48h Fg	72,444	18,437	3,929	0,000	0,010
WT 48h Neg-#2-9-4-9 48h Fg	86,500	18,437	4,692	0,000	0,000

Each row tests the null hypothesis that the Sample 1 and Sample 2 distributions are the same.

Asymptotic significances (2-sided tests) are displayed. The significance level is ,05.

a. Significance values have been adjusted by the Bonferroni correction for multiple tests.

Table Supplement 26: Descriptive statistics of fungal virulence genes Tri5 and Fgl1 expression analysis after infection of B. distachyon

		Statistic	Std. Error
Tri5	WT 48h Neg	Mean	2,082817756777780
		Median	0,506979740000000
		Variance	7,565
		Std. Deviation	2,750382768855850
	#2-9-4-9 48h Fg	Mean	0,730429884444444
		Median	0,685391402000000
		Variance	0,109
		Std. Deviation	0,330781260458797
	#2-9-6-30 48h Fg	Mean	1,970719370888890
		Median	1,328685814000000
		Variance	2,847
		Std. Deviation	1,687246011369450
Fgl1	#16-12-6-14 48h Fg	Mean	1,973098110222220
		Median	0,619853850000000
		Variance	7,274
		Std. Deviation	2,696995543961780
	#16-12-10-18 48h Fg	Mean	0,604394058222222
		Median	0,461691155000000
		Variance	0,232
		Std. Deviation	0,481237341076219
	#2-9-4-9 48h Fg	Mean	0,000059819494033
		Median	0,000018720800000
		Variance	0,000
		Std. Deviation	0,000089987729647
	#2-9-6-30 48h Fg	Mean	0,000068665001444
		Median	0,000076988400000

#16-12-6-14 48h Fg	Variance	0,000	
	Std. Deviation	0,000064834929752	
	Mean	0,000067521191778	0,000021289640027
	Median	0,000055198900000	
	Variance	0,000	
	Std. Deviation	0,000063868920081	
#16-12-10-18 48h Fg	Mean	0,000139785935311	0,000127801451848
	Median	0,000006781330000	
	Variance	0,000	
	Std. Deviation	0,000383404355544	

Table Supplement 27: Independent-Samples Kruskal-Wallis Test Summary of *TRI5* expression

Independent-Samples Kruskal-Wallis Test Summary	
Total N	45
Test Statistic	2,895 ^{a,b}
Degree Of Freedom	4
Asymptotic Sig.(2-sided test)	,576

a. The test statistic is adjusted for ties.

b. Multiple comparisons are not performed because the overall test does not show significant differences across samples.

Table Supplement 28: Descriptive statistics for the mean relative area of callose depositions at wounding sites 16 hours after wounding

Sorting	Statistic	Std. Error
Wild type	Mean	0,7039
	Median	0,6019
	Std. Deviation	0,39810
#2-9-4-9	Mean	0,4168
	Median	0,3054
	Std. Deviation	0,26159
#2-9-6-30	Mean	0,4341
	Median	0,3538
	Std. Deviation	0,31030
#16-12-6-14	Mean	0,3354
	Median	0,2999
	Std. Deviation	0,12751
#16-12-10-18	Mean	0,2681
	Median	0,2695
	Std. Deviation	0,03176

Table Supplement 29: Independent-Samples Kruskal-Wallis Test Summary for mean relative area of callose formation 16 hours after wounding

Total N	24
Test Statistic	7,420 ^{a,b}
Degree Of Freedom	4
Asymptotic Sig.(2-sided test)	0,115

a. The test statistic is adjusted for ties.

b. Multiple comparisons are not performed because the overall test does not show significant differences across samples.

Acknowledgments

An dieser Stelle möchte ich mich bei all den Menschen bedanken, die mir während der Dissertation fachlich und privat zur Seite standen.

Besonderer Dank gilt an erster Stelle Dr. Christian Voigt dafür das ich bei Ihm meine Promotion in Hamburg beginnen durfte, und nach dem Wechsel zur Universität Sheffield weiterhin mein Betreuer geblieben ist. Vielen Dank für die wissenschaftliche Betreuung sowie die Möglichkeiten die mir gegeben wurden und mein Leben bedeutend verändert haben.

Des Weiteren möchte ich mich gleichermaßen bei Prof. Dr. Stefan Hoth bedanken für die Übernahme der Gutachterfunktion dieser Dissertation und die damit verbundene Arbeit.

Ein weiterer großer Dank geht noch an Prof. Dr. Willi Schäfer für die Aufnahme in die Phytopathologie nach dem Wechsel von Dr. Christian Voigt, die damit verbundene Unterstützung und die anregenden Gespräche.

Ein großes Dankeschön gebührt auch den ehemaligen Mitarbeitern der Phytopathologie für die durchgehend aufbauende Unterstützung während der letzten vier Jahre. Die Hilfestellungen, Tipps und Diskussionen haben den Laboralltag selbst nach Rückschlägen noch aufgewertet. Dabei möchte ich mich bei Barbara, Petra, Annemarie, Kerstin, Chris, Björn und Marcel aus der ehemaligen PhyBi-Gruppe bedanken.

Was wäre jedoch die Zeit im Labor nicht ohne die Kollegen, mit denen man am meisten durch die Phasen der Promotion gegangen ist, vielen Dank an Chien, Gunnar, Christine, Anika, Sophie, Lewin, Brigitte, Birgit, Cathrin, Conni und Dave für die unvergesslichen Stunden während und nach der Arbeit. Besonderen Dank gilt noch Michael, der nicht nur ein guter Kollege, sondern auch ein guter Freund geworden ist und in den letzten Wochen aufbauend zur Seite stand. Auch die Kollegen aus Sheffield, besonders Henry, Nic, Peijun und Bastian, sollten nicht unerwähnt bleiben, danke für die freundliche Aufnahme in C45 und die lustigen Stunden im Labor. Ganz besonderen Dank noch an Anthony, der nicht nur ein guter Freund wurde, sondern auch die Arbeit auf sprachliche Richtigkeit überprüft hat.

Natürlich dürfen meine Freunde nicht unerwähnt bleiben, die mir beigestanden haben. Insbesondere Raphael, der sich so manches anhören musste.

Zum Schluß möchte ich mich noch bei meiner Familie bedanken für die Unterstützung während des langen Weges die mir in schwierigen Zeiten immer zur Seite standen.

Declaration of authorship

I hereby declare that I have written the present dissertation by my own, that I do not have used other than the acknowledge resources and aids. I further declare that I have not submitted this thesis to any other institution in order to obtain a degree.

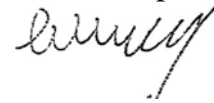
(Place and Date)

(Signature)

Confirmation of Linguistic Correctness

I hereby declare that I have read the thesis "Applicability of CRISPR/Cas9-mediated gene disruption in *Brachypodium distachyon* (L) P. Beauv to characterise the stress-induced 1,3- β -glucan synthase BdGSL3 in plant defence" by Tobias Hanak and can confirm, as a native English speaker, its linguistic correctness in English.

Sheffield, 25th September 2019



Anthony Hodder